FG

12

RADC-TR-76-105
Technical Report
April 1976

ABSORPTION OF DEUTERIUM FLOURIDE LASER RADIATION BY THE ATMOSPHERE

The Ohio State University

Sponsored By
Defense Advanced Research Projects Agency
ARPA Order No. 1279

Approved for public release;
distribution unlimited.

ROME AIR DEVELOPMENT CENTER
AIR FORCE SYSTEMS COMMAND
GRIFFISS AIR FORCE BASE, NEW YORK 13441

This report has been reviewed by the RADC Information Office (OI) and is releasable to the National Technical Information Service (NTIS). At NTIS it will be releasable to the general public, including foreign nations.

This report has been reviewed and approved for publication.

APPROVED: James W. Cusack
RADC Project Engineer

The views and conclusions contained in this document are those of the authors and should not be interpreted as necessarily representing the official policies, either expressed or implied, of the Defense Advanced Research Projects Agency or the U. S. Government.

Do not return this copy. Retain or destroy.

ABSORPTION OF DEUTERIUM FLOURIDE LASER RADIATION BY THE ATMOSPHERE

Frank S. Mills

Contractor: The Ohio State University
Contract Number: F30602-75-C-0029
Effective Date of Contract: 1 October 1974
Contract Expiration Date: 30 September 1974
Amount of Contract: $124,969.00
Program Code Number: 5E20
Period Covered: Mar 75 - Jul 75

Principal Investigator: Dr. Ronald K. Long
Phone: 614 422-6077

Project Engineer: James W. Cusack
Phone: 315 330-3145

Approved for public release;
distribution unlimited.

This research was supported by the Defense Advanced Research Projects Agency of the Department of Defense and was monitored by James W. Cusack RADC (OCSE), GAFB NY 13441.

UNCLASSIFIED

SECURITY CLASSIFICATION OF THIS PAGE (When Date Entered)

REPORT DOCUMENTATION PAGE

READ INSTRUCTIONS BEFORE COMPLETING FORM

1. REPORT NUMBER: RADC-TR-76-105
2. GOVT ACCESSION NO.
3. RECIPIENT'S CATALOG NUMBER
4. TITLE (and Subtitle): ABSORPTION OF DEUTERIUM FLUORIDE LASER RADIATION BY THE ATMOSPHERE
5. TYPE OF REPORT & PERIOD COVERED: Interim Report. 1 Jul 75 - 30 Sep 75
6. PERFORMING ORG. REPORT NUMBER: ESL-4054-3
7. AUTHOR(s): Frank S. Mills
8. CONTRACT OR GRANT NUMBER(s): F30602-75-C-0029; ARPA Order-1279
9. PERFORMING ORGANIZATION NAME AND ADDRESS: The Ohio State University/ElectroScience Laboratory, Department of Electrical Engineering, Columbus OH 43212
10. PROGRAM ELEMENT, PROJECT, TASK AREA & WORK UNIT NUMBERS: 62301E; 12790506; AF-1279
11. CONTROLLING OFFICE NAME AND ADDRESS: Defense Advanced Research Projects Agency, 1400 Wilson Blvd, Arlington VA 22209
12. REPORT DATE: April 1976
13. NUMBER OF PAGES: 192
14. MONITORING AGENCY NAME & ADDRESS (If different from Controlling Office): Rome Air Development Center (OCSE), Griffiss AFB NY 13441
15. SECURITY CLASS. (of this report): UNCLASSIFIED
15a. DECLASSIFICATION/DOWNGRADING SCHEDULE: N/A
16. DISTRIBUTION STATEMENT (of this Report): Approved for public release; distribution unlimited.

12 199p.

17. DISTRIBUTION STATEMENT (of the abstract entered in Block 20, if different from Report): Same
18. SUPPLEMENTARY NOTES: RADC Project Engineer: James W. Cusack (OCSE)
19. KEY WORDS (Continue on reverse side if necessary and identify by block number)

Absorption	Water Vapor
DF laser	Methane
Laser Propagation	Nitrous Oxide
Molecular Spectroscopy	Spectra
HDO	Atmosphere

20. ABSTRACT (Continue on reverse side if necessary and identify by block number)

Absorption of deuterium flouride (DF) laser radiation by atmospheric gases was measured for five absorbers and 8 laser lines using a single frequency, pulsed DF laser and a large multipass absorption cell. $N_2^{\Gamma}0$, CH_4^{Γ}, CO_2^{Γ}, HDO, and $H_2^{\Gamma}0$ absorption was investigated for the 2-1 P(6), P(7), P(8), P(10), and P(11) lines and the 3-2 P(6), P(7), and P(8) lines of the DF laser.

For the mid-latitude summer sea level atmospheric model (14.3 torr $H_2^{\Gamma}0$, 1.6 ppm

DD FORM 1 JAN 73 1473 EDITION OF 1 NOV 65 IS OBSOLETE

UNCLASSIFIED

SECURITY CLASSIFICATION OF THIS PAGE (When Data Entered)

402 251 LB

CH_4, 0.28 ppm N_2O, temperature 296K, total pressure 760 torr) the total molecular absorption coefficients are between 3.18×10^{-2} km^{-1} and 1.16×10^{-1} km^{-1} corresponding to a transmittance over a 10 km path of from 31 to 73 percent.

Assuming the mid-latitude summer model atmosphere, the water vapor continuum absorption coefficient for the eight lines is approximately 0.02 km^{-1}. The measured HDO absorption coefficients vary from 0.006 km^{-1} to 0.095 km^{-1} for the lines studied and the N_2O absorption coefficients vary from .002 km^{-1} to .045 km^{-1}. The CH_4 absorption coefficients were found to be on the order of 10^{-3} or 10^{-4} km^{-1}. The accuracy of the measured absorption coefficients is ±5%.

Measurements of H_2O absorption at 24°C with 14.3 torr H_2O and 760 torr total pressure confirm the water continuum absorption coefficients obtained by extrapolating the high temperature measurements of Burch.

The experimental results obtained in this study were compared with calculations made from the AFCRL line compilation. The theoretical background for making such calculations is thoroughly discussed, and listings of two computer programs written to perform the calculations are presented.

The calculated values for the N_2O absorption coefficients agree very well with the experimentally measured absorption cofficients. For other gases the agreement between calculation and measurement is not as good, although in most cases the calculated absorption coefficients are of the same order of magnitude as the experimentally measured results.

PREFACE

This technical report, Ohio State University Research Foundation Report 4054-3, was prepared by The Ohio State University ElectroScience Laboratory, Department of Electrical Engineering, Columbus, Ohio. Research was conducted under Contract F30602-75-C-0029. Mr. James W. Cusack, RADC (OCSE), of Rome Air Development Center, Griffiss Air Force Base, New York is the Project Engineer.

The author is grateful to his adviser, Professor Ronald K. Long, for suggesting this thesis problem and for his guidance and suggestions in the completion of the research program and the preparation of this manuscript. The author would also like to thank Professor Edward K. Damon and Dr. Gary L. Trusty for their many helpful discussions on experimental aspects of the problem.

The research reported in this dissertation was supported in part by Rome Air Development Center, Griffiss Air Force Base, and Defense Advanced Research Projects Agency.

The material contained in this report is also used as a dissertation submitted to the Department of Electrical Engineering, The Ohio State University as partial fulfillment for the degree Doctor of Philosophy.

TABLE OF CONTENTS

CHAPTER I

INTRODUCTION

Transmission of infrared radiation through the atmosphere is adversely affected by turbulence, scattering by aerosols, and molecular absorption. This study is restricted to certain aspects of the last problem.

An investigation of a low resolution solar spectrum from 1 to 15 μm, such as that shown in Fig. 1[1], reveals that there are certain regions of the spectrum where there is relatively little absorption by atmospheric gases. One of these regions from 3.5 to 4.0 microns corresponds to the wavelength range of the deuterium fluoride (DF) laser. This correspondence of DF laser wavelengths with an atmospheric window, along with the high power capability of this laser makes it very attractive for certain applications such as communications or laser radar.

Although the molecular absorption in the DF laser region is small, it does vary rapidly with frequency. This may be seen more clearly in the medium resolution spectrum obtained by Streete[2] over a 24.9 km sea-level path (Fig. 2). Straight lines corresponding to selected DF laser lines have been superimposed on the spectrum in Fig. 2.

In order for intelligent decisions to be made regarding the use of DF lasers in systems involving transmission of radiation through the atmosphere, a precise knowledge of the atmospheric transmittance at the laser frequencies is required. As may be seen in Fig. 2 this precise knowledge is very difficult to obtain using conventional spectroscopy techniques since the laser lines frequently occur at frequencies where the transmittance is changing very rapidly with frequency. Even the highest resolution conventional spectrometers tend to smooth this rapid variation because of their finite resolution. Thus, if precise knowledge of the atmospheric transmittance at a laser frequency is needed, it it necessary to measure it directly using the laser as the source. This is the approach taken in this study.

It can be seen from Fig. 1 that there are contributions to molecular absorption in the DF laser region from HDO, methane, nitrous oxide, and carbon dioxide. In addition there is a contribution from water continuum absorption presumably caused by

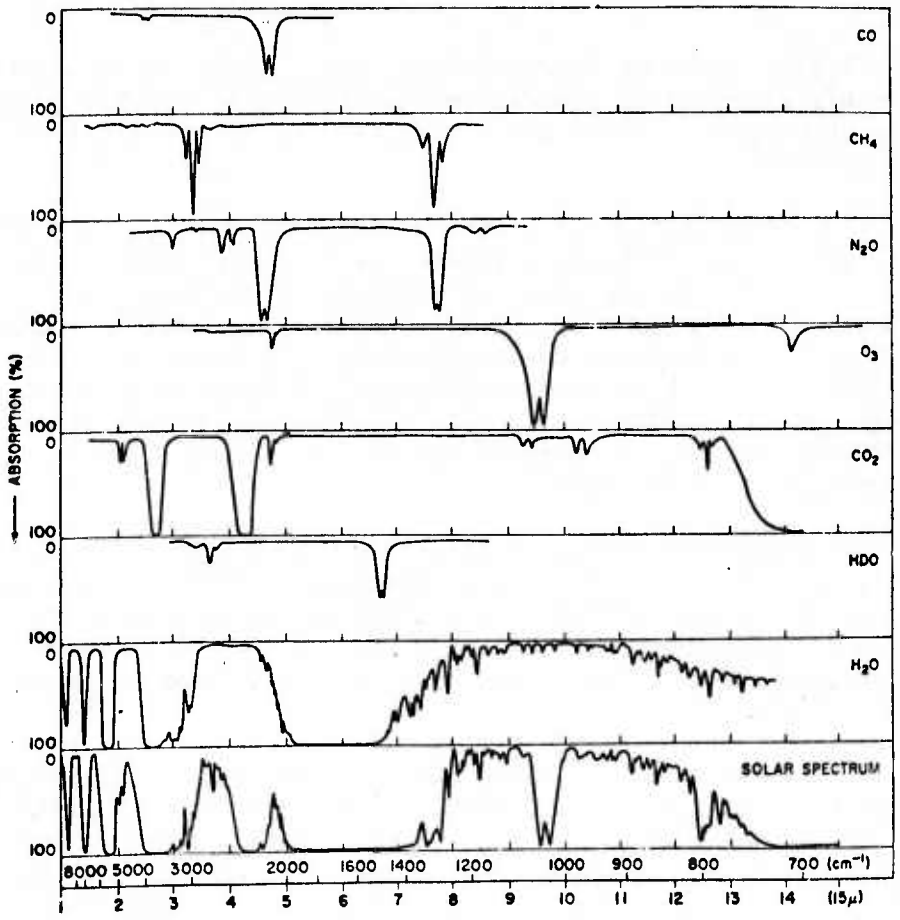

Fig. 1. Low resolution solar spectrum compared with laboratory spectra of atmospheric gasses (Shaw).

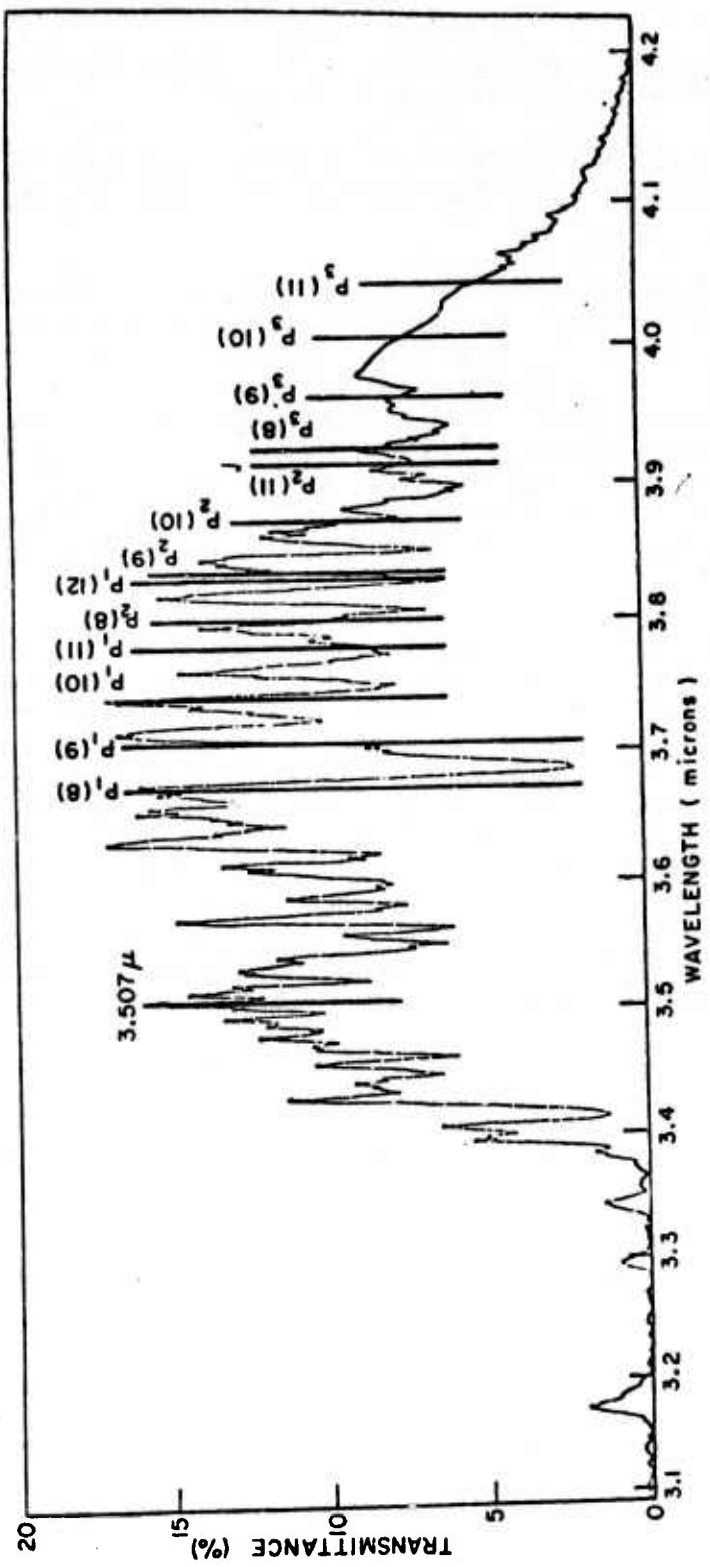

Fig. 2. Medium resolution relative transmittance of 3-4 infrared window (Streete).

the wings of the strong water vapor bands at 2.6 and 6.3 microns, and a small pressure-induced nitrogen continuum.

The purpose of this study was to measure accurately the absorption of selected DF laser lines by HDO, CH_4, N_2O, CO_2 and the water continuum.

The absorption was measured for each constituent separately using a long path laboratory absorption cell and a small, pulsed, single-frequency laser. DF laser lines selected for study were the 2-1 P(6), P(7), P(8), P(10), and P(11) lines and the 3-2 P(6), P(7), and P(8) lines. These lines are reported to be relatively intense in high-power lasers. Ideally one would wish to study the absorption on all lines. However, the lasers used in this study were capable of operation on about 30 lines, and it would have been prohibitively costly in terms of time and money to measure the absorption on all lines.

McClatchey, et al.[3] have compiled line data on the molecular absorption for the most important absorbers in the infrared region, and have made these data available to other workers on magnetic tape. The data are based on conventional spectra from many different sources. Using this tape it is possible to compute the atmospheric absorption at desired frequencies. The accuracy of such a computation is of course limited by the accuracy of the data on which it is based. However, even if the computation is off by a factor of two or more, it is still very useful as an aid in planning the necessary absorber concentration and path required to make accurate measurements of the absorption at the laser frequencies of interest. This was the approach taken in this study.

In Chapter II the theoretical basis of molecular absorption calculations is discussed, computer programs which calculate the absorption are described and calculations are presented for the DF laser lines. Also discussed in Chapter II are measurements made by Burch [4] of the water vapor and nitrogen continua using a conventional spectrometer and a long path absorption cell.

In Chapter III the experimental equipment used to make the absorption measurements is described.

In Chapter IV the absorption measurements are described and the results are discussed and compared with the experimental results of other workers and with the computer predictions. Also described is a laser spectroscopy technique which can be used to measure the frequency separation of an absorption line and a nearly coincident laser line.

CHAPTER II

MOLECULAR ABSORPTION CALCULATIONS

For many applications it is useful to compute both single frequency absorption and absorption spectra, for various situations of interest, from spectral data. The most complete set of standard spectral data currently available is the AFCRL Line Compilation[3]. This compilation lists data for over 100,000 absorption lines from 0.307 cm^{-1} to 15,000 cm^{-1}, and is available on magnetic tape. In this chapter the theoretical background for the absorption calculations will be presented, two computer programs which have been written to compute fixed frequency absorption and absorption spectra will be discussed, and results of calculations made for the DF laser region of the spectrum will be presented.

A. Theoretical Background

Assuming the photon density is low enough that nonlinear extinction processes do not occur, the change in intensity dI_ν of a parallel beam of electromagnetic radiation at frequency ν traversing an infinitesimal path $d\ell$ is given by Lambert's law

$$(1) \qquad dI_\nu = - k(\nu) I_\nu \, da$$

where da is the amount of absorber in a volume of unit cross-sectional area and length $d\ell$. The factor $k(\nu)$ is called the absorption coefficient.

The transmittance T_ν through an absorber amount a is found by integrating Eq. (1).

$$(2) \qquad T_\nu = \frac{I_\nu}{I_\nu^o} = e^{-k(\nu)a} \quad .$$

Here I_ν is the intensity of the beam after passing through the absorber and I_ν^o is the intensity of the beam before it enters the absorber.

The absorber amount a and absorption coefficient $k(\nu)$ may in general be expressed in any convenient units. The requirement is that the product $k(\nu)a$ be dimensionless. In making calculations using the AFCRL Line Compilation it is convenient to express the absorber amount a in mol cm^{-2}. The absorption coefficient is therefore in $(mol\text{-}cm^{-2})^{-1}$. In the experimental work presented later it is convenient to characterize the absorber amount by the length of the path containing the absorber. The absorber amount is then given in km and the absorption coefficient in km^{-1}. A more complete discussion of the units and conversion factors between various units is given in Appendix A.

The absorption of electromagnetic radiation by an absorbing medium is caused by the interaction of the electromagnetic fields with the energy states of the absorber. The energy of a molecule consists of its electronic, vibrational, and rotational energies and the interaction energies between these three energy modes. Energy levels are quantized so that the molecule can have only certain allowed values of energy. The absorption of one photon of electromagnetic radiation then involves a change of energy of one molecule from one energy state to a higher energy state, ignoring Raman and multiphoton processes. The difference in the energy states must be equal to the energy of the photon $h\nu$. In addition for a given type of molecule only transitions between certain energy states are allowed, and therefore only photons having energy equal to the difference in energy between those states will be absorbed. Thus, for a given absorber type, electromagnetic radiation will be absorbed at only those frequencies where the photon energy is equal to the energy difference of an allowed transition. The above discussion applies equally well to emission of radiation.

Allowed electronic energy states are normally widely separated, and the absorption or emission of radiation due to changes in electronic energy usually occurs in the visible or ultra-violet portion of the spectrum. Absorption or emission in the infrared portion of the spectrum of interest in this study is caused by changes in both the vibrational and rotational energies of the molecule while the electronic energy remains unchanged. Changes in rotational energy only result in emission or absorption in the far-infrared to microwave region of the spectrum.

Transitions occur from a higher energy state u to a lower energy state ℓ at a rate

$$W_{u\ell} = (B_{u\ell}\, \rho(\nu) + A_{u\ell})\ sec^{-1} \tag{3}$$

where $B_{u\ell}$ is the Einstein coefficient for stimulated emission, $\rho(\nu)$ is the radiation density per unit frequency interval, and $A_{u\ell}$

is the Einstein coefficient for spontaneous emission. The transition rate from lower level to upper level is given by

$$(4) \qquad W_{\ell u} = B_{\ell u}\, \rho(\nu) \ \text{sec}^{-1}$$

where $B_{\ell u}$ is the Einstein coefficient for absorption. In considering Planck's radiation law Einstein showed

$$(5) \qquad B_{\ell u} = B_{u\ell}\, \frac{g_u}{g_\ell}$$

where g_u and g_ℓ are the degeneracies of the upper and lower states respectively, and

$$(6) \qquad A_{u\ell} = \frac{8\pi h\nu^3}{c^3}\, B_{u\ell} \ \text{sec}^{-1} \quad .$$

The transition rates may now be written in terms of $A_{u\ell}$:

$$(7) \qquad W_{u\ell} = \left(\frac{\rho(\nu)\, c^3}{8\pi h\nu^3} + 1\right) A_{u\ell} \ \text{sec}^{-1}$$

$$(8) \qquad W_{\ell u} = \frac{g_u}{g_\ell}\, \frac{\rho(\nu)\, c^3}{8\pi h\nu^3}\, A_{u\ell} \ \text{sec}^{-1} \quad .$$

The transition rates are related to the transition moment by

$$(9) \qquad A_{u\ell} = \frac{64\pi^4\nu^3}{3hg_u}\, |\vec{m}_{u\ell}|^2 \ \text{sec}^{-1}$$

where $\vec{m}_{u\ell}$ is the electric dipole transition moment $\langle E^u \cdot |\vec{m}| E^\ell \rangle$. It is necessary to know $|E^u\rangle$ and $|E^\ell\rangle$ to calculate $|\vec{m}_{u\ell}|$. Since the states have a finite lifetime, the uncertainty principle says it is not possible to know the energy of the energy levels precisely. In addition, for a system of colliding molecules, the collision interaction energy must be included for the whole system. This is a many body problem which cannot be solved. The effect of these considerations is that the energy levels are smeared and

there is a finite transition probability for interaction with the radiation field over a range of frequencies.

This effect is taken into account by introducing a frequency dependent transition probability. The transition rates may then be written.

$$(10) \qquad W_{u\ell} = \int_{-\infty}^{\infty} \left(\frac{\rho(\nu)c^3}{8\pi h\nu^3} + 1 \right) A_{u\ell}\, g(\nu-\nu_o)\, d\nu$$

and

$$(11) \qquad W_{\ell u} = \int_{-\infty}^{\infty} \frac{g_u}{g_\ell} \frac{\rho(\nu)c^3}{8\pi h\nu^3} A_{u\ell}\, g(\nu-\nu_o)\, d\nu$$

where

$$\nu_o = \frac{E_u - E_\ell}{h}$$

and $g(\nu-\nu_o)$ is a normalized shape factor.

If $g(\nu-\nu_o)$ is small except for a narrow range of frequencies near ν_o, and

$$\frac{\rho(\nu)}{\nu^3}$$

is essentially constant over this range, then the transition rates are

$$(12) \qquad W_{u\ell} = \frac{\rho(\nu_o)c^3}{8\pi h\nu_o^3} A_{u\ell}$$

and

$$(13) \qquad W_{\ell u} = \frac{g_u}{g_\ell} \frac{\rho(\nu_o)c^3}{8\pi h\nu_o^3} A_{u\ell}$$

where the spontaneous emission term in $W_{u\ell}$ has been ignored (since its contribution to a collimated beam would be negligible) and

$$(14) \qquad \int_{-\infty}^{\infty} g(\nu-\nu_o)\, d\nu = 1 \quad .$$

When $\rho(\nu)$ is monochromatic,

$$(15) \qquad \rho(\nu') = \rho_o\, \delta\,(\nu-\nu') \quad ,$$

and Eqs. (11) and (10) become

$$(16) \qquad W_{\ell u} = \frac{g_u}{g_\ell}\, \frac{\rho_o\, c^3}{8\pi\, h\nu^3}\, A_{u\ell}\, g(\nu-\nu_o)$$

and

$$(17) \qquad W_{u\ell} = \frac{\rho_o\, c^3}{8\pi\, h\nu^3}\, A_{u\ell}\, g(\nu-\nu_o)$$

respectively.

The number of molecules per unit absorber in the upper energy level is related to the number of molecules per unit absorber in the lower energy level by the Boltzmann distribution

$$(18) \qquad N_u = N_\ell\, \frac{g_u}{g_\ell}\, e^{-\frac{(E^u-E^\ell)}{kT}} = N_\ell\, \frac{g_u}{g_\ell}\, e^{-\frac{h\nu_o}{kT}} \quad .$$

A monochromatic beam passing through an infinitesimal amount of absorber da will have an intensity change

$$(19) \qquad dI_\nu = (N_u\, W_{u\ell} - N_\ell\, W_{\ell u})\, h\nu\, da$$

or, from Eqs. (13) and (18)

$$(20) \qquad dI_\nu = \left(e^{-\frac{h\nu_o}{kT}} - 1\right) N_\ell\, W_{\ell u}\, h\nu\, da \quad .$$

From Eqs. (1) and (20)

$$(21) \qquad dI_\nu = - k(\nu) I_\nu \, da = \left(e^{- \frac{h\nu_o}{kT}} - 1 \right) N_\ell \, W_{\ell u} \, h\nu \, da \quad .$$

Equation (21) may be solved for the absorption coefficient

$$(22) \qquad k(\nu) = \left(1 - e^{- \frac{h\nu_o}{kT}} \right) \frac{N_\ell \, W_{\ell u} \, h\nu}{I_\nu} \quad .$$

Using $I_\nu = c \, \rho_o$ and $W_{\ell u}$ from Eq. (16)

$$(23) \qquad k(\nu) = N_\ell \frac{g_u}{g_\ell} \frac{A_{u\ell} \, c^2}{8\pi \, \nu^2} \left(1 - e^{- \frac{h\nu_o}{kT}} \right) g(\nu - \nu_o) \quad .$$

The line strength S is defined as the integral over all ν of $k(\nu)d\nu$

$$(24) \qquad S = \int_{-\infty}^{\infty} k(\nu) d\nu = N_\ell \frac{g_u}{g_\ell} \frac{A_{u\ell} \, c^2}{8\pi} \left(1 - e^{- \frac{h\nu_o}{kT}} \right) \times \int_{-\infty}^{\infty} \frac{g(\nu - \nu_o)}{\nu^2} \, d\nu \quad .$$

Again assuming $g(\nu - \nu_o)$ is small except for a narrow range of frequencies about ν_o, the integral in Eq. (24) becomes

$$(25) \qquad \int_{-\infty}^{\infty} \frac{g(\nu - \nu_o)}{\nu^2} \, d\nu = \frac{1}{\nu_o^2} \quad .$$

The line strength is then

$$(26) \qquad S = N_\ell \frac{g_u}{g_\ell} \frac{A_{u\ell} \, c^2}{8\pi \, \nu_o^2} \left(1 - e^{- \frac{h\nu_o}{kT}} \right) \quad ,$$

and the extinction coefficient is simply

$$k(\nu) = S\, g(\nu-\nu_o) \qquad (27)$$

If vibration-rotation interaction is neglected, N_ℓ is related to the total number of molecules of absorber by the rotational and vibrational partition functions Q_R and Q_V. The relationship of N_ℓ to N_T is given by

$$N_\ell = \frac{N_T}{Q_V\, Q_R}\, g_\ell\, e^{-\frac{E^\ell}{kT}} \qquad (28)$$

The line strength then becomes

$$S = \frac{N_T}{Q_V\, Q_R}\, g_u\, \frac{A_{u\ell}\, c^2}{8\pi\, \nu_o^{\,2}} \left(1 - e^{-\frac{h\nu_o}{kT}}\right) e^{-\frac{E^\ell}{kT}} \qquad (29)$$

The line strength per molecule per square centimeter S° at standard temperature T_o is found by evaluating Eq. (29) at temperature T_o and dividing by the number density N_T.

$$S^\circ = \frac{g_u}{Q_V^\circ Q_R^\circ}\, \frac{A_{u\ell}\, c^2}{8\pi\, \nu_o^{\,2}} \left(1 - e^{-\frac{h\nu_o}{kT_o}}\right) e^{-\frac{E^\ell}{kT}} \qquad (30)$$

The line strength at any other temperature is then

$$S = S^\circ\, \frac{Q_V^\circ Q_R^\circ}{Q_V\, Q_R}\, e^{\frac{E^\ell}{k}\left(\frac{T-T_o}{TT_o}\right)}\, \frac{\left(1 - e^{-\frac{h\nu_o}{kT}}\right)}{\left(1 - e^{-\frac{h\nu_o}{kT_o}}\right)} \qquad (31)$$

The AFCRL line compilation [3] gives for each line the line strength at 296°K. Equation (31) is used to correct the line strength for use in making calculations at other temperatures.

The vibrational partition function Q_V can be determined as follows.

For the Maxwell-Boltzmann distribution, the number of molecules in a vibrational state v, N_v, is proportional to the Boltzmann factor

$$e^{-E_V/kT} \quad .$$

For the vibrational states the term values G(v) are given by[5]

$$(32) \qquad G(v) = \omega_e(v + \tfrac{1}{2}) - \omega_e x_e(v + \tfrac{1}{2})^2 + \ldots .$$

where

$$(33) \qquad G(v) = \frac{E_v}{hc} \ \text{cm}^{-1} \quad .$$

Now let

$$G_0(v) = G(v) - G(0) \approx \omega_e \, v \quad ,$$

assuming that the simple harmonic oscillator function approximation is adequate. Then

$$(34) \qquad N_v = C_1 \, e^{-G_0(v) \, hc/kT}$$

where C_1 is a constant of proportionality. Again assuming the validity of the simple harmonic oscillator approximation

$$(35) \qquad N_0 = C_1$$

$$(36) \qquad N_1 = C_1 \, e^{-G_0(1) \, hc/kT}$$

$$(37) \qquad N_2 = C_1 \, e^{-G_0(2) \, hc/kT}$$

etc.

From Eq. (34)

$$(38) \qquad C_1 = \frac{N_v}{e^{-G_0(v)\ hc/kT}} \quad .$$

The total number of molecules is just the sum of the molecules in each state N_v.

$$(39) \qquad N = C_1 \left[1 + e^{-G_0(1)\ hc/kT} + e^{-G_0(2)\ hc/kT} + \ldots \right] \quad .$$

Substituting C_1 from Eq. (38) gives

$$(40) \qquad N = \frac{N_v}{e^{-G_0(v)\ hc/kT}} \left[1 + e^{-G_0(1)\ hc/kT} + e^{-G_0(2)\ hc/kT} + \ldots \right] .$$

Solving for N_v

$$(41) \qquad N_v = \frac{N\, e^{-G_0(v)\ hc/kT}}{\left[1 + e^{-G_0(1)\ hc/kT} + e^{-G_0(2)\ hc/kT} + \ldots \right]} \quad ,$$

or defining the denominator as Q_V

$$(42) \qquad N_v = \frac{N}{Q_v}\, e^{-G_0(v)\ hc/kT} \quad .$$

Assuming the harmonic oscillator approximation

$$(43) \qquad Q_v = \left[1 + e^{-\omega\ hc/kT} + e^{-2\omega\ hc/kT} + \ldots \right]$$

$$= \sum_{n=0}^{\infty} \left(e^{-\omega\ hc/kT} \right)^n$$

$$= \frac{1}{1 - e^{-\omega\ hc/kT}} \quad .$$

Now ωhc is approximately the difference between the vibrational energy levels of the absorbing transition, and since the difference in rotational energy levels is small it is also approximately the energy of the absorbed photon. Therefore

$$(44) \qquad Q_v \approx \frac{1}{1 - e^{-h\nu_o/kT}} \quad .$$

McClatchey, et al[3] have given a table of Q_v for the various molecules whose absorption lines are listed in the AFCRL Line Compilation which is repeated here as Table 1.

TABLE 1

VIBRATIONAL PARTITION FUNCTION VALUES FROM McCLATCHEY[3]

Molecule	Temperature °K						
	175	200	225	250	275	296	325
H_2O	1.000	1.000	1.000	1.000	1.000	1.000	1.001
CO_2	1.0095	1.0192	1.0327	1.0502	1.0719	1.0931	1.1269
O_3	1.004	1.007	1.013	1.022	1.033	1.046	1.066
N_2O	1.017	1.030	1.048	1.072	1.100	1.127	1.170
CO	1.000	1.000	1.000	1.000	1.000	1.000	1.000
CH_4	1.000	1.000	1.001	1.002	1.004	1.007	1.011
O_2	1.000	1.000	1.000	1.000	1.000	1.000	1.001

From Table 1 it appears that Q_v may be ignored for H_2O, CO, and CH_4. For the other molecules it appears that Eq. (44) is not a very good approximation. The table indicates no dependence on frequency although the above discussion indicates that there is a definite frequency dependence. Therefore it would seem that calculations made at frequencies lower than about 800 cm^{-1} would have reduced accuracy.

The rotational partition function Q_R is defined by

$$(45) \qquad Q_R = \sum_{J=0}^{\infty} g_J \, e^{-E_R(J)/kT}$$

The degeneracy g_J is different for different types of molecules. For a linear molecule (N_2O, CO_2, CO) Herzberg[5] gives as an approximation

(46) $$Q_R(T) = \frac{kT}{hcB}$$

so that

(47) $$\frac{Q_R^\circ}{Q_R} = \left(\frac{T_o}{T}\right)^{1.0} .$$

For asymmetric top molecules (H_2O, O_3) Herzberg[5] gives as an approximation

(48) $$Q_R = \sqrt{\frac{\pi}{ABC}\left(\frac{kT}{hc}\right)^3}$$

so that

(49) $$\frac{Q_R^\circ}{Q_R} = \left(\frac{T_o}{T}\right)^{1.5} .$$

For spherical top molecules (CH_4) Herzberg[5] gives

(50) $$Q_R = \sqrt{\frac{\pi}{B^3}\left(\frac{kT}{hc}\right)^3} .$$

So that

(51) $$\frac{Q_R^\circ}{Q_R} = \left(\frac{T_o}{T}\right)^{1.5} .$$

The line strength correction may now be written

(52) $$S = S_o \frac{Q_V^\circ}{Q_V}\left(\frac{T_o}{T}\right)^{BX} e^{\frac{E^\ell}{k}\left(\frac{T-T_o}{TT_o}\right)} \frac{\left(1 - e^{-\frac{h\nu_o}{kT}}\right)}{\left(1 - e^{-\frac{h\nu_o}{kT_o}}\right)}$$

where BX is either 1.0 or 1.5 depending on the molecule.

There are three effects which contribute to the line shape factor $g(\nu-\nu_0)$. The first of these is called natural broadening and results from the smearing of energy levels due to the Heisenberg uncertainty principle since the energy states have a finite lifetime. At temperatures and pressures normally occuring in the atmosphere this effect is negligible compared to other mechanisms and will not be considered further.

The second effect is called Doppler broadening and is caused by the rapid movement of the molecules while they are emitting or absorbing. The line shape factor due to Doppler broadening is given by[6]

$$(53) \qquad g(\nu-\nu_0) = \frac{1}{\alpha_D}\left(\frac{\ell n 2}{\pi}\right)^{1/2} e^{-[\ell n 2(\nu-\nu_0)^2/\alpha_D^2]}$$

where α_D is the Doppler half-width defined as half the width of the $g(\nu-\nu_0)$ versus ν curve at half the maximum amplitude. α_D is given by

$$(54) \qquad \alpha_D = \nu_0 \left(\frac{2kT}{mc^2}\ \ell n 2\right)^{1/2}$$

where ν_0 is the center frequency of the line, k is Boltzmann's constant, T is temperature in degrees Kelvin, m is the molecular mass, and c is the speed of light. For convenience of calculation this may be rewritten

$$(55) \qquad \alpha_D = 3.5812 \times 10^{-7}\left(\frac{T}{M}\right)^{1/2} \nu_0$$

where M is the molecular weight.

The third effect is caused by collisions between rapidly moving molecules in the absorbing medium and is called collision-broadening. This is the predominant effect at pressures higher than 50 to 100 torr. For frequencies near ν_0 the Lorentz line shape[7] gives a reasonable representation of the line shape factor $g(\nu-\nu_0)$.

$$(56) \qquad g(\nu-\nu_0) = \frac{1}{\pi}\ \frac{\alpha_L}{(\nu-\nu_0)^2 + \alpha_L^2} \ .$$

Here α_L is the Lorentz half-width defined as half the width of the $g(\nu-\nu_0)$ versus ν curve at one half maximum amplitude.

The AFCRL line compilation[3] gives for each line, the Lorentz half-width at 296°K and 1 atmosphere total pressure. For calculations at other temperatures and pressures the half-width must be modified. The form of the modification may be determined from a consideration of the Lorentz half-width given by kinetic theory[8]

$$(57) \qquad \alpha_L = \frac{F}{2\pi} = \frac{1}{4\pi} \sum_i N_i (D_{a,i})^2 \left[2\pi\, kT \left(\frac{1}{m_a} + \frac{1}{m_i} \right) \right]^{1/2}$$

where F is the collision frequency, N_i is the number of molecules of the ith type per unit volume, $D_{a,i}$ is the sum of the optical collision diameters of the absorbing molecule and a molecule of the ith type, k is Boltzmann's constant, T is the temperature in degrees K, m_a is the mass of the absorbing molecule, and m_i is the mass of a molecule of the ith type.

For a binary mixture of an absorbing gas a and a broadening gas b, Eq. (57) reduces to

$$(58) \qquad \alpha_L = \frac{1}{4\pi} \left\{ N_a (D_{a,a})^2 \left[2\pi kT \left(\frac{2}{m_a} \right) \right]^{1/2} + N_b (D_{a,b})^2 \left[2\pi kT \left(\frac{m_a + m_b}{m_a m_b} \right) \right]^{1/2} \right\}$$

or

$$(58a) \qquad \alpha_L = \left(\frac{kT}{8\pi} \right)^{1/2} \left[N_a (D_{a,a})^2 \left(\frac{2}{m_a} \right)^{1/2} + N_b (D_{a,b})^2 \left(\frac{m_a + m_b}{m_a m_b} \right)^{1/2} \right] .$$

Now define C_{aa}, C_{ab}, and B as follows

$$(59) \qquad C_{aa} = (D_{a,a})^2 \left(\frac{2}{m_a} \right)^{1/2}$$

$$(60) \qquad C_{ab} = (D_{a,b})^2 \left(\frac{m_a + m_b}{m_a m_b} \right)^{1/2}$$

(61) $$B = \frac{C_{aa}}{C_{ab}} \quad .$$

From the gas law the partial pressure of gas of the ith type is

(62) $$P_i = N_i \, kT \quad .$$

Using Eqs. (59), (60), and (62) Eq. (58a) becomes

(63) $$\alpha_L = \left(\frac{1}{8\pi \, kT}\right)^{1/2} [P_a \, C_{aa} + P_b \, C_{ab}] \quad .$$

Substituting B from Eq. (61) into Eq. (63) yields

(64) $$\alpha_L = \left(\frac{1}{8\pi \, kT}\right)^{1/2} C_{ab} \, [P_a \, B + P_b] \quad .$$

The total pressure P is $P_a + P_b$ so Eq. (64) may be rewritten

(65) $$\alpha_L = \left(\frac{1}{8\pi \, kT}\right)^{1/2} C_{ab} \, [P + P_a(b-1)]$$

or

(66) $$\alpha_L = \left(\frac{1}{8\pi \, kT}\right)^{1/2} C_{ab} \, P_e$$

where the equivalent pressure P_e may be defined

(67) $$P_e = P + P_a(B-1) \quad .$$

The modification to the Lorentz half-width α_{LO} given in the AFCRL line compilation for different temperature and pressure is then

(68) $$\alpha_L = \alpha_{LO} \left(\frac{P_e}{P_o}\right) \left(\frac{T_o}{T}\right)^{CX} \quad ,$$

where P_0 is one atmosphere and T_0 is 296°K. The exponent on T_0/T is given as CX rather than 1/2 since it has been determined experimentally that CX is actually about .62 for H_2O [9] and .58 for CO_2. The value of .58 for CO_2 is quoted by Deutschman and Calfee [10] as a private communication from Benedict.

B is called the self-broadening coefficient and represents the ratio of the effect on the half-width of collisions of absorbing molecules with each other to the effect of collisions between absorbing and non-absorbing molecules. B is usually defined with respect to nitrogen as the broadening gas since nitrogen is the major constituent of the atmosphere, and is not generally an infrared absorber.

Another situation of interest in this study is that of triple mixtures of an absorbing gas a and two non-absorbing gases b and nitrogen. For this situation Eq. (57) becomes

$$(69) \qquad \alpha_L = \frac{1}{4\pi}\left[N_a(D_{a,a})^2\left[2\pi\ kT\left(\frac{2}{m_a}\right)\right]^{1/2} + N_b(D_{a,b})^2\left[2\pi\ kT\left(\frac{m_a+m_b}{m_a m_b}\right)\right]^{1/2} + N_{N_2}(D_{a,N_2})^2\left[2\pi\ kT\left(\frac{m_a+m_{N_2}}{m_a m_{N_2}}\right)\right]^{1/2}\right] .$$

Now define

$$(70) \qquad C_{aa} = (D_{a,a})^2\left(\frac{2}{m_a}\right)^{1/2}$$

$$(71) \qquad C_{ab} = (D_{a,b})^2\left(\frac{m_b+m_a}{m_b m_a}\right)^{1/2}$$

$$(72) \qquad C_{a\,N_2} = (D_{a,N_2})^2\left(\frac{m_a+m_{N_2}}{m_a m_{N_2}}\right)^{1/2} .$$

Using Eqs. (70), (71), (72) and (62), Eq. (69) becomes

$$(73) \qquad \alpha_L = \left(\frac{1}{8\pi\ kT}\right)^{1/2} [P_a\ C_{aa} + P_b\ C_{ab} + P_{N_2}\ C_{aN_2} \quad .$$

Now B will be defined as before as the self-broadening coefficient of a with respect to N_2.

$$(74) \qquad B = \frac{C_{aa}}{C_{aN_2}} \quad .$$

For a broadening gas other than nitrogen a foreign broadening coefficient F_i is defined

$$(75) \qquad F_i = \frac{C_{ai}}{C_{aN_2}} \quad .$$

Using Eqs. (74) and (75), Eq. (73) becomes

$$(76) \qquad \alpha_L = \left(\frac{1}{8\pi\ kT}\right)^{1/2} C_{aN_2}\ [P_a\ B + P_b\ F_b + P_{N_2}]$$

or

$$(77) \qquad \alpha_L = \left(\frac{1}{8\pi\ kT}\right)^{1/2} C_{aN_2}\ P_e$$

where here P_e is

$$(78) \qquad P_e = P_a\ B + P_b\ F_b + P_{N_2} \quad .$$

Note that in the above discussion $D_{a,i}$, the sums of the optical collision diameters was assumed to be independent of temperature, pressure and frequency. This leads to the expectation that the half-width is the same for all lines in a vibration-rotation band and that the half-width depends on the temperature as $(1/T)^{1/2}$. In fact the half-width varies from transition to transition as do B and F_i and temperature dependence is not always $(1/T)^{1/2}$. Rice[11] gives a good discussion of the complexity of the determination of the Lorentz half-width and a discussion of other

derivations of the Lorentz half-width. For the purposes of the calculations used in this investigation the above theory will be assumed adequate.

At frequencies removed from line center, the Lorentz line shape does not in general give an accurate representation of the true line shape. Long, et al[12] found that water vapor window absorption between 5 and 6 microns could be more accurately predicted by a line shape having more absorption in the wings than the Lorentz profile. Also Benedict, et al[13] found that for the fundamental band of CO the absorption in the wings of lines was less than predicted by the Lorentz shape.

At pressures below about 0.5 torr the line shape is dominated by Doppler broadening, and at pressures greater than about 75 torr it is dominated by collision broadening. Between 0.5 torr and 75 torr both collision broadening and Doppler broadening are important. In this pressure range a line shape called the Voigt profile is used which reduces to the Doppler profile at low pressures and the Lorentz profile at high pressures. The line shape factor for the Voigt profile is given by[14]

$$(79) \qquad g(\nu-\nu_o) = \frac{\alpha_L}{\pi^{3/2}} \int_{-\infty}^{\infty} \frac{e^{-t^2}\, dt}{\alpha_L^2 + \left[\nu-\nu_c - \frac{\alpha_D\, t}{(\ell n 2)^{1/2}}\right]^2}$$

where α_D is the Doppler half-width as in Eq. (53) and α_L is the Lorentz half-width as in Eq. (56). A Fortran program for the evaluation of Eq. (79) has been made available by Charles Young [15]

B. Continuum Absorption

Continuum absorption in the DF laser region from 3.6 to 4 microns arises from two sources. One is water vapor absorption which is thought to be caused by the far wings of the strong water bands at 2.7 and 6.3 microns. The other is pressure induced nitrogen absorption. Burch[4] has investigated both these effects experimentally using a black-body source and a conventional spectrometer. Burch's results have been used in this study to help predict absorption at each of the DF laser lines.

In Burch's work the absorption coefficient has units molecules^{-1}-cm^2 and will be called k' in the following discussion. The absorber amount is then expressed in molecules-cm^2 and will

be called u here. For a given sample u may be determined from the partial pressures of the absorbing gas, the length of the sample and the temperature as follows

$$(80) \qquad u(\text{molecules/cm}^2) = 2.69 \times 10^{19}\ p(\text{atm})\ L(\text{cm})\ (273/T)$$

where p is the pressure of the absorbing gas in atmospheres, L is the path length in cm and T is the temperature in degrees Kelvin. The transmittance is then

$$(81) \qquad T = e^{-k'u} \quad .$$

Assuming for the moment that the Lorentz line shape is valid in the far wings of lines, k' for a single line is given by Eqs. (27) and (56)

$$(82) \qquad k' = \frac{S}{\pi} \frac{\alpha_L}{(\nu-\nu_o)^2 + \alpha_L^2} \qquad (\text{mol-cm}^{-2})^{-1}.$$

For $\nu-\nu_o >> \alpha_L$ this becomes

$$(83) \qquad k' = \frac{S\ \alpha_L}{\pi(\nu-\nu_o)^2} \qquad (\text{mol-cm}^{-2})^{-1}$$

where α_L is from Eq. (63)

$$(84) \qquad \alpha_L = \left(\frac{1}{8\pi\ kT}\right)^{1/2} [P_a\ C_{aa} + P_b\ C_{ab}] \quad .$$

Since α_L is proportional to pressure, k' is also proportional to pressure. It follows then that for continuum absorption due to far wings k' would be expected to have the form

$$(85) \qquad k' = C_S p_S + C_f\ p_f \qquad (\text{mol-cm}^{-2})^{-1} \ .$$

In order to obtain enough absorption to measure the water continuum accurately Burch was forced to use higher temperatures so that the water vapor pressure could be increased substantially

over that normally occurring in the atmosphere. He measured the water continuum between 2400 cm^{-1} and 2800 cm^{-1} by tuning his spectrometer to points in the spectrum which appeared to be free of local water lines and measuring the transmittance. He found that the absorption coefficient k' was proportional to pressure as indicated by Eq. (85). This incidentally does not indicate that the Lorentz line shape is valid in the far wings, but rather that the valid line shape has the same pressure dependence as the Lorentz shape.

Burch measured the continuum absorption of pure water samples at three temperatures and found that C_S is proportional to A exp (B/T) where A and B vary with frequency. Using this relationship Burch deduced a curve for the water vapor continuum at 296K from the data at higher temperatures. His data are reproduced in Fig. 3.

He measured C_{N_2} at one higher temperature and found that

$$\frac{C_{N_2}}{C_S} = 0.12 \pm 0.03. \tag{86}$$

Unfortunately C_{N_2} cannot be measured at normal atmospheric pressure and temperature since the absorption is too small so it is assumed that C_{N_2} and C_S have the same ratio at 296K as at the higher temperature.

It is useful to represent the extinction coefficient in units km^{-1}. From Eqs. (80) and (85)

$$k'u = (C_S\, p_S(atm) + C_f\, p_f(atm))\, 2.69 \times 10^{19}\, P_S(atm) L(cm) \times (273/T) \quad . \tag{87}$$

Rearranging gives k in units cm^{-1}

$$k = \frac{k'u}{L} = 7.34 \times 10^{21} \frac{p_S}{T} (C_S\, p_S + C_f\, p_f)\ cm^{-1} \quad . \tag{88}$$

The extinction coefficient k in km^{-1} is then

$$k = 7.34 \times 10^{26} \frac{p_S}{T} (C_S\, p_S + C_f\, p_f)\ km^{-1} \quad . \tag{89}$$

For the water continuum data at 296K, k can be written

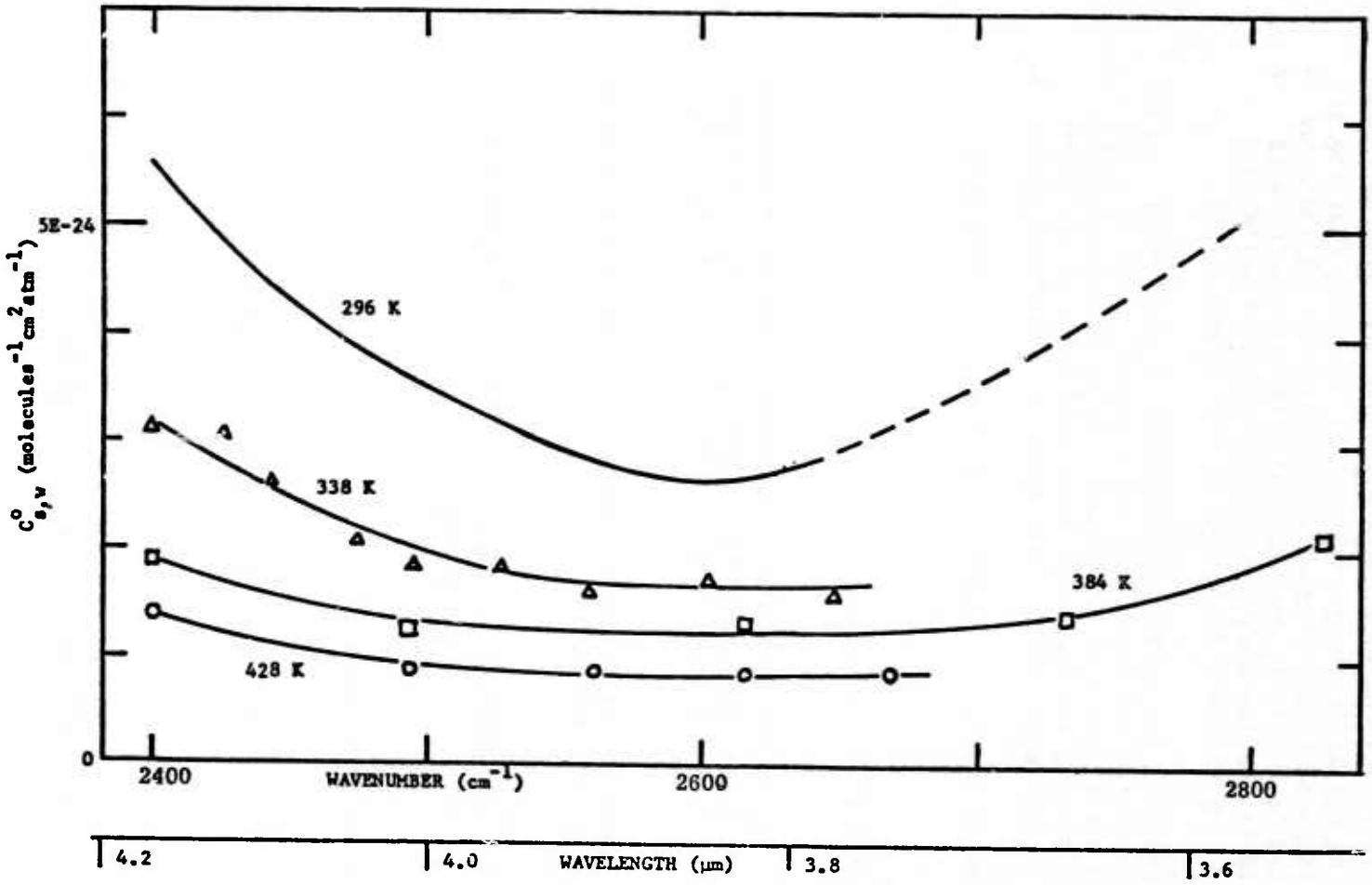

Fig. 3. Spectral plots of C_s° between 2400 and 2820 cm^{-1} for H_2O at four temperatures (Burch).

(90) $$k = 2.48 \times 10^{24}\ p_S(C_S\ p_S + 0.12\ C_S p_N)\ km^{-1}$$

or

(91) $$k = \frac{2.48 \times 10^{24}}{8.33}\ p_S C_S\ \ (8.33\ p_S + p_N)\ km^{-1}\ .$$

The total pressure P_T is P_S plus P_N so Eq. (91) may be rewritten

(92) $$k = 2.98 \times 10^{23}\ C_S p_S\ \ (7.33\ P_S + P_T) km^{-1}.$$

Figure 4 was derived by evaluating Eq. (92) at 14.26 torr H_2O and one atmosphere total pressure with C_S taken from Fig. 3.

The nitrogen continuum absorption arises from a pressure-induced band near 2200 cm^{-1}. A number of workers have investigated this absorption between 2400 cm^{-1} and 2640 cm^{-1}. Burch[4] has determined from his measurements and those of others that $(-\ln T)$ is proportional to p^2L just as for the pure water vapor continuum. Figure 5 is adapted from Burch and shows the nitrogen continuum between 2400 cm^{-1} and 2650 cm^{-1} at 296K.

C. Description of Calculation Programs

The basic quantity calculated by the programs is

(93) $$(-\ell n\ T) = k'u\ ,$$

where k' is in units $(mol - cm^{-2})^{-1}$ and u is in units $mol - cm^{-2}$. There are two different equations used to calculate k' depending on the total pressure. For pressures above about 75 torr the Lorentz profile is used:

(94) $$k' = \frac{S}{\pi}\ \frac{\alpha_L}{(\nu-\nu_0)^2 + \alpha_L^{\ 2}}\ \ \ (mol\text{-}cm^{-2})^{-1},$$

For lower pressures the Voigt profile is used.

(95) $$k' = \frac{S\alpha_L}{\pi^{3/2}}\ \int_{-\infty}^{\infty}\ \frac{e^{-t^2}\ dt}{\alpha_L^{\ 2} + \left[\nu-\nu_0\ \ \frac{\alpha_D t}{(\ell n 2)^{1/2}}\right]^2}\ .$$

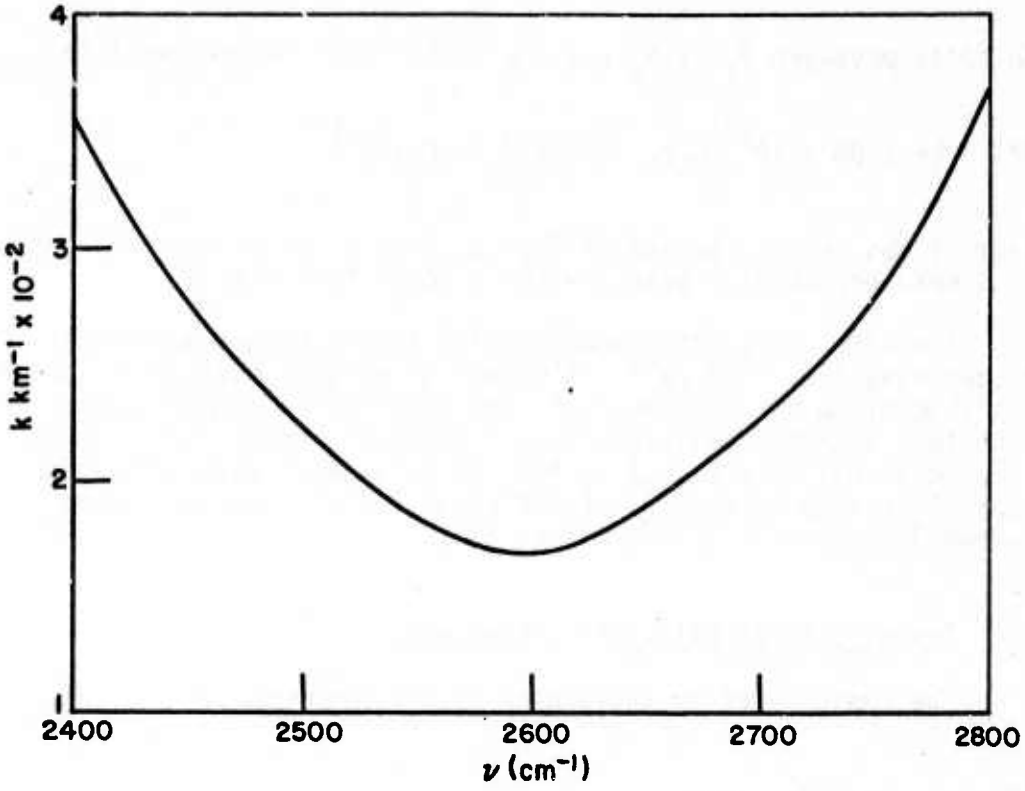

Fig. 4. Water vapor continuum absorption coefficient adapted from Burch for P_{H_2O}=14.2 torr and T=296K at 760 torr total pressure.

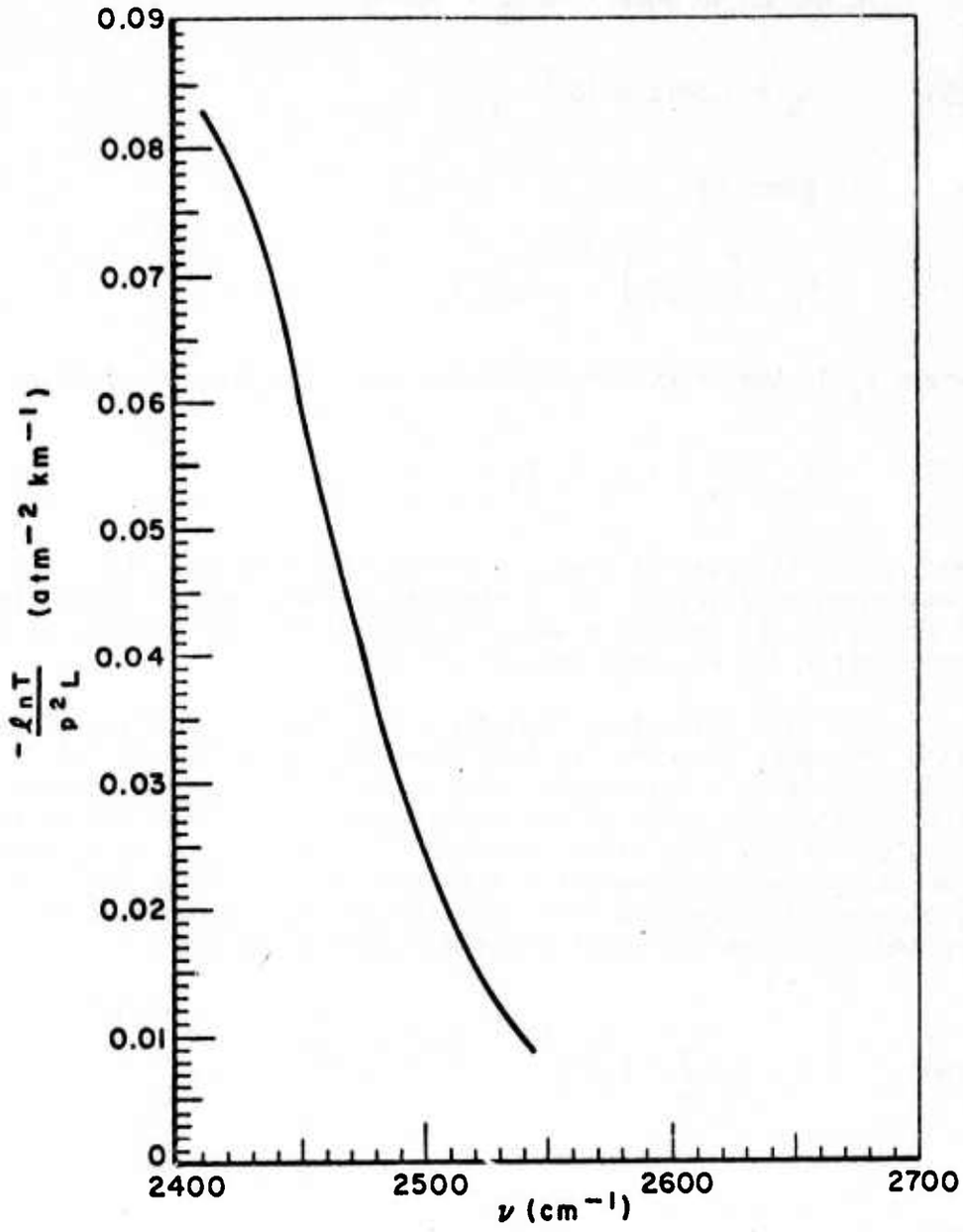

Fig. 5. Nitrogen absorption from Burch, T=296K.

In the above equations α_D is given by

$$\alpha_D = 3.5812 \times 10^{-7} \left(\frac{T}{M}\right)^{1/2} \nu_o \tag{96}$$

and α_L is given by

$$\alpha_L = \left(\frac{1}{8\pi\, kT}\right)^{1/2} C_{aN_2} P_e \tag{97}$$

where P_e is the effective broadening pressure given in general by

$$P_e = P_a B + \Sigma_i P_i F_i \quad . \tag{98}$$

Here P_a is the partial pressure of the absorbing gas, B is the self-broadening coefficient, P_i is the partial pressure of broadening gas i and F_i is the foreign broadening coefficient for broadening gas i. Note that F for nitrogen is defined to be 1.

For each absorption line the AFCRL line compilation gives the line frequency in cm^{-1}, the line strength in $(mol\text{-}cm^{-2})^{-1}\text{-}cm^{-1}$ at 296K, the Lorentz half-width in $cm^{-1}\text{-}atm^{-1}$ at 296K, the energy of the lower energy state of the transition in cm^{-1}, the energy levels involved in the transition, and the isotope and type of molecule. For use at temperatures other than 296K and pressures different from one atmosphere, the line strength and half-width must be corrected using the following equations derived earlier.

$$S = S_o \frac{Q_V^\circ}{Q_V} \left(\frac{T_o}{T}\right)^{BX} e^{\frac{E^\ell}{k}\left(\frac{T-T_o}{TT_o}\right)} \left\{ \frac{\left(1 - e^{-\frac{h\nu_o}{kT}}\right)}{\left(1 - e^{-\frac{h\nu_o}{kT_o}}\right)} \right\} \tag{99}$$

and

$$\alpha_L = \alpha_{LO} \left(\frac{P_e}{P_o}\right) \left(\frac{T_o}{T}\right)^{CX} \quad . \tag{100}$$

The programs described here have been used exclusively for frequencies greater than 800 cm^{-1} and for temperatures between 195K and 400K. For those conditions the term in brackets in Eq. (99) is very nearly one and may be safely ignored. Also the ratio of vibrational partition functions Q_V°/Q_V has been taken to be nearly one and therefore ignored although it could be included if uncertainties in line-shape and half-width were reduced to the point

where errors in Q_V°/Q_V were significant. Assuming 296K for T_o, 1 atm for P_o and using $k = .6951\ cm^{-1}/^\circ K$ the strength and half-width corrections become

$$(101) \qquad S = S_o \left(\frac{296}{T}\right)^{BX} e^{\frac{E_\ell}{.6951}\left(\frac{T-296}{296T}\right)}$$

and

$$(102) \qquad \alpha_L = \alpha_{LO}\ P_e \left(\frac{T_o}{296}\right)^{CX} .$$

The assumed values for the self-broadening coefficient B, BX, and CX are given for each molecule in Table 2.

TABLE 2

VALUES USED FOR B, BX, AND CX
IN ABSORPTION CALCULATIONS

	B	BX	CX
N_2O	1.24	1.0	.5
CH_4	1.3	1.5	.5
H_2O	5.0	1.5	.62
CO_2	1.3	1.0	.58
O_3	1.0	1.5	.5
CO	1.02	1.0	.5

Equation (94) gives the absorption coefficient k' for one absorption line. At any frequency there might be several lines contributing to the absorption. k' would then be given by the summation of all the individual line contributions.

$$(103) \qquad k' = \frac{1}{\pi} \sum_i \frac{S_i\ \alpha_{L_i}}{(\nu-\nu_i)^2 + \alpha_{L_i}^2} \quad (mol\text{-}cm^{-2})^{-1} .$$

The first program to be described calculates and plots k in km^{-1} versus wavenumber. Note that k in km^{-1} is k'u where u is evaluated using Eq. (80) with the path length L being one kilometer. Input parameters are the number of absorbers to be considered; the number of plots to be made; the beginning wavenumber of the first

plot; the number of wavenumbers per plot; the total pressure in torr; the temperature; the I.D. number, desired isotope, partial pressure in torr, and broadening coefficient for each absorber type; and descriptive information which is written on the plots. The user may specify a continuum of the form $k_c(\nu) = A_0 + A_1\nu + A_2\nu^2$ which is added to the calculated $k(\nu)$ at each point on the plot. The user may also specify a set of frequencies corresponding to laser lines or just frequencies of special interest, and the program will draw a vertical line on the plot at each specified frequency.

Figure 6 shows an example of the interactive (teletype) printout which occurs during execution of the program with the information provided by the operator underlined. The program then calculates u for each absorber from the partial pressure and temperature using Eq. (78) and P_e for each absorber from the partial pressure, total pressure and self-broadening coefficient. Data is read from the AFCRL tape as required and the strength and half-width are corrected for temperature and pressure using Eqs. (101) and (102). There is a parameter SLOW in the program which may be set to ignore all lines with strength less than SLOW and thus speed the calculation.

The heart of the program is the subroutine which calculates k'u. It is adapted from one written by Deutschman and Calfee[10]. At any point ν the subroutine considers contributions from absorption lines within BOUND of ν in either direction. Recognizing the uncertainty in the Lorentz line shape at frequencies far from line center, BOUND is usually set at 20 cm^{-1} or 25 cm^{-1}. For each separate absorption line in the range $\nu \pm$ BOUND the subroutine calculates the contribution using either Eq. (94) (Lorentz profile) or (95) (Voigt profile) and the appropriate u for the absorber being considered. Whether the Lorentz or Voigt profile is used is determined by the ratio α_L/α_D for each particular absorption line. If α_L/α_D is greater than five the Lorentz profile is used, otherwise the Voigt profile is used. The contributions from each absorption line are then added together to get the total k'u for local line absorption. If the user has specified a continuum, it is evaluated at this time at the frequency ν and added to k'u. This procedure is repeated for each point on the plot.

The program plots the absorption coefficient in km^{-1} on a logarithmic scale with the scale limits calculated automatically for the most effective presentation.

Another version of this program plots the transmittance rather than the absorption coefficient. It would seem however that this is less desirable since by improper choice of path length and absorber amount it would be possible to calculate a spectrum showing total absorption or total transmittance, whereas the absorption coefficient plot will always show the spectral structure no matter what absorber amount is specified.

```
 DATE 08/17/75  TIME 19:54:06

 ENTER THE NUMBER OF ABSORBERS AND THE NUMBER OF PLOTS1,1

 ENTER THE BEGINNING WAVENUMBER
 AND THE WAVENUMBER/PLOT.       2650,12

 ENTER THE TOTAL PRESSURE IN TORR.  760

 ENTER THE TEMPERATURE IN DEGREES F.69.8

 ENTER ID NUMBER, PARTIAL PRESSURE, AND BROADENING
 COEFFICIENT FOR EACH ABSORBER.

 ENTER ID NUMBER OF ABSORBER NO.1
 1=H20 2=C02 3=03 4=N20 5=CO 6=CH4 7=02
1

 ENTER NUMBER OF DESIRED ISOTOPE.
 IF ALL ISOTOPES ARE DESIRED ENTER 0.  162

 ENTER THE ABSORBER AMOUNT IN TORR. 14.26

 ENTER THE SELF-BROADENING COEFFICIENT.5

 DO YOU WISH A CONTINUUM?  NO

ENTER ABSORBER DESCRIPTION INFORMATION ON TWO LINES
 OF UP TO 42 CHARACTERS EACH.  THE FIRST LINE WILL
 APPEAR IMMEDIATELY TO THE RIGHT OF ABSORBERS: ,
 THE SECOND LINE WILL APPEAR TO THE RIGHT OF
 AMOUNT(TORR): AND IMMEDIATELY BELOW THE FIRST LINE.
HDO
14.26

 WHERE IS THE ABSORPTION LINE DATA?
 ENTER .MT0 OR .MT1  .MT1

 ENTER TAPE START POINT: FILE NUMBER AND RECORD NUMBER4,850

 WHICH TAPE UNIT WILL PLOT DATA BE WRITTEN ON?
 ENTER .MT0 OR .MT1  .MT0

 ENTER NUMBER OF FIRST FILE TO BE WRITTEN.216

 WHERE IS THE LASER LINE DATA?
 ENTER FILE AND USER NAME ON TWO LINES.
NDFLN
3271A

 DO YOU WISH TO RUN THIS PROGRAM IN BACKGROUND? YES
```

Fig. 6. Example run of spectra plotting program.

The program which calculates single frequency absorption is very similar with a few exceptions. The absorption coefficient is calculated for only one absorber at a time, however calculations may be made for a number of absorber pressures and frequencies at the same time.

The other main difference is that the Lorentz line shape is not used, but rather a modification of the Lorentz line shape suggested by Trusty[12]. The alternate shape has the form

$$k = \frac{C(\nu,\eta)S\ \alpha_L}{\pi\left[(\nu-\nu_o)^2 + \alpha_L^2\right]} \qquad 0 \le |\nu-\nu_o| \le \nu_m \tag{104}$$

$$k = \frac{C(\nu,\eta)S\ \alpha_L}{\pi\left[\nu_m^2 + \alpha_L^2\right]} \cdot \frac{\nu_m^{\eta}}{(\nu-\nu_o)^{\eta}} \qquad |\nu-\nu_o| \ge \nu_m \quad .$$

where

$$C(\nu_m,\eta) = \frac{S}{2\left[\int_0^{\nu_m} k\,d\nu + \int_{\nu_m}^{\infty} k\,d\nu\right]} \quad . \tag{105}$$

is added so that the line strength has the usual definition of the integrated absorption coefficient over the entire line. The integrations in Eq. (105) may be performed directly to give for $C(\nu_m,\eta)$

$$C(\nu_m,\eta) = \frac{\pi}{2\left[\mathrm{Tan}^{-1}(\nu_m) + \nu_m/((\nu_m^2+1)\ (\eta-1))\right]} \quad . \tag{106}$$

The modification location ν_m and modifier power η are specified by the user. For $\nu_m \ge 30\,\alpha_L$ and $\eta = 2$ the modified shape reduces to the Lorentz shape. For $\eta < 2$ the alternate line shape has more wing absorption than the Lorentz shape and for $\eta > 2$ the wing absorbtion is less.

Figure 7 shows an example of the interactive (teletype) printout which occurs during execution of the program with the information provided by the operator underlined.

Appendix B gives listings of the programs and a somewhat more detailed discussion of the mechanics of the programs.

```
 COMMANDS ARE
 PRESS, ABS, TEMP, NALFA, ETA, LINES, BROAD, DATA, EXE, END, SVE, STORE,
 VAR.

 DATE 08/17/78  TIME 19:48:22

 ENTER THE TOTAL PRESSURE IN TORR.  760

 ENTER THE TEMP IN DEG F.  69.8

ENTER IL NO. OF ABSORBER
 1=H2O 2=CO2 3=O3 4=N2O 5=CO 6=CH4 7=O2
1

 ENTER NUMBER OF DESIRED ISOTOPE.
 IF ALL ISOTOPES ARE DESIRED ENTER 0.  162

 HOW MANY ABSORBER PRESSURES WILL BE USED?1

 ENTER THEM ON ONE LINE, FREE FORMAT.
14.26

 ENTER THE SELF-BROADENING COEFFICIENT.5

 ENTER MODIFICATION LOCATION IN HALFWIDTHS.  30

 ENTER MODIFIER POWER.  2

 WILL CALCULATION FREQUENCIES BE READ FROM A "FILE" OR THE "TTY"? FILE

 ENTER FILE AND USER NAME ON TWO LINES.
NDFLN
3271A

 WHERE IS THE LINE DATA?
ENTER .MT0 OR .MTI
.MTI

ENTER TAPE START POINT:FILE NUMBER AND RECORD NO.  4,753

DO YOU WISH TO RUN OFF-LINE?  YES
```

Fig. 7. Example run of fixed-frequency program.

D. Calculations in the DF Laser Region

The programs described in the last section and the AFCRL line compilation were used to calculate both single frequency absorption and synthetic spectra for each laser line available from the probe laser used in this study.

Calculations were made for the AFCRL mid-latitude, sea-level, summer model[16]. The molecules considered in the calculation are H_2O, N_2O, CH_4, and CO_2. The contributions from pressure-induced N_2 absorption and water continuum absorption are obtained from Fig. 5 and Fig. 4 respectively. Parameters for the mid-latitude summer model are given in Table 3.

TABLE 3

AFCRL MID-LATITUDE SUMMER MODEL

T	=	294°K
P	=	760 torr
$P(H_2O)$	=	14.26 torr
$P(N_2O)$	=	2.13×10^{-4} torr (.28 ppm)
$P(CH_4)$	=	1.216×10^{-3} torr (1.6 ppm)
$P(CO_2)$	=	.251 torr (330 ppm)

The HDO line strengths on the AFCRL tape are scaled assuming an isotopic abundance of HDO relative to total water of 0.03%. SLOW was set at 10^{-27} for these calculations so that essentially all the absorption lines are included. BOUND was 20 cm^{-1}. B, BX, and CX used for each molecule are those given in Table 2. The DF laser frequencies used are those measured by Heath, et al[17] and are presumed accurate to ± .003 cm^{-1}.

The calculations at the individual laser frequencies are listed in Table 4. The calculations for each molecule are listed separately and then added together for the total predicted absorption. For the water contribution, the local HDO, local H_2O (excluding HDO), and H_2O continuum are tabulated separately so that the relative importance of each factor can be noted.

The synthetic spectra are presented in Figs. 8 through 35. They are vertical lines drawn on the plots to indicate laser line positions. The laser lines are identified by transition, and the major absorption lines near each laser line are identified. The water continuum and nitrogen absorption have not been included since it is slowly changing with respect to frequency and the effect would be to obscure the spectral structure.

TABLE 4

MID-LATITUOE SUMMER SEA LEVEL ABSORPTION COEFFICIENTS CALCULATED FROM AFCRL LINE DATA[3]

ν (cm^{-1})(a)	Line	N_2O (km^{-1})	CH_4 (km^{-1})	CO_2 (km^{-1})	HDO (km^{-1})	H_2O (km^{-1})	H_2O & HDO (km^{-1})	H_2O cont(b) (km^{-1})	N_2 (b) (km^{-1})	Total (km^{-1})
2419.070	3-2 P(13)	8.36E-5	1.79E-9	3.75E-4	2.64E-5	6.54E-5	9.17E-5	3.26E-2	8.1 E-2	1.14E-1
2445.356	3-2 P(12)	1.98E-3	4.26E-9	5.17E-3	2.72E-6	2.64E-5	2.90E-5	2.85E-2	6.6 E-2	1.02E-1
2471.245	3-2 P(11)	5.32E-3	1.96E-8	4.73E-5	6.07E-5	4.28E-3	4.34E-3	2.52E-2	4.6 E-2	8.09E-2
2496.721	3-2 P(10)	5.13E-4	1.17E-5	3.57E-8	3.95E-5	8.80E-4	9.20E-4	2.27E-2	2.5 E-2	4.91E-2
2500.428	2-1 P(13)	4.83E-4	2.85E-6	1.34E-8	6.43E-5	6.26E-5	1.27E-4	2.25E-2	2.5 E-2	4.81E-2
2521.769	3-2 P(9)	4.86E-4	2.69E-6	2.62E-7	1.66E-4	4.55E-5	2.12E-4	2.05E-2	1.5 E-2	3.62E-2
2527.391	2-1 P(12)	7.92E-4	1.82E-5	2.29E-7	2.89E-4	3.78E-6	2.92E-4	2.00E-2	1.4 E-2	3.51E-2
2546.375	3-2 P(8)	2.15E-2	1.11E-3	1.55E-7	1.13E-3	4.44E-5	1.18E-3	1.86E-2	8.0 E-3	5.04E-2
2553.953	2-1 P(11)	1.06E-2	7.67E-5	1.35E-7	5.07E-4	4.70E-6	5.12E-4	1.82E-2	7.1 E-3	3.65E-2
2570.522	3-2 P(7)	3.76E-2	3.20E-5	1.03E-7	4.53E-3	4.69E-5	4.58E-3	1.74E-2	5.0 E-3	6.46E-2
2580.097	2-1 P(10)	4.60E-2	2.50E-6	9.00E-8	2.65E-3	5.52E-6	2.66E-3	1.70E-2	3.6 E-3	6.93E-2
2583.486	1-0 P(13)	2.17E-2	4.88E-6	8.58E-8	3.77E-3	1.92E-5	3.79E-3	1.69E-2	3.45E-3	4.58E-2
2594.198	3-2 P(6)	2.26E-3	2.10E-5	7.46E-8	7.18E-3	3.54E-4	7.53E-3	1.68E-2	2.6 E-3	2.92E-2
2605.807	2-1 P(9)	5.02E-4	1.81E-4	6.47E-8	1.99E-2	6.75E-6	1.99E-2	1.68E-2	2.3 E-3	3.97E-2
2611.142	1-0 P(12)	8.89E-5	3.70E-6	6.08E-8	5.87E-3	2.53E-5	5.90E-3	1.70E-2	2.1 E-3	2.51E-2
2617.386	3-2 P(5)	1.11E-5	1.41E-4	5.67E-8	2.37E-3	3.98E-5	2.41E-3	1.72E-2	2.0 E-3	2.16E-2
2631.068	2-1 P(8)	4.65E-8	8.46E-4	4.90E-8	9.12E-3	4.73E-3	1.39E-2	1.78E-2	1.9 E-3	3.44E-2
2638.392	1-0 P(11)	2.04E-9	6.16E-4	4.56E-8	2.51E-1	7.63E-4	2.51E-1	1.82E-2	1.6 E-3	2.71E-1
2640.074	3-2 P(4)	5.73E-10	1.20E-4	4.48E-8	2.92E-2	4.64E-5	2.93E-2	1.83E-2		4.77E-2
2655.863	2-1 P(7)	1.11E-11	7.15E-4	3.86E-8	7.35E-2	4.42E-6	7.35E-2	1.93E-2		9.35E-2
2662.246	3-2 P(3)	1.31E-11	1.25E-5	3.65E-8	1.94E-2	3.13E-5	1.94E-2	1.98E-2		3.92E-2
2665.219	1-0 P(10)	1.42E-11	1.98E-3	3.56E-8	1.51E-2	9.80E-6	1.51E-2	2.00E-2		3.71E-2
2680.179	2-1 P(6)	2.30E-11	3.06E-4	3.14E-8	3.79E-2	2.34E-4	3.81E-2	2.12E-2		5.96E-2
2683.890	3-2 P(2)	2.64E-11	4.80E-4	3.04E-8	3.12E-3	5.66E-5	3.18E-3	2.15E-2		2.52E-2
2691.607	1-0 P(9)	3.66E-11	3.24E-3	2.86E-8	1.21E-2	3.72E-4	1.25E-2	2.20E-2		3.77E-2
2703.999	2-1 P(5)	7.12E-11	1.82E-6	2.61E-8	5.61E-3	1.12E-5	5.62E-3	2.30E-2		2.86E-2
2717.539	1-0 P(8)	9.34E-10	2.12E-6	2.36E-8	9.10E-2	7.56E-5	9.11E-2	2.41E-2		1.15E-1
2727.309	2-1 P(4)	1.60E-8	1.42E-4	2.21E-8	2.99E-2	1.27E-4	3.00E-2	2.51E-2		5.52E-2
2742.998	1-0 P(7)	4.31E-6	2.88E-4	1.99E-8	3.32E-2	4.75E-5	3.32E-2	2.69E-2		6.04E-2
2750.094	2-1 P(3)	4.13E-5	9.54E-4	1.90E-8	1.22E-2	4.66E-5	1.22E-2	2.75E-2		4.07E-2
2767.968	1-0 P(6)	1.02E-4	5.00E-3	1.70E-8	5.14E-2	6.87E-5	5.15E-2	3.08E-2		8.74E-2
2772.340	2-1 P(2)	1.05E-3	1.25E-3	1.66E-8	6.93E-1	1.04E-3	6.94E-1	3.14E-2		7.28E-1
2792.434	1-0 P(5)	8.03E-4	6.18E-4	1.48E-8	3.50E-2	1.55E-4	3.52E-2	3.50E-2		7.16E-2
2816.380	1-0 P(4)	1.16E-3	2.85E-3	1.30E-8	5.84E-2	1.60E-3	6.00E-2	4.00E-2		1.04E-1
2839.791	1-0 P(3)	3.24E-7	8.05E-4	1.15E-8	2.74E-2	2.44E-4	2.76E-2	4.50E-2		7.34E-2
2862.653	1-0 P(2)	7.60E-7	2.28E-3	1.03E-8	3.85E-2	1.59E-3	4.01E-2	5.00E-2		9.24E-2

(a) Heath, et al. [17]
(b) Burch, et al. [4]

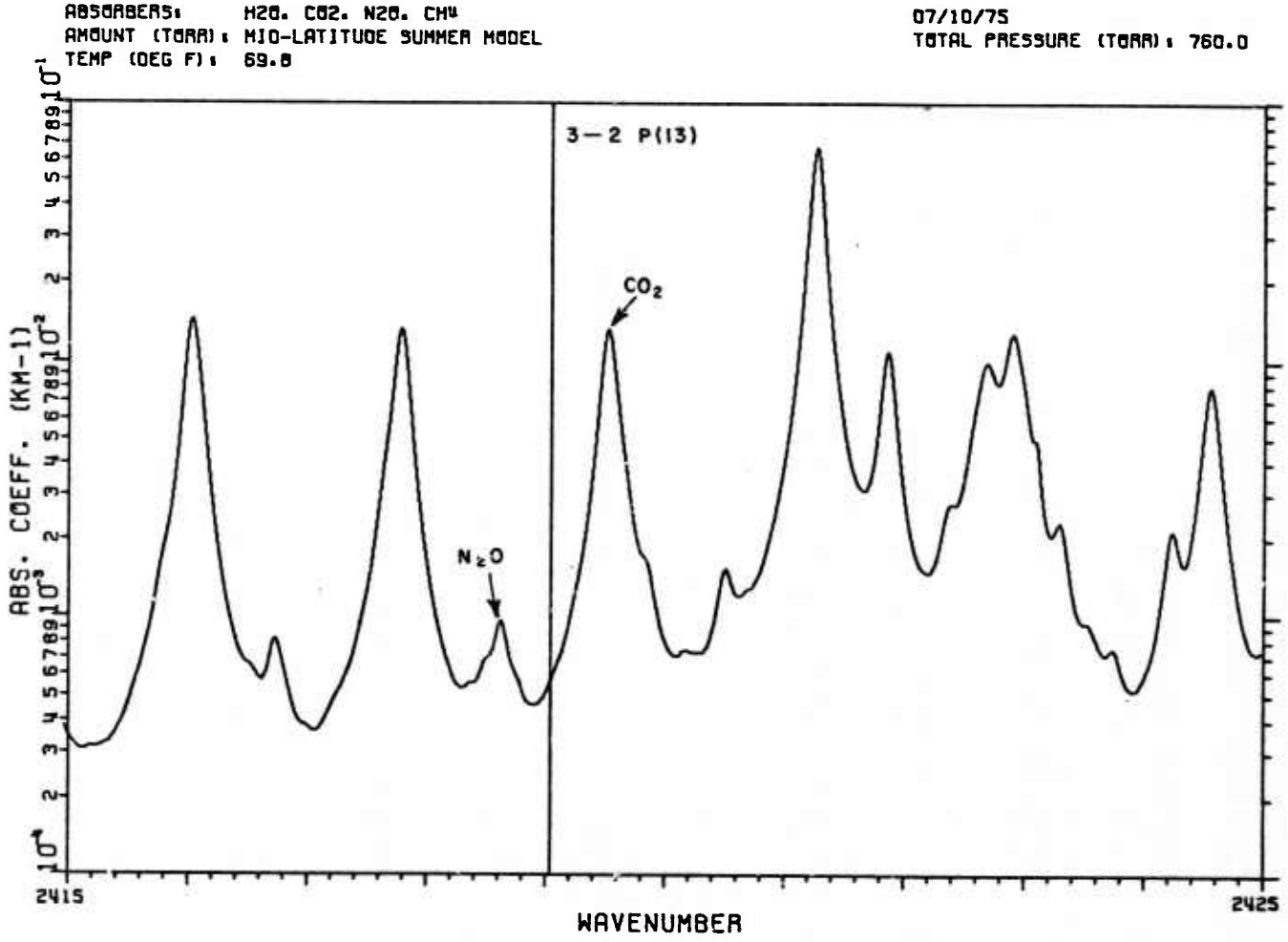

Fig. 8. Calculated spectrum near the 3-2 P(13) DF laser line.

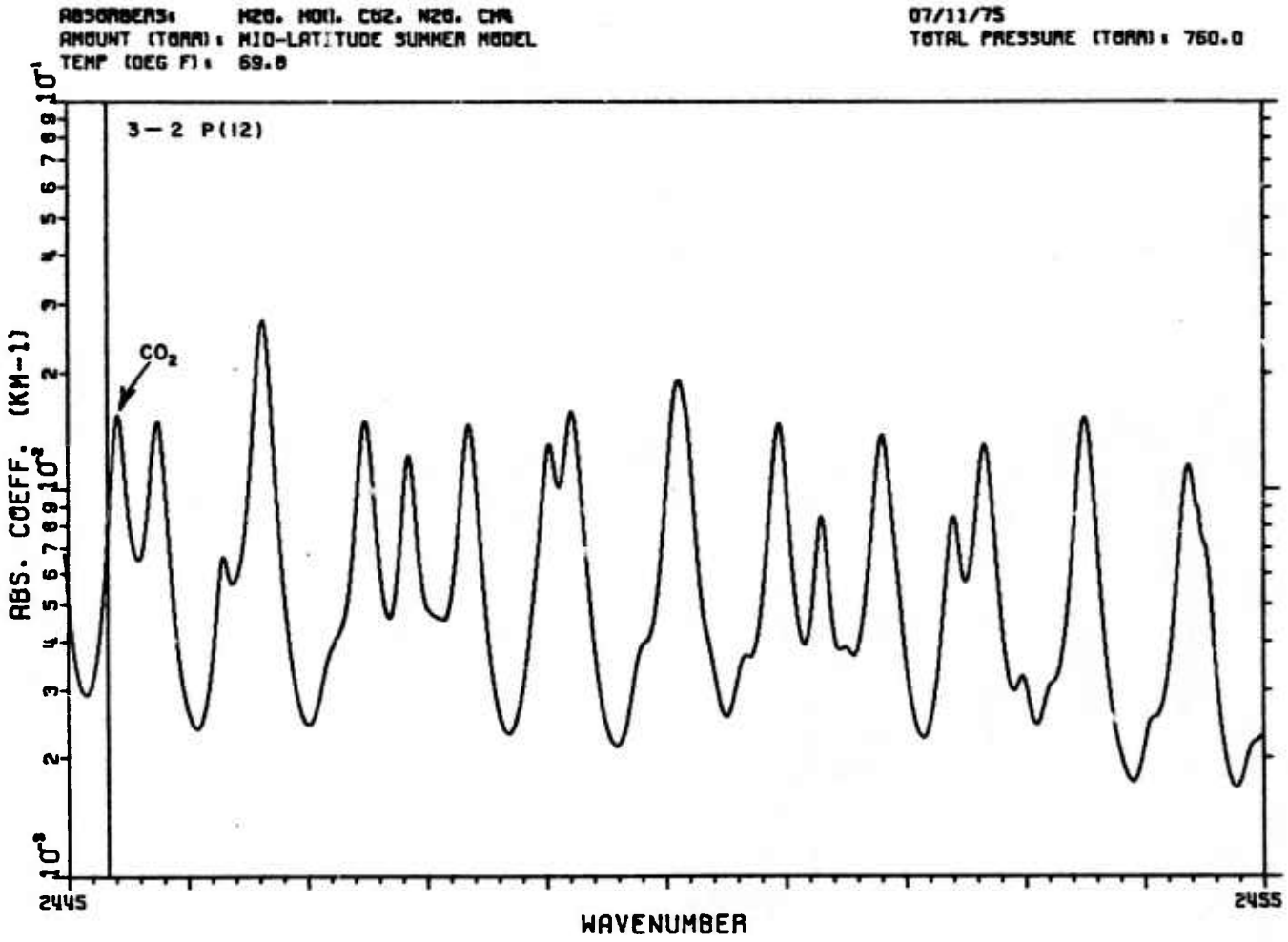

Fig. 9, Calculated spectrum near the 3-2 P(12) DF laser line.

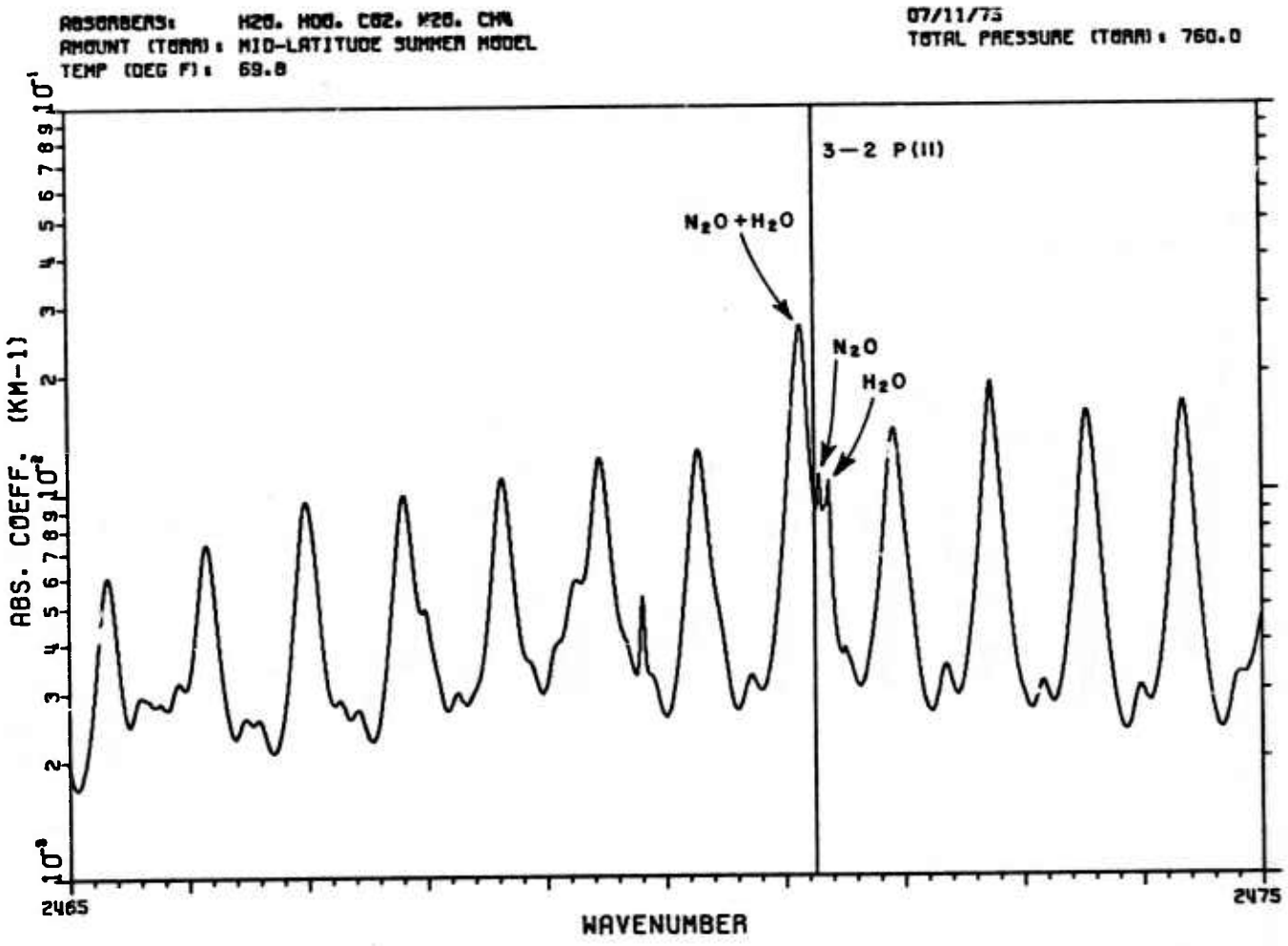

Fig. 10, Calculated spectrum near the 3-2 P(11) DF laser line.

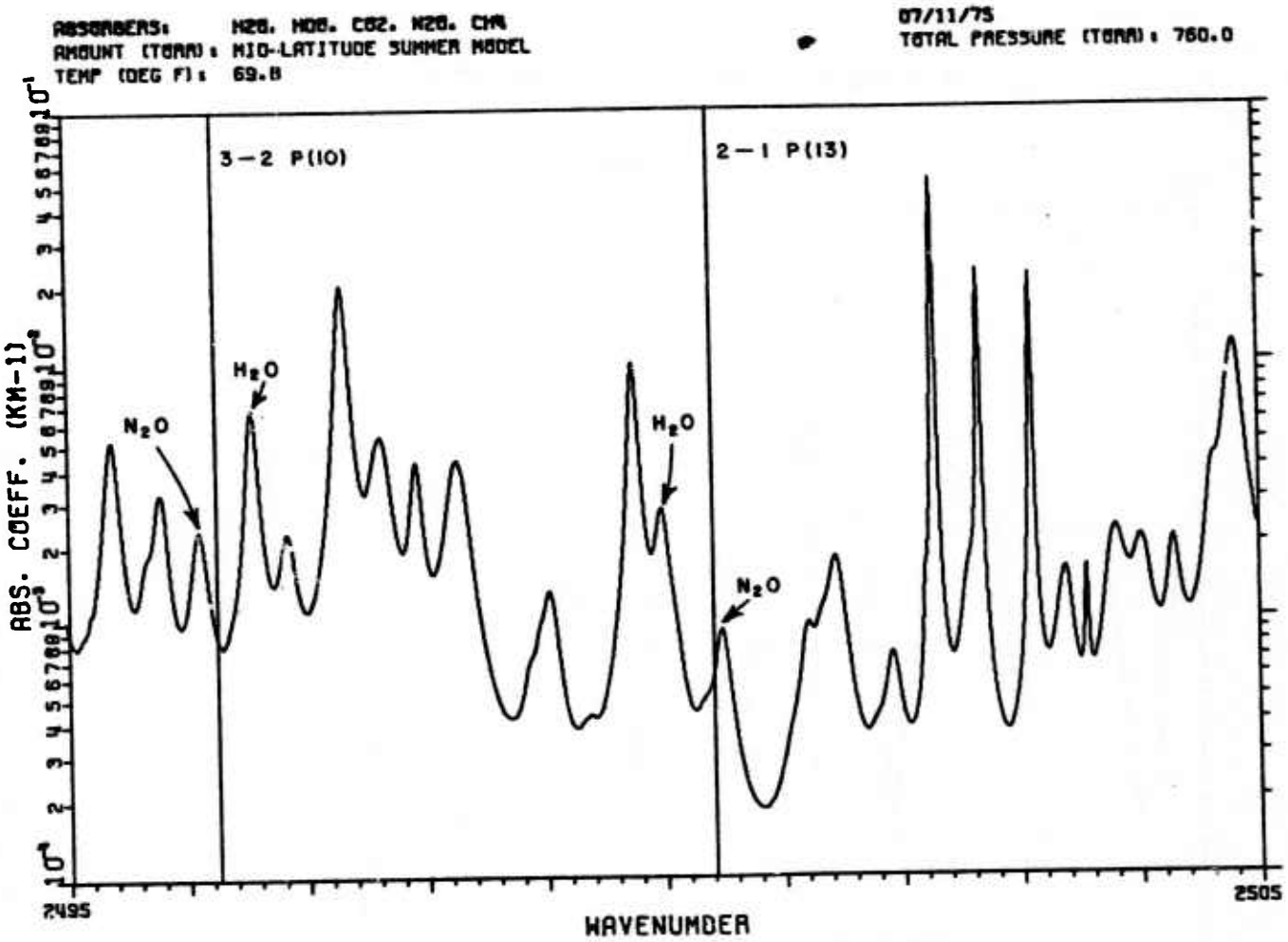

Fig. 11. Calculated spectrum near the 3-2 P(10) and 2-1 P(13) DF laser line.

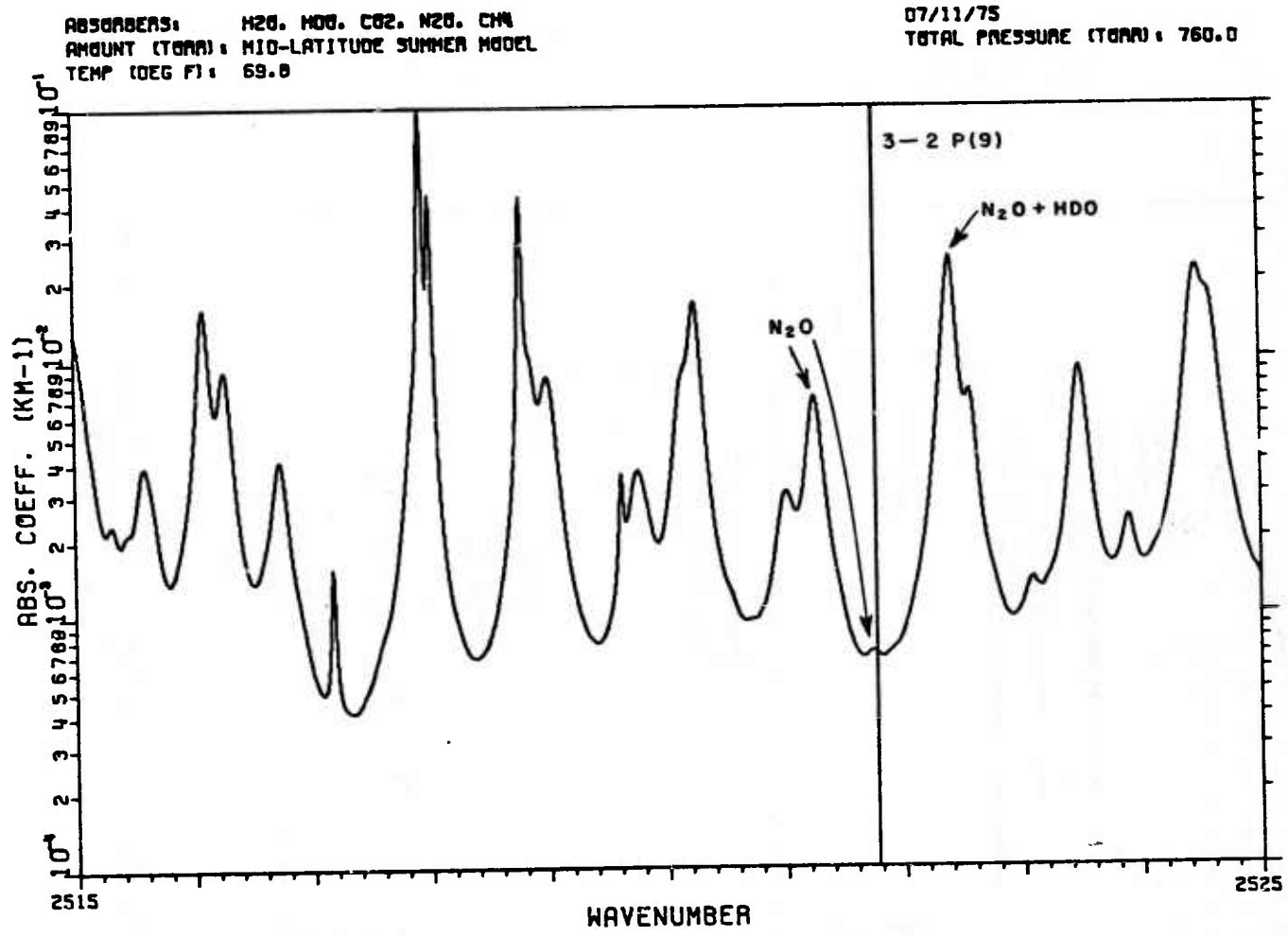

Fig. 12. Calculated spectrum near the 3-2 P(9) DF laser line.

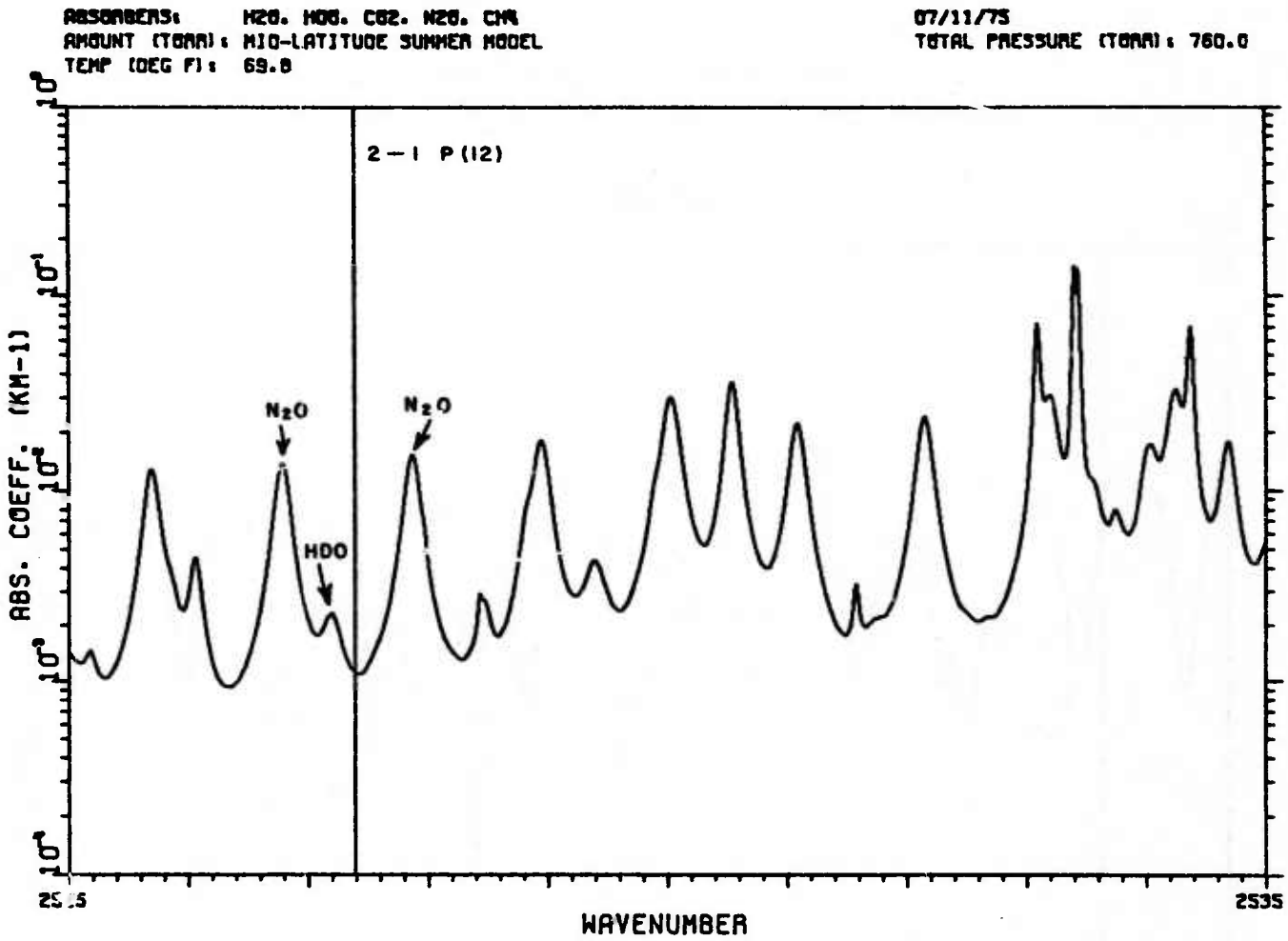

Fig. 13. Calculated spectrum near the 2-1 P(12) DF laser line.

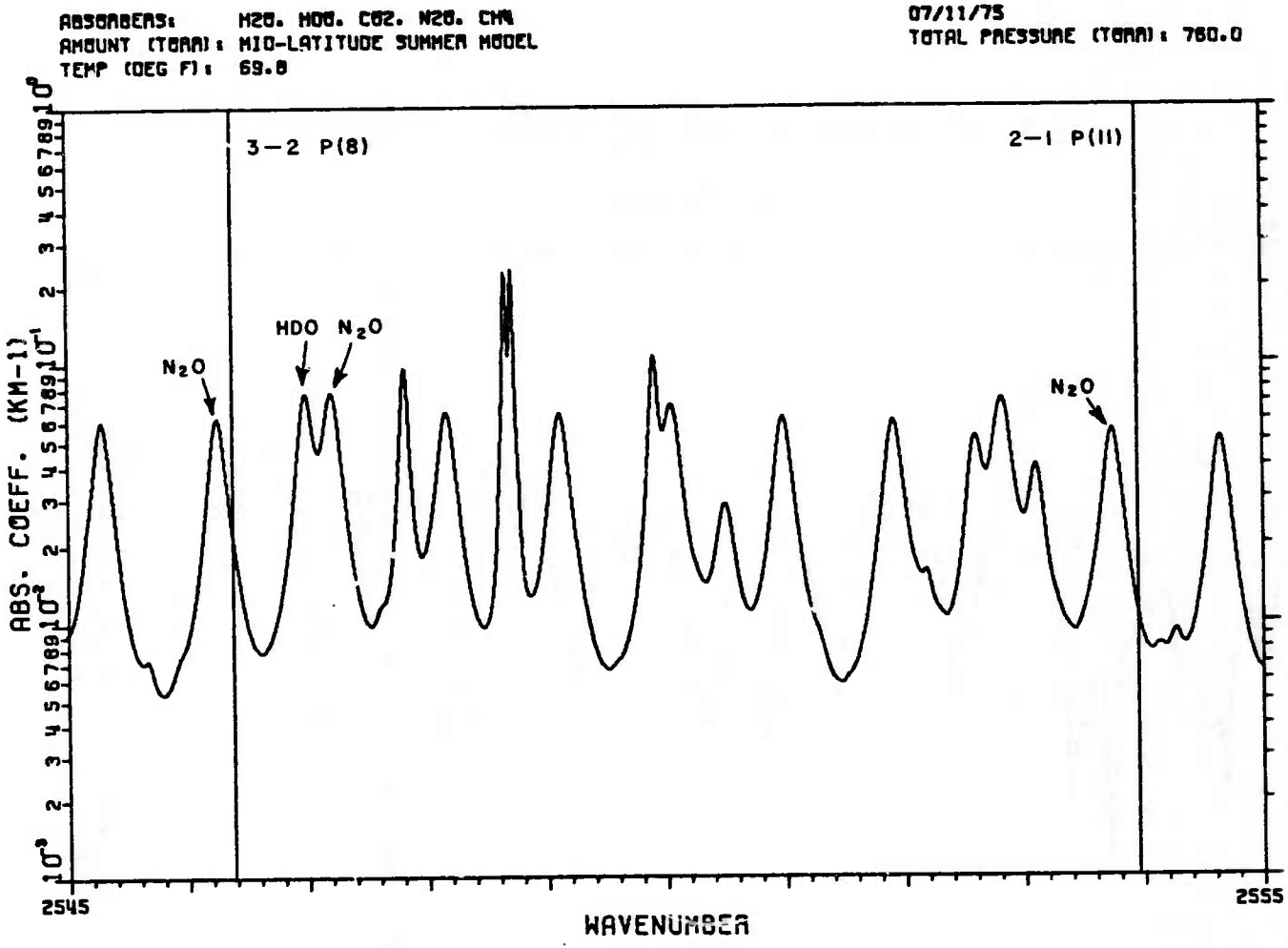

Fig. 14. Calculated spectrum near the 3-2 P(8) and 2-1 P(11) DF laser line.

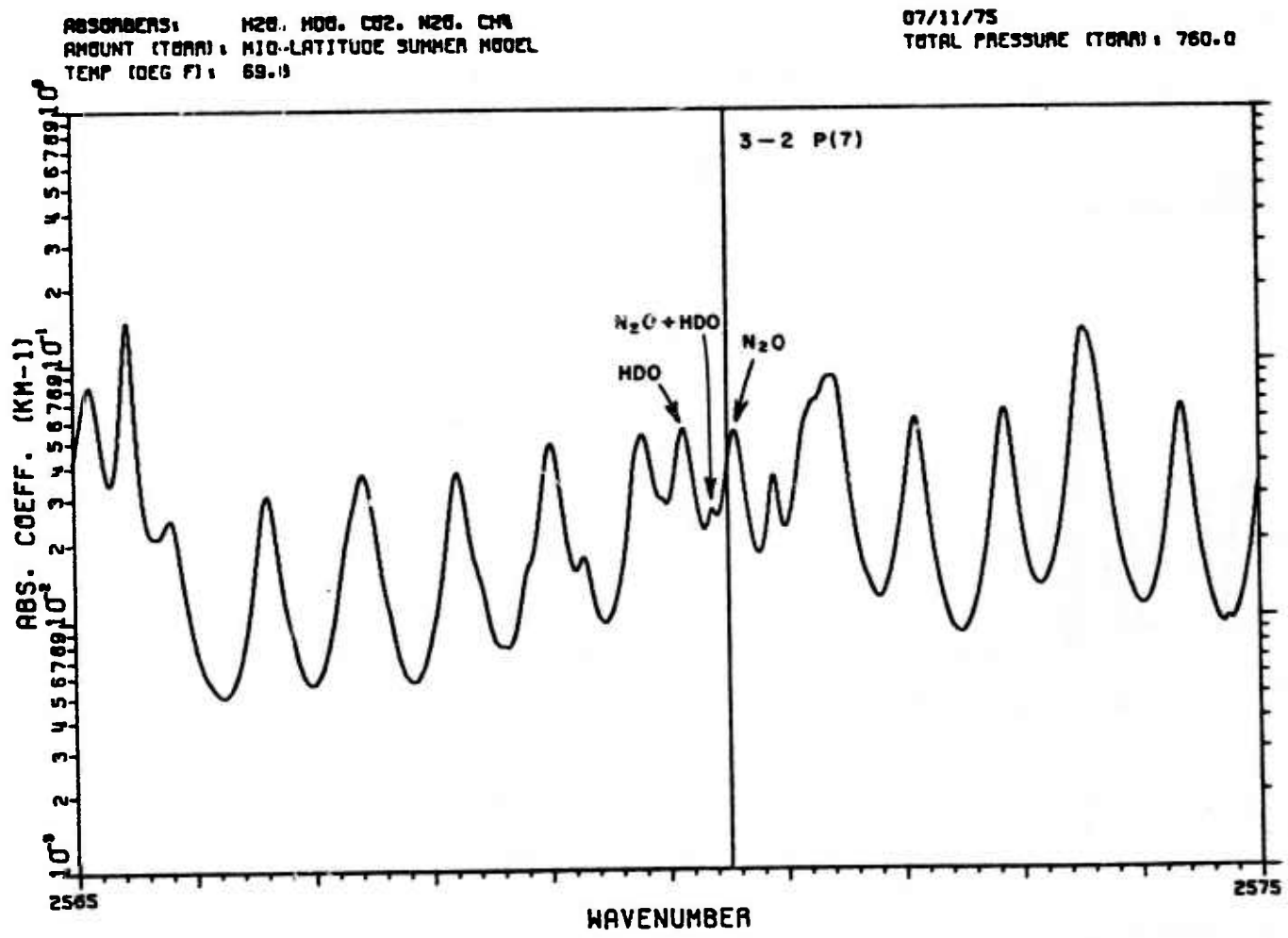

Fig. 15. Calculated spectrum near the 3-2 P(7) DF laser line.

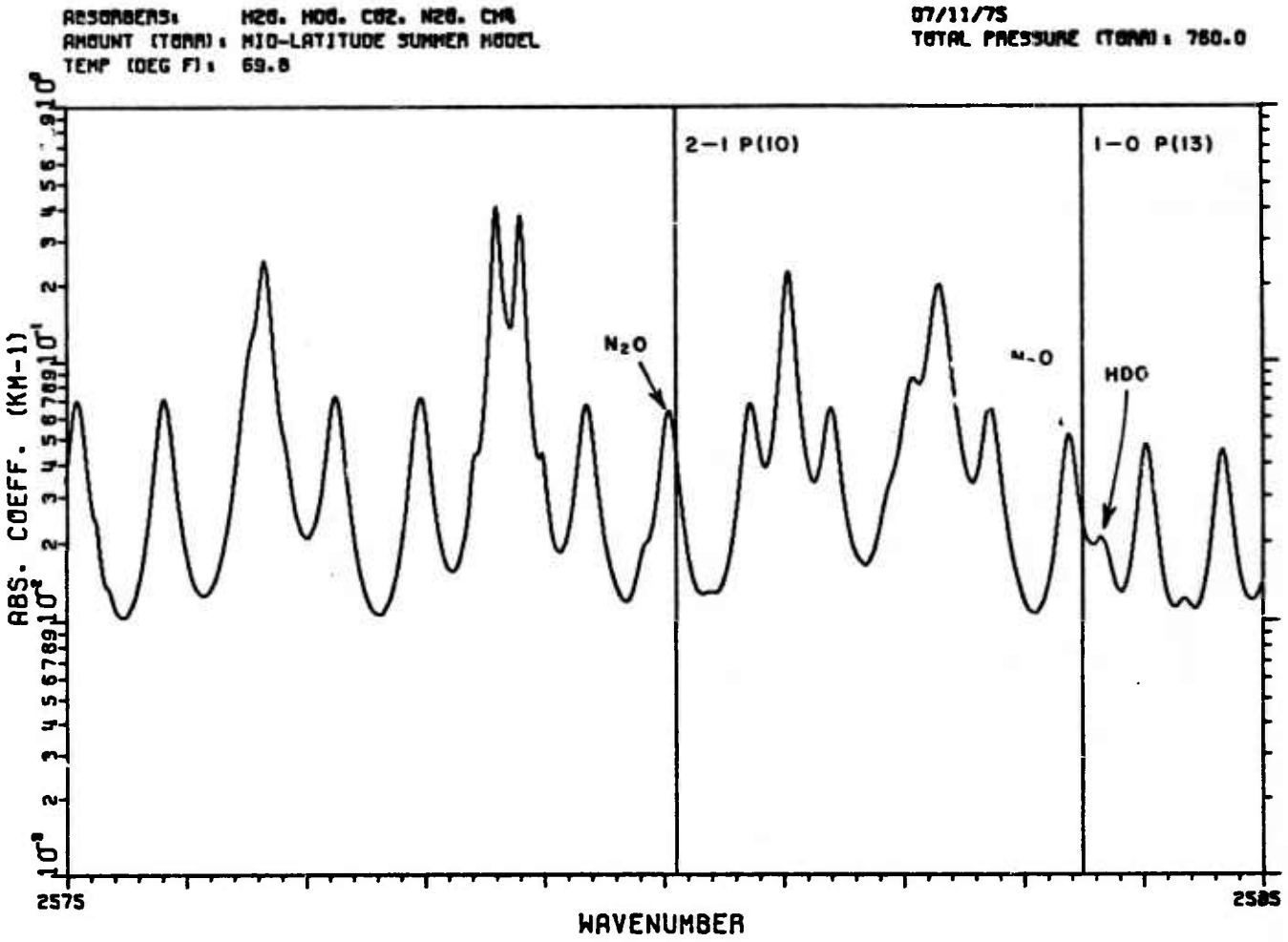

Fig. 16. Calculated spectrum near the 2-1 P(10) and 1-0 P(13) DF laser line.

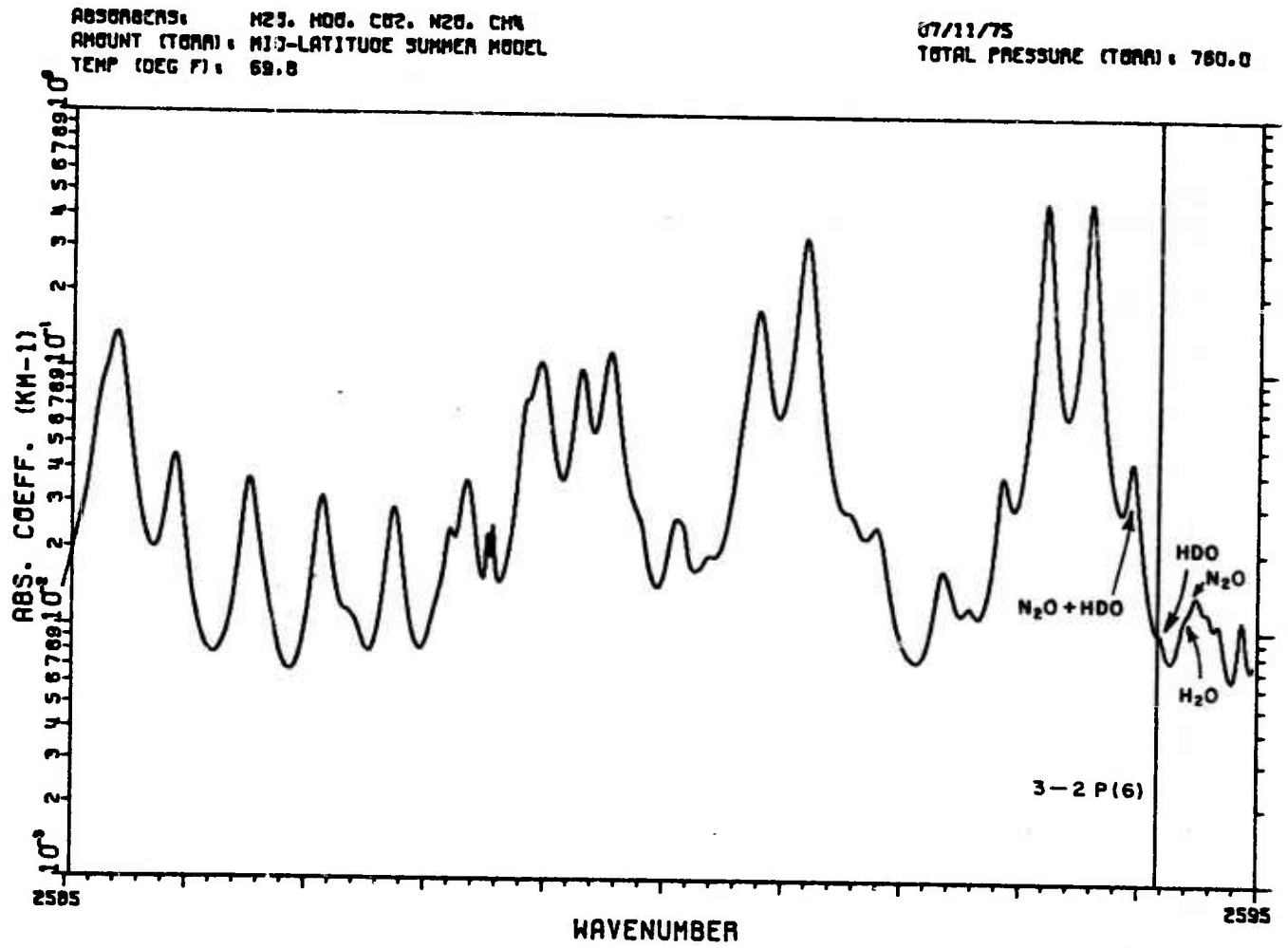

Fig. 17. Calculated spectrum near the 3-2 P(6) DF laser line.

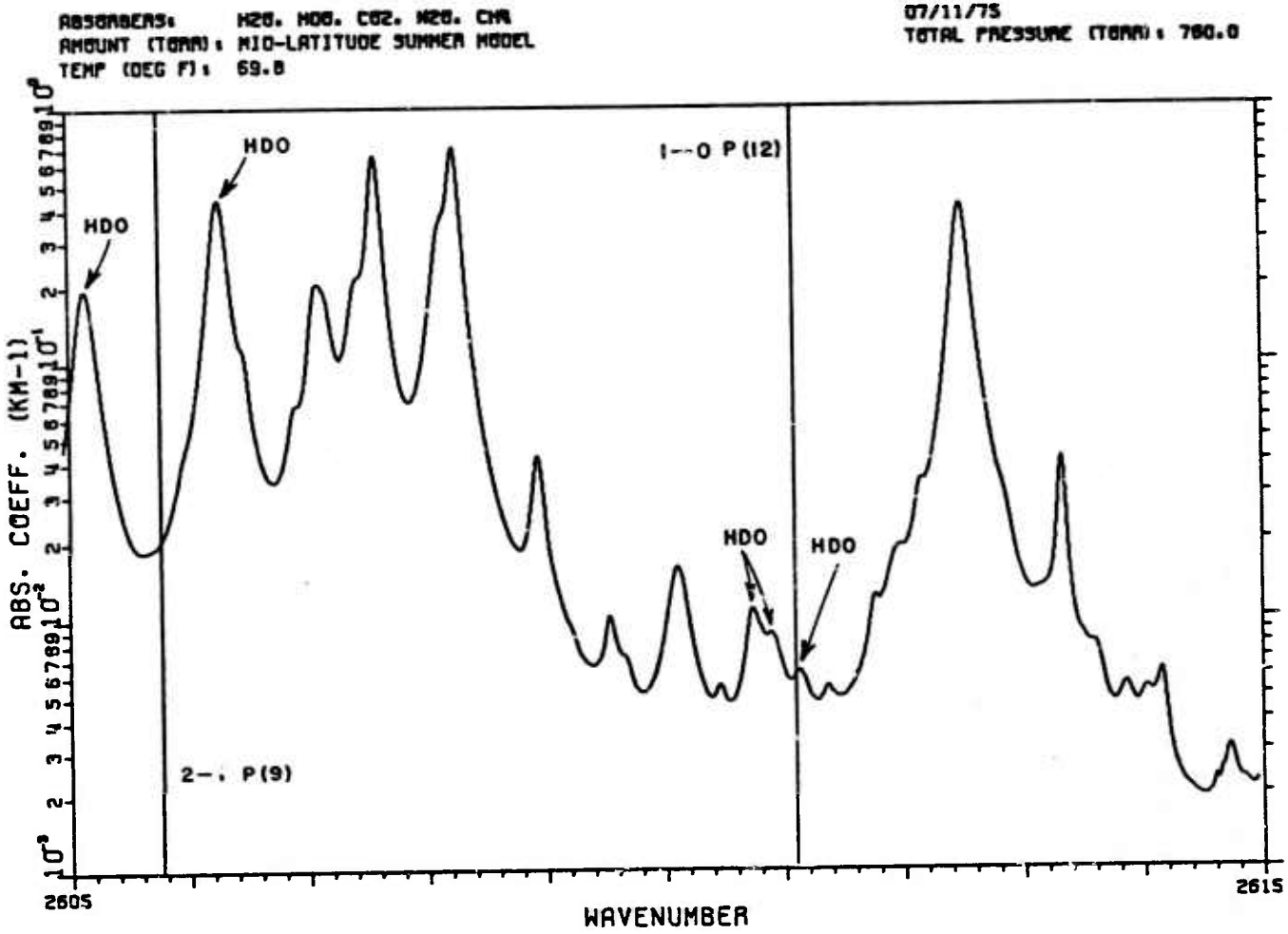

8. Calculated spectrum near the 2-1 P(9) and 1-0 P(12) DF laser lines.

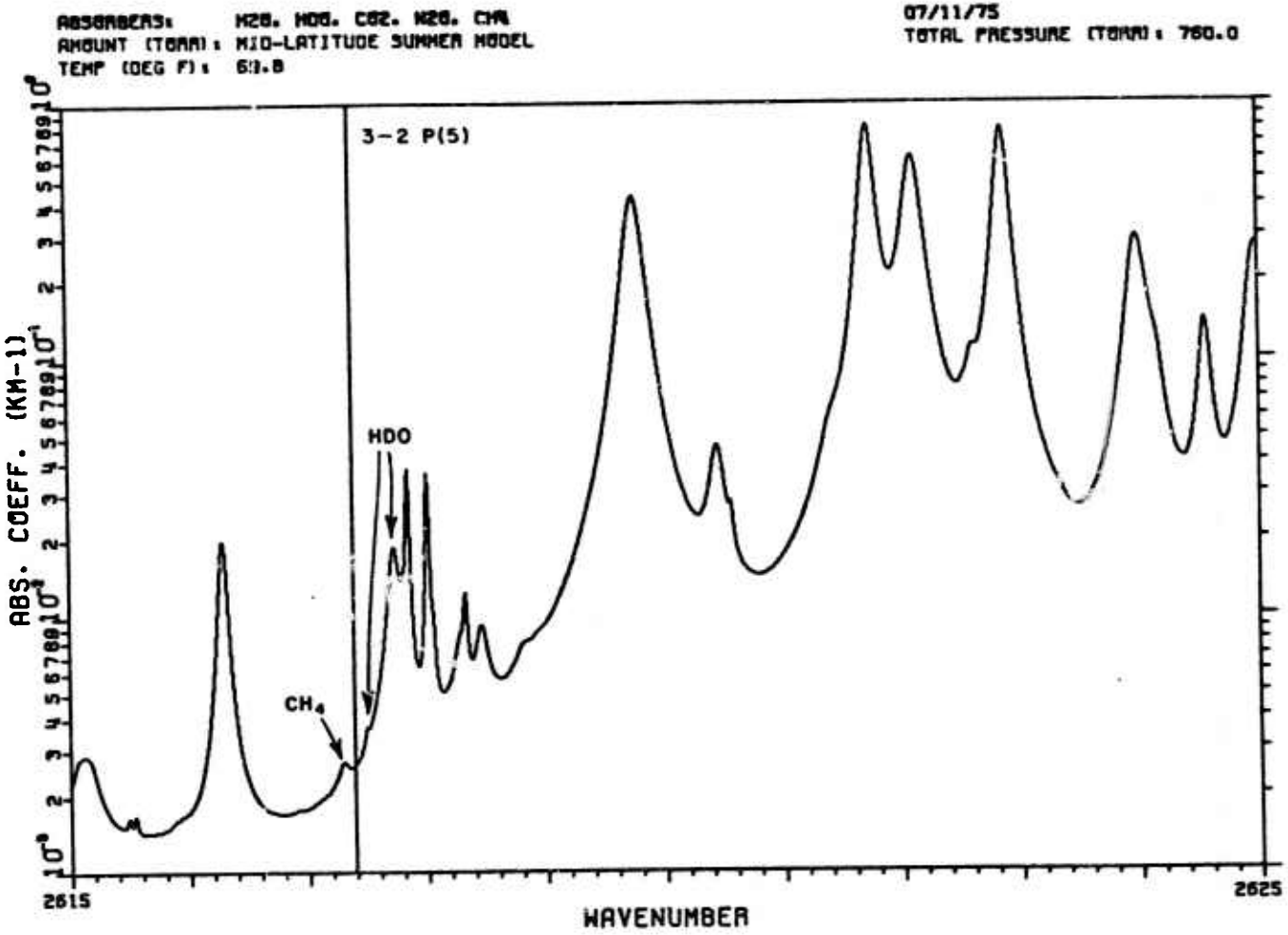

Fig. 19. Calculated spectrum near the 3-2 P(5) DF laser line.

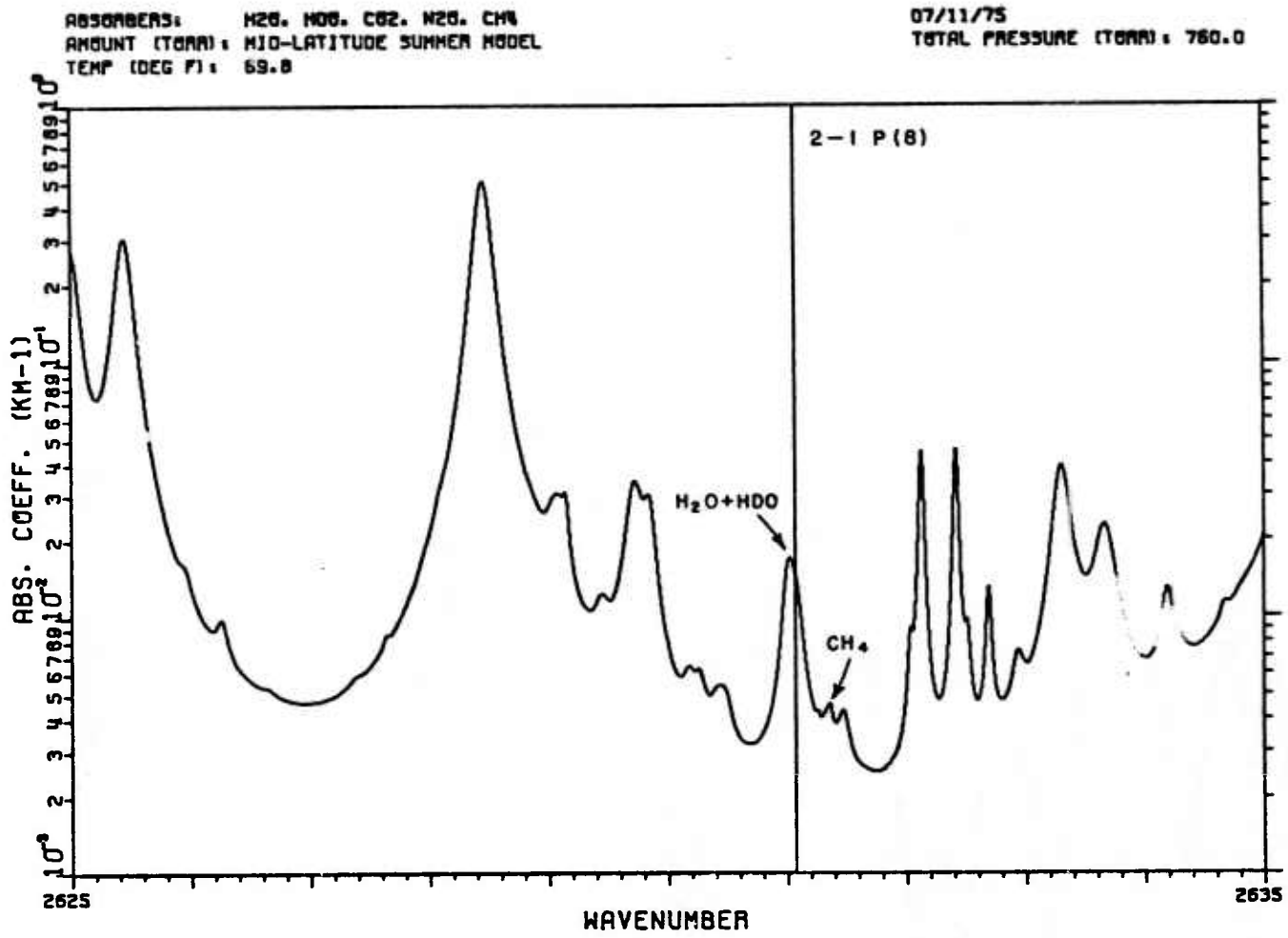

Fig. 20. Calculated spectrum near the 2-1 P(8) DF laser line.

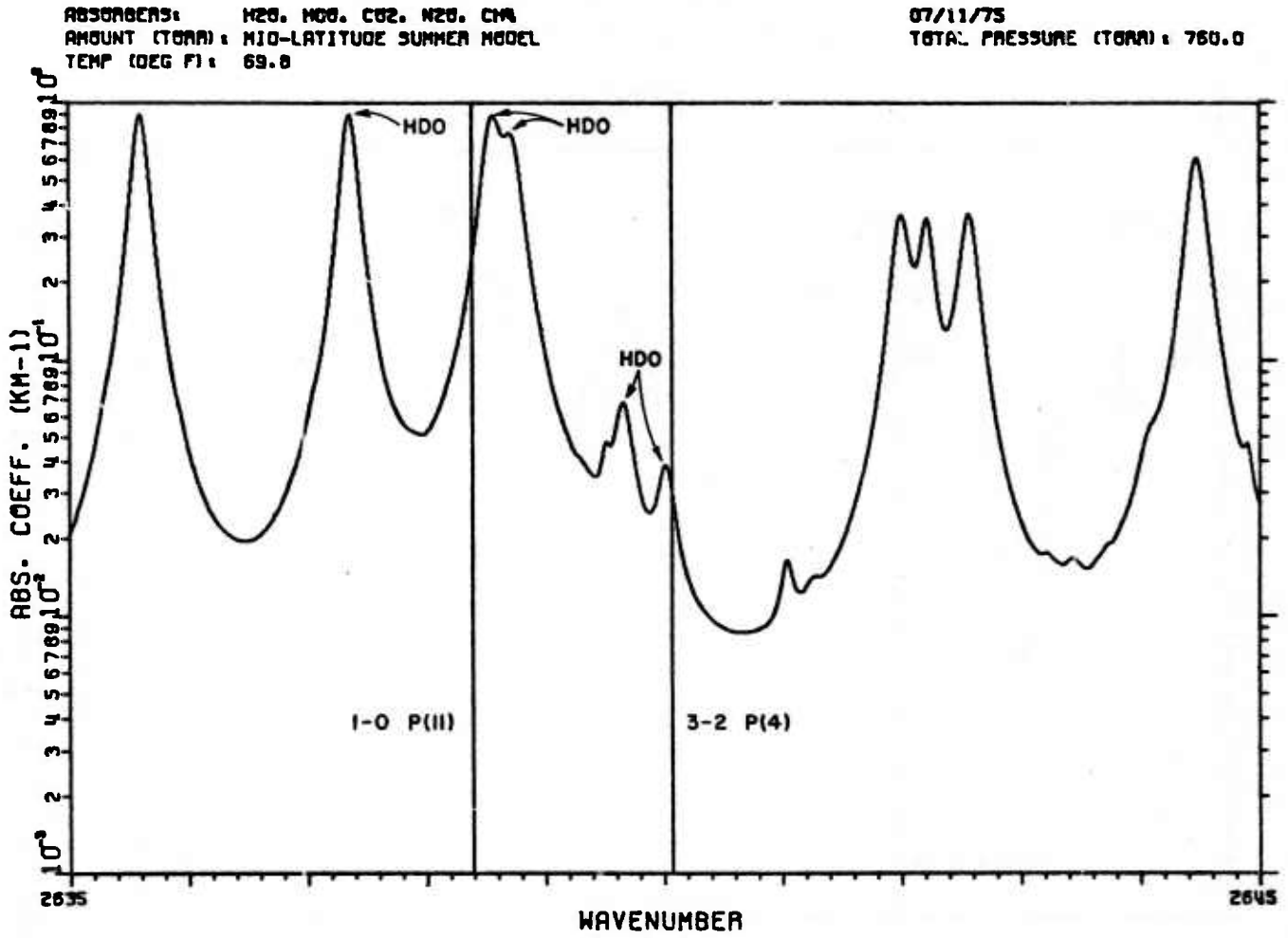

Fig. 21. Calculated spectrum near the 1-0 P(11) and 3-2 P(4) DF laser lines.

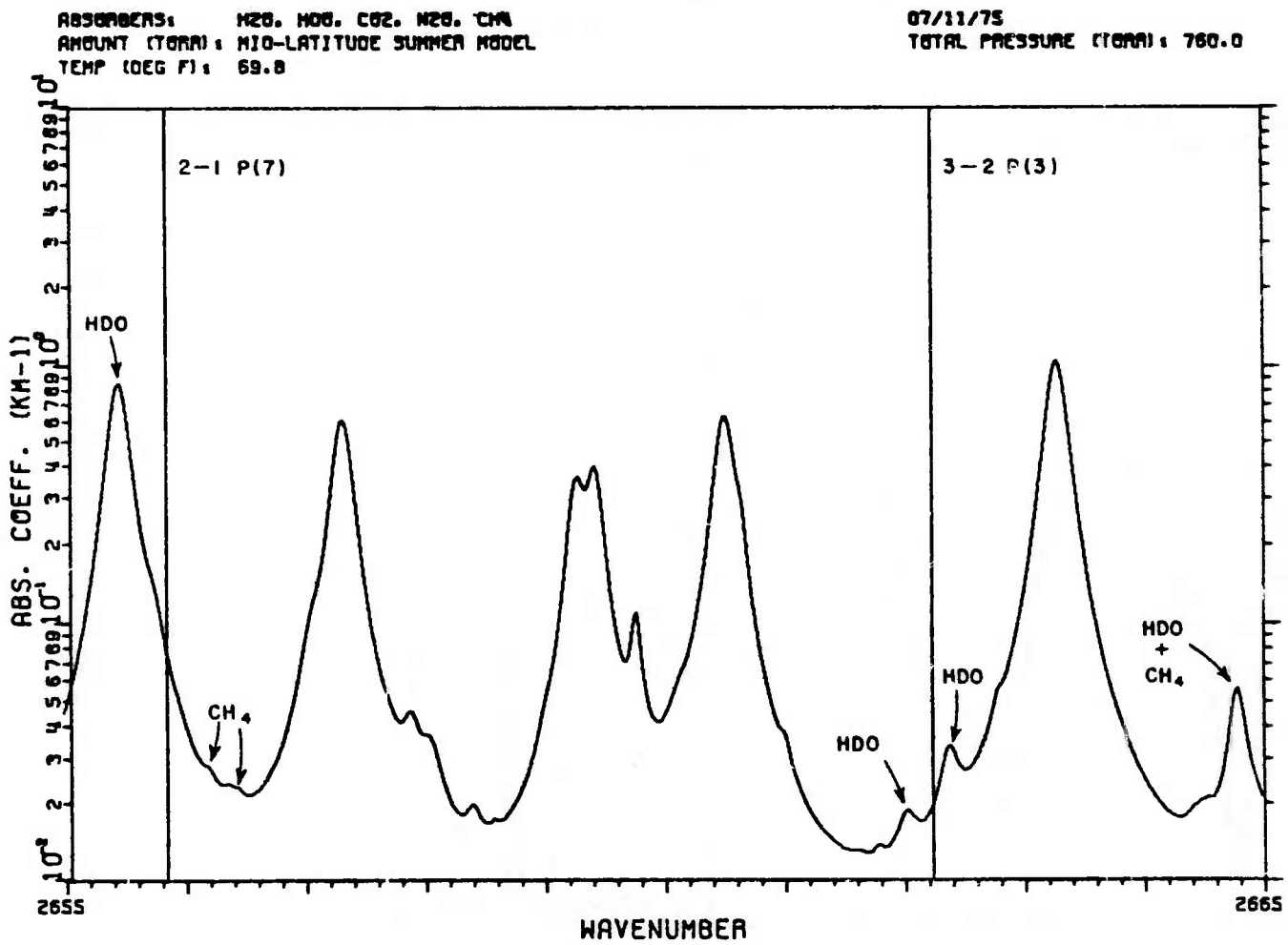

Fig. 22. Calculated spectrum near the 1-0 P(7) and 3-2 P(3) DF laser lines.

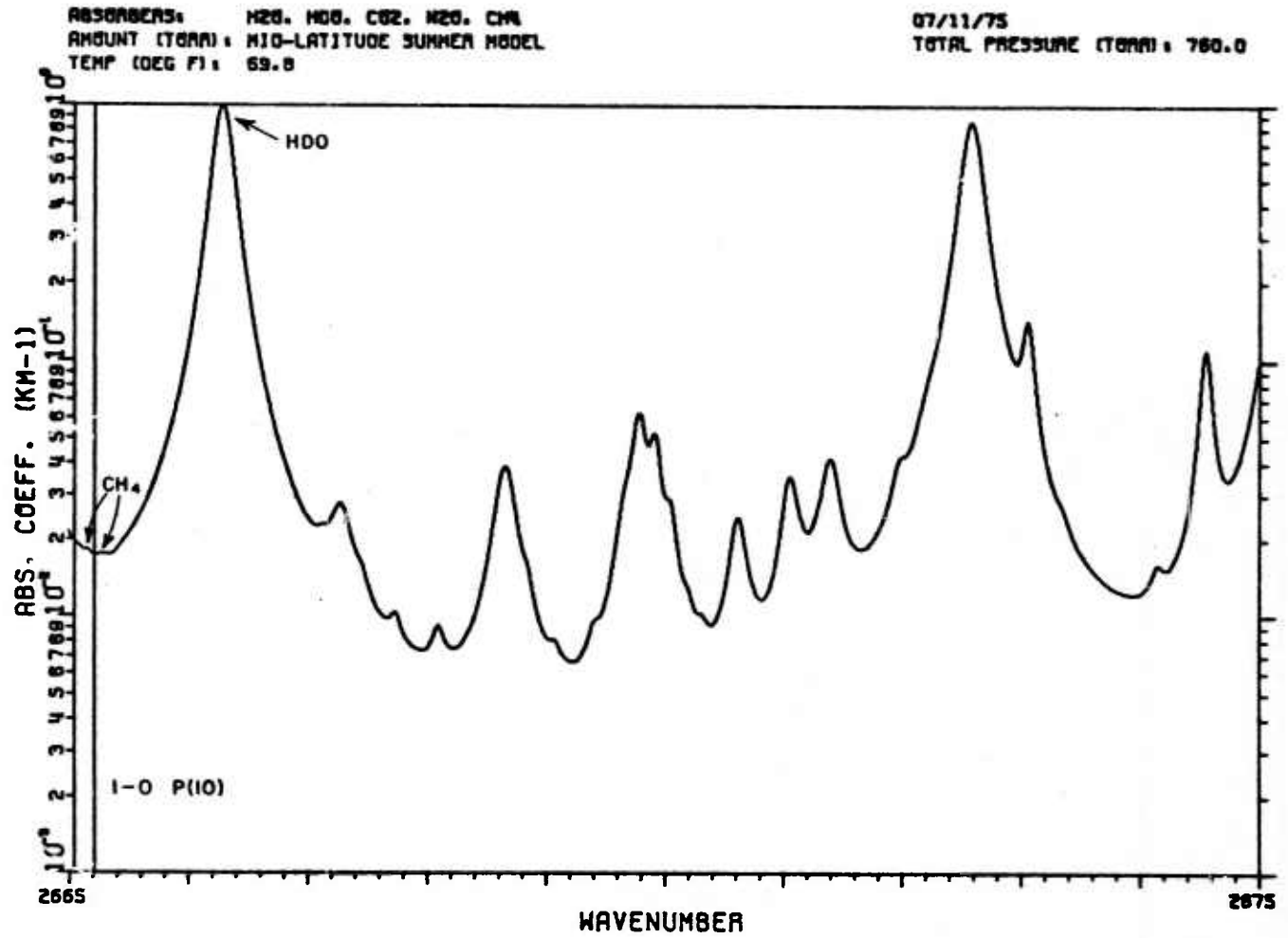

Fig. 23. Calculated spectrum near the 1-0 P(10) DF laser line.

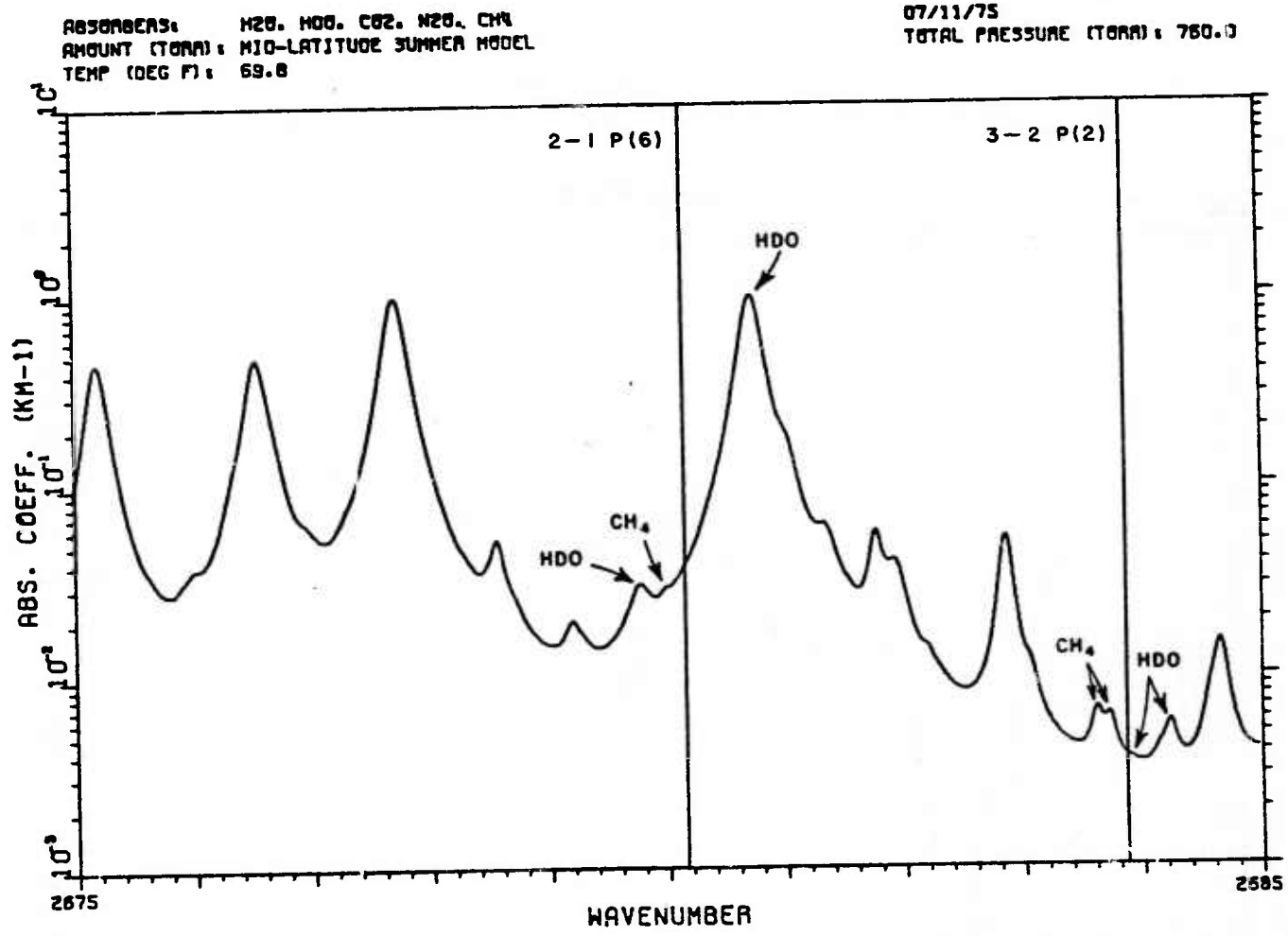

Fig. 24. Calculated spectrum near the 2-1 P(6) and 3-2 P(2) DF laser lines.

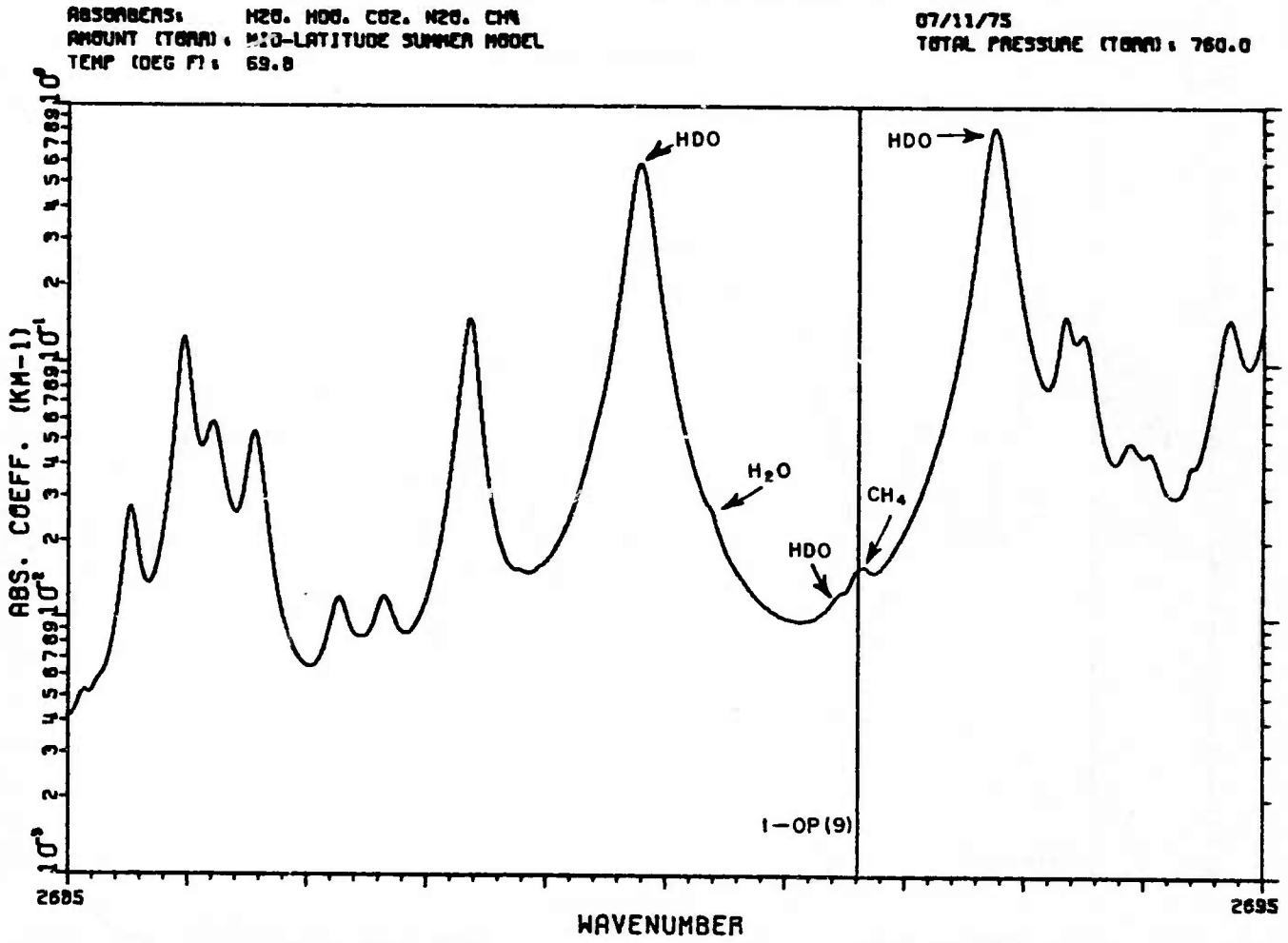

Fig. 25. Calculated spectrum near the 1-0 P(9) DF laser line.

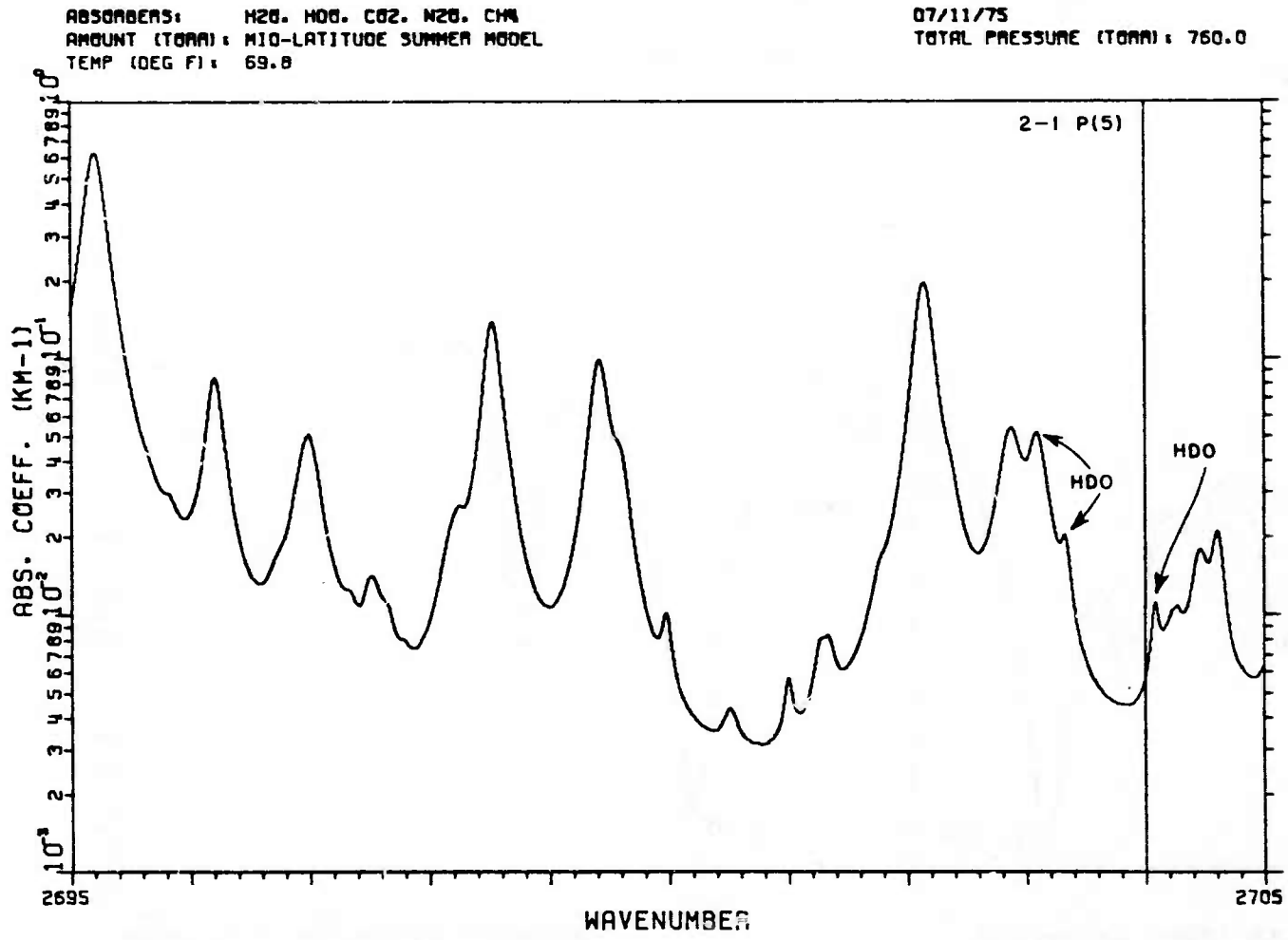

Fig. 26. Calculated spectrum near the 2-1 P(5) DF laser line.

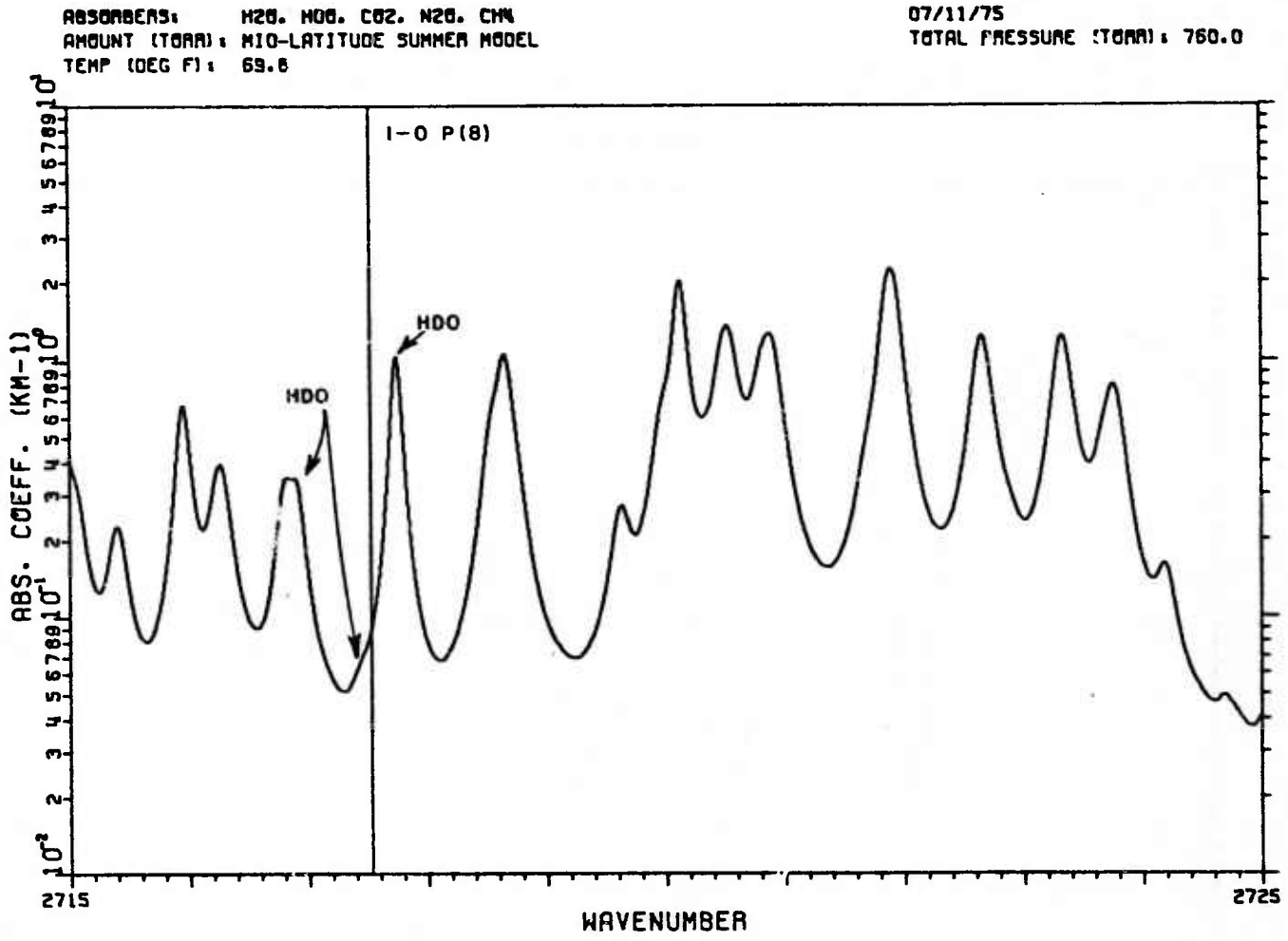

Fig. 27. Calculated spectrum near the 1-0 P(8) DF laser line.

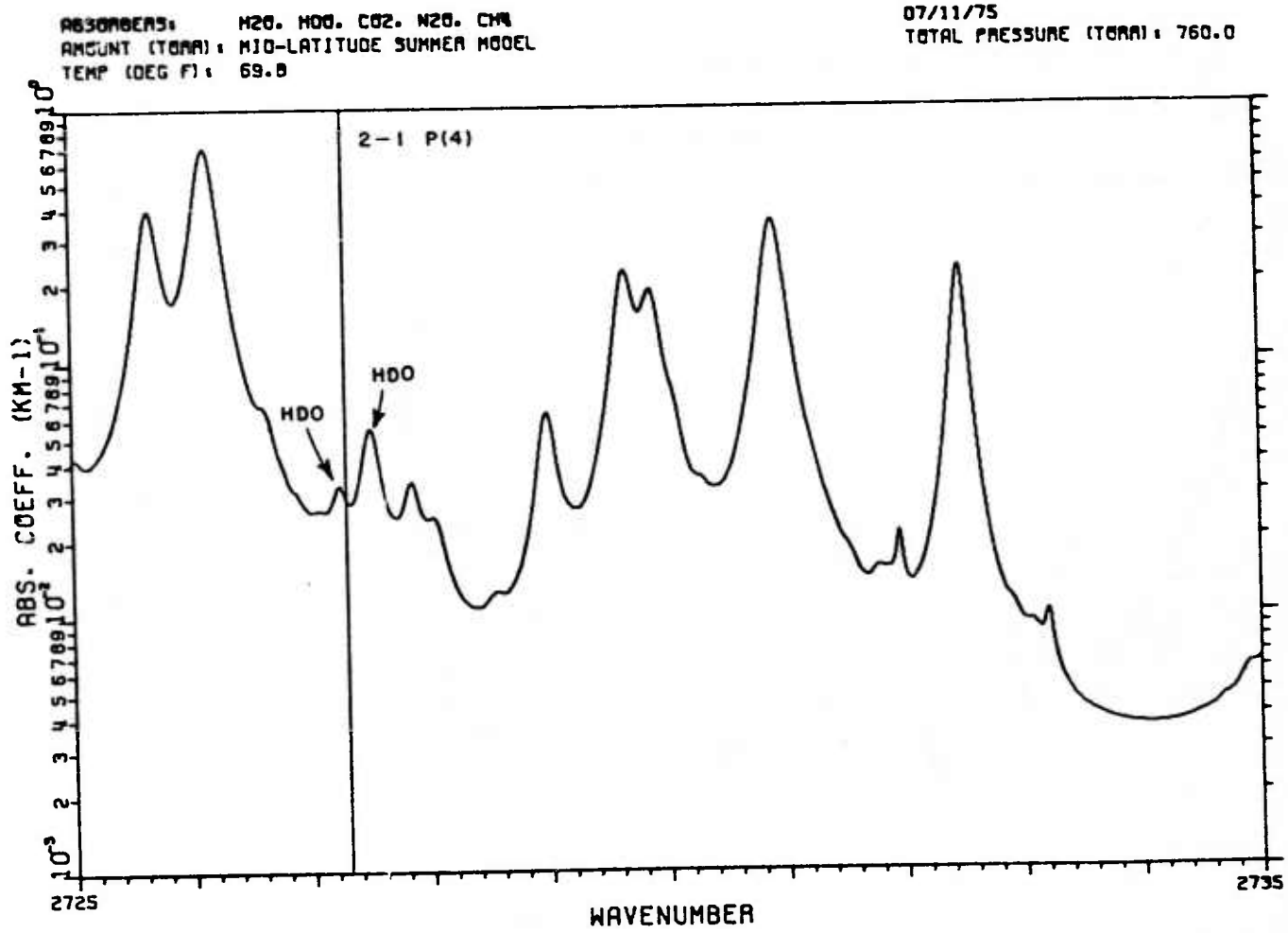

Fig. 28. Calculated spectrum near the 2-1 P(4) DF laser line.

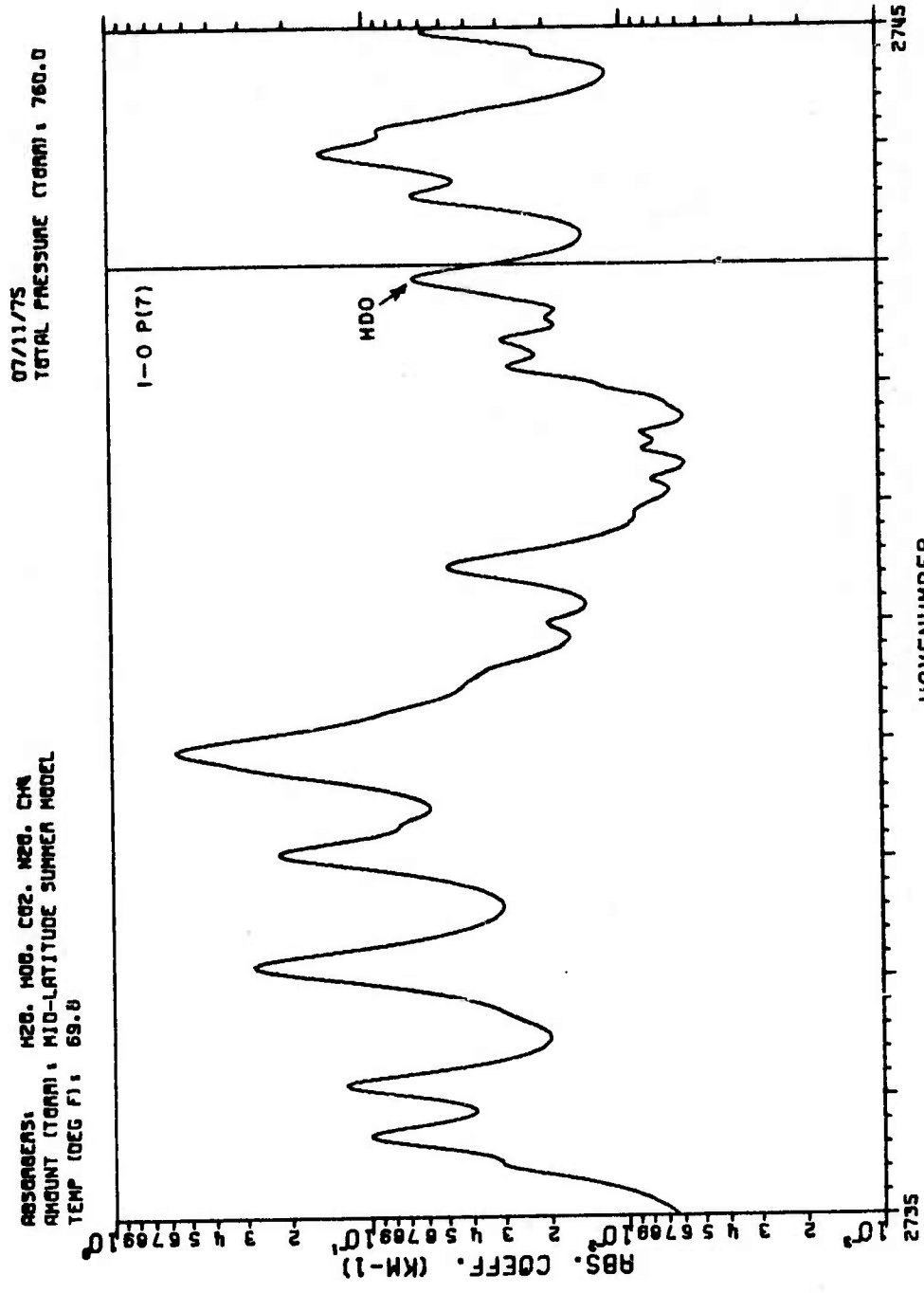

Fig. 29. Calculated spectrum near the 1-0 P(7) DF laser line.

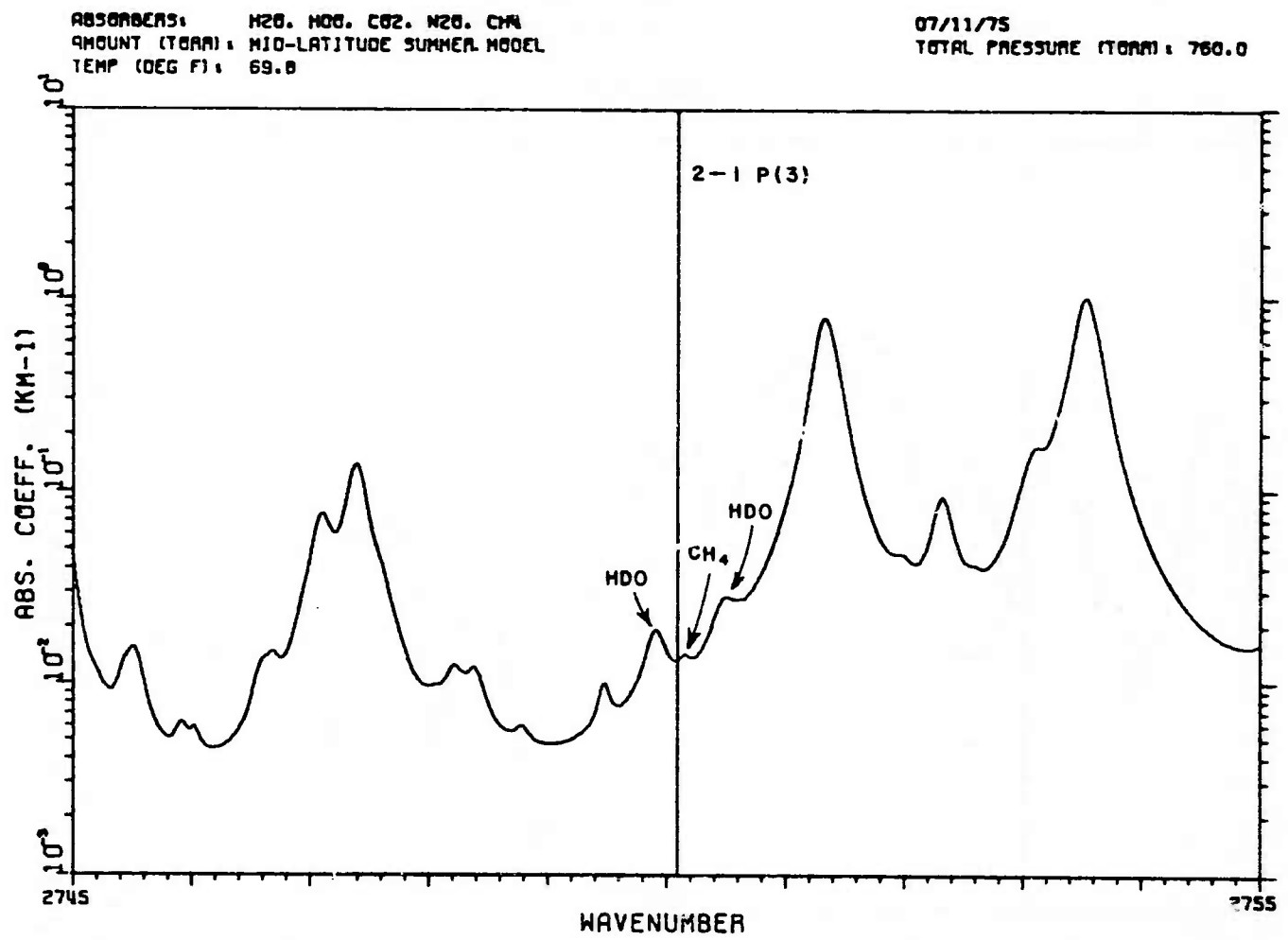

Fig. 30. Calculated spectrum near the 2-1 P(3) DF laser line.

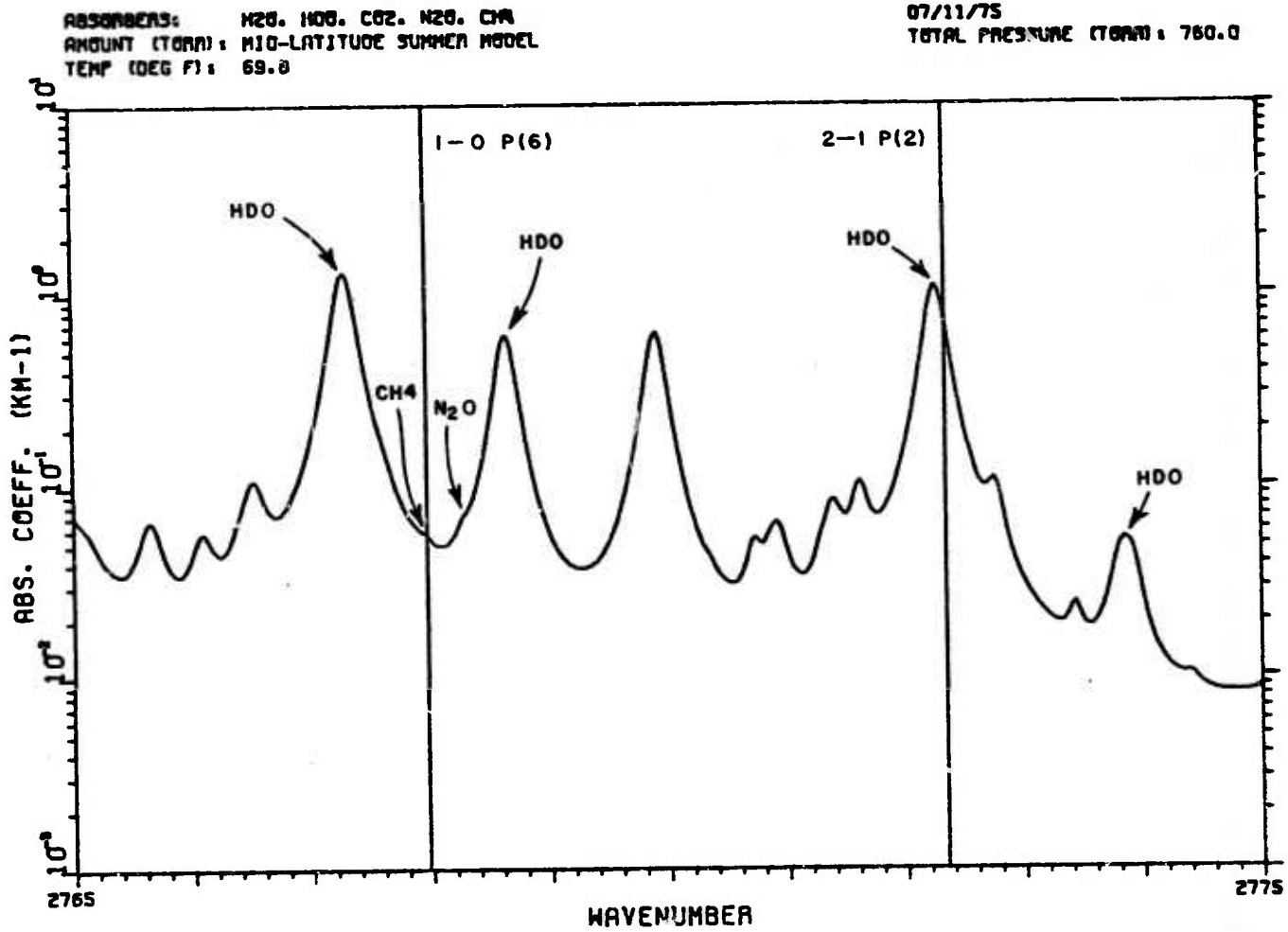

Fig. 31. Calculated spectrum near the 1-0 P(6) and 2-1 P(2) DF laser lines.

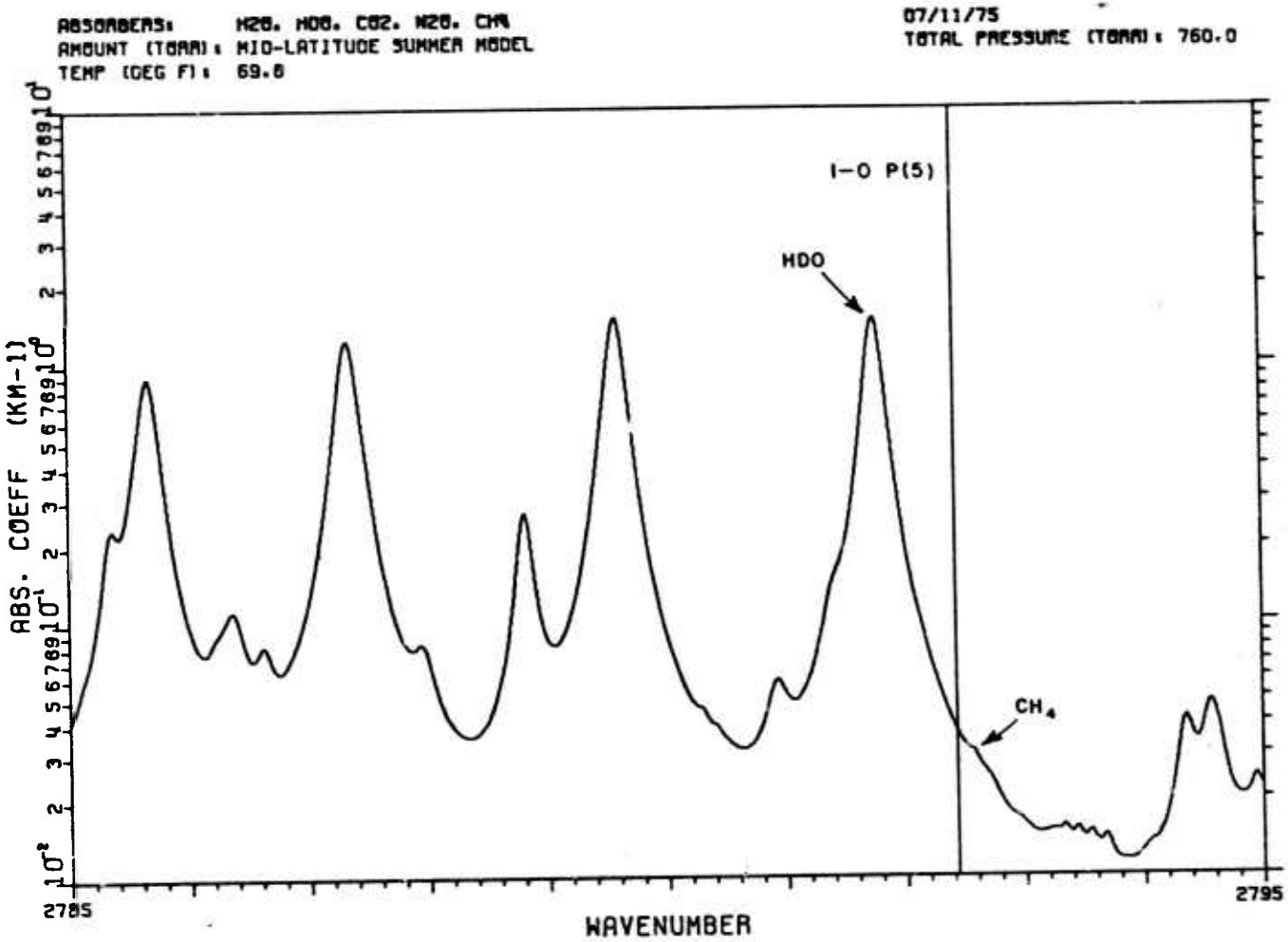

Fig. 32. Calculated spectrum near the 1-0 P(5) DF laser line.

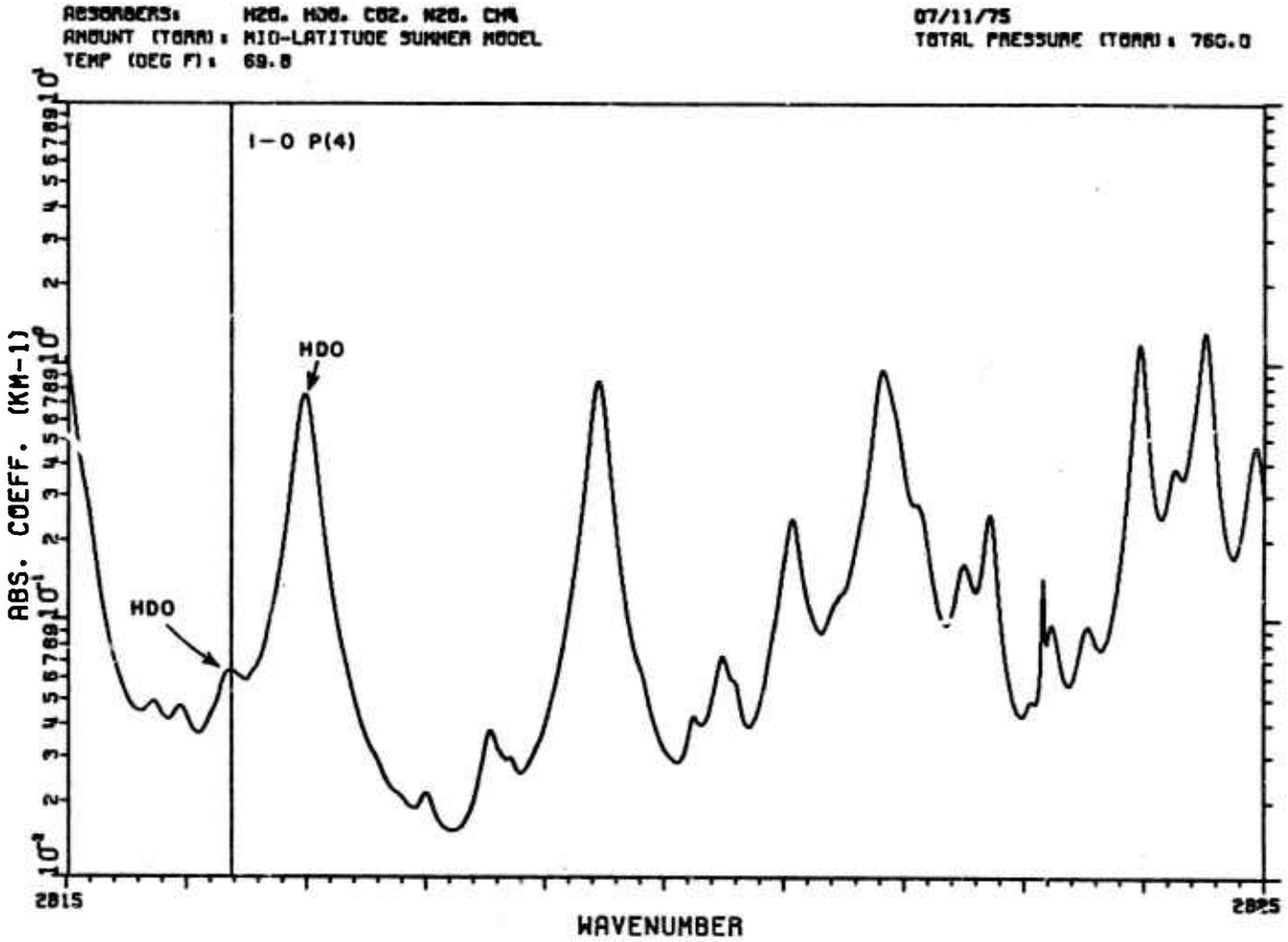

Fig. 33. Calculated spectrum near the 1-0 P(4) DF laser line.

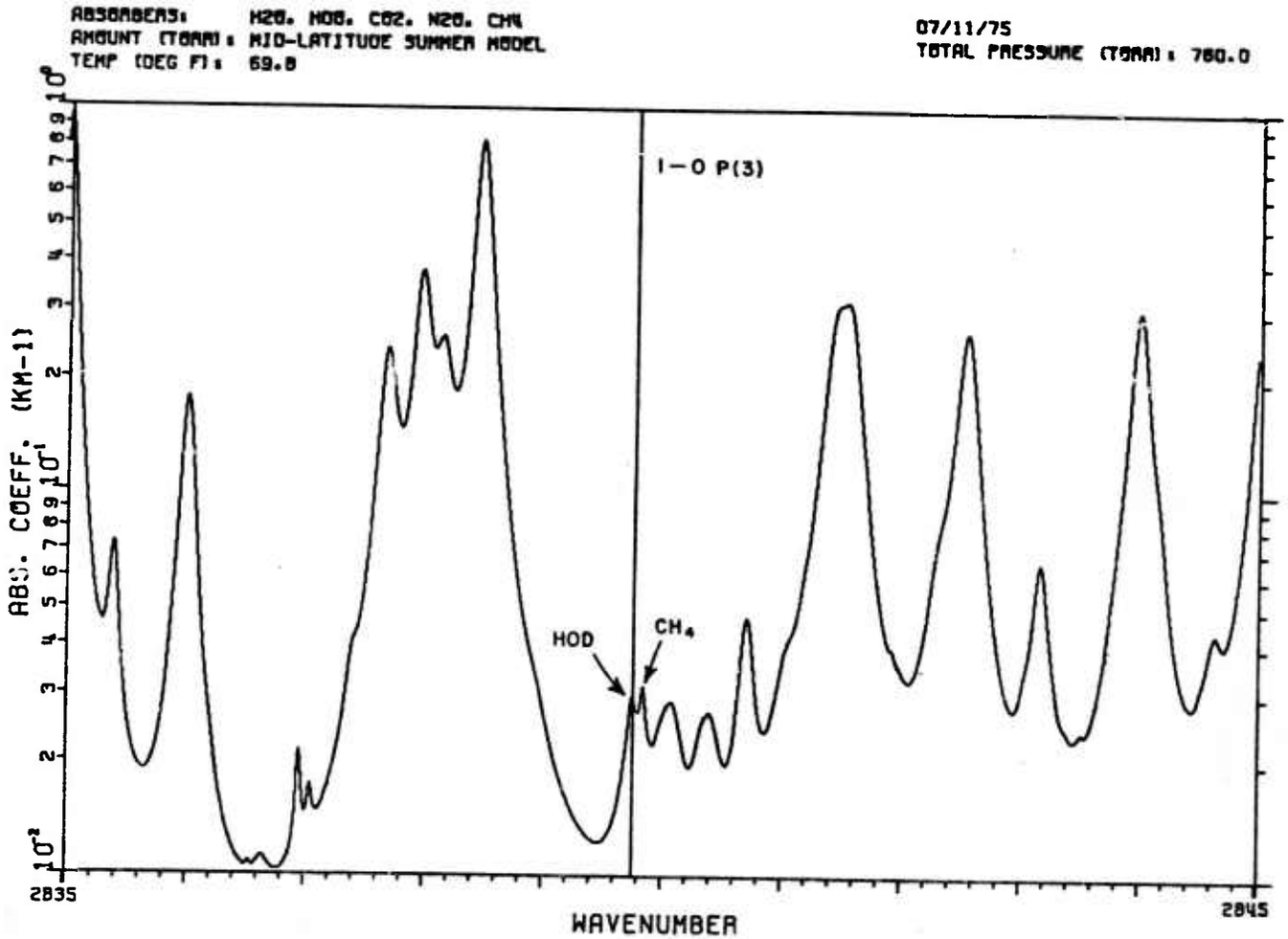

Fig. 34. Calculated spectrum near the 1-0 P(3) DF laser line.

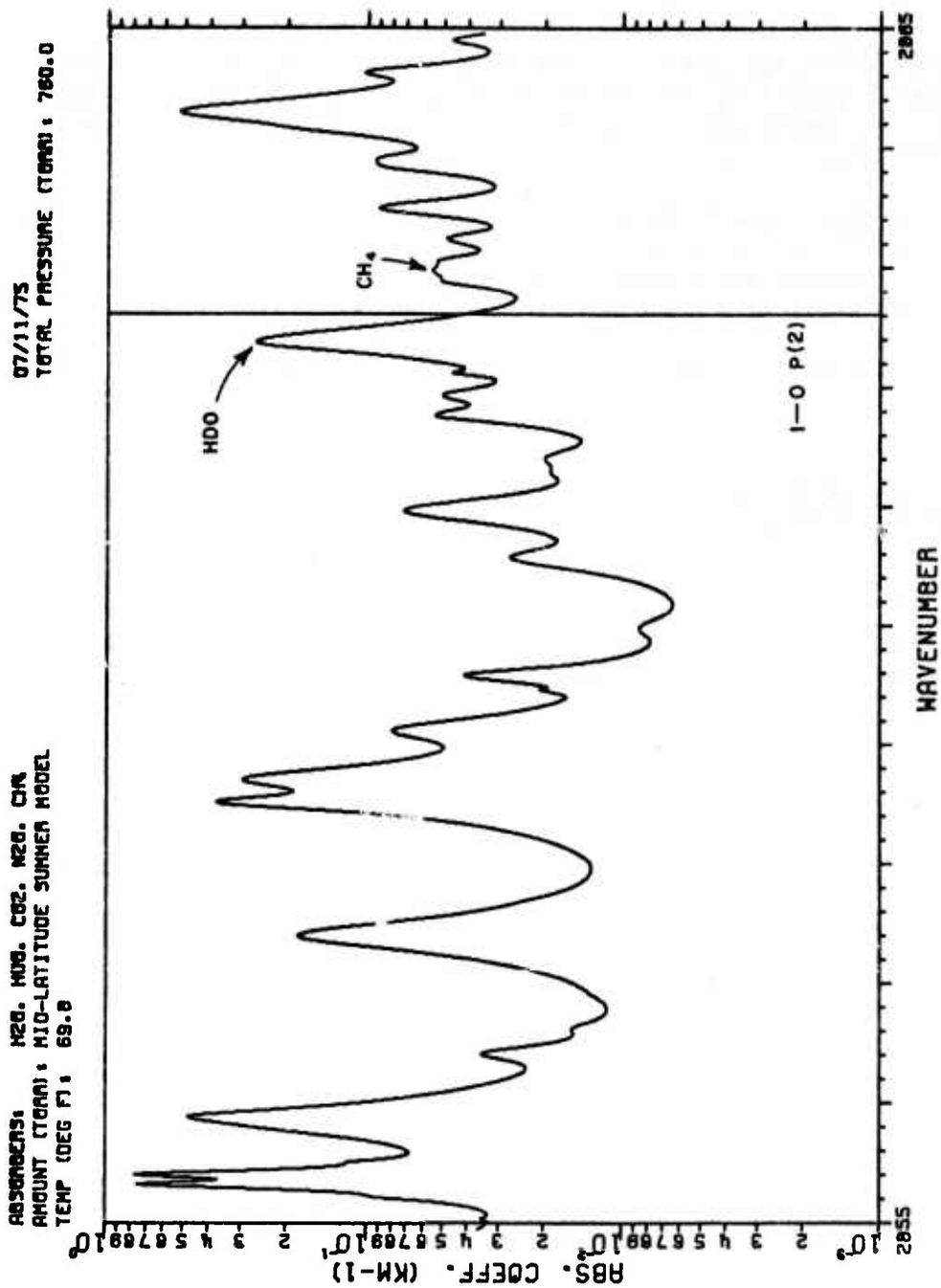

Fig. 35. Calculated spectrum near the 1-0 P(2) DF laser line.

CHAPTER III

EXPERIMENTAL EQUIPMENT

A very important part of this study was developing the experimental system necessary for making measurements of the desired high accuracy. The experimental apparatus making up this system can be divided into four groups:

1. Single line DF laser
2. Auxiliary optics
3. Detectors and electronics
4. Multiple traversal absorption cell .

The equipment in these groups will be described in this chapter.

A. Design and Construction of the DF Laser

1. Introduction

A probe laser for atmospheric absorption measurements should have the following characteristics:

1. It should operate on only a single line and be easily tunable from line to line.

2. It should be fairly easy to use , that is it should not require a full-time technician to operate.

3. It should be economical to operate.

4. Amplitude stability should be as good as possible.

At the time this study was begun and indeed even now such a DF laser is not commercially available. It was therefore necessary to design and construct the laser.

The DF laser is a chemical laser, that is the upper laser levels are populated by the release of energy from a chemical reaction. The lasers used in this study are similar but not identical

to one described by Ultee[18]. A mixture of helium, sulfur hexafluoride (SF_6), deuterium, and oxygen gases is introduced into the discharge tube. A 12 to 15 kv electrical pulse of less than one microsecond duration dissociates the SF_6 producing free fluorine which reacts with deuterium to form excited DF which then emits a laser pulse about one microsecond long. Helium is added to serve as a heat sink and promote discharge stability. A small amount of oxygen is added to keep sulfur deposits from forming on the walls of the discharge tube. Note that all the input gases are non-corrosive and non-poisonous and require no special handling,

2. Original DF laser

a. Gases

The gases used were helium, SF_6, deuterium, and oxygen as described in part 1. A conventional 15 cfm mechanical pump was used to maintain a pressure of 3 to 12 torr in the discharge tube and a flow rate sufficient to change the gas mixture between pulses. It was found that the optimum pressure and gas mix varied according to the particular line which was oscillating.

Estimated mass flow rates for operation at 6 torr are: helium, 21 gm/hour; SF_6 .49 gm/hour; deuterium, 1.4 gm/hour. Estimated operating cost with commercially supplied deuterium is $4.00/hour.

b. Laser tube geometry

The laser tube geometry is shown schematically in Fig. 36. The tube was constructed of 10 mm I.D. pyrex tubing with two inlet ports and three output ports. The electrodes were Kovar glass to metal seal. Swagelok fittings were used to make connections at the inlet and outlet ports.

The windows were calcium fluoride with the Brewster angle in the proper orientation for operation with a grating.

c. Optical cavity

The optical cavity consisted of a 300 line/mm grating blazed at 3 μm and a 20 m radius of curvature germanium mirror coated for greater than 80% reflectivity between 3 μm and 4 μm. The grating and the mirror were separated by 121 cm.

The grating mount was designed by Professor Damon at Ohio State so that the grating could be easily aligned, and so that the grating could be easily and reproducibly tuned to a specific laser

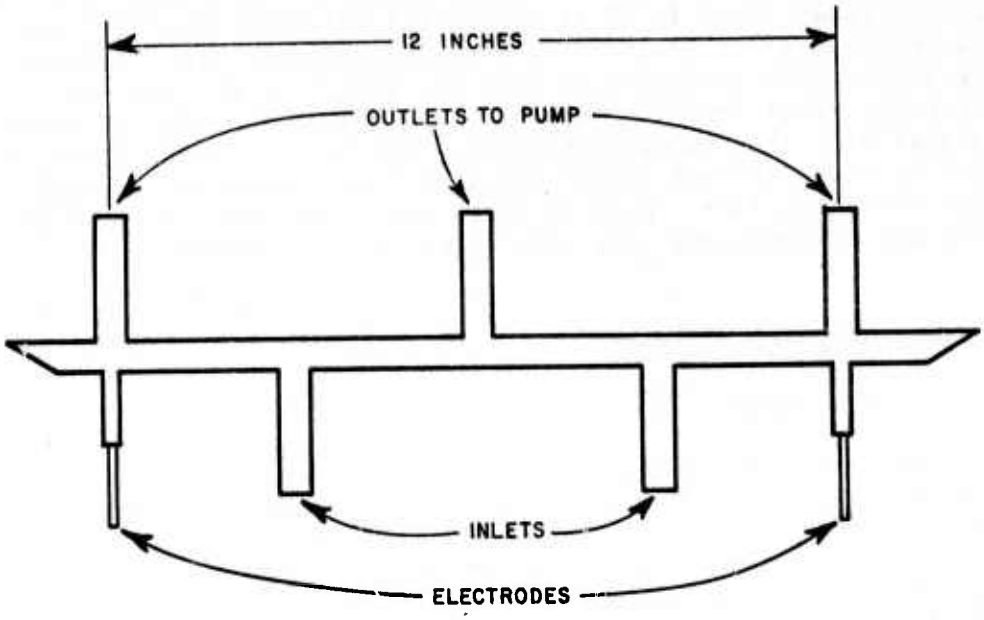

Fig. 36. Schematic diagram of first DF laser tube.

line. A photograph of the grating mount is shown in Fig. 37. This mount proved to be quite satisfactory and was used in all versions of the laser.

The output mirror was mounted in a piezoelectric drive which was part of a commercial gimbal mount which was mounted on a horizontal translation stage. The mirror could then be moved to adjust the longitudinal cavity mode for optimum operation on a single line. It was found however that longitudinal adjustment had no effect on the laser output, probably because of the extremely high gain for pulsed operation.

The grating mount, laser tube and mirror mount were all attached to a limestone slab five feet long, one foot wide, and three inches thick. This arrangement proved to be quite stable. Once the optical cavity was aligned it maintained alignment indefinitely with only minor adjustments required when the laser tube was changed.

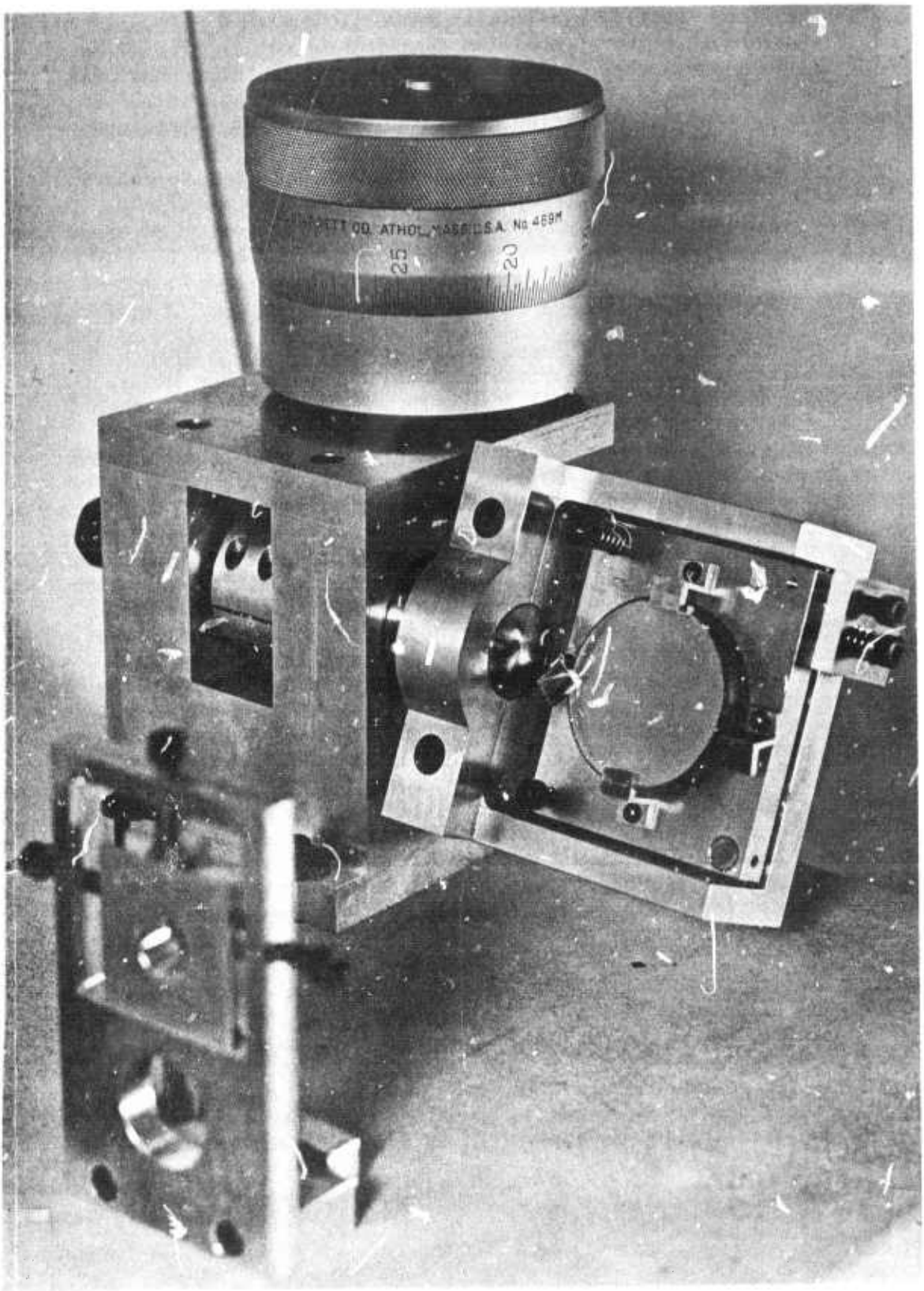

Fig. 37. Grating mount

d. Power supply

The laser reaction was initiated by discharging a 0.02 μfd capacitor through a thyratron. The capacitor was charged to 12 to 15 kv using a commercial high voltage power supply. The pulser was supplied by Aerospace Corporation and was capable of single pulse operation or repetitive pulsing up to about 100 pulses per second.

It was necessary to repackage the Aerospace pulser to reduce electrical noise problems. This is discussed in more detail in part f.

e. Laser alignment

The alignment of the laser was relatively simple although the output mirror was opaque to visible light. A helium-neon (HeNe) laser beam was first made collinear with the laser tube with the aid of small irises which were mounted at either end of the laser tube. Then a flat mirror was attached to the grating table and the grating mount was adjusted so the grating rotation axis was exactly perpendicular to the laser beam. This occurred when the flat mirror reflected the HeNe laser beam exactly back on itself. This could be easily determined because the reflected beam fed back into the HeNe laser and caused the output amplitude to fluctuate noticably. Then the flat mirror was removed and the grating was installed. The grooves of the grating were then aligned parallel with the axis of rotation of the grating by making sure that the 4th through 7th orders of the HeNe laser beam were reflected straight back to the laser as the grating angle was tuned. This insured that the grating was aligned for the wavelength range from 2.5 μm to 4.5 μm. The output mirror and mirror mount were now installed so that the output mirror was centered on the HeNe laser beam. Then the output mirror was adjusted so that the reflection of the HeNe laser beam from the back of the mirror went straight back to the laser. The output mirror could be adjusted closely enough this way so that with the laser operating and the grating tuned to the proper angle there would be oscillation. Fine adjustment of output mirror orientation could then be made to optimize the laser output. The grating micrometer tuning calibration could be determined from the micrometer positions where the 4th through 7th orders of the HeNe laser were exactly reflected. If a least square fit of a quadratic is then made to these four points, the micrometer position for any given laser line may then be determined from the fitted quadratic. This calibration method was tested by observing the laser output with a 1 meter Czerny-Turner spectrometer and found to be valid. This is hardly surprising since the laser cavity is equivalent to a 1.21 meter spectrometer with wide slits.

f. Laser performance

The laser was operated and found to oscillate on 25 lines with average power at 20 pulses per second of from .04 to 1 milliwatts per line. A drawing of an oscilloscope trace of the pulse is shown in Fig. 38. The laser could be operated up to about 35 pulses per second before the laser output per pulse started to deteriorate. The pulse rate was probably limited by the gas flow rate. There were however, two serious problems.

One was the great amount of RF electrical noise generated by the high-voltage pulser interfered with the operation of the electronics associated with the absorption measurement experiment. An attempt was made to reduce the noise by carefully repackaging the pulser. An improvement was observed, but the noise was still intolerable. The entire laser including the power supply was then placed in a shielded room with a double thickness of copper screen on all sides. The power to the shielded room was connected through line filters, and the room was separately grounded to an eight foot ground rod driven through the floor. The gas line and pumping lines came through brass or copper pipes. A one inch hole was cut in the wall to let the laser beam out. The pulse trigger signal was coupled through the wall using an infrared light emitting diode and a phototransistor. These rather drastic measures completely eliminated the RF noise problem.

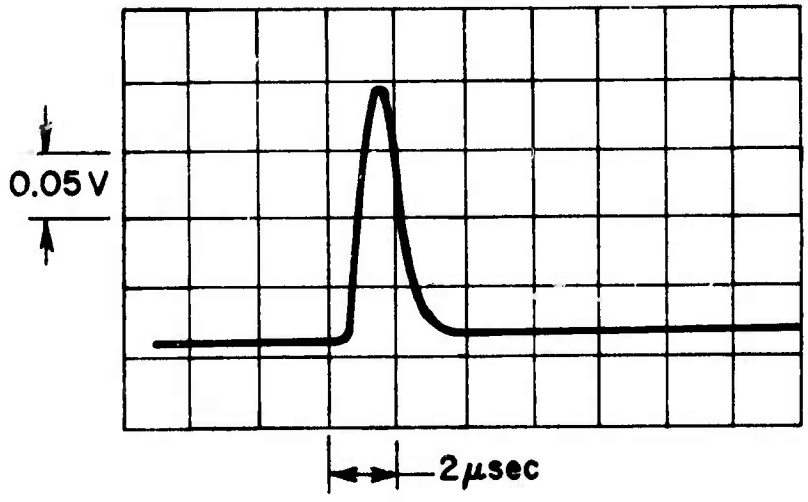

Fig. 38. Pulse shape of first DF laser.

The second problem which occured was sulfur depositing on the Brewster windows and on the inside of the laser tube. The deposit rate was such that the windows had to be cleaned after about one hour of operation. An attempt was made to reduce the sulfur deposit rate by adding more oxygen to the gas mixture. However this had the effect of drastically reducing the laser power.

3. Second DF laser

To solve the problem of window contamination a new tube was designed similar to the first but with ports added near each Brewster window. A schematic of the new tube is shown in Fig. 39. The idea is to admit helium through these additional ports to keep reaction products out of the area near the windows.

Other modifications were also made in the tube at this time. The tube I.D. was reduced to about 8.5 mm to improve discharge stability. The electrode configuration was changed from Kovar glass to metal seals to 1/8 inch copper tubing inserted as close to the active region as possible without obstructing the optical path. This was done to reduce the voltage and energy required to initiate the chemical reaction.

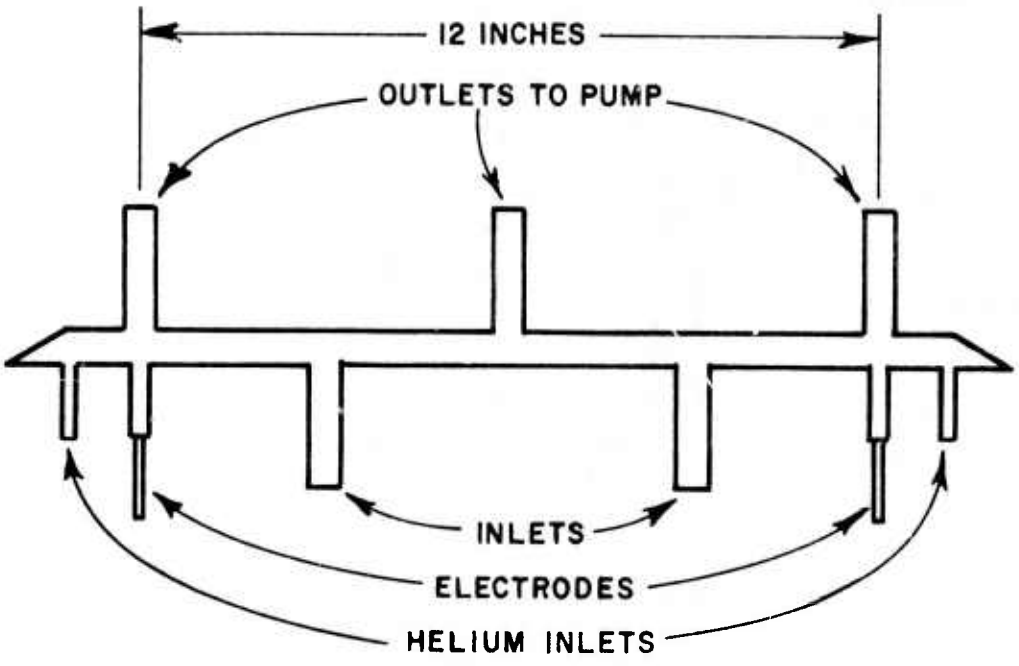

Fig. 39. Schematic diagram of second DF laser tube.

The new tube worked quite satisfactorily. The added helium flow at the windows not only had the expected effect of eliminating window contamination, but also the unexpected effect of reducing sulfur deposits in the tube. Thus the oxygen flow could be safely reduced to a point where the laser output was no longer affected. The helium flow rate past the windows was such that with the main gas mixture shut off the tube pressure was about 5 torr.

Both the output power and the pulse to pulse stability were somewhat improved with the new tube. The laser also operated on 30 lines instead of 25 with the added lines being primarily the lower rotational transitions of the 1-0 band. This may be because the helium flow at the windows removed unexcited DF from the optical path.

This second version of the laser worked reasonably well and most of the measurements described in the next chapter were made using this laser.

4. The portable DF laser

After operating the laser described above for a considerable time it was decided that a smaller more portable laser was needed. In particular a laser was needed which had very little RF noise generation, since the large shielded room was taking up much needed laboratory space. It was also felt that improved optical stability could be obtained if the laser could be mounted on the same table with the external optics.

The pulsed laser built by Ultee[18] used a different power supply design than that used in the Aerospace pulser. Ultee's power supply charged a 1 microfarad capacitor to about 600 volts and discharged it through a pulse transformer to get the high voltage required by the laser tube. This design has the advantage that the high-voltage pulses are restricted to the output of the pulse transformer and the laser tube. These components can be fairly easily shielded to eliminate RF noise emission. Using circuit diagrams provided by Ultee[19], a new pulser was constructed.

Also at this time a new tube was designed and built which had an active length of 20 centimeters and inside diameter of 5.5 millimeters. This compares to an active length of about 30 centimeters and inside diameter 8.5 millimeters for the previous tube. The new tube had one inlet at the center of the tube for the main gas mixture, and an exhaust port to either end as well as the helium inlet ports at the Brewster windows.

It had been observed on the previous laser that the copper electrodes became fouled after a period of time, particularly the one at the high voltage end. This could possibly have been copper

sulfate. A couple of different electrode configurations were tried to eliminate the fouling. The most satisfactory solution seems to be a nickel rod at the low voltage end and a tungsten rod at the high voltage end insulated with Teflon tape except at the tip.

The optical cavity for the new laser consisted of a 300 line/millimeter grating blazed at 3.5 μm and the same 20 meter radius of curvature germanium mirror used in the previous laser. The grating and end mirror were separated by 80 cm. The grating mount was of the same design as that used on the previous laser. The output mirror was mounted in a commercial gimbal mount as before, but there was no provision made for tuning the cavity length since it had been found to have little effect in the earlier laser.

The laser was constructed on a 3/4-inch aluminum plate, ten inches wide and thirty-nine inches long. Along one side of the laser was a 1/4-inch aluminum plate. Attached to the plate were a box containing the oscillator, feedthroughs for the gases and pumping port, and a vacuum gauge which reads the pressure at the exhaust ports of the laser tube. The mirror mount, grating mount, laser tube, storage capacitor, thyratron, and pulse transformer were all mounted on the base plate. There was an aluminum box attached to the base plate and side plate which enclosed everything but the mirror mount and grating mount. There were small holes in the ends of the box to let the laser beam out. Figure 40 shows the laser with the shield box removed.

Since the laser tube was not exactly the same as Ultee's, it was necessary to use a different pulse transformer and storage capacitor. The DC voltage to charge the capacitor is supplied by Power Designs Pacific, Inc., Model HV-1547 photomultiplier tube supply. The capacitor is charged to about 1200 to 1300 volts. Figure 41 shows the electrical schematic of the Ultee power supply as modified. Ultee used an E.G&G. Model TS-185 pulse transformer rather than an E.G&G. Model TS-146A and a one microfrad capacitor instead of a .333 μfd capacitor. When the laser is operating at 50 pulses per second the photomultiplier supply provides about 1600 volts at about 20 ma. The capacitor is charged to about 1250 volts since the charging time between pulses is 1.5 time constants.

The new laser completely eliminated the RF noise emission experienced with the earlier laser, and in addition the average power in the new laser was increased by a factor of four or five. Part of the increase comes from a faster pulse rate (50 pps rather than 35 pps) made possible because the tube was smaller and the vacuum pump was the same. Figure 42 shows a photograph of an oscilloscope trace of the pulse.

A laser very similar to that just described was built and loaned to Professor Rao of the Ohio State University Physics department so the laser line frequencies could be accurately determined using a very accurate grating spectrometer. Using the laser emission

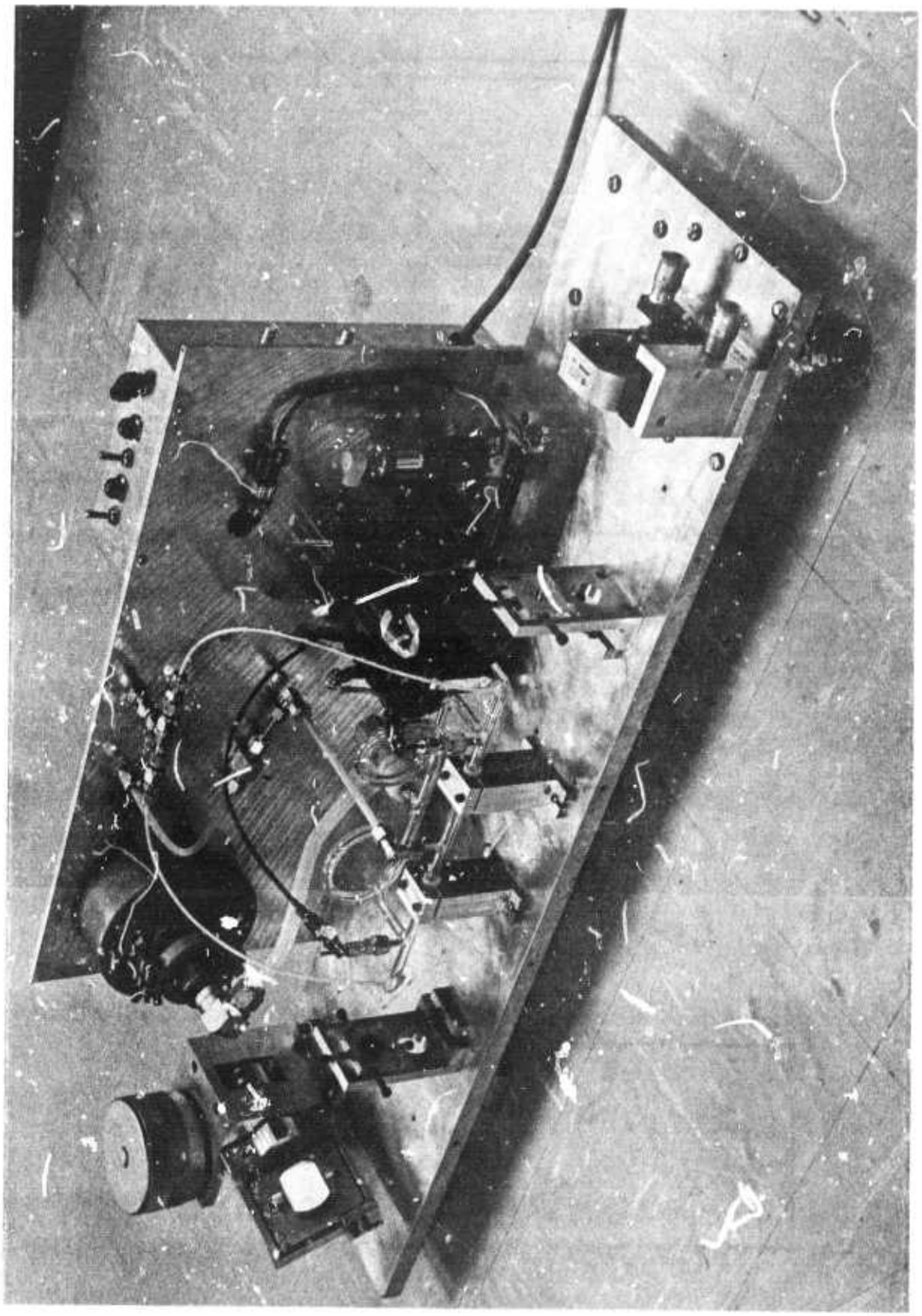

Fig. 40. Portable DF laser with shield box removed.

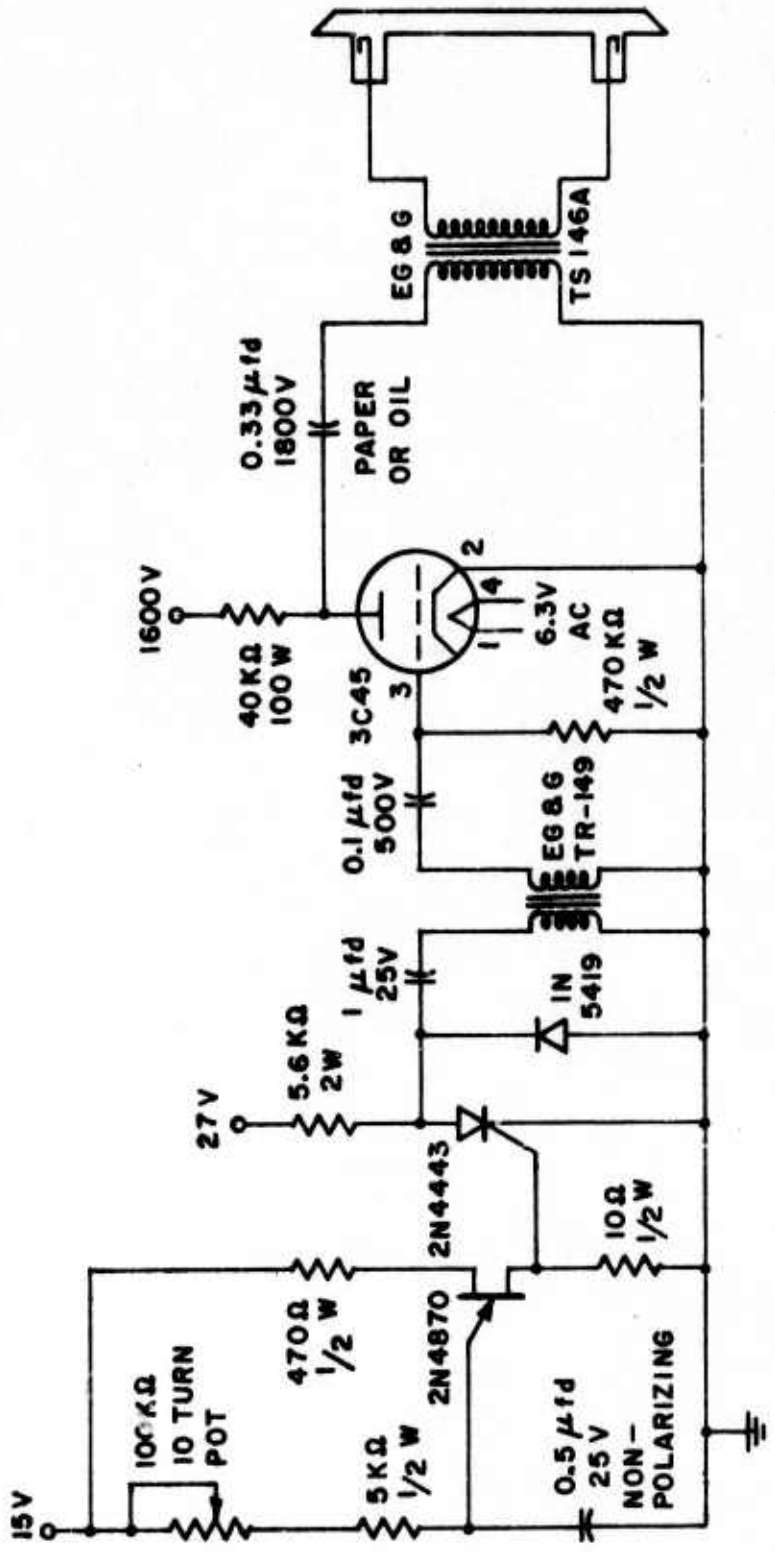

Fig. 41. Circuit diagram of the power supply for the portable, pulsed DF laser.

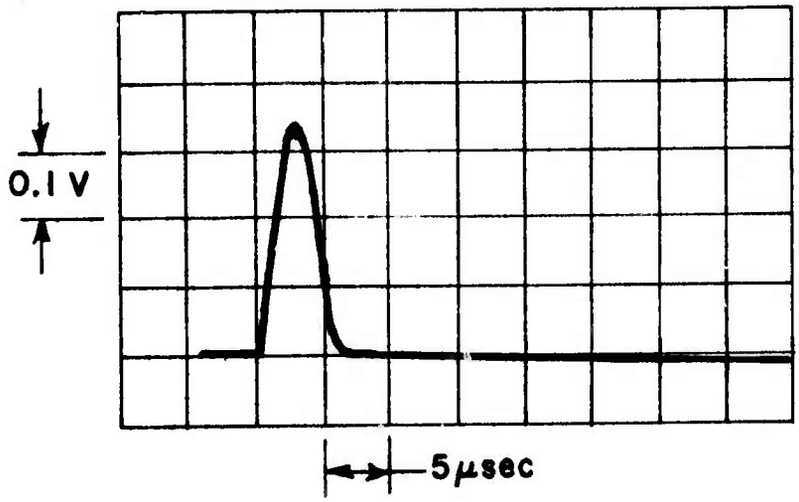

Fig. 42. Output of portable DF laser.

spectra in conjunction with DF absorption spectra, the values for the laser frequencies were determined to an accuracy of ± .003 cm^{-1}. These frequency values are given in Table 5 for each of the lines observed in the pulsed lasers described here.

B. Optics

The next important aspect of the experimental system is the optics necessary to focus the laser beam into the absorption cell and onto the detectors. There were two optical setups used, one with the DF laser mounted separately in a shielded room, and the other with the DF laser mounted on the main optical table with the White cell entrance optics.

The first optical layout to be described is the one used with the DF laser mounted separately in the screen room. This is the arrangement which was used in making most of the measurements described in the next chapter. The layout is shown schematically in Fig. 43.

The DF laser beam comes from the shielded room and is directed onto the main optical table by mirror M1. Mirror M2 is used to align a visible HeNe laser beam collinear with the DF laser beam and is removed during measurements. The N_2O cell and mirror M7 are used in detector calibration (described later) and are also removed during a measurement. The apertures are used as an aid in aligning the visible HeNe laser beam. Mirror M5 and M6 are used to direct the beam into the White cell. M6 is a spherical mirror with 0.76 m focal length which is positioned to focus the DF laser beam at the plane of mirror M10 in the absorption cell without overfilling mirror M11. The beamsplitter is an uncoated BaF_2 ½° wedge which reflects a small percentage of the incident beam to the reference detector which is positioned near the focal point of the beam. Mirrors M8 and M9 are used to direct the laser beam onto the signal detector after it has passed through the White cell, with M9 being used to focus the beam on the detector. All mirrors used in the system are aluminum coated first surface reflectors.

The proper position of the focusing mirrors M6 and M9 and the proper detector positions were determined with the aid of a computer program based on the optical resonator chart developed by Collins [20]. The program is a generalization of one written by Trusty[21], and calculates the spot size and distance from the focal point at any desired location in an optical system consisting of a laser and up to ten focusing elements (mirrors or lenses). A listing of the program is given in Appendix C.

The program assumes a laser resonator consisting of a flat mirror on one end and a spherical mirror at the output end. This is equivalent to a resonator with a flat grating on one end and a spherical output mirror such as the one used with the DF lasers described earlier. The program accounts for the fact that the output mirror is also a diverging lens when making the calculations.

TABLE 5
FREQUENCIES OF OBSERVED DF LASER LINES

Identification Band	Transition	Frequency (cm^{-1}) (a)	Identification Band	Transition	Frequency (cm^{-1}) (a)
1-0	P(2)	2862.653	2-1	P(8)	2631.068
1-0	P(3)	2839.791	2-1	P(9)	2605.807
1-0	P(4)	2816.380	2-1	P(10)	2580.097
1-0	P(5)	2792.434	2-1	P(11)	2553.953
1-0	P(6)	2767.968	2-1	P(12)	2527.391
1-0	P(7)	2742.998	2-1	P(13)	2500.428
1-0	P(8)	2717.539			
1-0	P(9)	2691.607	3-2	P(2)	2683.890
1-0	P(10)	2665.219	3-2	P(3)	2662.246
1-0	P(11)	2638.392	3-2	P(4)	2640.074
1-0	P(12)	2611.142	3-2	P(5)	2617.386
1-0	P(13)	2583.486	3-2	P(6)	2594.198
			3-2	P(7)	2570.522
2-1	P(2)	2772.340	3-2	P(8)	2546.375
2-1	P(3)	2750.094	3-2	P(9)	2521.769
2-1	P(4)	2727.309	3-2	P(10)	2496.721
2-1	P(5)	2703.999	3-2	P(11)	2471.245
2-1	P(6)	2680.179	3-2	P(12)	2445.356
2-1	P(7)	2655.863	3-2	P(13)	2419.070

(a) Frequencies determined to ± 0.003 cm^{-1} by Heath, et.al[18]

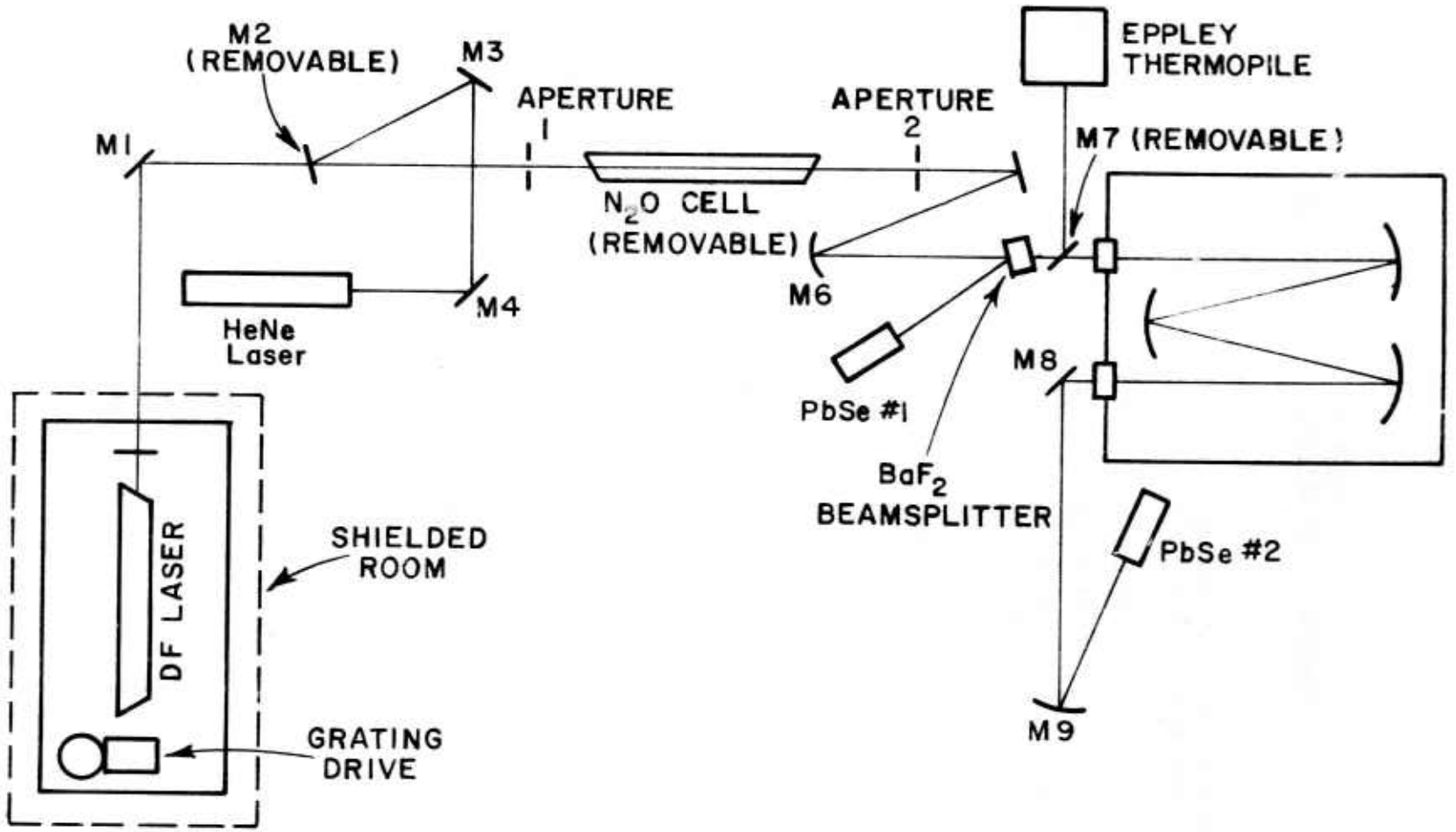

Fig. 43. Block diagram of the optics used with the DF laser located in the shielded room.

Aligning the HeNe laser beam collinear with the DF laser beam was rather difficult since the DF laser beam was invisible and the average power was too low to permit using the fluorescent screens which are useful in observing higher power infrared laser beams.

The first alignment method made use of an uncoated calcium fluoride flat in place of mirror M2 in Fig. 43. A small hand held lead selenide detector was used to find the approximate location of the DF laser beam on the calcium fluoride flat. Mirror M3 was then used to direct the visible laser beam to that spot. Then the small detector was used to find the location of the DF laser beam near mirror M5. The calcium fluoride flat was adjusted so that the HeNe laser beam struck the small detector. The coincidence of the HeNe and DF laser beams was then checked again near the calcium fluoride flat and mirror M3 used again to refine the alignment of the visible beam. If adjustment was required, the alignment was again checked near mirror M5 and adjusted if necessary. The last two steps in the alignment were repeated until the alignment of the two laser beams was as close as possible.

This method proved to be somewhat unsatisfactory since the DF laser spot was fairly large and the center of the spot was difficult to determine.

The second method and the one which proved to be most satisfactory made use of the adjustable apertures shown in Fig. 43. The idea is to exactly center the apertures on the DF laser beam with mirror M2 removed and then insert mirror M2 and adjust M2 and M3 so that the helium neon laser beam goes exactly through the apertures.

The difficult part of this method is getting the apertures centered properly on the DF laser beam.

The DF laser beam was directed to the reference detector using the small handheld detector to make sure the beam fell entirely on M1, M5, M6, and the barium fluoride (BaF_2) beamsplitter. The beamsplitter was then adjusted for maximum signal on the reference detector. The reference detector was located near the focus of the DF laser beam and was large enough to collect the entire beam.

The location and approximate size of the DF laser beam at the apertures was determined by observing the reference detector signal as the beam was obstructed by slowly moving a card into the beam from the top and bottom and from either side. Using this technique, the apertures could be accurately positioned.

With the HeNe laser beam adjusted collinear with the DF laser beam and the apertures opened up, the rest of the optical alignment could be performed rather easily using the HeNe laser beam as the visible reference.

Mirrors M5 and M6 were used to direct the beam into the White cell properly. The White cell was adjusted to the desired path length using the HeNe laser as a reference. The BaF_2 beamsplitter was then adjusted to direct the HeNe laser beam to the reference detector, and mirrors M8 and M9 were used to direct the laser beam to the signal detector after it had passed through the White cell. Fine adjustment of the detector alignment was made with mirror M2 removed and the DF laser operating.

The second optical layout (Fig. 44) is the one used when the DF laser was mounted on the main optical table with the White cell entrance optics.

The apertures were used to align the visible HeNe laser beam collinear with the DF laser as before.

Since the DF laser used in this configuration had more average power, Eppley thermopiles were used as the reference and signal detectors. Because the Eppley thermopiles are relatively slow they could not be easily used to adjust the DF laser for optimum operation on a desired line. Therefore provision was made for directing the reference beam to a lead selenide detector for laser adjustment and to the Eppley thermopile for absorption measurements. This was done by mounting mirror M7 on a kinematic mount which could be removed and replaced without affecting the optical alignment.

C. Detectors

Early attempts to measure absorption in the White cell with the first pulsed laser made use of Eppley thermopiles as the reference and signal detectors. The average laser power was too low however and air currents and temperature changes in the room caused detector responses which were a noticable fraction of the laser signal. This resulted in a low signal to noise ratio and very poor repeatability in the measurements. It was necessary therefore to use fast detectors which could respond to the peak laser power in each pulse rather than the average power.

The first fast detectors used were mercury cadmium telluride photoconductive detectors manufactured by Mullard Inc. The detectors had an operating temperature range of 273-300°K, a time constant of 0.15 μsec, and were .25 mm square. The detectors had adequate sensitivity, however their small size made it necessary that the optical alignment be very closely maintained. This is almost impossible, particularly at the output of the absorption cell after the beam has traveled three-fourths of a kilometer or more.

The next detectors were lead selenide photoconductive detectors manufactured by Santa Barbara Research Center. These detectors operated at ambient temperature ($\sim$ 296°K) with a time constant of

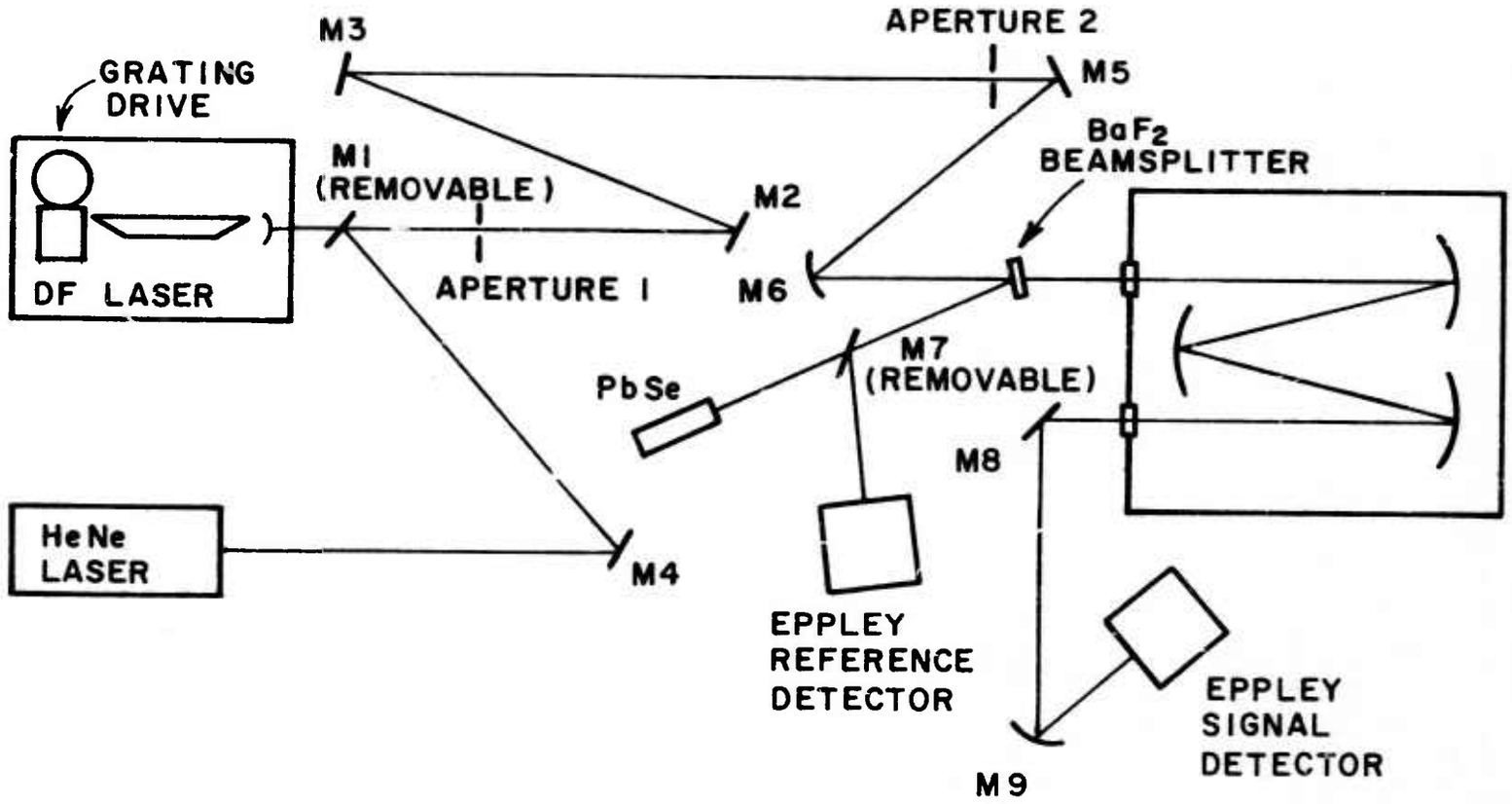

Fig. 44. Block diagram of the optics used with the portable DF laser mounted on the main optics table.

1-3 μsec and were 4 mm square. These detectors also had the required sensitivity and their relatively large size made alignment less critical, although great care was still needed.

The use of pulse detectors presented three additional problems. The pulse to pulse instability of the laser made it necessary to use pulse averaging electronics, and the propagation delay of about 2.5 microseconds in the absorption cell made it necessary to look at the reference and signal pulses at different times or to "save" the reference pulse. The solution to these problems is discussed in the next section.

The third problem was the possibility of detector non-linearity. Although the average laser power was only about 1 milliwatt, the peak pulse power was about 25 or 30 watts. Accounting for the fact that the reference detector received a small percentage of this power and the signal detector only about a fourth (because of White cell insertion loss), the detectors still received from 1 to about 8 watts peak power.

The possibility of detector non-linearity was investigated by intercomparing the reference detector with an Eppley thermopile. While the thermopile detectors could not be used to make the absorption measurements because of the low reflectivity of the beamsplitter and White cell insertion loss, it was possible to use a thermopile to make the detector comparison by placing it where it received most of the laser power. The Eppley thermopile was known to be linear in this low average power region, so if the lead selenide detector was also linear, a plot of voltage from the thermopile detector versus voltage from the lead selenide detector would be a straight line. In fact the relationship observed was not a straight line, so the lead selenide detector was indeed non-linear as suspected.

The detectors were calibrated against the Eppley thermopile using the following procedure.

The experimental layout is that shown in Fig. 43. The idea is to compare the reference detector PbSe #1 to the Eppley thermopile over a wide range of signal levels with mirror M7 in place. Then the mirror is removed and the reference detector and signal detector PbSe #2 are compared with the White cell evacuated.

At first it was thought that the signal level to the detectors could be changed by changing the gas mix and excitation voltage in the laser. This procedure gave unsatisfactory and unrepeatable results. This could have been caused by pulse shape changes as gas mix and discharge voltage are changed since the electronics associated with the lead selenide detectors responded to only the peak of the pulse while the thermopile responded to the energy in the pulse.

It was necessary therefore to use an external attenuator and leave the laser undisturbed during the calibration runs. The signal to the detectors was attenuated step by step by introducing N_2O into the 21 cm cell shown in Fig. 43. The first part of the experiment comparing the thermopile and the reference detector PbSe #1 was repeated three times on three separate days, as was the second part of the experiment comparing the reference detector and the signal detector PbSe #2. At each signal level the signals from the two detectors were read and recorded on the typewriter by the computer using the data taking program which will be described later.

A least squares fit of the data from the first part of the experiment was made to a third-order polynomial. This results in an expression of the form

$$E_1 = A_0 + A_1 X_1 + A_2 X_1^2 + A_3 X_1^3 \tag{107}$$

relating the reference detector voltage X_1 to the Eppley thermopile voltage E_1 (Fig. 45). The voltages are those read by the computer after arbitrary fixed amplifications.

Similarly the data from the second part of the experiment was used to obtain an expression of the form

$$X_1 = C_0 + C_1 X_2 + C_2 X_2^2 + C_3 X_2^3 \tag{108}$$

where X_2 is the signal detector voltage as read by the computer and X_1 is the reference detector voltage (Fig. 46).

From Eqs. (107) and (108) the following expression relating the signal detector voltage X_2 to an equivalent Eppley voltage E_2 was determined (Fig. 47):

$$E_2 = B_0 + B_1 X_2 + B_2 X_2^2 + B_3 X_2^3 \tag{109}$$

The linearity correction expressions determined by the above procedure were tested by incorporating them into the data-taking program and repeating the second part of the calibration experiment. At each signal level the computer read the voltages X_1 and X_2 from the reference and signal detectors and used Eqs. (107) and (109) to determine E_1 and E_2 respectively. If the linearity corrections are good, a plot of E_2 versus E_1 should be a straight line. Figure 48 shows that this was indeed the case.

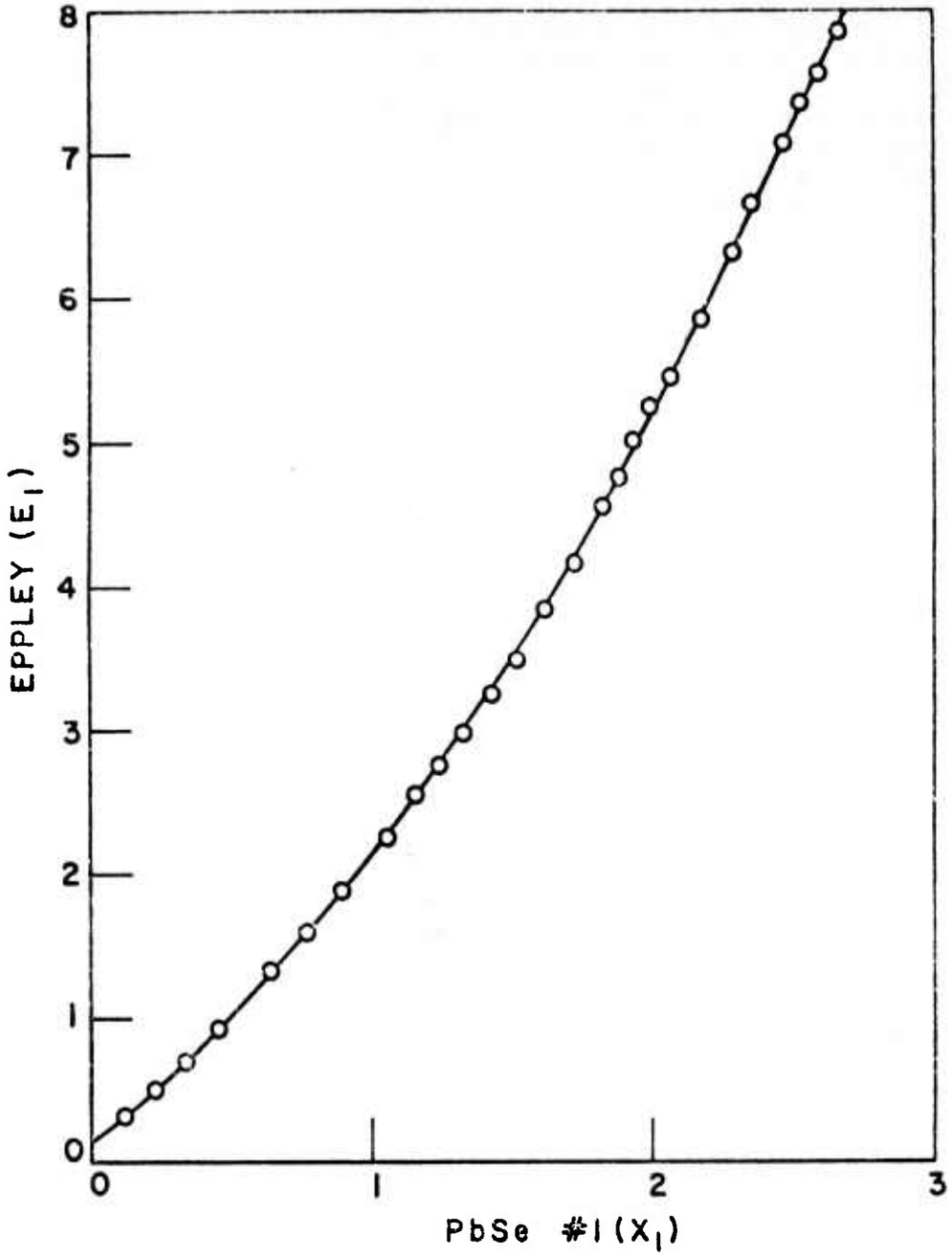

Fig. 45. Eppley thermopile calibration signal versus lead selenide detector number one. Units are volts at A/D converter after arbitrary amplifications.

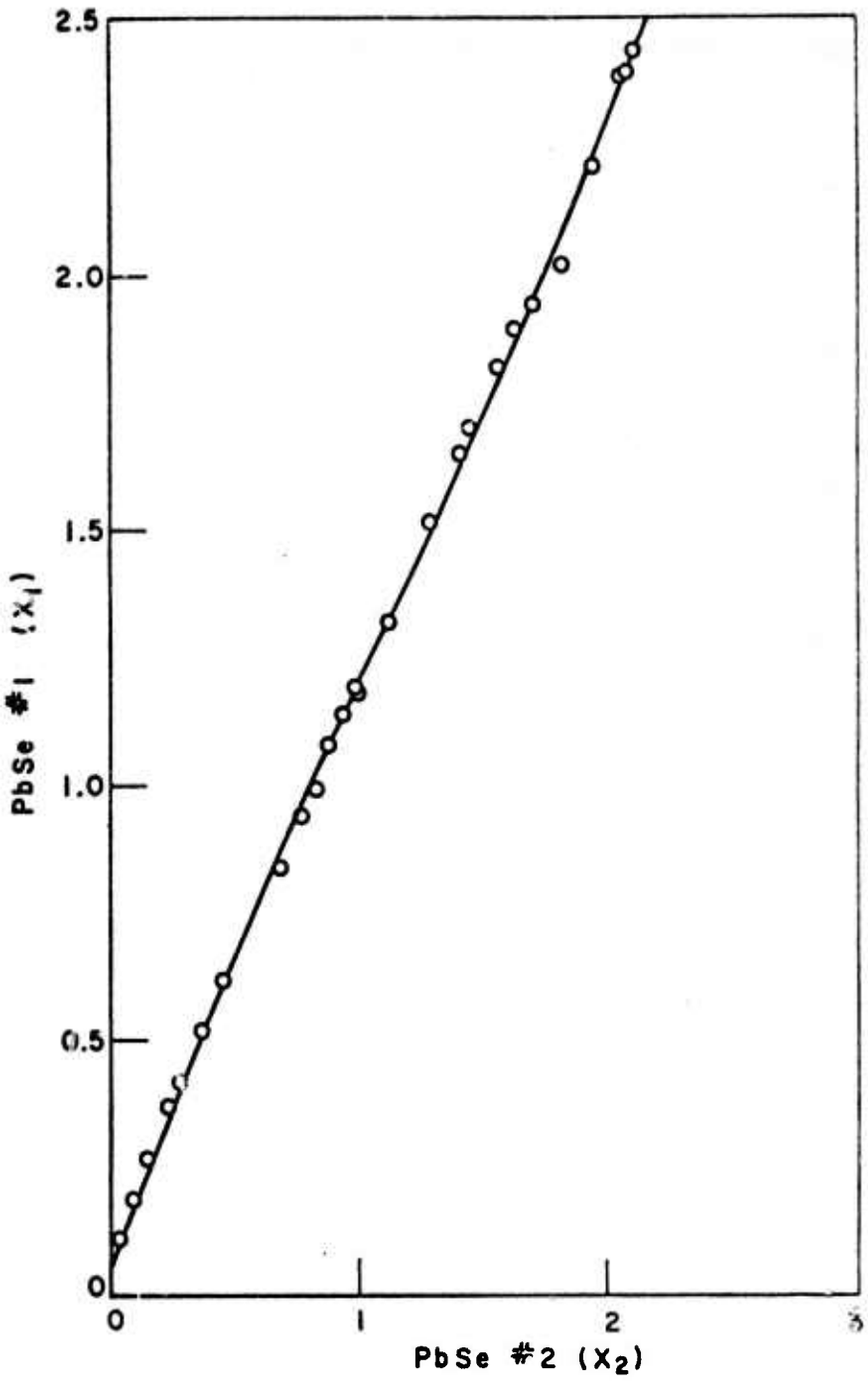

Fig. 46. Calibration of lead selenide detector #2 in terms of lead selenide detector #1. Units are volts at A/D converter after arbitrary amplification.

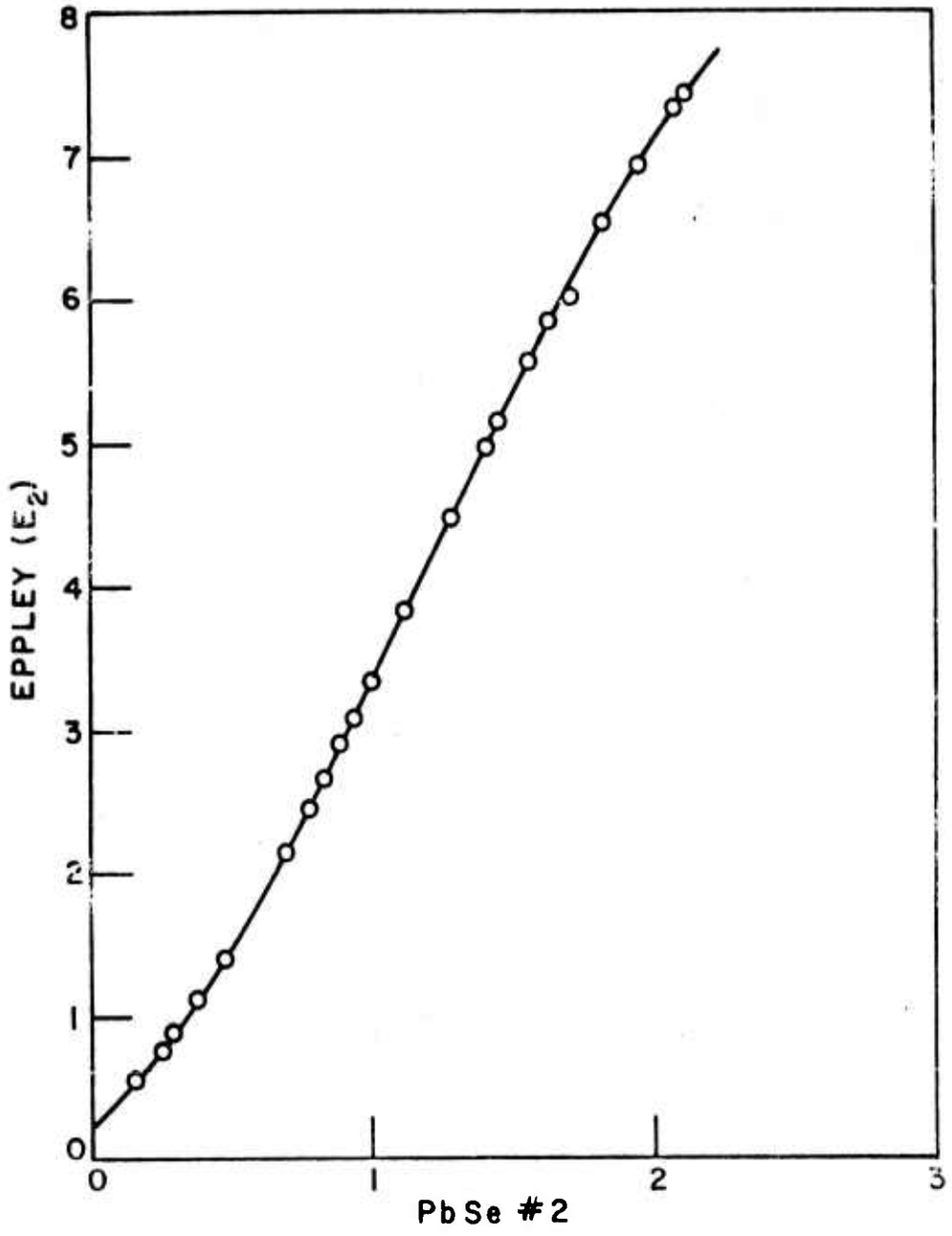

Fig. 47. Derived curve relating PbSe #2 detector to Eppley thermopile. Units are volts at A/D converter after arbitrary amplifications.

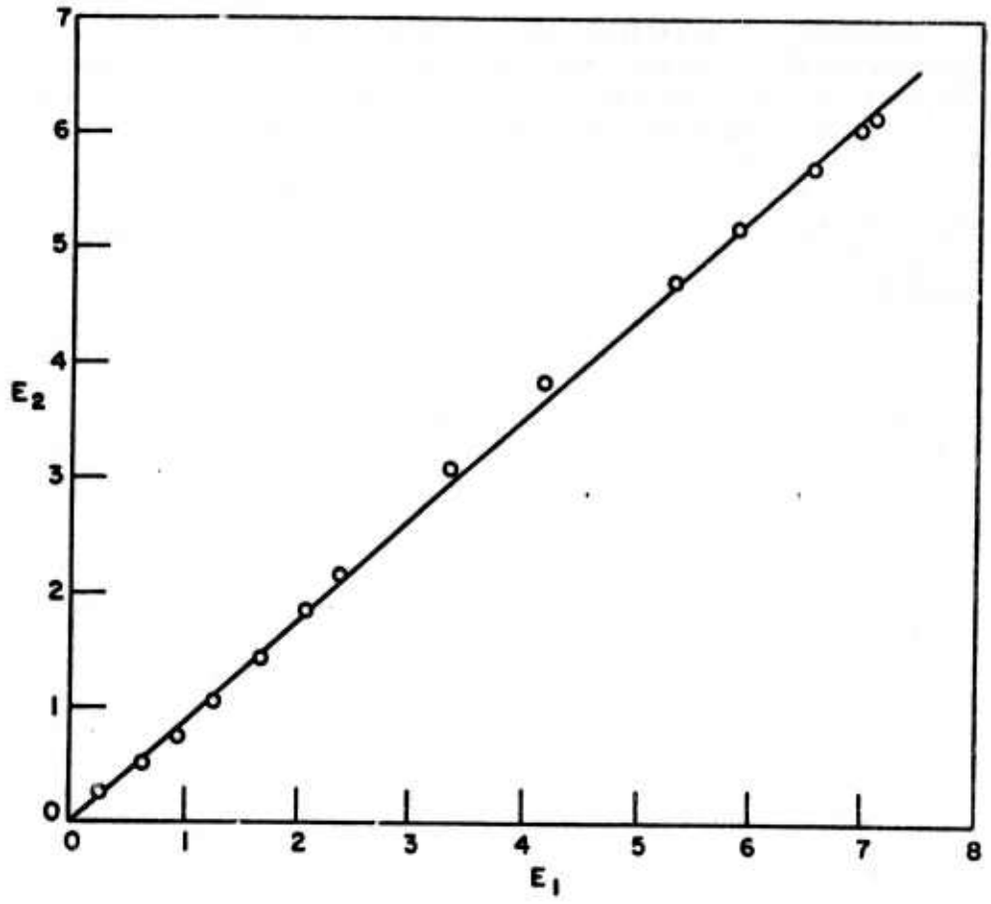

Fig. 48. Results of experiment to check calibration linearity.

The first attempt to determine the linearity correction used quadratic rather than cubic expressions. It was found, however, that the quadratic expressions were not sufficient to correct the nonlinearity.

Subsequent calibrations used a somewhat different procedure. The experimental technique used was the same. However, before the second part of the experiment was performed, the data from the first part of the experiment was used to obtain the expression in Eq. (107). This expression was incorporated into the data taking program. The data from the second part of the experiment was then in the form corresponding to Fig. 47 or Eq. (109) rather than Fig. 46 or Eq. (108). The two procedures yield the same results, however the second requires less hand manipulation of the data.

The detectors described above were used with the original laser mounted in the shielded room. The small portable laser which was built later could be mounted on the main optical table and had four or five times as much average power. This made possible the use of thermopile detectors. This was desirable since the thermopile detectors respond to the average laser power and they are known to be linear in the low average power region.

Some care was required in the use of the thermopile detectors since they readily respond to room temperature fluctuations and air currents. To help eliminate these problems the thermopiles were each encased in a 4 inch block of styrofoam with a small hole to admit the laser beam. Boxes were also constructed of 1 inch thick styrofoam to completely enclose the detectors, with a small hole cut in the boxes to admit the laser beam.

The styrofoam boxes and insulating blocks protected the detectors from short term temperature fluctuations and air currents. However the detectors did respond to long term temperature changes. Therefore if the room thermostat setting was changed or a heat load was suddenly introduced in the room it was necessary to wait until the temperature had stabilized before attempting to make measurements. This usually took no more than thirty minutes to an hour.

D. Electronics

Another important part of the system was the electronics used to amplify and record the detector signals. There were two separate systems used with the two different types of detectors. The lead selenide detectors which were fast enough to respond to each laser pulse required the use of commercial box-car integrators and some other specially built electronics. The Eppley thermopiles were relatively slow and therefore responded only to the average laser power. DC amplifiers were used with these detectors. The output of the electronics in either case was read by an XDS 920 computer through a 24 channel, 14 bit A/D converter.

The boxcar integrators and associated electronics will be described in part 1, the DC amplifiers will be described in part 2, and the computer and A/D converter will be described in part 3 below.

1. Boxcar integrators and associated electronics

Boxcar integrators were needed with the fast lead selenide detectors for two reasons: 1) to average out variations caused by pulse to pulse instability and 2) to provide a DC voltage proportional to the pulse height which could be read by the computer.

A block diagram of the pulse detector electronics is shown in Fig. 49. The pulse amplifiers, dual gate generator, and differential gated integrators were manufactured by Molectron Corporation. The 2-channel peak holding circuit, the optical trigger coupler, and the detector bias circuits, were specially built for this particular experiment.

The key components of the system are the differential integrators (Molectron Mdl. 112). Typical operation of one of the differential gated integrators is depicted in Fig. 50 and Fig. 51.

The diode bridges are back-biased when the gates are off. When a gate is on (gate input greater than 2 volts) the diode bridge is forward biased and the integrator side of the bridge follows the signal side. Thus if the voltage on the integrator capacitor is less than the signal voltage, current flows from the bridge to charge the capacitor, and if the signal voltage is less than the capacitor voltage, the capacitor discharges. In the back-biased mode the diodes have extremely high impedance, and the buffer amplifier following the integrator has extremely high impedance. These factors reduce leakage currents from the integrating capacitor to less than 0.5 picoamperes.

The integrating time constant is selected by changing R and C in the integrator. If the input is a continuous string of pulses as shown in Fig. 51, and the two gates are adjusted as shown, the output is just the pulse height and varies with a time constant equal to $RC(T/\tau_g)$.

The gate pulses and the input signal are superimposed at the monitor jack for convenience in adjusting the gate timing. The signal at the monitor jack is one tenth the input signal and the gate pulses are fixed at 25 millivolts.

The time constants of the integrators in both channels are matched to within 0.5%

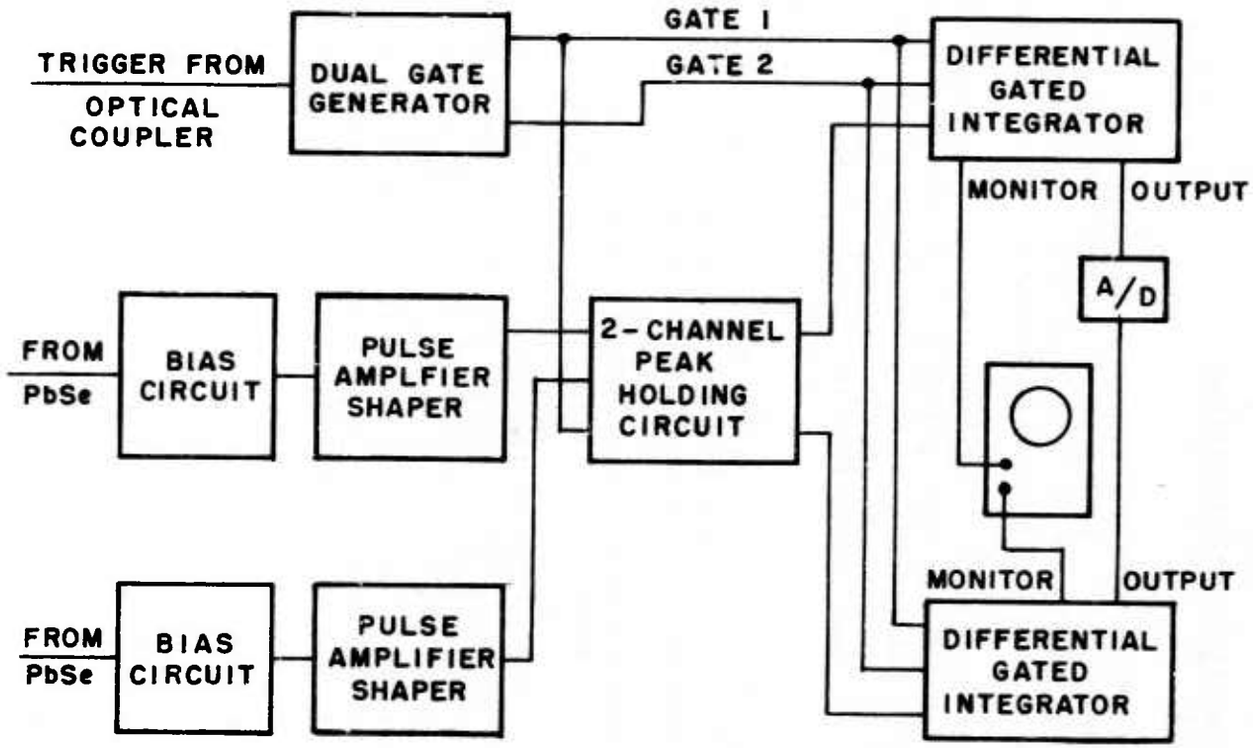

Fig. 49. Block diagram of pulse detector electronics.

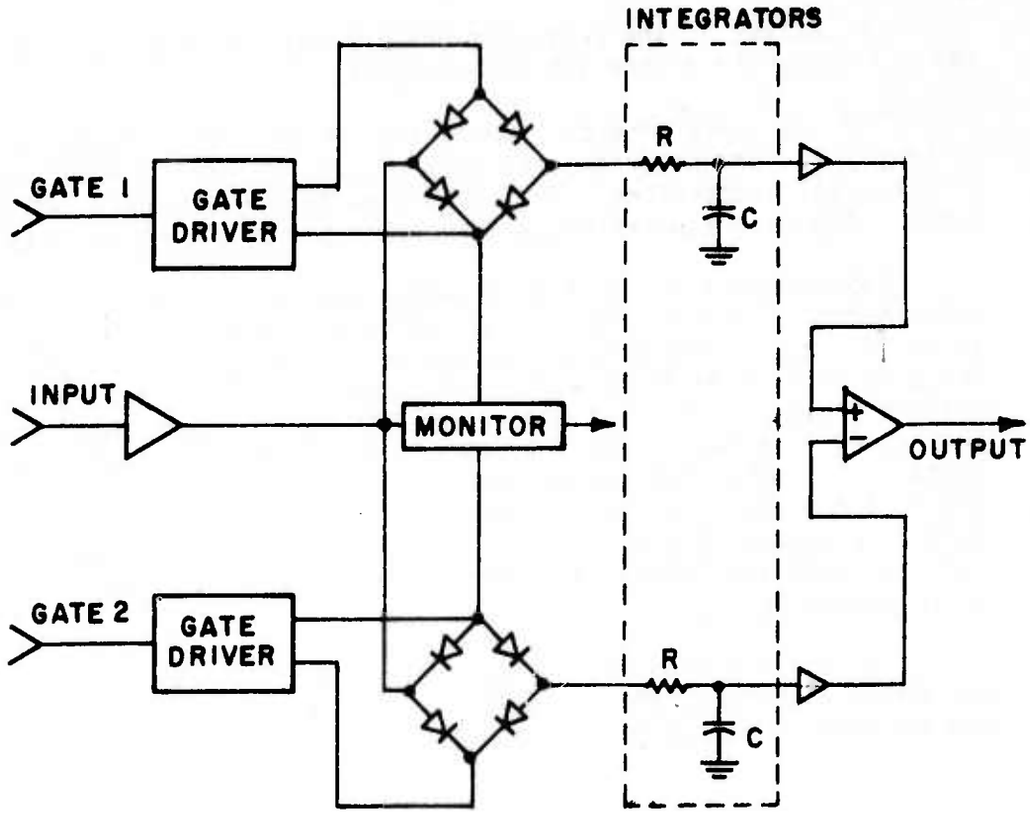

Fig. 50. Block diagram showing gated integrator operation.

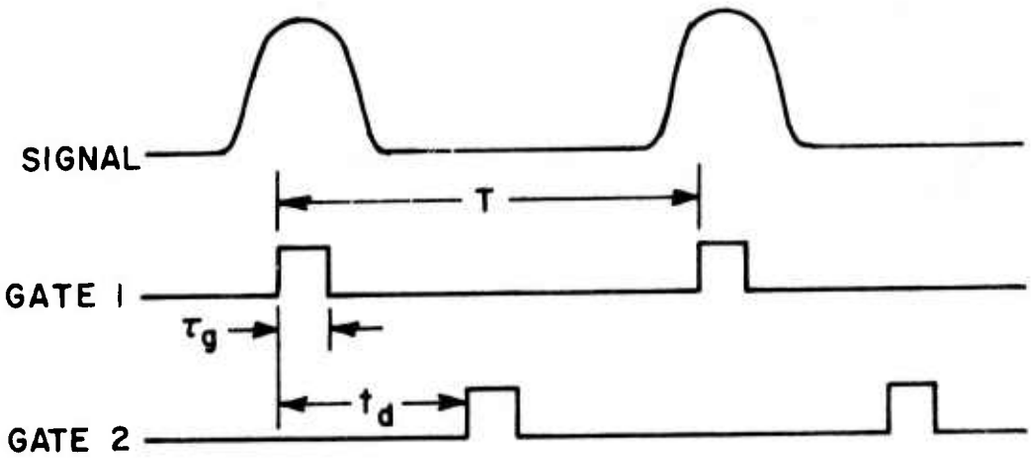

Fig. 51. Gated integrator signal timing diagram.

The output of the gated integrators was fed directly into the A/D converter on the XDS 920 computer.

The dual gate generator (Molectron Model 122) accepted the trigger pulse and generated the gate signals required by the two differential integrators. The delay time from the trigger pulse to gate 1, the gate separation, and the gate width are all adjustable.

The response of the lead selenide photoconductive detectors to an increase in the intensity of infrared radiation striking them is an increase in electrical conductivity. The primary purpose of the bias circuit is to convert this increase in conductivity to a voltage change. A circuit diagram of the bias circuits used in this study is shown in Fig. 52. R1 is adjusted to maintain the bias voltage at 160v as the battery ages, C1 is a filter capacitor, R2 is the load resistor, C2 insures that the steady state voltage at the output connector is zero, R3 and C3 integrate the pulse, and S2 is used to short the output and prevent high voltage transients when S1 is opened or closed.

The signals from the detector bias circuits were processed by the pulse amplifiers (Molectron Model 131) which shaped the pulses and amplified them up to five volts.

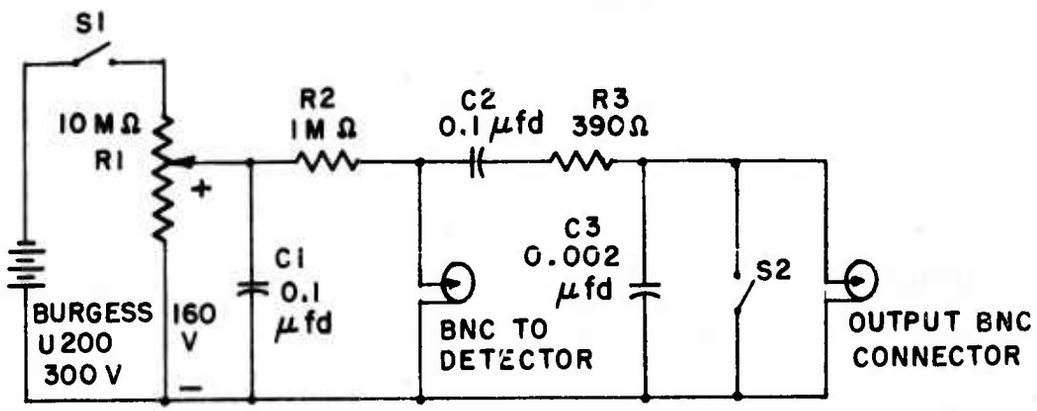

Fig. 52. Lead selenide detector bias circuit diagram.

One problem which had to be solved was the delay between the reference pulse and the signal pulse caused by the transit time of the White cell. The solution to this problem was a peak-holding circuit which held the peak of each pulse until after gate 1 was off. This circuit is shown in Fig. 53. When the input voltage exceeds the output voltage D1 conducts and charges C1 to the new input voltage. As the input voltage decreases, D1 becomes reversed biased and the peak voltage is held on C1 (discharging slowly through R5). R1 in series with D1 limits the charging current. To discharge C1, a positive pulse of approximately 2 volts (Gate 1) is applied to the reset terminal. Q1 inverts the reset pulse and C2 and R4 differentiate the inverted reset pulse. D2 suppresses the negative spike from the differentiator (caused by the leading edge of the reset pulse). The positive spike (caused by the trailing edge of the reset pulse) causes the two FET's to conduct and discharge the storage capacitors C1.

Another problem was caused by the very large high frequency noise associated with the trigger pulse from the laser. An attempt was made to suppress the noise with an RC filter. This attempt was unsuccessful. The trigger pulse was then coupled optically through the screen room wall using an LED and a photo transistor as shown in Fig. 54. This optically coupled trigger worked quite well and eliminated the noise completely.

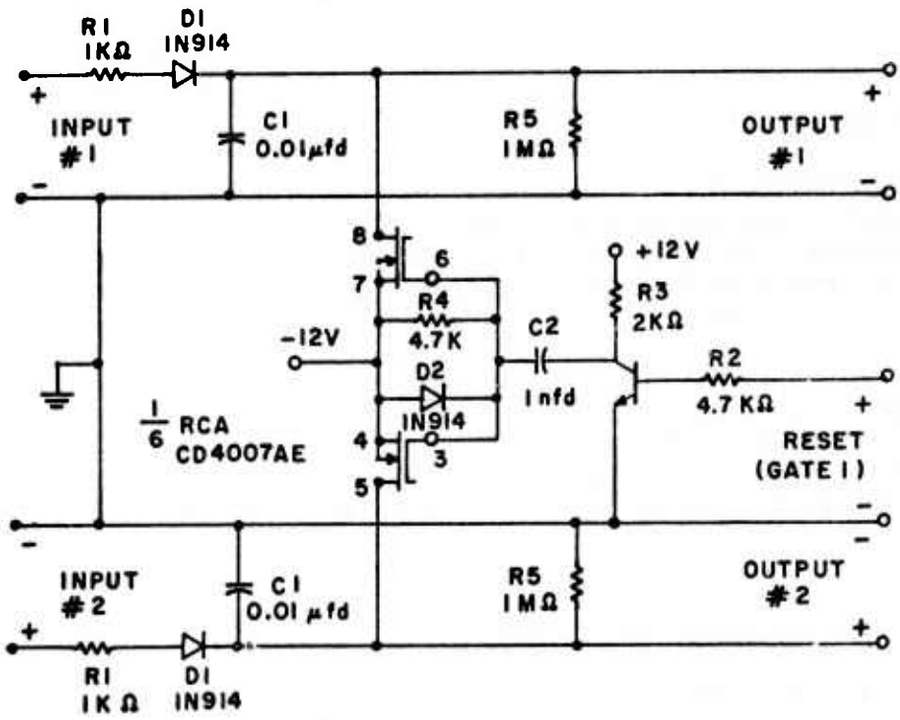

Fig. 53. Peak holding circuit diagram.

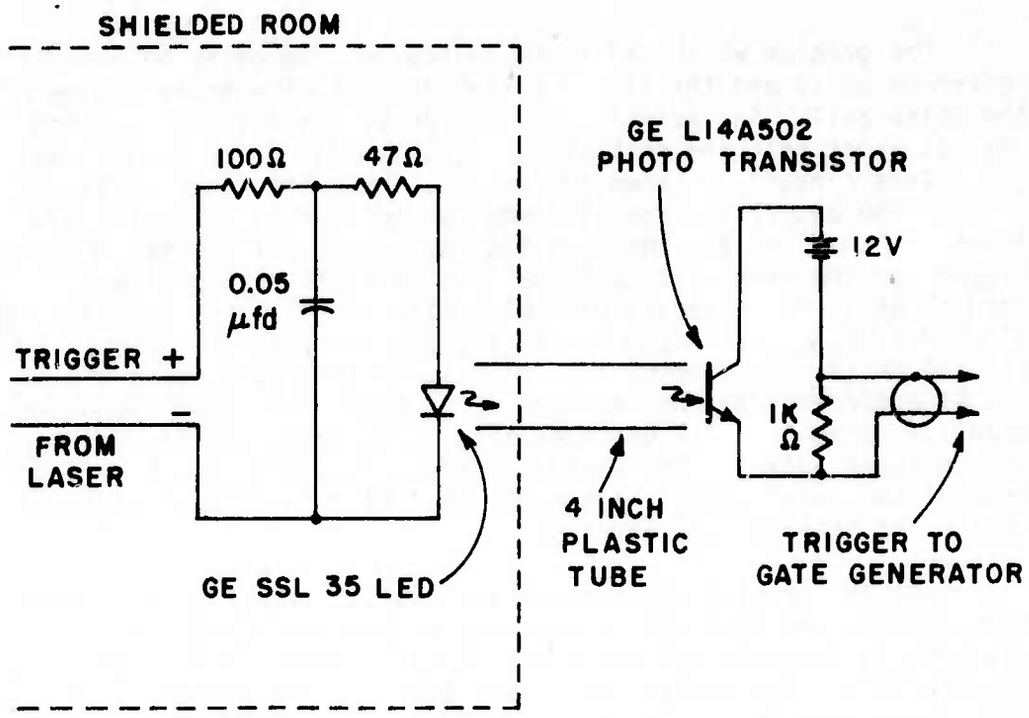

Fig. 54. Optical trigger circuit diagram.

2. DC amplifiers

When the thermopiles were used, the required electronics was much simpler since the only requirement was that the thermopile signal be amplified to about a plus or minus ten volt range without introducing noise so that full advantage could be taken of the A/D converter resolution.

The signals were first fed into HP425A microvoltmeters whose output was a maximum of plus or minus one volt. The outputs of the microvoltmeters were then amplified to plus or minus ten volts by Alinco Model 518A differential amplifiers. The output of the Alinco amplifiers was read directly by the A/D converter on the XDS 920 computer.

3. A/D converter and computer

The XDS 920 computer used in this experiment has 4096 24 - bit words of core memory with a cycle time of 8 microseconds and a fairly powerful instruction set,and input/output capability which makes it easily adaptable to laboratory experimental applications.

The cycle time of 8 microseconds is slow compared with modern computers, however the speed is quite adequate for the present application.

The analog to digital converter was manufactured by Epsco, Incorporated. It has a 24 channel multiplexer with an input impedance of 100,000 ohms and an input range from -10 to 10 volts. The digital output word is 14 bits long which means the resolution is about 1.24 millivolts per bit.

Programs for the computer are written primarily in Fortran except for some subroutines which control special devices such as the analog to digital converter which are written in assembly language. The program used to take the data in this study is described in the next chapter along with the experimental procedure.

E. The Absorption Cell

The absorption cell used in this study was originally designed and built by Long[22]. The cell is 0.61 meter in diameter and 16.15 meters long with a sample volume of 4.72 cubic meters or 4720 liters. The cell walls were honed smooth during construction in order to reduce water vapor adsorption effects.

Path lengths of well over one kilometer are easily obtainable in the cell using a three mirror optical system of the type first described by White[23]. The White optical system used in this cell is shown in Fig. 55. The mirrors all have a radius of curvature of 15.24 meters, and mirrors A and B are separated from mirror C by the common radius of curvature 15.24 meters. Mirrors A and B were obtained by cutting a 51 centimeter diameter mirror into two halves. Mirror C is 30.48 centimeters in diameter with notches cut out as shown for the entrance and exit beams.

The number of traversals and hence the path length is adjusted by tilting mirrors A and B as shown in Fig. 55. The external optics are adjusted so that the incoming laser beam is focused just as it passes the front surface of mirror C and with proper optics external to the cell it diverges to almost fill mirror A. The White optical system then has the property that the beam is focused at the plane of mirror C after every second traversal of the cell if the distance from mirror C to mirrors A and B is exactly the radius of curvature of mirrors A and B. The number of traversals is determined by counting the spots on mirror C. The number of traversals is just two more than twice the number of spots.

The entrance and exit windows of the cell are barium fluoride half-degree wedges. Wedges are used rather than flats to eliminate interference effects.

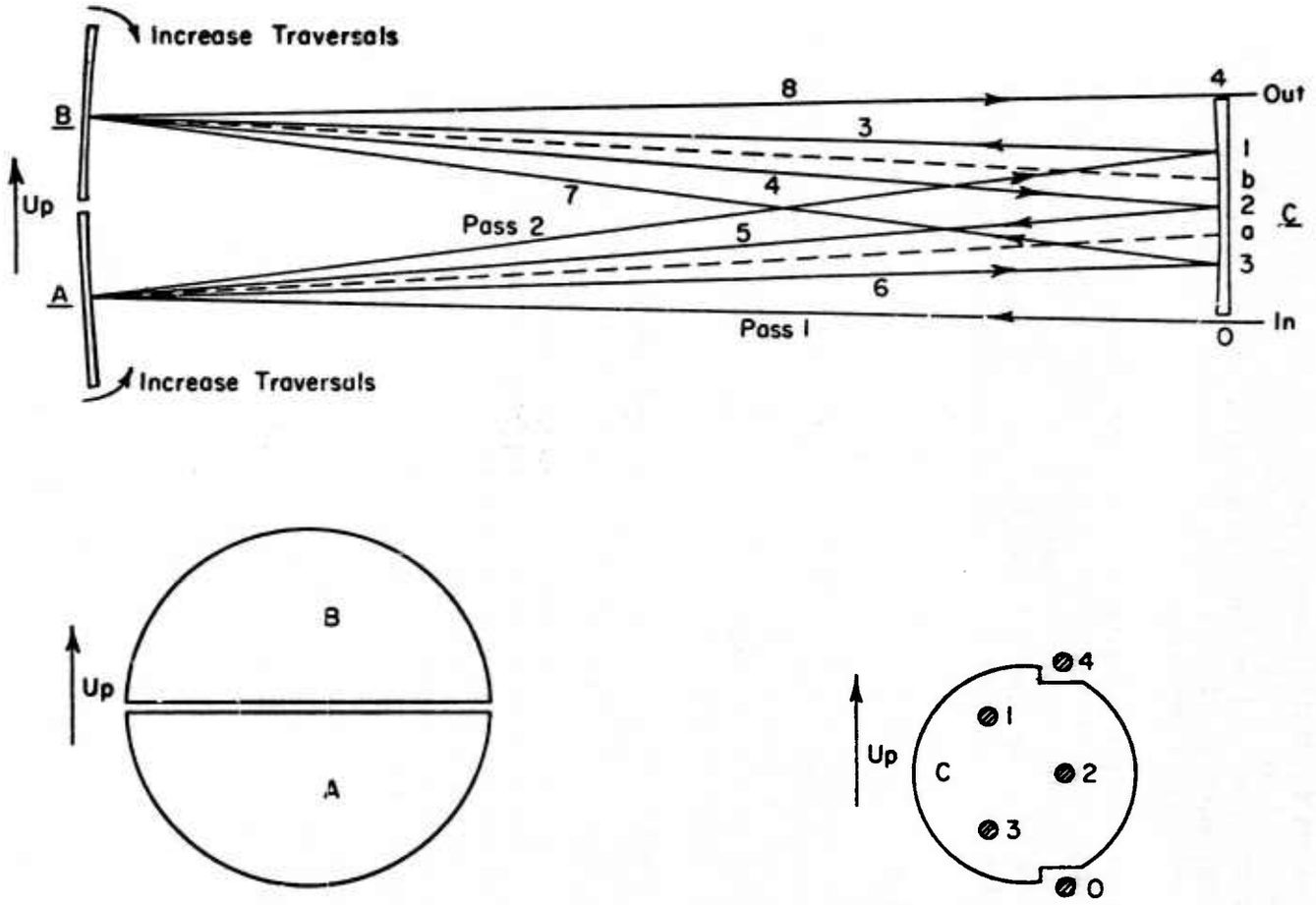

Fig. 55. Ray diagram of White cell (8 traversals).

For most of the measurements reported in the next chapter, the cell was set for 48 traversals or 731.7 meters. For some of the measurements however a longer path was required. The cell was therefore set at 88 traversals or 1.341 kilometers. It was discovered that at the longer path length the output spot was so large that the spots on mirror C overlapped. Using the spot size program described earlier, it was discovered that a small error in mirror separation would cause the spot on mirror C to become larger as the number of traversals became greater.

The mirror separation was then adjusted using a white light source. An image was formed at point O in the plane of mirror C which then diverged to fill mirror A. The image was observed in the plane of mirror C at the output with the cell set for 64 passes. The mirror separation was then adjusted to make that image as sharp as possible. It was found that the mirrors had been about 1 cm too far apart. Since the mirror separation is 15.24 meters, this is not a large error. It does however cause problems if long path lengths are desired.

From the above discussion it is obvious that for a White cell which is designed to be either heated or cooled some provision must be made in the design for keeping the mirrors properly separated as the cell expands and contracts.

The cell is evacuated using a 100 cubic foot per minute mechanical pump and a six inch diffusion pump connected near the center of the cell through pneumatically operated valves.

Gases are admitted to the cell through three ports located near the center of the cell and at each end. The ports are connected to a common manifold where various gases can be admitteed.

There are two small fans, one at each end, inside the cell to aid in mixing the gas samples.

There are several different types of vacuum gauges attached to the cell. The vacuum pumps' operation is monitored by a set of thermocouple gauges and an Alphatron 530 gauge. Gas sample pressure is monitored by three separate mercury gauges. Sample pressures up to two torr were measured with a McLeod gauge. Sample pressures from 1 torr to 50 torr are measured with a Roger Gilmont Instruments Model 906 mercury micrometric manometer. This instrument can be read to .025 torr. Pressures up to 1000 torr are measured with a U-tube manometer which can be read to 1 torr.

The dew-point of the water vapor-air or water vapor-nitrogen mixtures was measured with a dew-point hygrometer which optically senses the formation of dew or frost on a thermo-electrically cooled metal mirror. Two different hygrometers were used. One was a Cambridge Systems Model 880 which used a precision aged thermistor to

measure the dew-point temperature. This instrument was calibrated against a mercury micrometric manometer in this laboratory. The other hygrometer used was a Cambridge Systems Model 992 which used a precision platinum resistance thermometer to sense the dew-point temperature. The calibration on this instrument is traceable to the National Bureau of Standards.

The cell temperature was monitored using Stow Laboratories platinum resistance thermometers installed near the center of the cell and at either end.

Also connected to the cell was a mass spectrometer residual gas analyzer which could be used to monitor the composition of a gas sample over a period of time to determine whether selective adsorption might be occurring.

CHAPTER IV

DISCUSSION OF MEASUREMENTS

Absorption measurements were made for five absorbers and eight different DF laser lines. The absorbers studied were N_2O, CH_4, CO_2, HDO, and H_2O. The laser lines studied were the 2-1 P(6), P(7), P(8), P(10), and P(11) lines and the 3-2 P(6), P(7), and P(8) lines.

Absorption by all constituents was not measured for each line. For the 2-1 P(6) - P(8) lines and the 3-2 P(6) - P(8) lines the goal was to measure the molecular absorption accurately. Therefore only those constituents which caused significant absorption for these lines were measured. This determination was made by studying the calculations described in Chapter II and preliminary measurements made by Spencer, et al.[24]. In addition N_2O absorption was also measured on the 2-1 P(10) and P(11) lines since they were the only other lines for which N_2O absorption was significant.

Also a laser spectroscopy technique was used to determine the frequencies of the 3-2 P(7) and 2-1 P(10) lines by measuring their separation from N_2O absorption lines.

A. N_2O Absorption Measurements, 760 Torr, 23°C

Measurements of the absorption by nitrous oxide samples broadened to 760 torr with dry nitrogen were made for the 3-2 P(6) - P(8) lines and the 2-1 P(10) and P(11) lines. For these measurements the White cell was set for a path length of 0.7317 kilometers.

Assuming the calculations in Chapter II are in error by no more than ±100%, it is not possible to measure the N_2O-N_2 absorption coefficients with acceptable accuracy in a path of 0.7317 kilometers unless the N_2O concentration is increased above the normally assumed sea-level concentration of 0.28 ppm. Therefore the N_2O concentrations used were from 10 to 1000 times the normal concentration (2.8 to 280 ppm). These concentrations are still quite low and the results can be linearly extrapolated to normal N_2O abundance without distortion which might arise from the difference between the self-broadened and foreign-broadened half-width. This can be seen from the following.

Assuming the Lorentz line shape, the absorption coefficient in km^{-1} may be written as follows

$$(110) \qquad k(km^{-1}) = \frac{S}{\pi} \frac{\alpha_L \quad u}{(\nu-\nu_o)^2 + \alpha_L^2}$$

where u is the absorber concentration in molecules-cm^{-2}.

Now u is directly proportional to the absorber partial pressure P_a and α_L is given for 296K from Eqs. (67) and (68) by $\alpha_{LO}(P_T + (B-1)P_a)$. Therefore the absorption coefficient can be written

$$(111) \qquad k(km^{-1}) = \frac{CS}{\pi} \frac{\alpha_{LO} P_a (P_T + (B-1)P_a)}{(\nu-\nu_o)^2 + \alpha_{LO}^2 (P_T + (B-1)P_a)^2}$$

where C is a proportionality constant relating u to P_a. If the absorber pressure P_a is very small compared to the total pressure, $P_T + (B-1)P_a$ is very nearly P_T and the absorption coefficient k is directly proportional to the absorber pressure P_a. Thus if the absorption coefficient is known at some absorber pressure P_a, the absorption coefficient at some lower pressure P_a is just P_L/P_a times the absorption coefficient at P_a.

For each experimental run, the absorption was measured on a single DF laser line for a number of N_2O concentrations. First the cell was evacuated and the signal detector and reference detector voltages were read by the computer and their ratio calculated and recorded on the computer typewriter. Any detector linearity correction determined from calibration experiments was made automatically at this time. Next a predetermined amount of a mixture of 1% N_2O in Nitrogen was admitted to the cell and the cell filled to 760 torr with dry nitrogen. The 1% mixture was used to admit the sample rather than pure N_2O so the absorber amount could be accurately measured. Even at the highest N_2O concentration used (250 ppm) the N_2O partial pressure was still only 0.2 torr. With the mercury pressure gauges which are used on the absorption cell, pressures between 1 and 50 torr can be measured with greater accuracy than pressures less than 1 torr. Therefore a mixtrue of 1% N_2O in nitrogen was used as the absorbing gas.

The cell now contained the absorbing mixture at the highest N_2O concentration to be measured in the current run. This sample was permitted to mix for about one hour. Then the ratio of signal voltage to reference voltage was read and recorded by the computer as before. The proper mixing time was determined by monitoring the transmittance of the cell continuously until it was observed to be stable. Next the mixture was partially pumped out, the pressure

measured, and the cell refilled with nitrogen to 760 torr. This procedure reduced the N_2O concentration by a known amount. This new sample was allowed to mix for about one hour and the signal to reference ratio was read and recorded as before. This procedure was repeated to obtain data at several N_2O concentrations. At the end of the day, the cell was evacuated, and the signal to reference ratio recorded.

The above procedure was repeated several times on different days for each laser line. All measurements were made at room temperature ($\sim$ 23°C).

Although the laser was tunable from line to line, it was found the desired repeatability in transmittance could not be obtained unless the laser was left tuned to one line for the duration of a measurement run. This is presumably due to optical alignment difficulties associated with moving the grating.

For these measurements the optical arrangement shown in Fig. 43, with the DF laser in the shielded room and the lead selenide detectors was used. The procedure used for making each measurement took advantage of the averaging capability offered by the computer. Before each measurement, the laser beam was blocked. On command from the typewriter the computer then read the signal channel and reference channel 300 times in about 15 seconds, computed the averages and recorded them on the typewriter. These zero readings represented the offset introduced by the electronics and were subtracted from all subsequent readings. Next the beam was unblocked and the signal and reference readings were allowed to stabilize. On command from the typewriter the computer then made a series of five measurements. For each measurement, the signal and reference voltage were read 100 times in a period of about 5 seconds and averaged, the zero offsets measured before were subtracted, and the readings were corrected for linearity using the cubic equation for each detector derived from the calibration experiments. The computer then printed the corrected signal voltage and reference voltage, the standard deviations of each measurement, and the ratio of signal to reference voltage. After this had been repeated five times, the average signal voltage, reference voltage and ratio were recorded on the typewriter. A sample data run is shown in Fig. 56. Five sets of 100 samples were used rather than one set of 500 samples so that short term trends in the readings such as zero drifts, alignment instabilities or laser power changes could be observed. All of the parameters of the measurement procedure could be modified by the user such as number of measurements, number of samples and delay between sample readings. In addition a threshold value of standard deviation could be set which if exceeded caused the measurement to be ignored in the final average.

Figures 57 - 61 show the measured absorption coefficients versus N_2O concentration for the five lines studied. In each case a least squares fit of the data to a straight line through the origin was

```
9.
DATA TAKING PROGRAM.  REVISED OCT. 25,1973

--------
TODAYS DATE IS:
11/16/73
--------


VARIABLE VALUES ARE:
AD1      3
AD2     18
DLY      50.000
SAM    100
ASTDV   1.0000
NOA      5


-OPTION
17.
ENTER DETECTOR CALIBRATION COEFFICIENTS FOR THE CUBIC Y=A0+A1*X+A2*X**2+A3*X**3
ENTER A0,...,A3 FOR SIGNAL DETECTOR.
.2511,1.7147,1.8987,-.52312,
ENTER A0,...,A3 FOR REFERENCE DETECTOR.
.11762,1.3011,.72959,-.015012,

-OPTION
5.
ZERO ADJUST.  BLOCK BEAM, CARRIAGE RETURN TO CONTINUE.

          ZERO1 IS  -.0418        STANDARD DEVIATION IS    .0268
          ZERO2 IS   .0005        STANDARD DEVIATION IS    .0425


-OPTION
5.
ZERO ADJUST.  BLOCK BEAM, CARRIAGE RETURN TO CONTINUE.

          ZERO1 IS  -.0423        STANDARD DEVIATION IS    .0266
          ZERO2 IS   .0433        STANDARD DEVIATION IS    .0140


-OPTION
5.
ZERO ADJUST.  BLOCK BEAM, CARRIAGE RETURN TO CONTINUE.

          ZERO1 IS  -.0424        STANDARD DEVIATION IS    .0265
          ZERO2 IS   .0188        STANDARD DEVIATION IS    .0286


-OPTION
8.
          CHANNEL  3          CHANNEL 18
          SIGNAL              REFERENCE
          VOLTAGE  STD DEV    VOLTAGE  STD DEV      SIG/REF
  1        5.4207   .0271      6.9426   .0269        .78078
  2        5.4173   .0266      6.9533   .0267        .77910
  3        5.4770   .0267      6.9186   .0270        .79163
  4        5.4484   .0265      6.9521   .0266        .78370
  5        5.4292   .0265      6.9077   .0264        .78595

AVERAGE:   5.4385              6.9349                .78423  TAKEN   5 TIMES
```

Fig. 56. Example run of data-taking program.

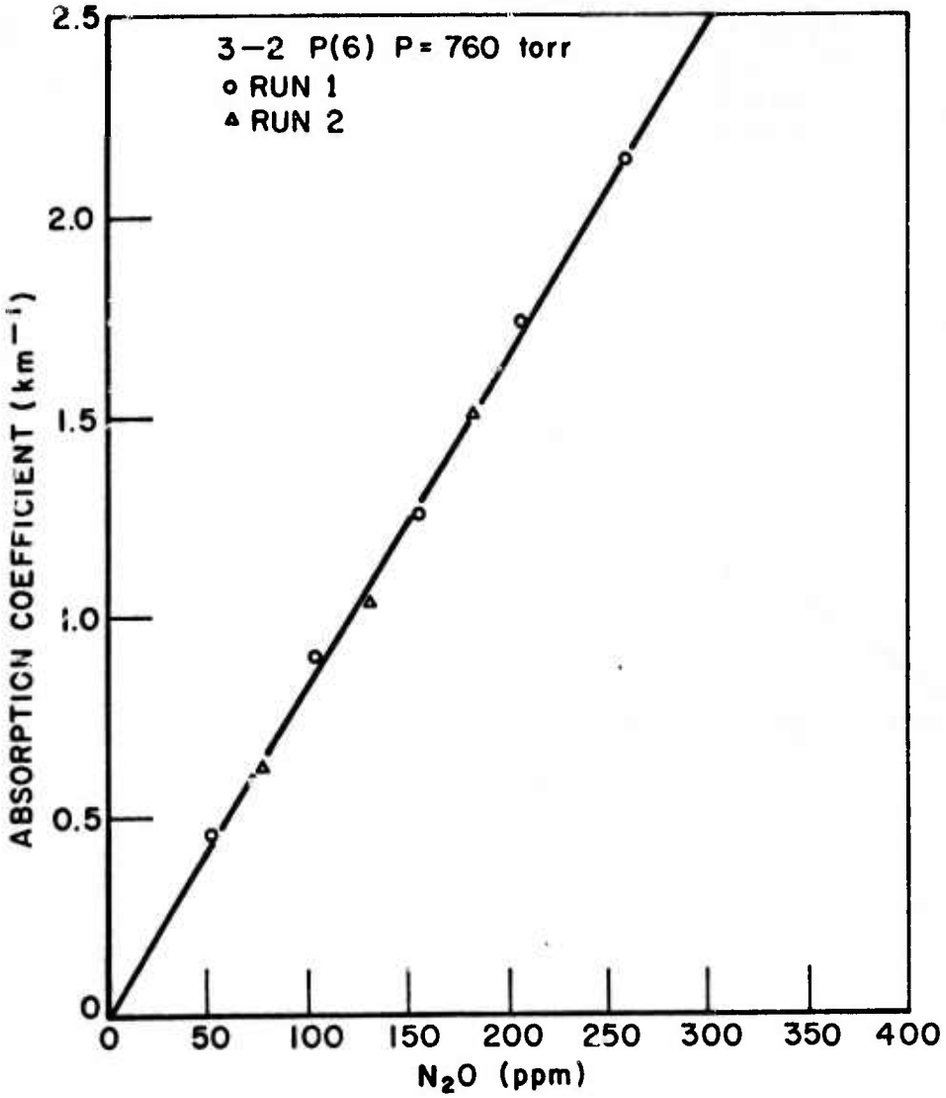

Fig. 57. Measured N_2O absorption for the 3-2 P(6) line at 2594.198 cm^{-1} (23°C).

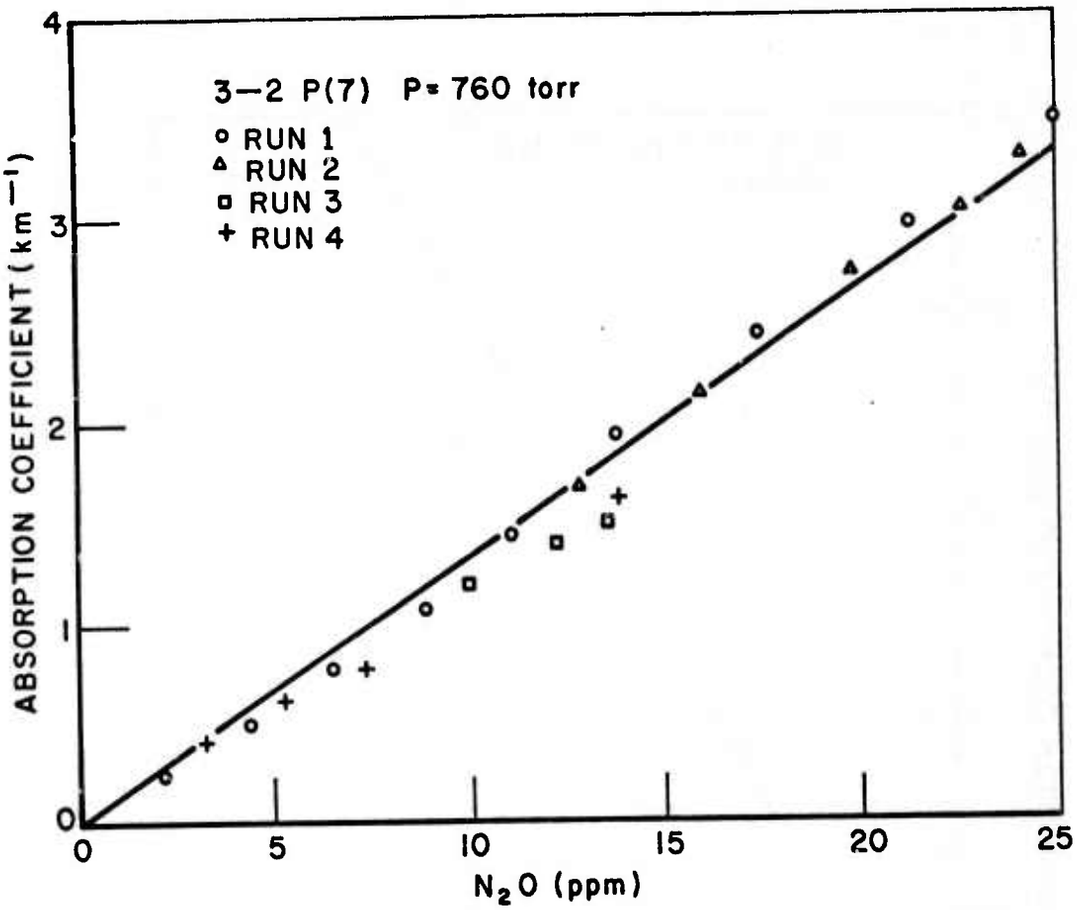

Fig. 58. Measured N_2O absorption for the 3-2 P(7) line at 2570.522 cm^{-1} (23°C).

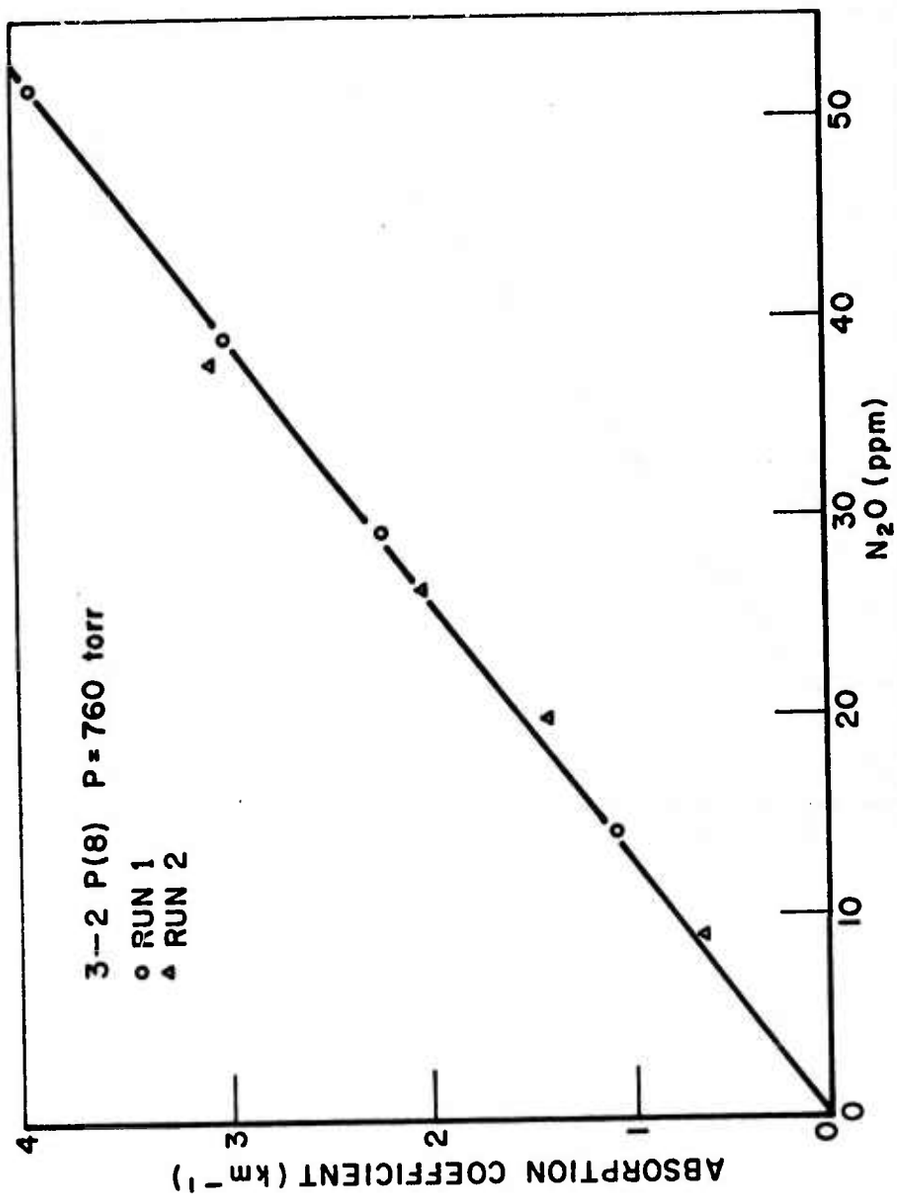

Fig. 59. Measured N2O absorption for the 3-2 P(8) line at 2546.522 cm^{-1} (23°C).

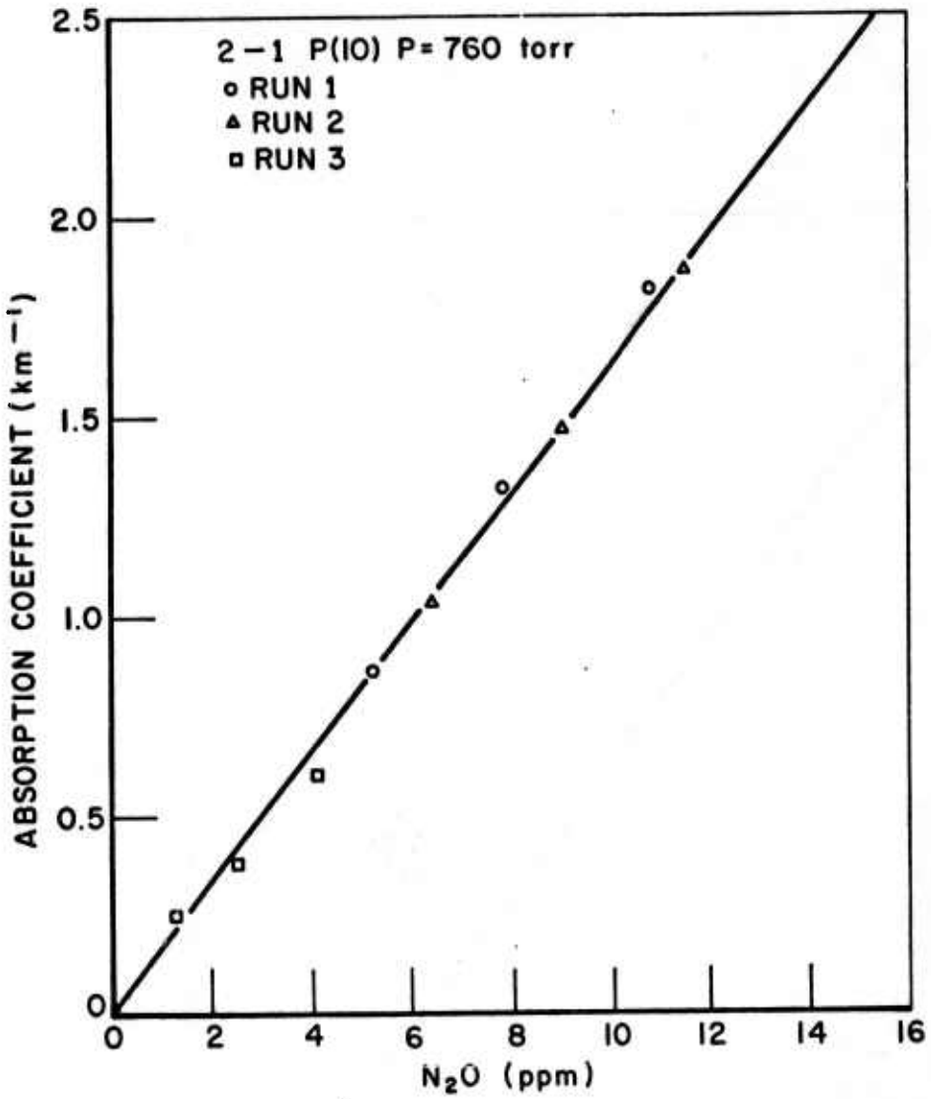

Fig. 60. Measured N_2O absorption for the 2-1 P(10) line at 2580.097 cm^{-1} (23°C).

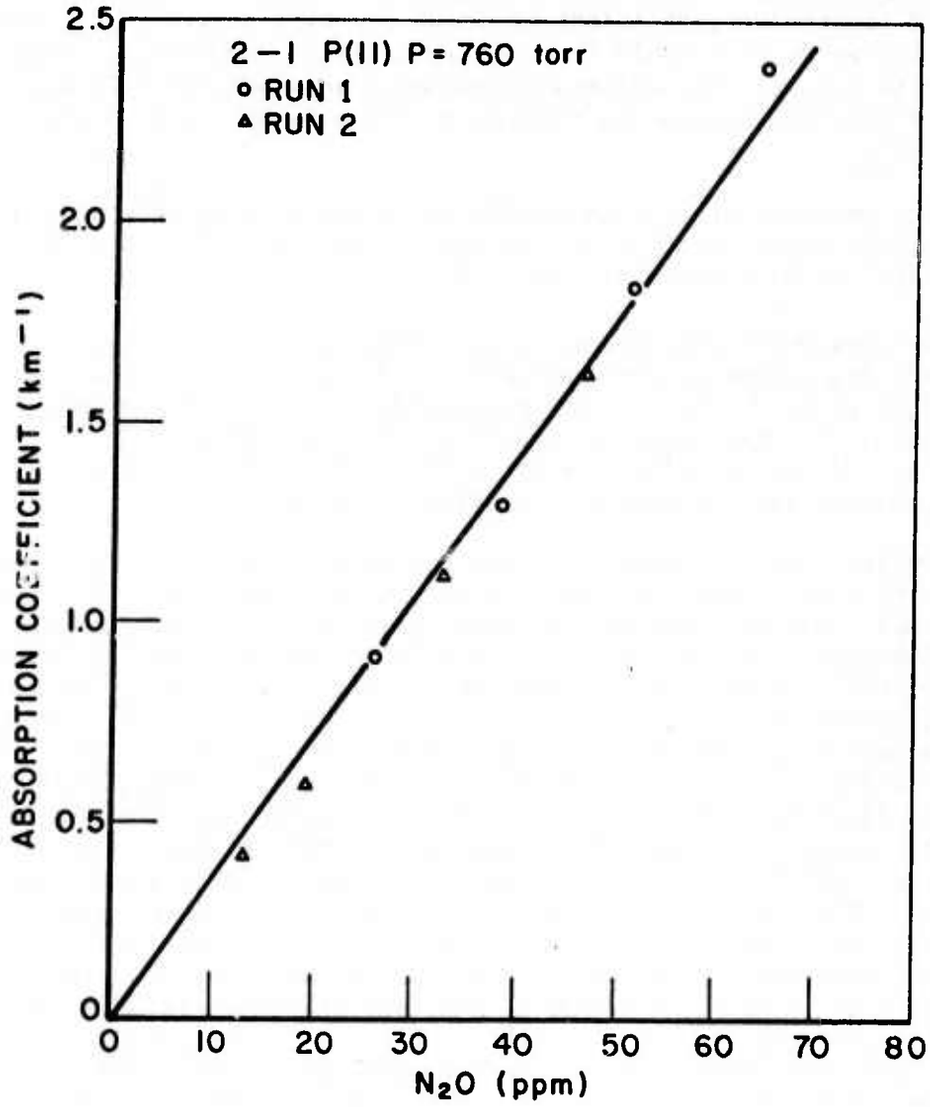

Fig. 61. Measured N_2O absorption for the 2-1 P(11) line at 2553.953 cm^{-1}.

made. The fact that the data points fall almost on a straight line is the best indication of the validity of the detector linearity correction procedure described in Chapter III. Table 6 gives the measured absorption coefficient per part per million along with the calculated value from Table IV. The absorption coefficients extrapolated to the normally assumed atmospheric abundance of 0.28 ppm are also given along with the results obtained by Spencer[24] and Deaton[25].

The measured absorption coefficients and calculated absorption coefficients agree within 1 or 2 percent except for the 2-1 P(11) line where the difference is about 10%.

The agreement with Spencer's measurements is not as good. Spencer's measurements were made with pure N_2O in a 1 or 10 cm cell. The values given in Table 6 are extrapolated from Spencer's measurements at 760 torr assuming a self-broadening coefficient for N_2O of 1. If the self-broadening coefficient in not 1, this extrapolation could introduce a substantial error.

Deaton's measurements were made using a differential spectrophone with flat windows and N_2O concentrations from 1 to 1000 times the normally assumed atmospheric concentration. The spectrophone was calibrated using the N_2O data from this study for the 3-2 P(6), P(7) and P(8) lines. The calibration factors determined by Deaton were different for the three lines. He attributed this difference to experimental errors and took the average of the three as the correct value. The fairly good agreement for the 3-2 P(6), P(7), and P(8) lines then is to be expected since Deaton used the data from this study for those three lines as his calibration. The data for the 2-1 P(10) line is not in good agreement. There are a couple of things which could account for this. The data in this study is valid for 760 torr total pressure. Deaton's measurements and calibrations were made at 630 torr. There is no certainty that the 760 torr data could be used to calibrate at 630 torr and calibration errors could be introduced which were different for different lines. Also Peterson[26] has found that the spectrophone calibration can be frequency dependent since the flat spectrophone windows are also low-finesse Fabry-Perot etalons.

For two of the laser lines, 3-2 P(7) and 2-1 P(10), the assumed laser frequency differs from the assumed frequency of an N_2O absorption line. In this situation, it is possible to determine parameters of the absorption line from a plot of absorption coefficient versus total pressure with the absorber pressure constant.

This can be shown by the following[27]. For an isolated Lorentz line the following expression may be written

$$k = \frac{S}{\pi} \frac{\alpha}{(\Delta\nu)^2 + \alpha^2} \tag{112}$$

TABLE 6

Measured N_2O Absorption Coefficients for Five DF Laser Lines

Line	ν (cm^{-1})	K_{exp}^{OSU} / ppm (km^{-1})	K_{calc} / ppm (km^{-1})	K_{exp}^{OSU} 0.28ppm (km^{-1})	$K^{(a)}$ 0.28ppm Spencer (km^{-1})	$K^{(b)}$ 0.28ppm Deaton (km^{-1})
3-2P(6)	2594.198	0.00811	0.00807	0.00227	0.00244	0.00233
3-2P(7)	2570.522	0.133	0.134	0.0373	0.0333	0.039
3-2P(8)	2546.375	0.0764	0.0768	0.0214	0.0230	0.0196
2-1P(10)	2580.097	0.162	0.164	0.0453	0.0465	0.0704
2-1P(11)	2553.953	0.0346	0.0379	0.00969	0.0123	-

(a) From Spencer, et al. (24)

(b) From Deaton, et al. (25)

where k is the absorption coefficient,

$$(113) \qquad \alpha = \alpha_o \frac{P}{P_o}\left(\frac{T_o}{T}\right)^m$$

is the half-width of the absorption line, P_o = 1 atm, $\Delta\nu$ is the difference in the frequencies of the laser line and the absorption line, P is the total pressure, and S is the line strength. For a constant temperature and P in atmospheres, α becomes

$$(114) \qquad \alpha = \alpha_o P \quad .$$

On a curve of k versus total pressure P, the condition for zero slope with $\Delta\nu$ constant is

$$(115) \qquad \frac{dk}{d\alpha} = \frac{S}{\pi}\left[\frac{(\Delta\nu)^2 + \alpha^2 - 2\alpha^2}{((\Delta\nu)^2 + \alpha^2)^2}\right] = 0$$

or,

$$(116) \qquad \alpha = \Delta\nu \quad .$$

Therefore, as a first approximation (i.e., assuming a single isolated Lorentz line) when the slope of the k versus P curve is zero

$$(117) \qquad \alpha_o P = \Delta\nu \quad .$$

Thus, if the frequency difference between the laser line and the absorption line is known, the half-width can be determined. Similarly, if the half-width is known the frequency difference can be determined.

Now if $\alpha_o P = \Delta\nu$ is substituted into Eq. (112) the following is obtained

$$(118) \qquad k = \frac{S}{\pi}\frac{\Delta\nu}{2(\Delta\nu)^2}$$

or

$$(119) \qquad S = 2\pi k(\Delta\nu) \quad .$$

Thus the line strength may also be determined.

When this experiment was performed, the laser frequencies had not yet been accurately measured. Therefore the line widths and frequencies listed for the N_2O absorption lines on the AFCRL tape[3] were assumed to be correct and this technique was used to better determine the laser line frequencies.

It should be mentioned that Eq. (117) is strictly true only if the pressure is high enough that the Voigt profile does not have to be used to describe the absorption line shape, there is no pressure shift in the frequency of the absorption line, and there are no other absorption lines close enough to contribute to the absorption at the laser frequency. In the present study, the first assumption is valid, the second one is probably valid, but the third assumption is not valid.

A first approximation of the effect of additional absorption lines on Eq. (117) can be obtained by including the nearest absorption line on either side of the nearly coincident line. In this case Eq. (112) becomes

$$(120) \qquad k = \frac{S}{\pi} \frac{\alpha}{(\Delta\nu)^2 + \alpha^2} + \frac{S_1}{\pi} \frac{\alpha_1}{(\Delta\nu_1)^2 + \alpha_1^2} + \frac{S_2}{\pi} \frac{\alpha_2}{(\Delta\nu_2)^2 + \alpha_2^2}$$

where the non-subscripted terms refer to the nearly coincident absorption line and the subscripts 1 and 2 refer to the lines on either side of the coincident line.

Assume the half-widths and line strengths are all about the same and $\Delta\nu_1$ and $\Delta\nu_2$ are about 10 times $\Delta\nu$. This is the case for the N_2O band under consideration here. Equation (120) then becomes

$$(121) \qquad k = \frac{S}{\pi} \left[\frac{\alpha}{(\Delta\nu)^2 + \alpha^2} + \frac{\alpha}{(\Delta\nu_1)^2 + \alpha^2} + \frac{\alpha}{(\Delta\nu_2)^2 + \alpha^2} \right] .$$

Differentiating Eq. (118) with respect to α gives

$$(122) \qquad \frac{dK}{d\alpha} = \frac{S}{\pi} \left[\frac{\Delta\nu^2 - \alpha^2}{((\Delta\nu)^2 + \alpha^2)^2} + \frac{\Delta\nu_1^2 + \alpha^2}{((\Delta\nu_1)^2 + \alpha^2)^2} + \frac{\Delta\nu_2^2 - \alpha^2}{((\Delta\nu_2)^2 + \alpha_2)^2} \right] = 0$$

Now assume that the two additional lines cause only a small change in the single line solution which is $\alpha = \Delta\nu$. Substitute $\alpha = \Delta\nu$ in the denominator of the first term of Eq. (122) and drop α in the second and third terms of Eq. (122) since $(\Delta\nu_1)^2$ and $(\Delta\nu_2)^2$ are both much greater than α^2, and substitute $\Delta\nu_1 = \Delta\nu_2 = 100\,\Delta\nu$. Equation (122) then becomes

(123) $$\frac{dk}{d\alpha} = \frac{S}{\pi}\left[\frac{\Delta\nu^2 - \alpha^2}{4(\Delta\nu)^4} + \frac{100\,\Delta\nu^2}{10000\Delta\nu^4} + \frac{100\,\Delta\nu^2}{10000\Delta\nu^4}\right] = 0$$

or

(124) $$\frac{dk}{d\alpha} = \frac{S}{\pi}\left[\frac{\Delta\nu^2 - \alpha^2}{4\Delta\nu^4} + \frac{\Delta\nu^2}{50\Delta\nu^4}\right] = 0$$

(125) $$\frac{dk}{d\alpha} = \frac{S}{\pi}\left[\frac{\Delta\nu^2 - \alpha^2 + .080\Delta\nu^2}{4\Delta\nu^4}\right] = 0$$

Solving for α^2

(126) $$\alpha^2 = 1.08\ \Delta\nu^2 \quad .$$

Substituting Eq. (126) into Eq.(122) and solving for α^2 again yields

(127) $$\alpha^2 = 1.0865\ \Delta\nu^2 \quad .$$

Repeating the process one more time gives

(128) $$\alpha^2 = 1.087\ \Delta\nu^2$$

or

(129) $$\alpha_o P = 1.043\ \Delta\nu \quad .$$

The effect of additional absorption lines then is to add four or five percent to the right side of Eq. (117)

For the two lines studied, the experimental plot of absorption coefficient versus total pressure was used to make a first estimate of the laser frequency. Curves of absorption coefficient versus total pressure were calculated for several laser frequencies close to the estimated frequency using the computer program described in Chapter II. These calculated curves were then plotted along with the experimental data. The calculated curve which best fit the experimental data was then taken to represent the correct laser frequency

Figure 62 shows the experimental data for the 3-2 P(7) line with N_2O pressure constant at 6.51×10^{-3} torr and total pressure varying from 50 - 850 torr along with calculated curves for the same N_2O pressure and laser frequencies 2570.505 cm^{-1}, 2570.510 cm^{-1}, and 2570.515 cm^{-1}. The laser frequency determined from Fig. 62 is 2570.51 $\pm$ .01 cm^{-1}. This compares with 2570.522 $\pm$ .003 cm^{-1} determined by Heath, et al.[17].

Figures 63 and 64 show the experimental data for the 2-1 P(10) line with N_2O pressures 6.82×10^{-3} torr and 1.73×10^{-2} torr respectively and total pressures from 50 torr to 760 torr. Also shown are calculated curves for the same N_2O pressures and laser frequencies 2580.100 cm^{-1}, 2580.105 cm^{-1}, and 2580.110 cm^{-1}. The laser frequency determined from the plots is 2580.10 $\pm$ .005 cm^{-1}. This compares with 2580.097 $\pm$ .003 cm^{-1} determined by Heath, et al.[17].

For the 2-1 P(10) line the frequency determined results in $\alpha_o P = 1.043\ \Delta\nu$ at the zero slope point. This is in exact agreement with Eq. (129). This is probably coincidental considering the assumptions which were made in the derivation. For the 3-2 P(7) line at the zero slope point $\alpha_o P = 1.068\ \Delta\nu$ which is a little higher than predicted.

The technique described here is certainly useful provided proper precautions are taken in interpreting the results.

B. CH_4 Absorption Measurements, 760 Torr, 23°C

Measurements of the absorption by methane samples broadened to one atmosphere total pressure by dry air were made for the 2-1 P(6), P(7) and P(8) DF laser lines. The White cell was set at 0.7317 km for these measurements.

As with the nitrous oxide measurements the methane concentration had to be increased substantially over the normal atmospheric abundance in order to have sufficient absorption so that it could be measured accurately in a 0.7317 km path. The highest partial pressure of methane used was 1.72 torr which corresponds to 2263 parts per million. The normally assumed atmospheric concentration is 1-6 parts per million. Even though the concentration is greatly enhanced over the normal concentration the methane partial pressure is still low enough that the results can be linearly extrapolated without distortion caused by self-broadening.

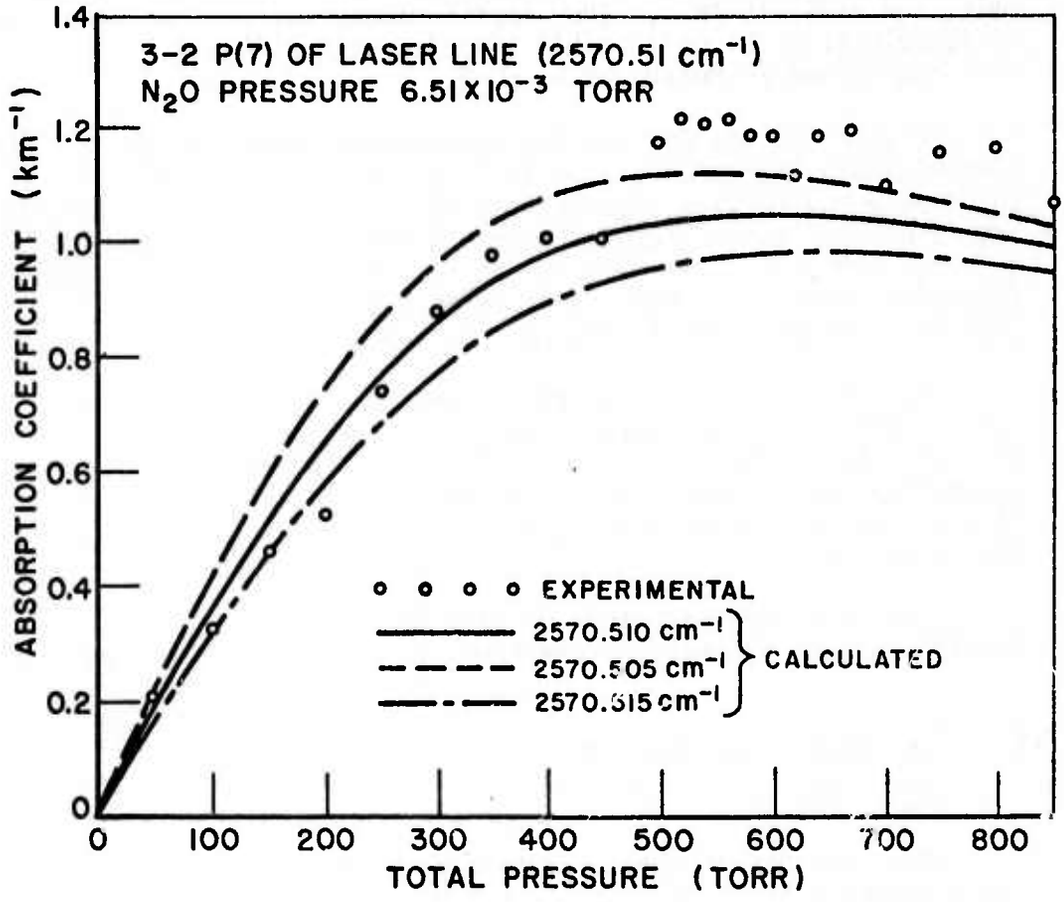

Fig. 62. Absorption coefficient vs total pressure for 3-2 P(7) line at 6.51 x 10^{-3} torr N_2O.

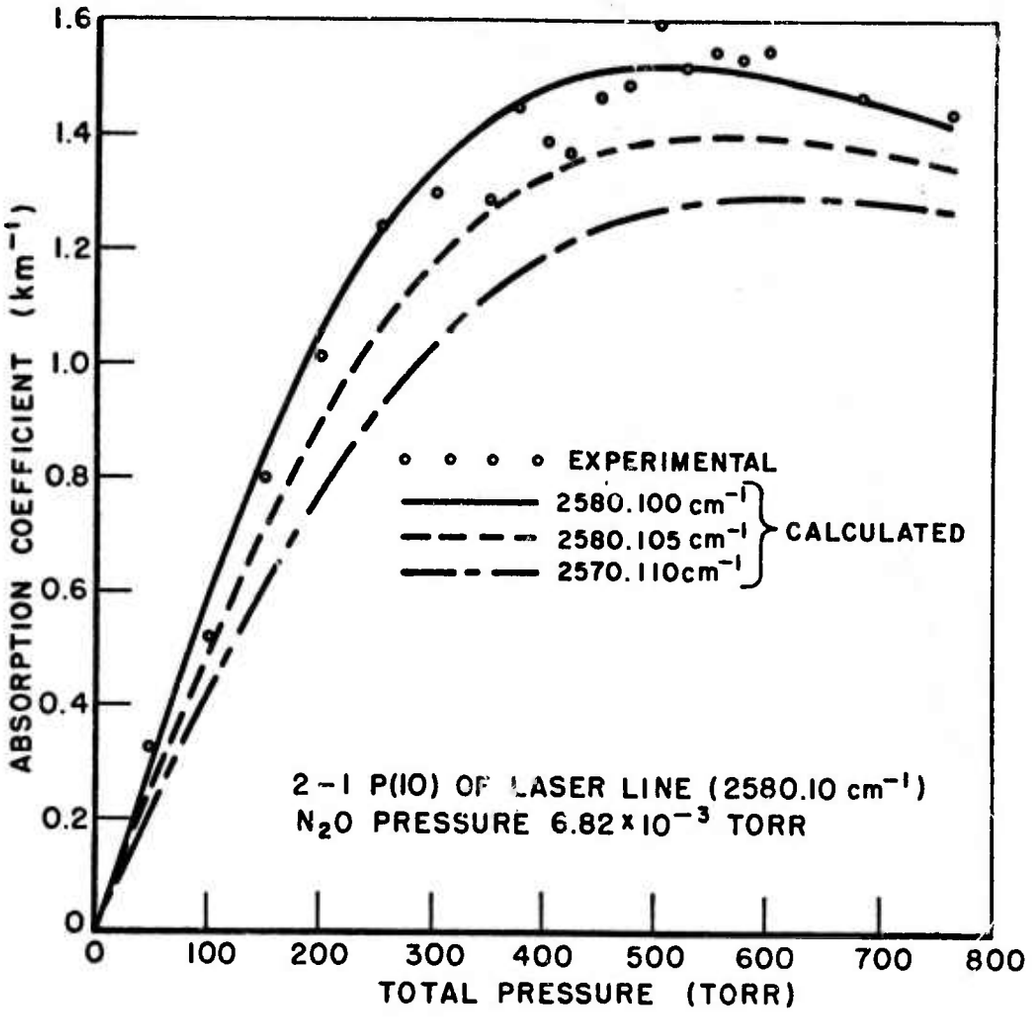

Fig. 63. Absorption coefficient vs total pressure for 2-1 P(10) line at 6.82 x 10^{-3} torr N_2O.

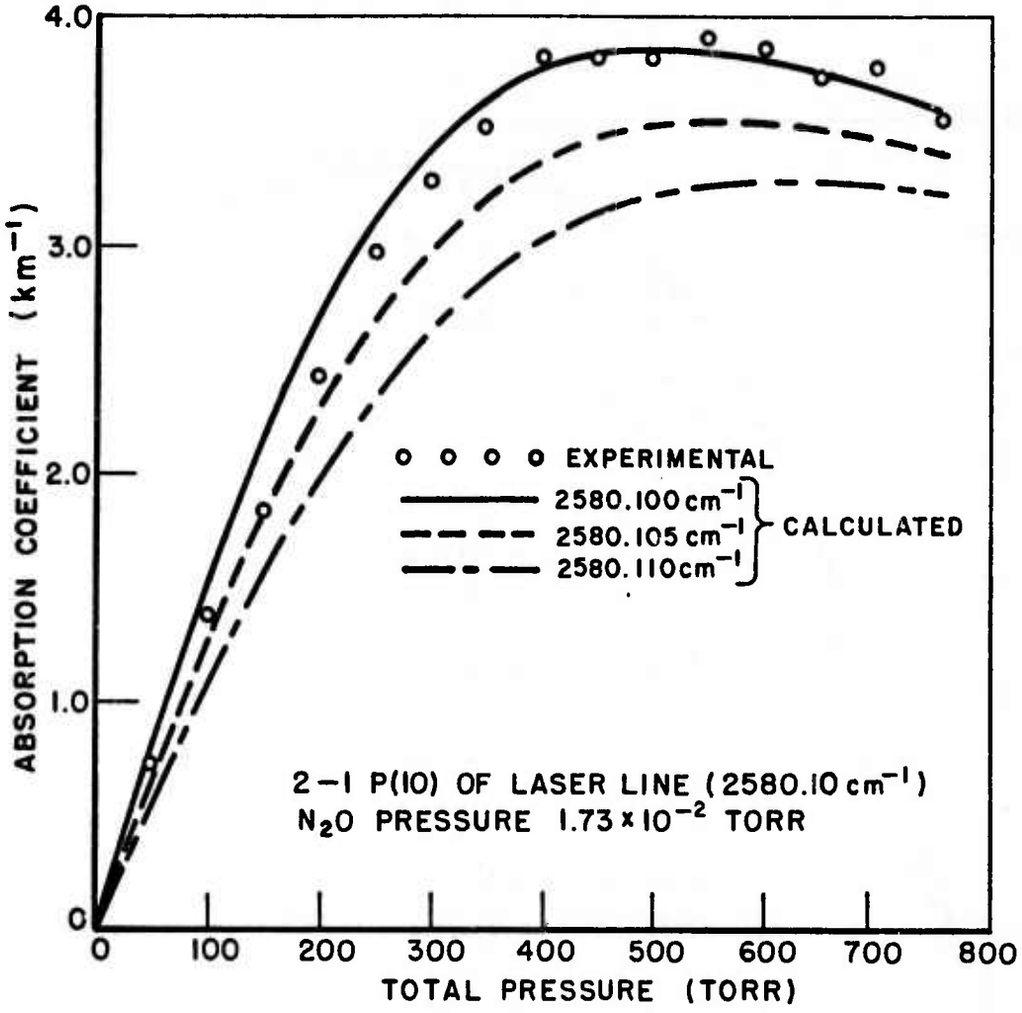

Fig. 64. Absorption coefficient vs total pressure for 2-1 P(10) line at 1.73 x 10^{-2} torr N_2O.

Assuming the calculations presented in Chapter II are in error by no more than ±100%, the absorption due to methane for the six high-power lines in the 2-1 and 3-2 bands is negligible compared with the absorption due to HDO and the water continuum. One of the purposes of these measurements then was to verify that the methane absorption was indeed small. The second purpose of these measurements was to provide calibration data for a spectrophone experiment which has been reported elsewhere[28].

The procedures and experimental setup used for making the methane measurements were the same as those used in making the nitrous oxide measurements except that all three laser lines were studied in one experimental run.

Figures 65, 66, and 67 show the measured absorption coefficients versus methane concentration for the 2-1 P(6), P(7), and P(8) lines respectively. For each laser line a least squares fit of the absorption data to a straight line through the origin was made.

Assuming a natural CH_4 abundance of 1.6 ppm[16], Table 7 gives the CH_4 absorption coefficients for the three laser lines as extrapolated from the experimental data. For comparison the measurements reported by Spencer, et al.[24] and Deaton, et al.[26] are also presented along the the calculated values from Chapter II.

TABLE 7.

METHANE ABSORPTION COEFFICIENTS ASSUMING 1.6 ppm CH_4 IN AIR AT SEA LEVEL

Line	ν (cm^{-1})	k (km^{-1}) calculated	k (km^{-1}) OSU exp.	k (km^{-1}) Deaton (a)	k (km^{-1}) Spencer (b)
2-1 P(6)	2680.179	3.061×10^{-4}	15.2×10^{-4}	11.0×10^{-4}	19.8×10^{-4}
2-1 P(7)	2655.863	7.147×10^{-4}	11.3×10^{-4}	11.4×10^{-4}	12.9×10^{-4}
2-1 P(8)	2631.068	8.458×10^{-4}	8.59×10^{-4}	9.79×10^{-4}	8.88×10^{-4}

(a) From Deaton, et.al.[25]
(b) From Spencer, et.al.[24]

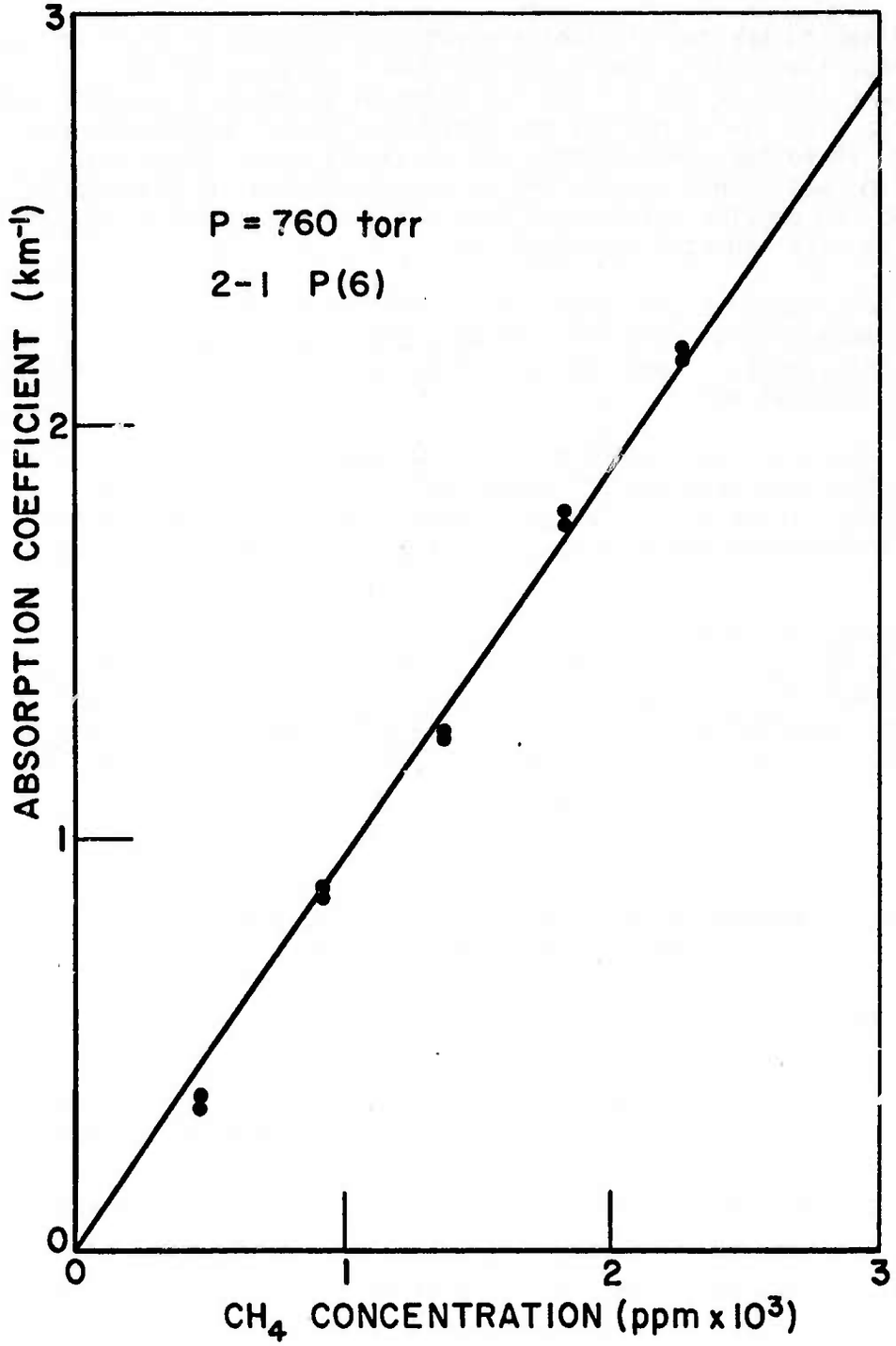

Fig. 65. Measured CH_4 - Air absorption coefficient for 2-1 P(6) line at 2680.179 cm^{-1}.

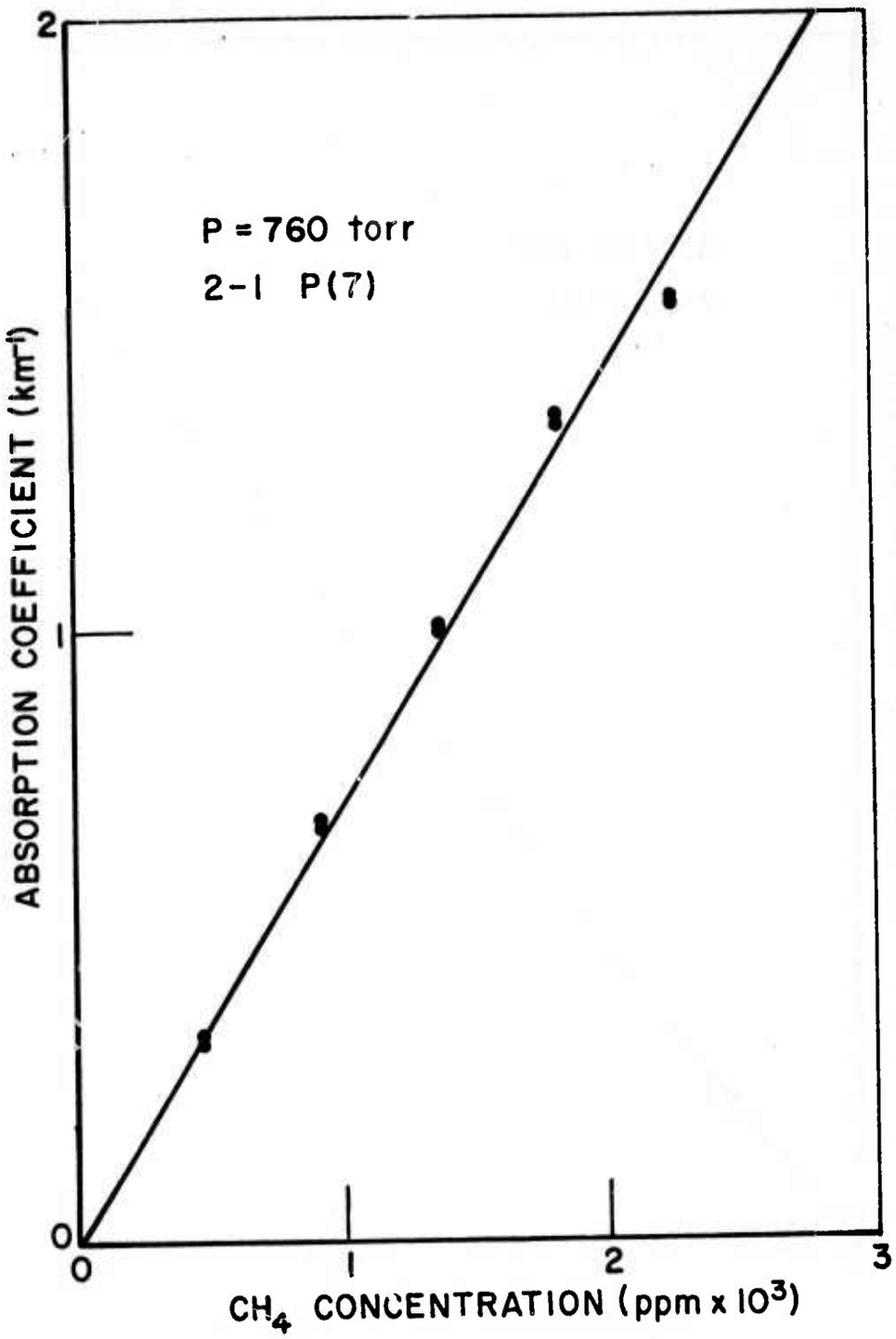

Fig. 66. Measured CH_4 - Air absorption coefficient for 2-1 P(7) line at 2655.863 cm^{-1}.

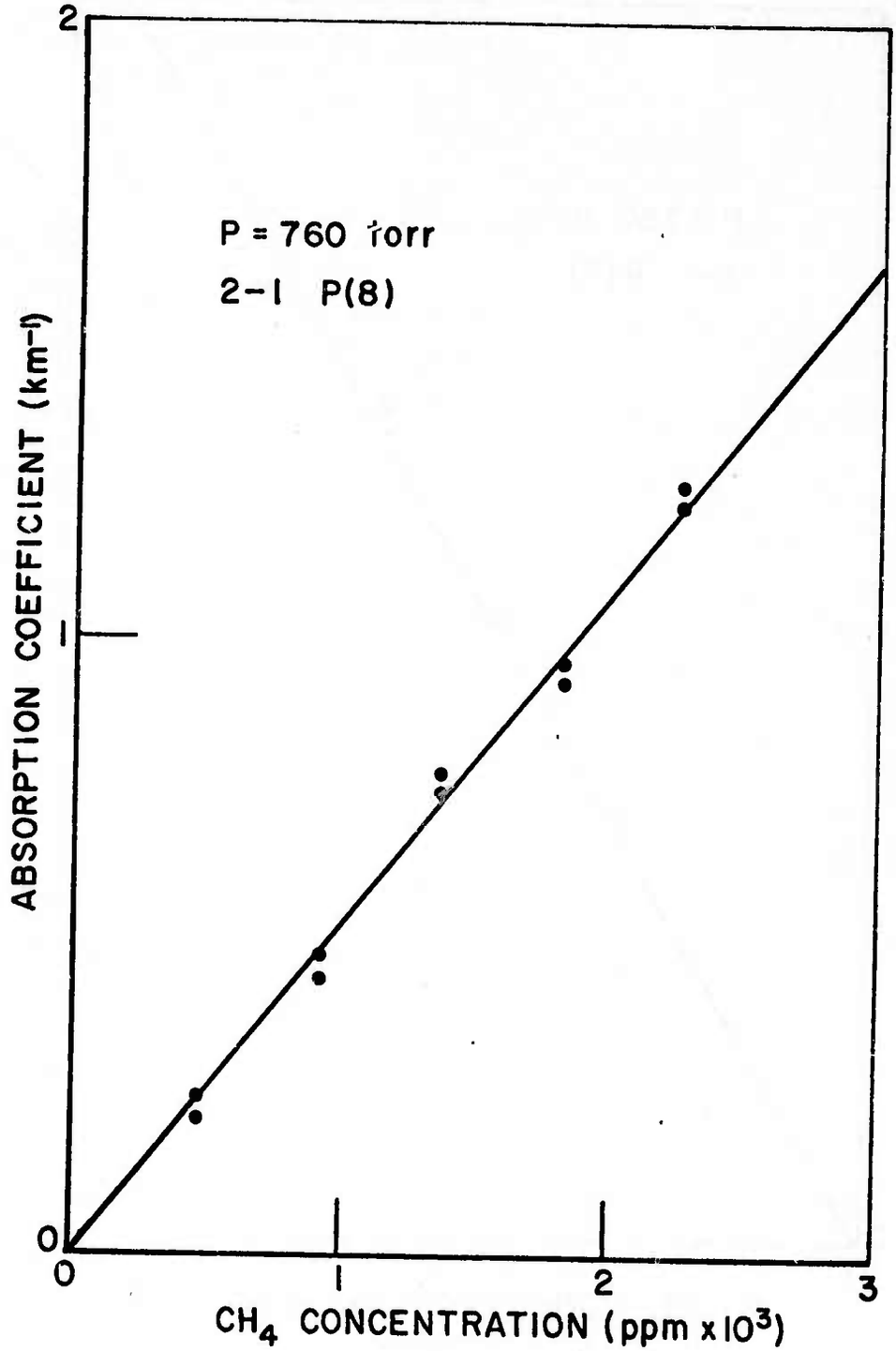

Fig. 67. Measured CH_4 - Air absorption coefficient for 2-1 P(8) line at 2631.068 cm^{-1}.

The measured absorption coefficients are in reasonable agreement with the calculated absorption coefficients only on the 2-1 P(8) line. For the other two lines the agreement is not good at all. According to Benedict[29] the methane data on the AFCRL line data tape[3] may be in error. Therefore the calculations made using this data would also be in error.

The CH_4 measurements reported by Deaton were made using the same apparatus and procedures as for the N_2O measurements. The same calibration factor was used and the measurements were made at 630 torr in both cases. Considering those factors the agreement of the results of this study with those reported by Deaton is as good as could be expected.

The measurements reported by Spencer were made using a 200 cm cell and pure methane. The results given in Table 7 were obtained by extrapolating his measurements at 760 torr to 1.6 ppm assuming a self-broadening coefficient of 1. The agreement of the results of this study with those reported by Spencer is reasonably good except for the 2-1 P(6) line. On this line some error could be introduced in extrapolating Spencer's measurement to 1.6 ppm.

The results of this study along with the results reported by Deaton, et.al. and Spencer, et.al. confirm that the methane absorption is indeed quite small compared to absorption due to HDO or the water vapor continuum.

C. CO_2 Absorption Measurements

The calculations presented in Chapter II indicate CO_2 absorption coefficients for the six laser lines of interest in the 3-2 and 2-1 bands of about 10^{-7} or 10^{-8} km^{-1}. Myers[30] has investigated the CO_2 absorption experimentally using a DF laser and has found that the absorption coefficient for some lines is four orders of magnitude higher than the calculations predict. This absorption is apparently due to an isotopic or weak CO_2 band which was not included in the AFCRL compilation.

Absorption of the 2-1 P(8) DF laser line by pure CO_2 was measured for CO_2 pressures of 248, 503, and 761 torr in a path of 0.7317 km. The optical setup and detectors were the same as for the N_2O and CH_4 measurements. Myers found that this line had higher absorption than any of the other six lines of interest in this study. The results of the measurement are shown in Fig. 68. The results of this experiment are probably less reliable than the results of the N_2O and CH_4 measurements because the detector calibration was not sufficiently well known. The point at 761 torr is probably within 10% with the other two points being somewhat worse.

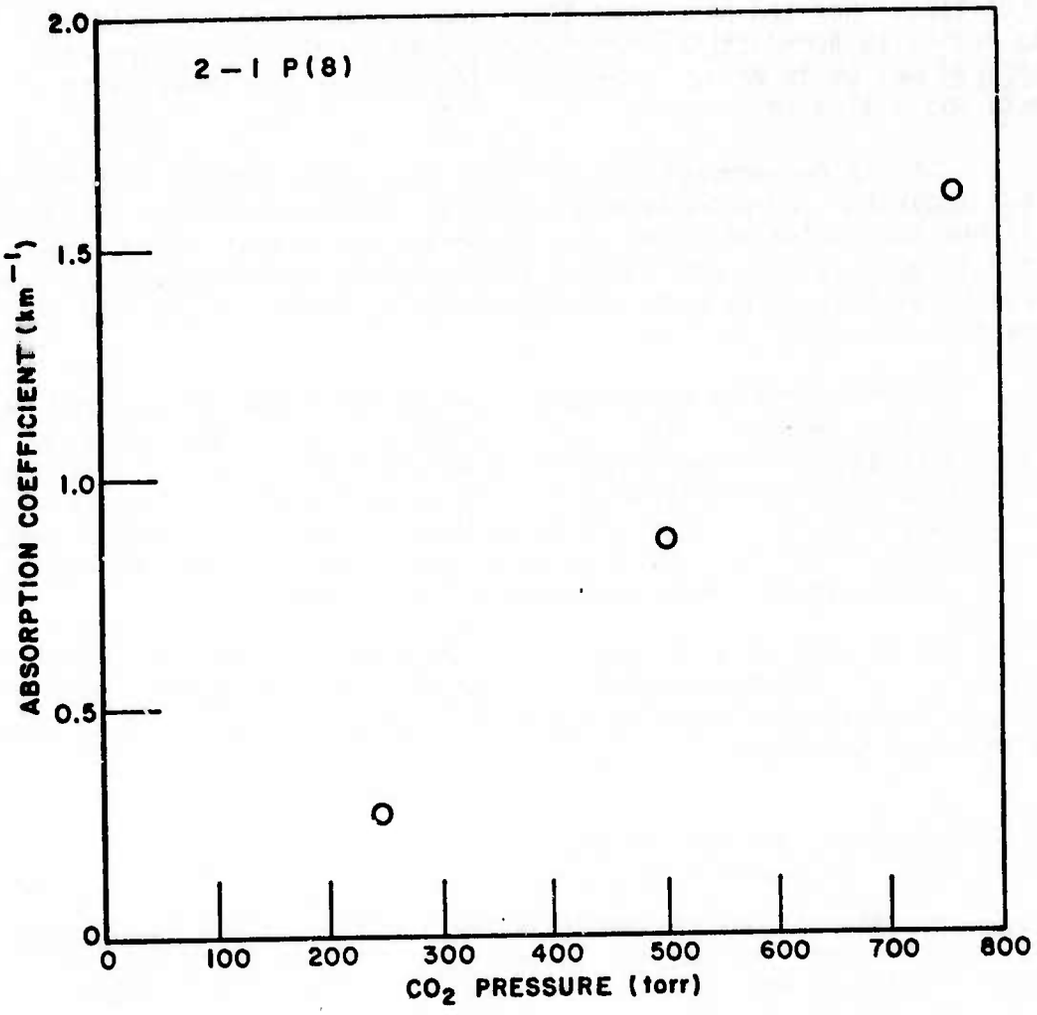

Fig. 68. Measured CO_2 absorption coefficient for 2-1 P(8) line at 2631.068 cm^{-1}.

The measured absorption coefficient was 1.6 km^{-1} at 761 torr. Assuming a self-broadening coefficient of 1 for CO_2 this corresponds to 5.3×10^{-4} km^{-1} at 330 ppm CO_2 and 1 atmosphere total pressure. Assuming a self-broadening coefficient of 1.3 and using the data in Fig. 68, a value of 4.7×10^{-4} km^{-1} at 330 ppm and one atmosphere is obtained. Table 8 lists the absorption coefficients obtained by Myers for the six high power laser lines along with the result obtained in this study for the 2-1 P(8) line.

TABLE 8

MEASURED CO_2 ABSORPTION COEFFICIENTS FOR 6 DF LASER LINES

Line	ν (cm^{-1})	k (km^{-1}) Myers (a)	k (km^{-1}) this study
2-1 P(6)	2680.179	$.19 \times 10^{-4}$	
2-1 P(7)	2655.863	1.85×10^{-4}	
2-1 P(8)	2631.068	9.26×10^{-4}	5.3×10^{-4}
3-2 P(6)	2594.198	6.85×10^{-4}	
3-2 P(7)	2570.522	5.24×10^{-4}	
3-2 P(8)	2546.375	4.21×10^{-4}	

(a) From Myers[30]

The difference between the absorption coefficient for the 2-1 P(8) line measured in this study and that measured by Myers is not completely accounted for. Myers has indicated that the numbers he has quoted are not as accurate as would be indicated by the number of significant figures. In any case the CO_2 absorption coefficients are small compared to the HDO and water continuum absorption coefficients.

D. HDO Absorption Measurements, 760 torr, 24°C

Absorption of the 2-1 P(6), P(7) and P(8) and the 3-2 P(6), P(7) and P(8) DF laser lines by HDO-nitrogen mixtures was measured. The detectors, optical arrangement, and data recording procedures were the same for these measurements as for the N_2O absorption measurements.

As with the N_2O and CH_4 absorption, the HDO absorption for the six laser lines of interest in this study is too low in normal atmospheric samples to be measured in a 0.7317 km path. In addition, the calculations presented in Chapter II indicate that the HDO absorption is the same order of magnitude as the water-vapor continuum absorption. Therefore it was necessary to enhance the HDO concentration relative to the H_2O concentration for two reasons. First, the HDO enhancement was necessary in order to obtain high enough absorption to accurately measure in a 0.7317 km path. Second it was necessary to enhance the HDO concentration so that the HDO absorption was much greater than the water vapor continuum absorption. The small continuum absorption would not then cause any appreciable error in the measurement of HDO absorption.

In these experiments it was necessary to devise a careful sample preparation procedure.

In the steady state, HDO does not exist alone but rather in equilibrium with H_2O and D_2O according to the following equation:

$$(130) \qquad H_2O + D_2O \rightleftharpoons 2HDO \quad .$$

The relative concentrations of the three types of water can be calculated from the equilibrium constants, $K_{292°} = 3.543$ and $K_{293} = 3.506$[24] for the liquid and gas phases respectively.

The procedure used in preparing the samples for the work presented here was to mix a known amount of D_2O with a known amount of H_2O and calculate the resulting amount of HDO using the equilibrium constant. A formula relating the final amount of HDO to the initial amounts of D_2O and H_2O can be derived as follows:

For a mixture of H_2O, D_2O, and HDO where the molal concentrations of the three types of water are A, B, and C respectively, the equilibrium concentrations of each of the three types of water are related by

$$(131) \qquad \frac{C^2}{AB} = K$$

where the appropriate K for the liquid or gas phase is used.

Let C_{H_2O} be the initial volumes of H_2O, C_{D_2O} be the initial volume of D_2O and C_{HDO} be the final volume of HDO. The final concentrations of H_2O and D_2O are then $(C_{H_2O} - C_{HDO}/2)$ and $(C_{D_2O} - C_{HDO}/2)$ respectively. Substituting these definitions for A, B, and C in Eq. (131) gives

$$(132) \qquad \frac{(C_{HDO})^2}{(C_{H_2O} - C_{HDO}/2)(C_{D_2O} - C_{HDO}/2)} = K$$

or

$$(133) \qquad \frac{(C_{HDO})^2}{C_{H_2O}\,C_{D_2O} - \frac{C_{HDO}}{2}(C_{H_2O} + C_{D_2O}) + \frac{(C_{HDO})^2}{4}} = K \quad .$$

Equation (133) may be written as follows:

$$(134) \qquad (C_{HDO})^2(4-K) + 2K\,C_{HDO}\,(C_{D_2O} + C_{H_2O}) - 4K\,C_{H_2O}\,C_{D_2O} = 0 \quad .$$

Equation (134) may now be solved for C_{HDO} using the quadratic formula:

$$(135) \qquad C_{HDO} = \frac{-K(C_{H_2O}+C_{D_2O}) + \sqrt{K^2(C_{H_2O}+C_{D_2O})^2 + 4K(4-K)C_{H_2O}\,C_{D_2O}}}{(4-K)}$$

Three separate mixtures containing different HDO concentrations were used. The appropriate mixture was chosen for each laser line so that the absorption could be measured accurately in a 0.7317 km path. The samples used were: for the 2-1 P(6) line, .01% D_2O, 1.99% HDO, balance H_2O; for the 2-1 P(7) line, .003% D_2O, 1.02% HDO, balance H_2O; and for the 2-1 P(8), 3-2 P(6), 3-2 P(7), and 3-2 P(8) lines, .12% D_2O, 6.22% HDO, balance H_2O. The percentages were calculated using the gas phase equilibrium constant K = 3.506.

There is a potential problem which could be encountered when the enhanced sample is introduced into the White cell. This is caused by the fact that HDO is less volatile than H_2O and therefore remains preferentially in the condensed phase. It has been reported[31] that in thermodynamic equilibrium, water vapor over liquid water will contain 8% fewer HDO moleucles than the liquid water. When the water vapor is being introduced into the White cell, the liquid and gas are certainly not in thermodynamic equilibrium, so the HDO concentration in the cell could be quite uncertain. This problem was overcome by filling a small bottle with just enough of the specially prepared water to fill the White cell with the desired amount of water vapor and evaporating the sample completely.

Another problem which could affect the HDO concentration would be preferential adsorption of one water isotope relative to the other.

The cell has been tested several times for H_2O adsorption and none has been observed. A mass spectrometer residual gas analyzer was added to the cell so that the HDO/H_2O ratio could be monitored as a function of time in order to evaluate this problem. The instrument was not accurate enough for absolute concentration determination. A water vapor sample containing an enhanced concentration of HDO was admitted to the cell and the HDO/H_2O ratio was monitored using the mass spectrometer over a period of several hours. Within the accuracy limits of the instrument, no change in the ratio was observed. A more complete discussion of this experiment is given in Appendix D.

Figures 69 through 74 show the results of the HDO absorption measurements for the 2-1 P(6), P(7), and P(8) lines and the 3-2 P(6), P(7), and P(8) lines respectively. The absorption cell path length was 0.7317 km. The cell originally contained 15 torr of the appropriate special water sample plus nitrogen to a total pressure of 760 torr. The lower points on the curves were obtained by partially pumping the cell out and refilling to 760 torr with nitrogen.

For each line a least squares fit of the data to an expression of the form $k = AP+BP^2$ was made, where k is the absorption coefficient and p is the partial pressure of enriched water in torr. The derived expression for a laser line is presumed to be a more accurate characterization of the absorption coefficient than any individual data point. The expressions for the measured absorption coefficients for the three lines are presented in Table 9. The expressions are valid for 760 torr total pressure with p being the partial pressure of the enriched water.

In Table 10 the expressions from Table 9 are extrapolated to an assumed abundance of HDO to H_2O of 0.03%. This was done by multiplying the coefficients A and B by $.03/x$ where x is the percent HDO concentration of the mixture used to make the measurements. This procedure assumes that line broadening caused by HDO - HDO collisions is not greatly different from line broadening due to HDO - H_2O collisions. These expressions have been evaluated at 14.26 torr for each line and the values listed in Table 10 along with the absorption coefficients calculated in Chapter II. It should be pointed out that the expressions for absorption coefficients in Table 10 are only valid at 24°C and 760 torr total pressure. The temperature dependence and total pressure dependence of the absorption coefficients have not been investigated.

Since the samples used to make the measurements also contained an enhanced D_2O concentration as well as enhanced HDO, it is possible that some error might be introduced due to D_2O absorption. This possibility was investigated by measuring the absorption of a sample of pure D_2O vapor broadened with dry air. The D_2O vapor pressure was 0.21 torr which is 12-500 times the D_2O partial pressure at the highest water vapor pressure for the HDO measurements in Figs. 69

TABLE 9

MEASURED HDO ABSORPTION COEFFICIENTS FOR SIX DF LASER LINES

Line	ν (cm^{-1})	HDO concentration	k (km^{-1})
2-1 P(6)	2680.179	1.99%	$2.25\times10^{-1}p + 1.36\times10^{-3}p^2$
2-1 P(7)	2655.863	1.02%	$2.02\times10^{-1}p + 1.78\times10^{-3}p^2$
2-1 P(8)	2631.068	6.22%	$7.07\times10^{-2}p + 1.20\times10^{-3}p^2$
3-2 P(6)	2594.198	6.22%	$2.31\times10^{-1}p + 1.58\times10^{-3}p^2$
3-2 P(7)	2570.522	6.22%	$9.77\times10^{-2}p + 1.93\times10^{-3}p^2$
3-2 P(8)	2546.375	6.22%	$3.00\times10^{-2}p + 4.01\times10^{-4}p^2$

TABLE 10

HDO ABSORPTION COEFFICIENTS EXTRAPOLATED TO .03%
RELATIVE HDO ABUNDANCE

Line	K (km^{-1}) .03% HDO 760 torr total pressure	K (km^{-1}) 14.26 torr H_2O	K (km^{-1}) 14.26 torr calculated
2-1 P(6)	$3.39\times10^{-3}p + 2.05\times10^{-5}p^2$	5.24×10^{-2}	3.79×10^{-2}
2-1 P(7)	$5.94\times10^{-3}p + 5.24\times10^{-5}p^2$	9.54×10^{-2}	7.35×10^{-2}
2-1 P(8)	$3.38\times10^{-4}p + 5.78\times10^{-6}p^2$	6.00×10^{-3}	9.12×10^{-3}
3-2 P(6)	$1.11\times10^{-3}p + 7.62\times10^{-6}p^2$	1.74×10^{-2}	7.18×10^{-3}
3-2 P(7)	$4.71\times10^{-4}p + 9.31\times10^{-6}p^2$	8.61×10^{-3}	4.53×10^{-3}
3-2 P(8)	$1.45\times10^{-4}p + 1.93\times10^{-6}p^2$	2.46×10^{-3}	1.13×10^{-3}

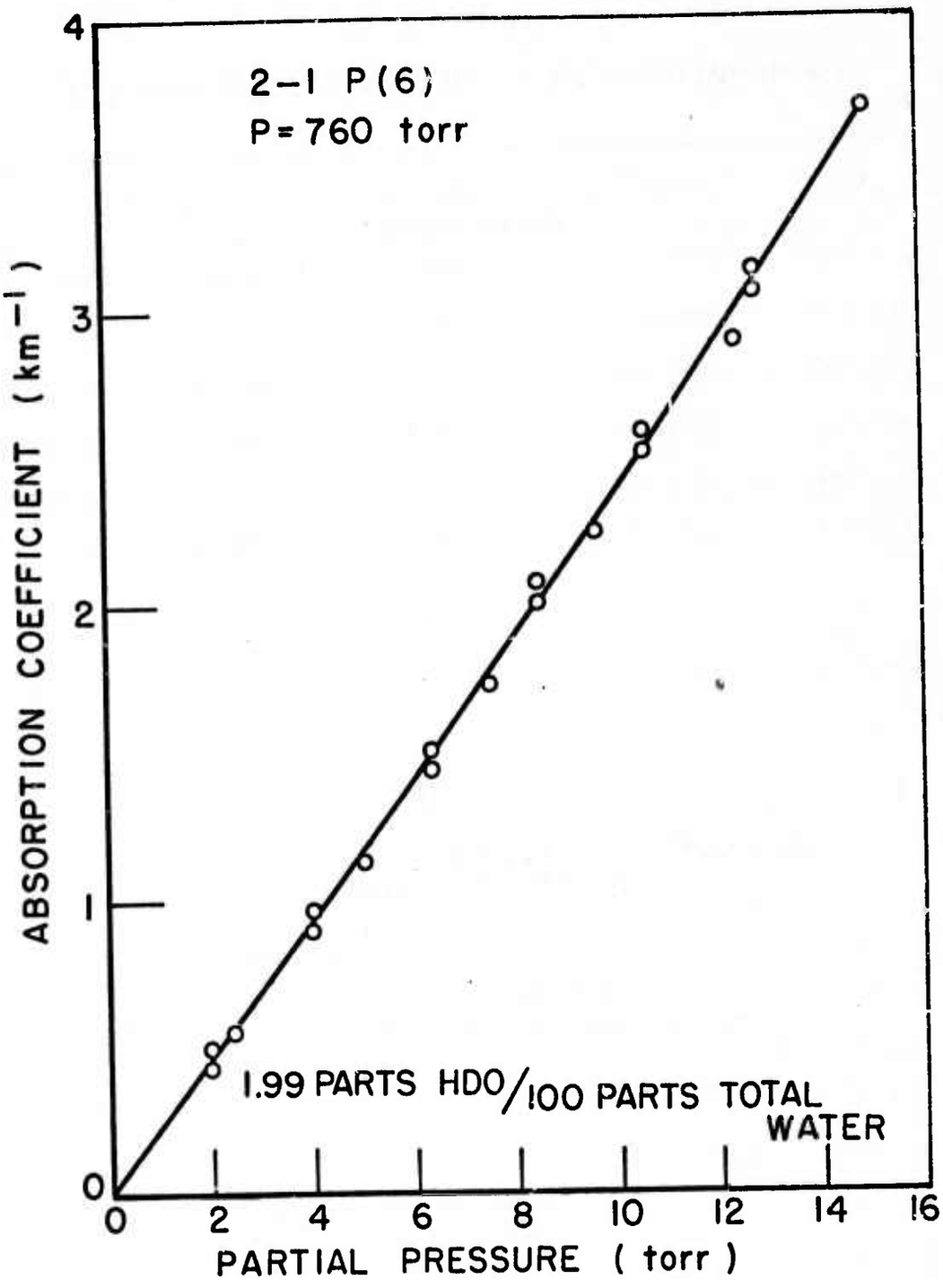

Fig. 69. Measured HDO-N_2 absorption coefficient for the 2-1 P(6) line at 2680.179 cm^{-1}.

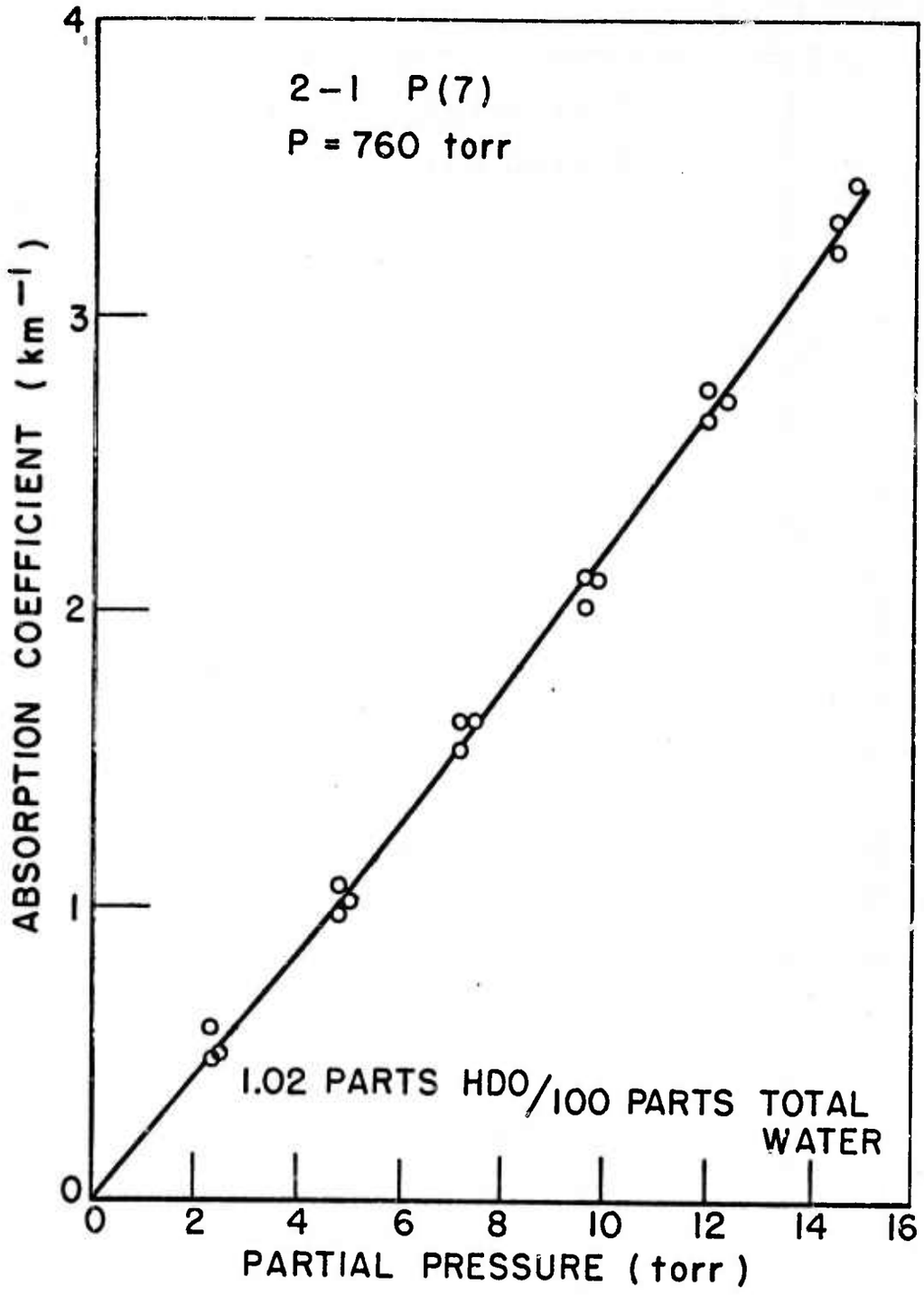

Fig. 70. Measured HDO-N_2 absorption coefficient for 2-1 P(7) line at 2655.868 cm^{-1}.

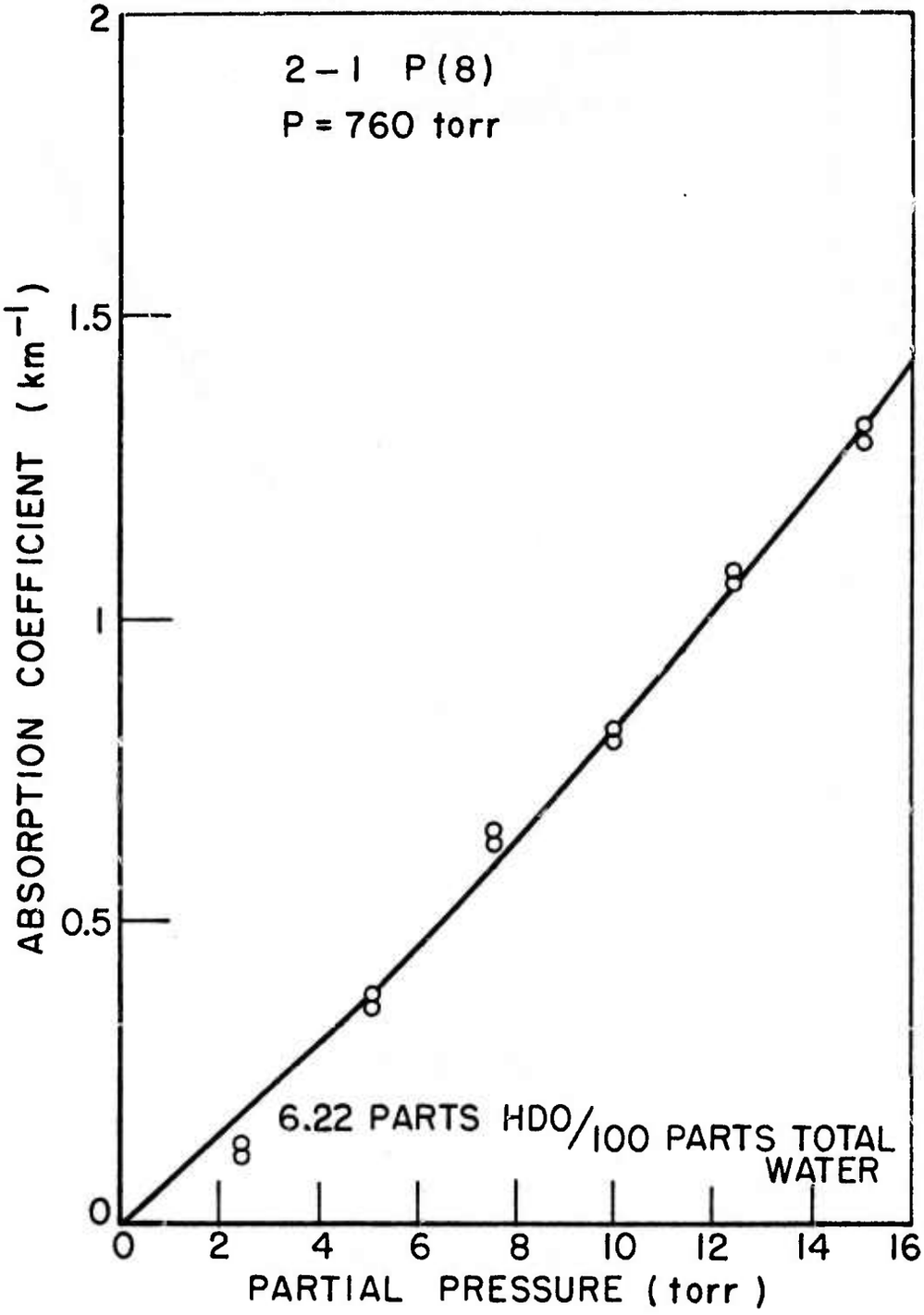

Fig. 71. Measured HDO-N_2 absorption coefficient for 2-1 P(8) line at 2631.068 cm^{-1}.

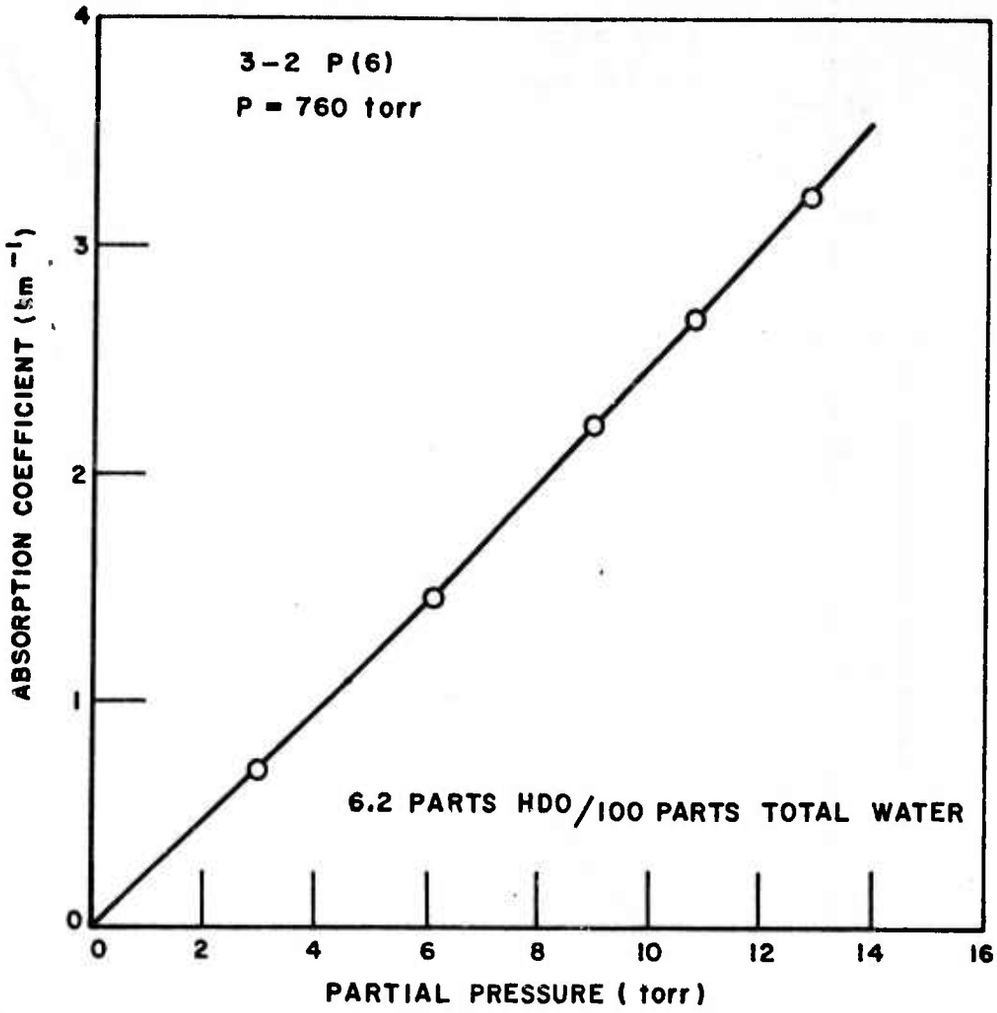

Fig. 72. Measured HDO-N_2 absorption coefficient for 3-2 P(6) line at 2594.198 cm^{-1}.

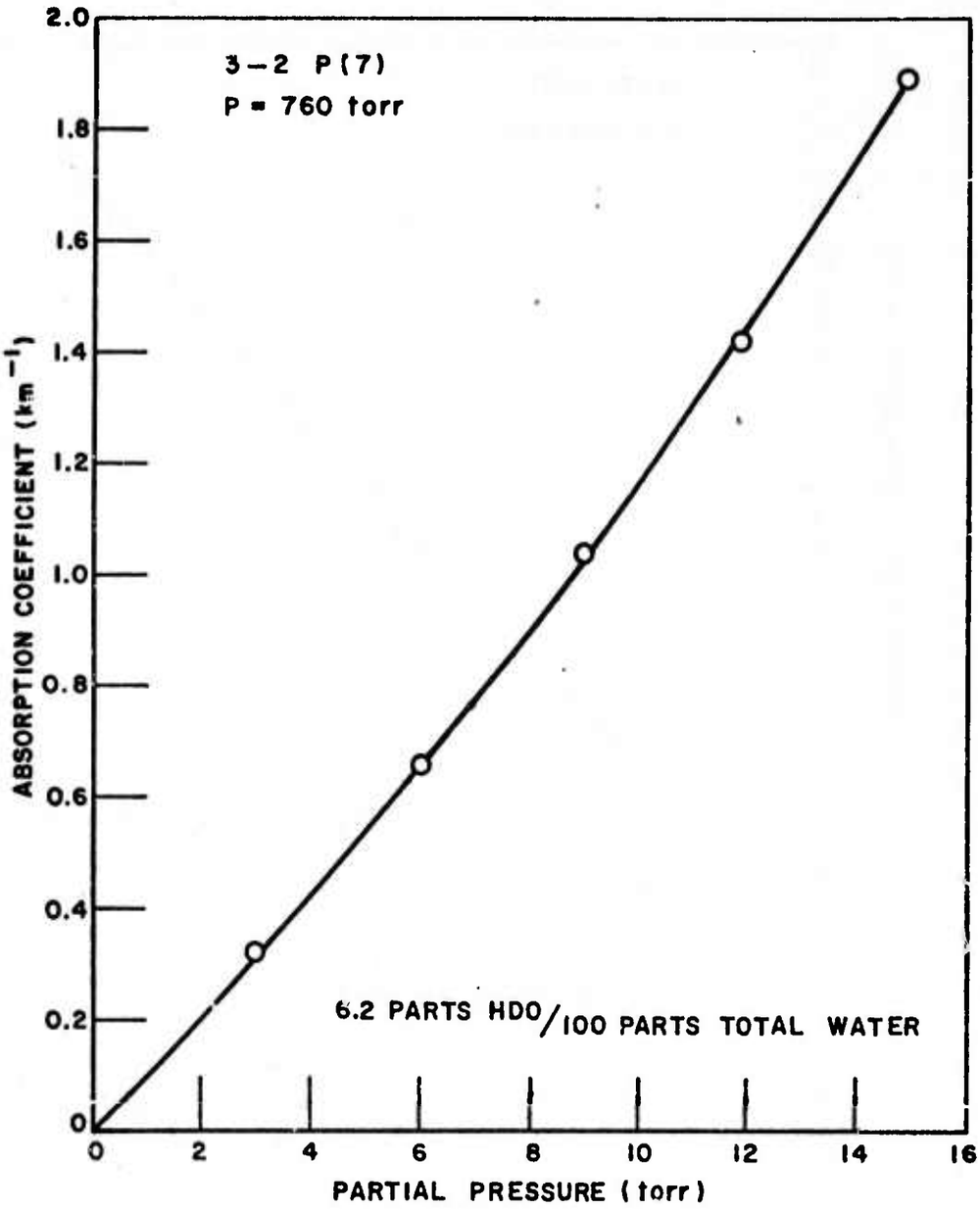

Fig. 73. Measured HDO-N_2 absorption coefficient for 3-2 P(7) line at 2570.522 cm^{-1}.

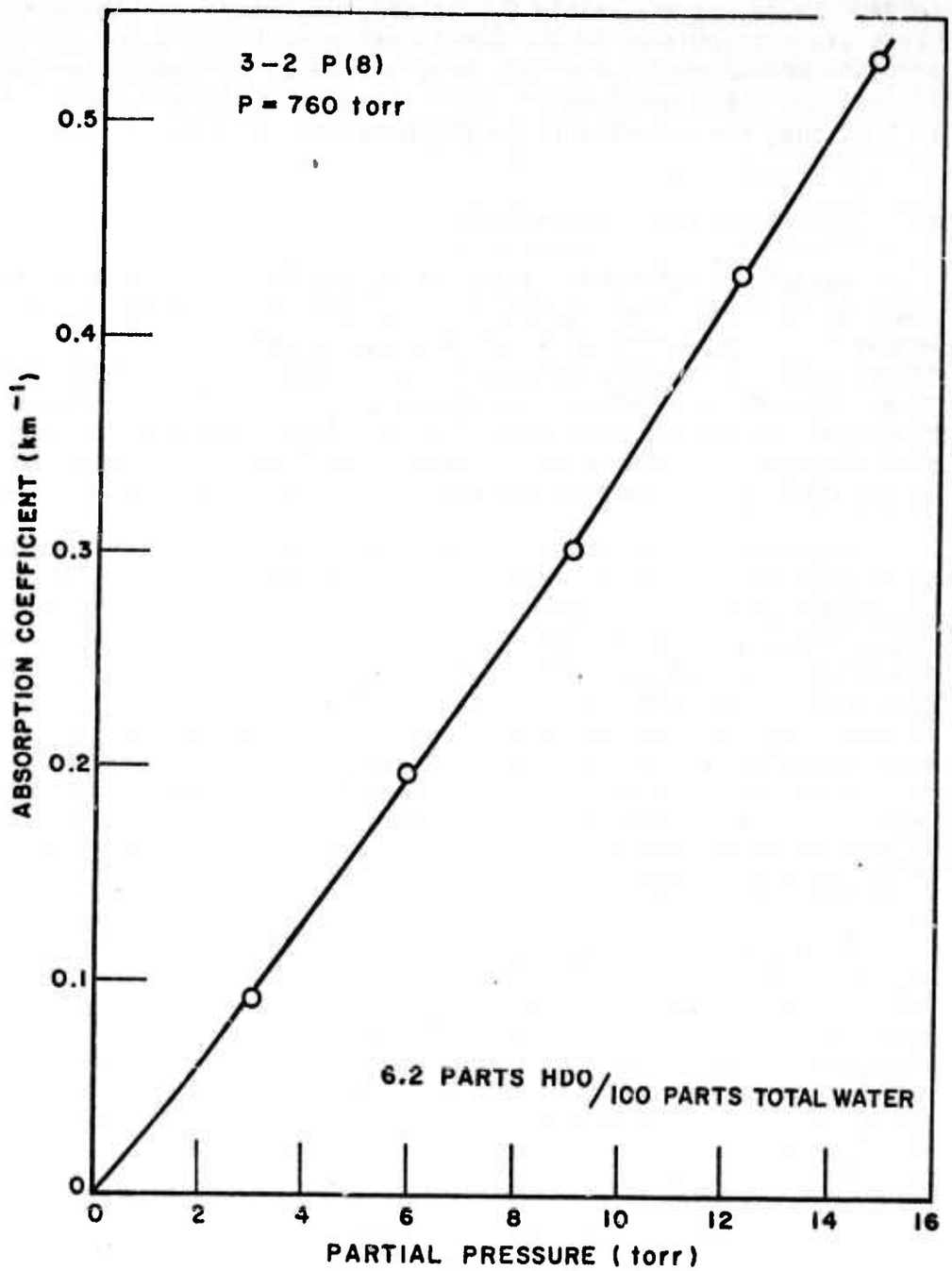

Fig. 74. Measured HDO-N_2 absorption coefficient for 3-2 P(8) line at 2546.375 cm^{-1}.

to 74. There was measurable D_2O absorption, however if the measurements are extrapolated to the conditions prevailing in the HDO absorption measurements, the D_2O contribution to the absorption coefficients at the highest water vapor pressure is .02 or .03 km^{-1} which is less than the uncertainty in the experimental data.

E. H_2O Absorption Measurements

Absorption of the 2-1 P(6), P(7), and P(8) and 3-2 P(6), P(7), and P(8) DF laser lines by H_2O-air and H_2O-nitrogen mixtures was measured. It was originally thought that water vapor absorption would be too small to measure accurately in the White cell at room temperature. However preliminary spectrophone measurements[28] indicated higher absorption on some lines than had been expected. It was therefore decided that with a very carefully performed experiment it might be possible to measure the absorption directly using the White cell.

Improvements in the White cell optics which were discussed in Chapter II made it possible to increase the path length to 1.341 kilometers with only a small increase in insertion loss. Also a new pulsed laser was constructed (described in Chapter III) which was primarily intended to eliminate RF noise emission. While testing the new laser it was also found that the average power was improved significantly over the earlier model. This made possible the use of thermopile detectors which eliminated the need for detector linearity correction which had been a source of error with the measurements using the lead selenide detectors. The thermopiles were carefully shielded in styrofoam to reduce the effect of air currents and short term fluctuations in room temperature.

In previous measurements the ratio of input power to output power for the evacuated cell and the cell filled with the desired sample had been determined by making 500 separate measurements of the ratio over about a one minute period and using the average as the final value. The sample transmittance was then just the quotient of the ratio obtained with the sample in the cell and the ratio obtained with the cell evacuated. The absorption coefficient was then obtained by dividing the negative of the natural logarithm of the transmittance by the path length.

For the measurements of HDO, N_2O, and CH_4 absorption it was possible to measure the absorption coefficient at several absorber concentrations and use least-squares curve-fitting techniques to reduce the uncertainty of the measurements. This was not possible for the H_2O measurements however since the absorption at the highest water vapor pressure was still quite low.

The procedure used therefore was to repeat the measurement of input to output ratio described above several times in a period of a half-hour. These ratios were then averaged to obtain a final

value. Also the ratio of input power to output power for the evacuated cell was measured both before and after the measurement of the ratio for the sample. Transmittances could then be calculated using each empty cell ratio separately or the average of the ratios. The entire procedure was repeated two or three times for each line, i.e., on different days and using different water samples.

The optical setup shown in Fig. 44 was used for these measurements. Measurements were made with a path length of 1.341 km, water vapor pressure of 14.3 torr and total pressure including dry air or nitrogen of 760 torr. Both dry air and nitrogen were used as broadening gases, and within error limits no difference in absorption coefficient was observed. Also there was no observable difference between the transmittance of the evacuated cell and the transmittance of the cell when filled with either dry air or nitrogen.

The water vapor sample was introduced into the cell from a bottle containing distilled water attached to the sample-mixing manifold. When the water bottle was first attached to the manifold it was pumped on for several hours to remove all dissolved gas. The water bottle was heated about 5°C above room temperature in order to speed the filling process. About 2½ hours was required to fill the cell with 14.3 torr of water vapor. The water vapor pressure was determined approximately using the mercury micromanometer as the water vapor was introduced. When the desired amount of water vapor had been introduced, the cell was filled to 760 torr with either nitrogen or dry air and the fans at each end of the cell were turned on and the sample was allowed to mix over night. The actual water vapor pressure was determined using the E.G. & G. Model 992 Dew Point Hygrometer at the time the transmittance measurement was made.

The data are presented in Tables 11, 12, 13, 14, 15, and 16 for the 2-1 P(6), P(7), and P(8) and 3-2 P(6), P(7), and P(8) DF laser lines. The ratio of input to output measured with the sample in the cell is designated R_i. The ratio measured for the evacuated cell before the sample is admitted is BK_{i1} and the ratio measured when the cell is evacuated after measuring the sample is designated BK_{i2}

In Table 17 the average values for each line are compared with the HDO measurements presented in Table 10 calculated H_2O values from Table 4, and H_2O continuum values obtained using Burch's data[4].

On the 2-1 P(6) line, the calculated H_2O absorption coefficient is very small, and the measured HDO absorption coefficient plus the water continuum absorption coefficient determined from Burch's measurements agree quite well with the measured H_2O absorption coefficient. Agreement is not as good on the 2-1 P(7) line although the measured HDO absorption coefficient added to water continuum absorption coefficient obtained from Burch's measurements is certainly

within the experimental scatter shown in Table 12. On the 2-1 P(8) line agreement is again only fair, although here the difference might be attributable to an error in the calculated H_2O absorption coefficient. For the 3-2 P(6), P(7), and P(8) lines the measured H_2O absorption coefficient is somewhat greater than the measured HDO absorption coefficient added to the water continuum absorption coefficient obtained from Burch's measurements (Column 4 in Table 17) in each case. For all three lines however the value in Column 4 of Table 17 is within the experimental scatter shown in Tables 14, 15, and 16.

One conclusion to be drawn from the direct measurements of H_2O absorption presented here is that the water continuum absorption obtained by extrapolating Burch's high temperature measurements is probably correct. A series of carefully performed spectrophone measurements would be the best way to determine the water continuum absorption accurately. This was beyond the scope of this study since a CW DF laser was not available. The only spectrophone measurements of the water continuum performed thus far[28] did not have the required accuracy due to experimental difficulties.

F. Summary of Molecular Absorption for the Eight Lines Studied

Table 18 gives the contribution to the molecular absorption due to each absorber at each of the 8 laser lines investigated for the sea-level mid-latitude summer model whose parameters are given in Table 3. The values listed are believed to be the most accurate available at this time. For N_2O, CH_4, and HDO the values given are those measured in this study for those lines where they are available. For CH_4, the absorption coefficients for the remaining lines are those obtained by Deaton, et al. [25] or the calculated values from Table 4. For HDO, the absorption coefficients for the lines not measured in this study are taken from the calculations in Table 4. For CO_2, the absorption coefficients are those obtained by Myers [30] except for the 2 - 1 P(8) line which was measured in this study. The contributions due to local water lines are obtained from the calculations in Table 4. The water vapor continuum absorption and the pressure induced nitrogen contributions are those obtained by Burch [4].

For each line the total absorption coefficient due to molecular absorption is presented. From the total molecular absorption coefficients the transmittance of a ten kilometer sea level path was calculated for each line. These values are also presented in Table 18. The transmittance over a ten kilometer sea level path varies from 0.31 for the 2 - 1 P(7) line to 0.73 for the 2 - 1 P(8) line. It should be pointed out that the actual transmittance through a real atmosphere would probably be lower than shown in Table 18 because of aerosol scattering and absorption.

TABLE 11

H_2O ABSORPTION ON THE 2-1 P(6) DF LASER LINE AT 2680.179 cm^{-1}

	T	K (Km^{-1})	Avg. K (Km^{-1})
R_1/BK_{11} = 1.071/1.183	0.905	0.074	0.075
R_1/BK_{12} = 1.071/1.182	0.906	0.074	
R_2/BK_{21} = 1.071/1.181	0.907	0.073	
R_2/BK_{22} = 1.071/1.192	0.898	0.080	
$R_1 \Big/ \left(\frac{BK_{11} + BK_{12}}{2}\right)$ = 1.071/1.1825	0.906	0.074	0.075
$R_2 \Big/ \left(\frac{BK_{21} + BK_{22}}{2}\right)$ = 1.071/1.1865	0.903	0.076	

TABLE 12

H_2O ABSORPTION ON THE 2-1 P(7) DF LASER LINE AT 2655.863 cm^{-1}

	T	K (Km^{-1})	Avg. K (Km^{-1})
R_1/BK_{11} = 1.055/1.196	0.882	0.094	0.103
R_1/BK_{12} = 1.055/1.204	0.876	0.099	
R_2/BK_{21} = 1.033/1.204	0.858	0.114	
R_2/BK_{22} = 1.033/1.211	0.853	0.119	
R_3/BK_{31} = 1.045/1.211	0.863	0.110	
R_3/BK_{32} = 1.045/1.170	0.893	0.084	
$R_1 \Big/ \left(\frac{BK_{11} + BK_{11}}{2}\right)$ = 1.055/1.200	0.879	0.096	0.103
$R_2 \Big/ \left(\frac{BK_{21} + BK_{22}}{2}\right)$ = 1.033/1.208	0.855	0.116	
$R_3 \Big/ \left(\frac{BK_{31} + BK_{32}}{2}\right)$ = 1.045/1.191	0.878	0.097	

TABLE 13

H_2O ABSORPTION ON THE 2-1 P(8) DF LASER LINE AT 2631.068 cm^{-1}

	T	K (Km^{-1})	Avg. K (Km^{-1})
R_1/BK_{11} = 1.422/1.499	0.949	0.039	0.0376
R_1/BK_{12} = 1.422/1.484	0.958	0.032	
R_2/BK_{21} = 1.414/1.484	0.953	0.036	
R_2/BK_{22} = 1.414/1.498	0.944	0.043	
$R_1 / \left(\frac{BK_{11} + BK_{12}}{2}\right)$ = 1.422/1.492	0.953	0.036	0.038
$R_2 / \left(\frac{BK_{21} + BK_{22}}{2}\right)$ = 1.414/1.491	0.948	0.040	

TABLE 14

H_2O ABSORPTION ON THE 3-2 P(6) DF LASER LINE AT 2594.198 cm^{-1}

	T	K (Km^{-1})	Avg. K (Km^{-1})
R_1/BK_{11} = 1.151/1.230	0.936	0.050	
R_2/BK_{21} = 1.182/1.336	0.885	0.091	
R_2/BK_{22} = 1.182/1.329	0.889	0.087	
R_3/BK_{31} = 1.248/1.329	0.939	0.047	0.059
R_3/BK_{32} = 1.248/1.329	0.939	0.047	
R_4/BK_{41} = 1.296/1.357	0.955	0.034	
R_4/BK_{42} = 1.296/1.392	0.931	0.053	
R_1/BK_{11} = 1.151/1.230	0.936	0.050	
$R_2 / \left(\frac{BK_{21} + BK_{22}}{2}\right)$ = 1.182/1.333	0.887	0.089	
$R_3 / \left(\frac{BK_{31} + BK_{32}}{2}\right)$ = 1.248/1.329	0.939	0.047	0.057
$R_4 / \left(\frac{BK_{41} + BK_{42}}{2}\right)$ = 1.296/1.375	0.943	0.044	

TABLE 15

H_2O ABSORPTION ON THE 3-2 P(7) DF LASER LINE AT 2570.522 cm^{-1}

	T	K (Km^{-1})	Avg. K (Km^{-1})
R_1/BK_{11} = 1.324/1.389	0.953	0.036	0.035
R_1/BK_{12} = 1.324/1.397	0.948	0.040	
R_2/BK_{21} = 1.357/1.428	0.950	0.038	
R_2/BK_{22} = 1.357/1.422	0.954	0.035	
R_3/BK_{31} = 1.357/1.422	0.954	0.035	
R_3/BK_{32} = 1.357/1.403	0.967	0.025	
R_4/BK_{41} = 1.355/1.417	0.956	0.033	
R_4/BK_{42} = 1.355/1.420	0.954	0.035	
$R_1 \Big/ \left(\frac{BK_{11} + BK_{12}}{2}\right)$ = 1.324/1.393	0.950	0.038	0.035
$R_2 \Big/ \left(\frac{BK_{21} + BK_{22}}{2}\right)$ = 1.357/1.425	0.952	0.036	
$R_3 \Big/ \left(\frac{BK_{31} + BK_{32}}{2}\right)$ = 1.357/1.413	0.961	0.030	
$R_4 \Big/ \left(\frac{BK_{41} + BK_{42}}{2}\right)$ = 1.355/1.419	0.955	0.034	

TABLE 16

H_2O ABSORPTION ON THE 3-2 P(8) DF LASER LINE AT 2546.375 cm^{-1}

	T	K (Km^{-1})	Avg. K (Km^{-1})
R_1/BK_{11} = 1.352/1.422	0.951	0.038	0.029
R_2/BK_{21} = 1.394/1.469	0.949	0.039	
R_2/BK_{22} = 1.394/1.429	0.976	0.018	
R_3/BK_{31} = 1.383/1.429	0.968	0.024	
R_3/BK_{32} = 1.383/1.432	0.966	0.026	
R_1/BK_{11} = 1.352/1.422	0.951	0.038	0.031
$R_2 \Big/ \left(\frac{BK_{21} + BK_{22}}{2}\right)$ = 1.394/1.449	0.962	0.029	
$R_3 \Big/ \left(\frac{BK_{31} + BK_{32}}{2}\right)$ = 1.383/1.431	0.967	0.025	

TABLE 17

H_2O MEASUREMENTS COMPARED WITH CALCULATED H_2O VALUES, MEASURED HDO VALUES, AND THE H_2O CONTINUUM

Line	1 H_2O calc (km^{-1})	2 HDO exp (km^{-1})	3 H_2O (a) cont. (km^{-1})	4 1+2+3 (km^{-1})	5 H_2O measured (km^{-1})
2-1 P(6)	2.34×10^{-4}	5.24×10^{-2}	2.12×10^{-2}	7.38×10^{-2}	7.5×10^{-2}
2-1 P(7)	4.42×10^{-6}	9.54×10^{-2}	1.93×10^{-2}	1.15×10^{-1}	1.03×10^{-1}
2-1 P(8)	4.73×10^{-3}	6.00×10^{-3}	1.78×10^{-2}	2.85×10^{-2}	3.8×10^{-2}
3-2 P(6)	3.54×10^{-4}	1.74×10^{-2}	1.68×10^{-2}	3.46×10^{-2}	5.7×10^{-2}
3-2 P(7)	4.69×10^{-5}	8.6×10^{-3}	1.74×10^{-2}	2.60×10^{-2}	3.5×10^{-2}
3-2 P(8)	4.44×10^{-5}	2.46×10^{-3}	1.86×10^{-2}	2.11×10^{-2}	3.1×10^{-2}

(a) From Burch [4]

TABLE 18

SUMMARY OF MOLECULAR ABSORPTION COEFFICIENTS FOR 8 DF LASER LINES
MID-LATITUDE SUMMER MODEL

Line	N_2O (km^{-1})	CH_4 (km^{-1})	CO_2 (km^{-1})	HDO (km^{-1})	H_2O (local)[c] (km^{-1})	H_2O (cont.)[e] (km^{-1})	N_2[e] (km^{-1})	Total (km^{-1})	Transmittance 10 km path
3-2 P(8)	2.14E-2 [a]	4.11E-4 [b]	4.21E-4 [d]	2.46E-3 [a]	4.44E-5	1.86E-2	8.0E-3	5.13E-2	0.60
2-1 P(11)	9.69E-3 [a]	7.67E-5 [c]	2.1E-4 [d]	5.07E-4 [c]	4.70E-6	1.82E-2	7.1E-3	3.58E-2	0.70
3-2 P(7)	3.73E-2 [a]	2.47E-4 [b]	5.24E-4 [d]	8.61E-3 [a]	4.69E-5	1.74E-2	5.0E-3	6.91E-2	0.50
2-1 P(10)	4.53E-2 [a]	1.77E-4 [b]	5.7E-5 [d]	2.65E-3 [c]	5.52E-6	1.70E-2	3.6E-3	6.88E-2	0.50
3-2 P(6)	2.27E-3	1.49E-4 [b]	6.85E-4 [d]	1.74E-2 [a]	3.54E-4	1.68E-2	2.6E-3	4.03E-2	0.67
2-1 P(8)		8.59E-4 [a]	5.3E-4 [a]	6.00E-3 [a]	4.73E-3	1.78E-2	1.9E-3	3.18E-2	0.73
2-1 P(7)		1.13E-3 [a]	1.85E-4 [d]	9.54E-2 [a]	4.42E-6	1.93E-2		1.16E-1	0.31
2-1 P(6)		1.52E-3	1.9E-5	5.24E-2	2.34E-4	2.12E-2		7.54E-2	0.47

(a) This Study
(b) From Deaton [26]
(c) Theoretical (from Table 4)
(d) From Myers [31]
(e) From Burch, et al. [4]

CHAPTER V

SUMMARY

The purpose of this study was to determine, as accurately as possible, the absorption of DF laser radiation by atmospheric gases.

Computer programs were written which can be used to calculate the absorption of radiation by atmospheric gases from the AFCRL Line Compilation [3]. Using these programs, absorption coefficients for all the DF laser lines and all the atmospheric absorbers were calculated. These calculated absorption coefficients were used to plan experiments to measure accurately the absorption coefficients for selected DF laser lines. Lines selected for study were the 2-1 P(6), P(7), and P(8) lines and the 3-2 P(6), P(7), and P(8) lines. For these lines absorption coefficients were measured for N_2O, CH_4, CO_2, HDO, and H_2O. For a given laser line, the absorption coefficient was measured for those gases which were significant absorbers at that frequency, and not necessarily for all gases. In addition to the lines listed above, the N_2O absorption coefficient was measured for the 2-1 P(10) and P(11) lines since they were the only other DF laser lines for which N_2O absorption was significant.

The results of the measurements were compared with the calculations and with results obtained by other workers. It was found that the calculated values for the N_2O absorption coefficients agreed very well with the measured absorption coefficients. For the other gases the agreement between calculation and measurement was not as good, although in most cases the calculations and measurements were of the same order of magnitude. For CO_2 the calculated absorption coefficients are about 10^{-7} km^{-1}. Myers [30] found that the CO_2 absorption coefficients were actually about 10^{-4} km^{-1}. The CO_2 absorption coefficient was measured for the 2-1 P(8) line and found to be of the same order of magnitude as that measured by Myers. The discrepancy in the calculations is probably caused by a weak isotope band which is not included in the AFCRL tapes. The H_2O absorption measurements confirmed that the values for water continuum absorption obtained by extrapolating the high temperature measurements of Burch, et.al. [4] are close to the correct values.

The transmittance of a ten kilometer sea level path for the Mid Latitude Summer model [16] was calculated from the most accurate values of the molecular absorption coefficients for each of DF laser

lines investigated in this study. The calculated transmittance varied from 31% to 83% for a ten kilometer path. The actual transmittance over a ten kilometer path in the real atmosphere would be somewhat lower since attenuation due to turbulence and aerosol scattering and absorption has not been accounted for.

Further work in this area should include an extension of these measurements to other DF laser lines and measurements over a range of total pressure and temperature. There is also a need for carefully performed spectrophone measurements to more accurately determine the water contiuum absorption and the pressure induced nitrogen absorption.

APPENDIX A

UNITS AND CONVERSION FACTORS USED IN MOLECULAR ABSORPTION CALCULATION PROGRAMS

The information in this appendix has appeared in earlier reports [32,33]. It is presented here for completeness and easy reference.

A. Basic Equation for Lorentz Line

(136) $$\ell n\ T = -\ ku$$

where T = transmittance
u = absorber concentration
k = extinction coefficient

and

(137) $$k_\nu = \sum_i \frac{S_i\ \alpha_i}{\pi[(\nu-\nu_i)^2 + \alpha_i^2]}$$

where S_i = line strength
ν = wavenumber
ν_i = line center wavenumber
α_i = half-width at half intensity.

B. Units of S and u

1. It is necessary to specify the units of S and u so that the product ku is dimensionless.

   It has been common to use different units for CO_2 and other gases and for water vapor. Recently, however, Calfee and others have begun to use similar units for all gases. All of these units will be discussed.

2. Units of S

H_2O: S is in $cm^{-1}/gm\ cm^{-2}$
(pr-cm and $gm\ cm^{-2}$ are the same)

CO_2: S is in $cm^{-1}/atm\text{-}cm$.

H_2O and CO_2 (uniform system): S is in $cm^{-1}/molecules\ cm^{-2}$.

3. Units of Absorber Concentration, u .

H_2O: $gm\ cm^{-2}$ or pr-cm

$$u_{H_2O} = \rho\ell = \frac{288.34 \times 10^{-4} p_{H_2O,torr}\ \ell_{mtr}}{T_{o_K}} \quad \text{pr-cm} \tag{138}$$

for reference

$$\rho_{H_2O} = \frac{1.05821 \times 10^{-6}\ p_{H_2O,\ torr}}{1 + .00367\ T_{o_C}}\ gm/cm^3 \tag{139}$$

CO_2: $atm\text{-}cm_{T_{o_K}}$

$u_{CO_2} = p_{CO_2} \times \ell$.

It is necessary to specify the temperature since pressure depends on temperature through the gas law $p = NkT$, i.e., p_{CO_2} is CO_2 pressure in atm. at T_o.

ℓ = path length in cm.

H_2O and CO_2 (uniform system): $molecules/cm^2$

4. Conversion factors between separate and uniform system[34].

(140) $u[\text{atm-cm}_{STP}] \times 2.689 \times 10^{19} = u[\text{molecules/cm}^2]$

(141) $u[\text{pr cm}_{H_2O}] \times 3.34 \times 10^{22} = u[\text{molecules/cm}^2]$

(142) $S_o[\text{cm}^{-1}/\text{atm-cm}_{STP}] \times 3.72 \times 10^{-20} = S_o[\text{cm}^{-1}/\text{molecules cm}^{-2}]$

(143) $S_o[\text{cm}^{-1}/\text{pr cm}] \times 2.991 \times 10^{-23} = S_o[\text{cm}^{-1}/\text{molecules cm}^{-2}]$.

It is most convenient to have one computer program for all gases. Thus, the uniform system is to be recommended.

C. Conversion of $(\text{atm-cm})_{STP}$ to molecules cm^{-2}[16]

The molecular weight, M, of any gas in grams occupies 22.4136 liters at STP [12] so one cm^3 of any gas at STP weighs

$$\frac{M}{2.24136 \times 10^4} \text{ grams.}$$

Since 1 atm-cm_{STP} is equivalent to one cm of gas at STP per cm^2

(144) $$1 \text{ atm-cm}_{STP} = \frac{M}{2.24136 \times 10^4} \text{ gm cm}^{-2}.$$

Avogardro's number [35] car be used to compute the number, n of molecules per cm^3 of any gas

(145) $$n = \frac{6.02252 \times 10^{23}}{2.24136 \times 10^4} = 2.687016 \times 10^{10} \text{ molecules cm}^{-3}.$$

Hence the desired result is

(146) $$\boxed{\text{one atm-cm}_{STP} = 2.6870 \times 10^{19} \text{ molecules cm}^{-2}} \quad .$$

D. Conversion of Precipitable Centimeters of Water to mol cm^{-2} [6]

(147) $$1 \text{ atm-cm}_{STP,H_2O} = \frac{M}{2.24136 \times 10^4} = \frac{18.016}{2.24136 \times 10^4}$$

(148) $$1 \text{ atm-cm}_{STP,H_2O} = 8.03798 \times 10^{-4} \text{ gm cm}^{-2}.$$

Using the constant developed in paragraph C, above we have the desired result.

(149) $$\boxed{1 \text{ pr-cm} = 3.3429 \times 10^{22} \text{ mol cm}^{-2}} \quad .$$

E. Partial pressure of Water Vapor from Density and Temperature [36].

From the referenced tables we have the relation

(150) $$\rho = \frac{10^3 a \, \delta \, p_a / 760}{1 + \alpha T} \quad \text{gm m}^{-3}$$

where

(151) a = weight of one cubic meter of dry air at 0°C and 760 torr = 1.29278 kg.

(152) δ = density of aqueous vapor relative to dry air = .62168

(153) p_a = partial pressure H_2O in torr

(154) α = coefficient of expansion of air for 1°C = .00366.

Rearranging we have the desired result

(155) $$\boxed{p_a = .9456 \, (1 + .00366 \, T) \, \rho \text{ torr}}$$

where T = temperature in deg C

ρ = water vapor density in gm/m^3

F. Precipitable centimeters H_2O from partial pressure, temperature, and path length

(156) $$w = \rho \ell \quad .$$

Using the relation from paragraph C,

(157) $$w = \frac{1.05821\ p_a \cdot 10^{-6}}{1 + .00367\ (T_{\circ K} - 273.13)} \cdot \ell \cdot 10^2$$

where ℓ is the path length in meters

p_a is water vapor pressure in torr.

Since the third term in the denominator is nearly unity, we can write

(158) $$\boxed{w = \frac{2.8834 \times 10^{-2}\ p_a\ \ell}{T} \text{ pr-cm}} \quad .$$

G. Conversion to atm-cm_{STP} from pressure, path length, and temperature of sample [16]

$$\text{atm-cm}_{STP} = \frac{\ell p_a}{760} \quad \frac{273.13}{T}$$

(159) $$\boxed{\text{atm-cm}_{STP} = 3.5938 \times 10^{-1} \quad \frac{p_a\ \ell}{T}}$$

where p_a = absorber pressure in torr

ℓ = path length in cm

T = temperature in deg K.

H. Density computed from partial pressure, molecular weight, and temperature

This is of course the Gas Law

(160) $$\rho = 1.6035 \times 10^{-5} \frac{p_a M}{T} \text{ gm cm}^{-3}$$

where p_a = pressure in torr
M = molecular weight
T = deg K.

I. Partial pressure of water vapor from mixing ratio [14]

(161) $$p_a = \frac{r P}{.62168 + r} \text{ torr}$$

where r is the mixing ratio and P is the total pressure in torr.

From the data in the AFCRL models [16], one should compute mixing ratio as follows:

(162) $$r = \frac{\rho_{H_2O}}{\rho_{air} - \rho_{H_2O} \frac{28.9785}{18.0153}}$$

Note that the constant .62168 in Eq. (7) is the ratio of the molecular weight of water vapor to that of dry air at STP, i.e., 18.0153/28.9785, see reference 35. In the Smithsonian tables [36] the value used is 0.62197 apparently based on older molecular weight data.

J. Ozone partial pressure from density for AFCRL mid-latitude summer model [16]

$$(163) \quad p_a' = \frac{d}{q} \times 760 \times \frac{6.0 \times 10^{-5}}{1.191 \times 10^{3}} \text{ torr}$$

where d = air density at STP = 28.9785(35),
q = molecular weight of ozone = 47.9982 (35),

and 6.0×10^{-5} g/m^3 is the density of ozone and 1.191×10^{3} g/m^3 is the air density, both at sea level, of the AFCRL mid-latitude summer model. The result is 2.31×10^{-5} torr.

APPENDIX B

ABSORPTION CALCULATION PROGRAM LISTINGS

A. Single Frequency Calculation Program

A listing of the program is given on pages 156 to 167. The program was written to operate on the ElectroScience Laboratory time-sharing system and contains some statements which are incompatible with other computer systems.

In line 34 the statement OPTIONS 32K allows the program to use over 60,000 words of program storage although the computer only has 27,000 words of program storage available. The rest of the storage is on disc and is swapped into the computer memory as needed.

In line 49, CALL ESC ($100) causes the program to branch to statement 100 immediately if the escape key on the teletype is pressed.

The statement CALL COMDFL ($100) in line 50 and the CALL COMD(----) statements in lines 66, 73, 82, 96, 112, 119, 140, 162, 209, 306, 364, 384, 389, 405 are used to enable the user to branch easily from one part of the program to another. When the CALL COMD(----) statement is executed the computer types < > on the teletype and waits for input from the user. The user responds by typing a character string of 1-6 characters long and a carriage return. The computer then branches to the first executable statement following the CALL COMD(----) statement having the character string as its argument. For example if the statement CALL COMD(5HPRESS) in line 66 is executed, the computer will type < >. If the user types PRESS, the computer will branch to the statement in line 70. If the user types SUB, the computer will branch to the statement in line 86. For another computer system a similar set of subroutines could be written. They would have to be written in assembly language and would require some knowledge about how arguments are passed to subroutines. Alternatively, a control routine could be written in Fortran which performed the same function using UF statements and computed GO TO statements.

The CALL ASSIGN (----) statements in lines 185, 218, 353, and 399 are associated with the ElectroScience Laboratory timesharing file system and are used to assign logical unit numbers to physical devices or to disc files.

The TPFILE and TPRKD subroutines called in lines 244 and 245 are system subroutines which are used to skip files and records on a magnetic tape.

For the single frequency calculation program there is a limit on the size of the frequency interval over which calculations may be made at one time. This limit is caused by the size of the array in which the absorption line data is stored (AD(4,5600) in line 40). For a set of calculations covering the frequency range VL to VH, the program requires all the data for absorption lines of the correct substance with strength greater than SLOW in the frequency range from VL - BOUND to VH + BOUND. For the ElectroScience Laboratory computer system the maximum storage allowed for the program and the data is 60,000 words. This is enough room for the calculation program and the data for 5600 absorption lines.

The data is stored in one 4 by 5600 array rather than four 560-word arrays in order to increase the efficiency of the program on a timesharing computer.

```
      C     PROGRAM NAME: LEVEL
      C
      C     COPYRIGHT 1975 THE OHIO STATE UNIVERSITY
      C
      C     CALCULATES SINGLE FREQUENCY,LEVEL PATH
      C     ABSORPTION COEFFICIENTS.
      C
      C     PROGRAM AUTHORS: G. L. TRUSTY AND F. S. MILLS
      C                      THE OHIO STATE UNIVERSITY
      C                      ELECTROSCIENCE LABORATORY
      C                      1320 KINNEAR ROAD
      C                      COLUMBUS, OHIO 43212.
      C
      C     USABLE COMMANDS ARE PRESS, BROAD, NALFA, ETA, ABS,
      C     TEMP, LINES, EXE, END, DATA, SUB, STORE, VAR,RESULT.
      C****
      C     CALCULATION CAN BE MADE FOR A MAXIMUM OF 175
      C     FREQUENCIES.  LAST ENTRY IN DATA FILE SHOULD BE 0.0
      C     IF FILE CONTAINS FEWER THAN 175 LINES.  FIRST
      C     LINE MUST BE LOWEST FREQUENCY AND LAST LINE HIGHEST.
      C******
      C     LOGICAL DEVICE ASSIGNMENTS FOR THIS PROGRAM
      C          0   AFCRL LINE DATA TAPE (INPUT)
      C          2   FILE CONTAINING CALCULATION FREQ. (INPUT)
      C          3   FILE OF FREQUENCIES AND CALCULATED
      C              ABSORPTION COEFFICIENTS (OUTPUT)
      C          6   ,OUT FILE (LINE PRINTER OUTPUT)
      C          7   MSG,3271A (PROGRAM WRITES TIME WHEN
      C              OFF-LINE CALCULATION IS COMPLETED)
      C          8   TELETYPE (OPERATOR COMMUNICATION,
      C              INPUT OR OUTPUT)
      C          JJ  OUTPUT DEVICE SELECTOR (6 OR 8)
      C
            OPTIONS 32K
            LOGICAL FIRST,RWOUND, TELE
            REAL NALFA
            DIMENSION ICARD(5),ABS(5),IDATE(3)
            COMMON JJ
            DIMENSION Y(5,175),VL(175),BX(7),CX(7),MA(7),ITIM(3)
            COMMON/Z/AD(4,5600),CAY
            DATA ITTY/3HTTY/,BOUND/20.0/,TEMP0/296.0/,S_BW/.1E-26/
            DATA MA/18,44,45,44,28,16,32/,IYES/3HYES/
            DATA CX/.62,.58,0.5,0.5,0.5,0.5,0.5,0.5/
            DATA BX/1.5,1.0,1.5,1.0,1.0,1.5,1.0/
      C
      C     PRINT LIST OF USABLE COMMANDS ON TELETYPE.
      C
            WRITE(8,2070)
            CALL ESC($100)
            CALL COMDFL($100)
      C
      C     FLAGS USED THRU THE PROGRAM:
      C     FIRST -- SIGNIFIES FIRST TIME THRU THE PROGRAM
```

```
C     RWOUND - DATA FILE HAS BEEN REWOUND
C     TELE ---- FREQUENCIES TO BE ENTERED ON TELETYPE
C
      JJ=6
      FIRST=.TRUE.
      RWOUND=.FALSE.
      TELE=.TRUE.
C
C     WRITE DATE AND TIME ON THE TELETYPE.
C
      CALL CLOCK
      GO TO 150
100   CALL COMD(5HPRESS)
C
C     READ THE TOTAL PRESSURE IN TORR.
C
150   WRITE(8,2000)
      READ(8,-)P1
      IF(FIRST)GO TO 200
      CALL COMD(4HTEMP)
C
C     READ THE TEMP IN DEG F.
C
      REWIND 0
      RWOUND=.TRUE.
200   WRITE(8,1980)
      READ(8,-)TF
      IF(FIRST)GO TO 300
      CALL COMD(3HSUB)
C
C     GET SUBSTANCE ID NUMBER
C
300   WRITE(8,3020)
      READ(8,-)NSUB
C
C     GET ISOTOPE INFORMATION
C
      WRITE(8,3030)
      READ(8,-)ISOTOP
      IF(FIRST)GO TO 400
      RWOUND=.TRUE.
      REWIND 0
      CALL COMD(3HABS)
C
C     READ THE ABSORBER PRESSURES IN TORR. 5 MAXIMUM.
C
400   WRITE(8,2010)
C
C     NTORRS IS THE NUMBER OF ABSORBER PRESSURES TO BE USED.
C
      READ(8,-)NTORRS
      IF(NTORRS.GT.5)NTORRS=5
      WRITE(8,2020)
C
C     ABS(I) ARE THE ABSORBER PRESSURES IN TORR
```

```
109     C
110           READ(8,-)(ABS(I),I=1,NTORRS)
111           IF(FIRST)GO TO 500
112           CALL COMD(5HBROAD)
113     C
114     C     READ THE SELF-BROADENING COEFFICIENT.
115     C
116     500   WRITE(8,1990)
117           READ(8,-)BROAD
118           IF(FIRST)GO TO 600
119           CALL COMD(5HNALFA)
120     C
121     C     READ THE NUMBER OF HALFWIDTHS WHERE LINE SHAPE
122     C     MODIFICATION TAKES PLACE.
123     C
124     600   WRITE(8,1970)
125           READ(8,-)NALFA
126           IF(FIRST)GO TO 700
127     C
128     C     CALCULATE CNORM, THE NORMALIZING FACTOR FOR MODIFIED
129     C     LINE SHAPE. SEE MILLS NOTEBOOK #4320 PG 104 FOR DETAILS.
130     C     NOTE IN THE FOLLOWING LINES THAT CNORM IS COMPUTED
131     C     AT TWO PLACES. THIS MUST BE DONE IN ORDER FOR THE
132     C     TIMESHARING  COMD  FUNCTION TO WORK PROPERLY FOR
133     C     BOTH NALFA AND ETA.
134     C
135           IF(ETA.EQ.2.)GO TO 650
136           CNORM=3.14159/(2.*(ATAN(NALFA)+NALFA/((NALFA*NALFA+1.)*
137          1(ETA-1.))))
138           GOTO 690
139     650   CNORM=1.
140     690   CALL COMD(3HETA)
141     C
142     C     READ THE MODIFIER POWER (ETA).
143     C
144     700   WRITE(8,1960)
145           READ(8,-)ETA
146     C
147     C     CHECK TO SEE IF ETA IS LESS THAN ONE.
148     C
149           IF(ETA.GT.1.)GO TO 710
150           WRITE(8,2050)
151           GO TO 700
152     C
153     C     CALCULATE CNORM, THE NORMALIZING FACTOR FOR MODIFIED
154     C     LINE SHAPE. SEE MILLS NOTEBOOK #4320 PG 104 FOR DETAILS.
155     C
156     710   IF(ETA.EQ.2.)GO TO 730
157           CNORM=3.14159/(2.*(ATAN(NALFA)+NALFA/((NALFA*NALFA+1.)*
158          1(ETA-1.))))
159           GOTO 740
160     730   CNORM=1.
161     740   IF(FIRST)GO TO 800
162           CALL COMD(5HLINES)
163     C
```

```
C     READ CALCULATION FREQUENCIES INTO VL. 175 MAXIMUM.
C
      REWIND 0
      RWOUND=.TRUE.
      TELE = .TRUE.
      CLOSE 2
C
C     ARE FREQUENCIES TO BE ENTERED ON TELETYPE
C
800   WRITE(8,1020)
      READ(8,1030)IIN
      IF(IIN.NE.ITTY)TELE=.FALSE.
      IF(TELE)GO TO 155
C
C     REQUEST LOCATION OF FILE WITH CALCULATION FREQUENCIES
C     LAST LINE OF FILE MUST BE 0.0 IF THERE ARE FEWER THAN
C     175 CALCULATION FREQUENCIES.
C
      WRITE(8,1000)
      READ(8,1010)FILEL
      READ(8,1010)USERL
      CALL ASSIGN(FILEL,USERL,2)
      LUNIT=2
      GO TO 160
155   LUNIT=8
160   CONTINUE
      IF(LUNIT.EQ.8)WRITE(8,2030)
C
C     IVL IS THE NUMBER OF CALCULATION FREQUENCIES USED.
C
      IF(LUNIT.EQ.8)READ(8,-)IVL
      IF(LUNIT.EQ.8)WRITE(8,2040)
      IF(LUNIT.EQ.2)IVL=175
      DO 110 I=1,IVL
      IF(LUNIT.EQ.8)WRITE(8,1950)I
C
C     CALCULATION FREQUENCY FILE MAY HAVE BAND ID'S FOR USE WITH
C     REPORT,3271T
C
      READ(LUNIT,3000)VL(I)
3000  FORMAT(F13.0)
      IF(VL(I).EQ.0.0)GO TO 130
110   CONTINUE
130   IVL=I-1
      IF(FIRST)GO TO 900
      CALL COMD(4HDATA)
      RWOUND=.TRUE.
C
C     REQUEST LOCATION OF LINE DATA
C
900   WRITE(8,950)
      WRITE(8,1001)
      READ(8,1010)FILED
      CLOSE 0
      CALL ASSIGN(FILED,0,0,0)
```

```
      C
      C     GET THE FILE AND RECORD NUMBERS ON THE TAPE
      C     WHERE THE PERTINENT ABSORPTION DATA IS LOCATED.
      C
            WRITE(8,3010)
            READ(8,*)NFILE,NRKD
            NFILE=NFILE-1
            NRKD=NRKD-1
      840   IF(.NOT.FIRST)GO TO 115
      C
      C     SHOULD CALCULATION BE PERFORMED  OFF-LINE  ?
      C
            WRITE(8,3040)
            READ(8,1030)IDUM
            IF(IDUM.EQ.IYES)CALL DEASSN
            FIRST=.FALSE.
      C
      C     J IS THE TOTAL NUMBER OF SUBSTANCES TO BE CONSIDERED.
      C     SET NUMBER EQUAL 1 FOR NOW
      C
      850   J=1
      C
      C     POSITION DATA TAPE.
      C
            REWIND 0
            CALL TPFILE(0,NFILE)
            CALL TPRKD(0,NRKD)
            I = 0
      C
      C     READ DATA FROM AFCRL LINE DATA TAPE.
      C     FOR LINE I, AD(1,I) IS THE FREQUENCY, AD(2,I) IS
      C     THE LINE STRENGTH, AD(3,I) IS THE HALFWIDTH, AND
      C     AD(4,I) IS THE ENERGY OF THE LOWER STATE OF THE
      C     TRANSITION.
      C
            GO TO 22
      20    CLOSE 0
            GO TO 23
      C
      C     CHECK FOR SLOW
      C
      21    IF((AD(1,I).LT.SLOW).OR.(AD(1,I).LT.VL(I)-BOUND))I=I-1
            IF(AD(1,I).GT.VL(IVL)+BOUND)GO TO 27
      22    I=I+1
            IF(I.GT.5600)GO TO 27
      23    READ(0,3,END=20) AD(1,I),AD(2,I),AD(3,I),AD(4,I),ISTOP,NABS
      C
      C     CHECK FOR PROPER SUBSTANCE AND ISOTOPE.
      C
            IF(NABS.NE.NSUB)GO TO 23
            IF(ISOTOP.EQ.0)GO TO 26
            IF(ISOTOP.NE.ISTOP)GO TO 23
      26    IF(AD(1,I))21,27,21
      27    ICARD(J)=I-1
            CLOSE 0
```

```
274           P=P1
275           ICRD=ICARD(J)
276     C
277     C     TEMP IN DEG K IS
278     C
279           TEMP=5./9.*(TF-32.)+273.2
280           ICRD=ICARD(J)
281           I1=ICARD(J)
282           I7=1
283     C
284     C     CALCULATE TEMPERATURE CORRECTION CONSTANTS.
285     C
286     52    CS1=(TEMP0-TEMP)/(TEMP0*TEMP*.6951)
287     53    CS2=(TEMP0/TEMP)**BX(NSUB)
288     54    CA=(TEMP0/TEMP)**CX(NSUB)
289     C
290     C     CALCULATE THE DOPPLER HALF-WIDTH DIVIDED BY FREQUENCY
291     C
292           DN2=ALOG(2.)
293           ALFAD=3.5812E-7*SQRT(TEMP/MA(NSUB))
294     C
295     C     CHANGE THE STRENGTHS AND WIDTHS TO NEW TEMPERATURE
296     C
297           DO 71 I=I,I1
298           AD(2,I)=AD(2,I)*CS2*EXP(-AD(4,I)*CS1)
299     C
300     C     PRESSURE CORRECTION TO HALFWIDTH (CA) IS MADE
301     C     IN ABSV02 SUBROUTINE.
302     C
303           AD(3,I)=AD(3,I)*CA
304     71    CONTINUE
305           GO TO 116
306     115   CALL COMD(3HEXE)
307     C
308     C     NOTE:  IF EXE COMMAND IS GIVEN AFTER COMPLETION
309     C     OF A CALCULATION WITH NO VARIABLE CHANGES, THE
310     C     CALCULATION WILL BE REPEATED WITH SAME DATA AND
311     C     IF ON-LINE ENTER OUTPUT DEVICE NUMBER WILL BE
312     C     PRINTED ALMOST IMMEDIATELY LEADING USER TO THINK
313     C     THAT NO NEW CALCULATION HAS TAKEN PLACE.  IF NEW
314     C     DATA IS WANTED DUE E.G. TO SUSPECTED TAPE READ
315     C     PROBLEM, GIVE DATA COMMAND FIRST WHICH WILL CAUSE
316     C     TAPE TO BE REWOUND AND READ AGAIN.
317     C
318           WRITE(8,3040)
319           READ(8,1030)IDUM
320           IF(IDUM.EQ.IYES)CALL DEASSN
321           IF(RWOUND)GO TO 850
322           IF(IDUM.EQ.IYES)GO TO 116
323     116   CONTINUE
324           DO 90 I=1,IVL
325           DO 85 M=1,NTORRS
326     C
327     C     FOR A ONE KM PATH THE ABSORBER AMOUNT
328     C     IN MOLECULES/CM2 IS
```

```
      C
            W = .733952E22*(ABS(M)/760./TEMP)*1E5
      C
      C     EFFECTIVE PRESSURE IN ATM IS.
      C
            P=(P1+(BROAD-1.)*ABS(M))/760.
            V=VL(I)
            CALL ABSV02(V,BOUND,I7,I1,P,NALFA,ETA,ALFAD)
            CAYW=CAY*W*CNORM
      C
      C     CAYW DOES NOT HAVE UNITS. IT EQUALS LN
      C     OF TRANSMITTANCE.
      C     Y(M,I) WILL BE USED FOR THE ABSORPTION COEFF
      C     IN KM-1. I.E. LN(T)/1.0
      C
            Y(M,I)=+CAYW/1.000
   85       CONTINUE
   90       CONTINUE
      C
      C     WRITE MESSAGE IN MSG,3271A TELLING WHEN THE CALCULATION
      C     IS FINISHED.
      C
            CLOSE 6
            CLOSE 7
            CALL ASSIGN(4HMSG ,5H3271A,7)
            CALL GETDAT(IDATE)
            CALL GETTIM(ITIM)
            WRITE(7,3050)ITIM,IDATE
            CLOSE 7
      C
      C     WHEN REASSIGNED AFTER OFF-LINE CALCULATION PROGRAM
      C     WRITES EXECUTIVE SIGN (<>).  RESULTS MAY
      C     THEN BE OBTAINED BY USE OF STORE COMMAND
      C     (ABBREVIATED VERSION) OR RESULT COMMAND.
      C
            CALL COMD(6HRESULT,0)
      C
      C     WRITE OUT FINAL ANSWERS IF CALCULATION
      C     IS  ON-LINE .
      C
      C
      C     SHOULD CALCULATION RESULTS BE PRINTED
      C     ON TELETYPE OR WRITTEN ON .OUT FILE ?
      C
            WRITE(8,1940)
            READ(8,-)JJ
            CALL CLOCK
            WRITE(JJ,13)BX(NSUB),CX(NSUB),BOUND,SLOW,ICARD(J)
            WRITE(JJ,206C) CNORM
            DO 666 I=1,IVL
            WRITE(JJ,120)VL(I),(ABS(K),Y(K,I),K=1,NTORRS)
  120       FORMAT(/' AT THE FREQUENCY'F10.3//
           1' ABS '8X'K'6X/' TORR'6X'I/KM'
           221(/1X,0PF6.2,1PE11.3))
```

```
  666   CONTINUE
        CALL COMD(3HVAR)
C
C       PRINT LIST OF PROGRAM PARAMETERS ON THE TELETYPE
C
        WRITE(8,3060)P1,ABS(1),TF,NALFA,ETA,BROAD,NSUB,ISOTOP
        CALL COMD(5HSTORE)
C
C       NOW WRITE PARTIAL DATA, IF DESIRED, FOR USE IN FURTHER
C       DATA REDUCTION PROGRAMS.
C
        WRITE(8,4000)
        WRITE(8,1000)
        READ(8,1010)FILES
        READ(8,1010)USERS
        CLOSE 3
        CALL ASSIGN(FILES,USERS,3)
        DO 10 I=1,IVL
        WRITE(3,2080)VL(I),Y(1,I)
  10    CONTINUE
        CLOSE 3
        RWOUND=.FALSE.
        CALL COMD(3HEND)
        CALL EXIT
  1     FORMAT(6E10.4)
  3     FORMAT(2F10.4,F5.2,F10.2,38X,I4,I3)
  13    FORMAT(' BX='F5.2/' CX ='F5.2,/
       2' BOUND ='F7.2/,' SLOW ='
       3E9.2,/' NUMBER OF LINES USED =',I5/)
 950    FORMAT(' WHERE IS THE LINE DATA?')
1000    FORMAT(' ENTER FILE AND USER NAME ON TWO LINES.'/)
1001    FORMAT('ENTER .MT0 OR .MT1 '/)
1010    FORMAT(A6)
1020    FORMAT(' WILL CALCULATION FREQUENCIES BE READ FROM'
       2' A  FILE  OR THE  TTY ?')
1030    FORMAT(A3)
1940    FORMAT(' ENTER OUTPUT DEVICE NUMBER.')
1950    FORMAT(I3,2H =)
1960    FORMAT(' ENTER MODIFIER POWER.')
1970    FORMAT(' ENTER MODIFICATION LOCATION IN HALFWIDTHS.')
1980    FORMAT(' ENTER THE TEMP IN DEG F.')
1990    FORMAT(' ENTER THE SELF-BROADENING COEFFICIENT.')
2000    FORMAT(' ENTER THE TOTAL PRESSURE IN TORR.')
2010    FORMAT(' HOW MANY ABSORBER PRESSURES WILL BE USED?')
2020    FORMAT(' ENTER THEM ON ONE LINE, FREE FORMAT.'/)
2030    FORMAT(' HOW MANY LASER LINES WILL BE USED?')
2040    FORMAT(' ENTER THEM ONE PER LINE IN INCREASING ORDER.'/)
2050    FORMAT('MODIFIER POWER MUST BE STRICTLY GREATER THAN 1!')
2060    FORMAT(' THE NORMALIZATION FACTOR = ' ,F5.3)
2070    FORMAT(' COMMANDS ARE '/
       2' PRESS, ABS, TEMP, NALFA, ETA, LINES, BROAD,'
       3' DATA, EXE, END, SUB, STORE, VAR,RESULT.'//)
2080    FORMAT(1X,F10.3,1PE12.3)
3010    FORMAT('ENTER TAPE START POINT:FILE NUMBER AND RECORD NO.')
3020    FORMAT('ENTER ID NO. OF ABSORBER'/
```

```
438          2 ' 1=H20 2=C02 3=03 4=N20 5=C0 6=CH4 7=02'/)
439     3030  FORMAT(' ENTER NUMBER OF DESIRED ISOTOPE.'/
440          1       ' IF ALL ISOTOPES ARE DESIRED ENTER 0.')
441     3040  FORMAT('DO YOU WISH TO RUN OFF-LINE?')
442     3050  FORMAT('CALCULATION FINISHED AT ',3A3,', ',3A3)
443     3060  FORMAT(/F6.1,1PE11.2,0PF7.1,F7.1,F7.2,F6.1,I4,I6/)
444     4000  FORMAT('WHERE WILL DATA BE STORED?')
445           END
446     C
447     C     THE FOLLOWING SUBROUTINE CALCULATES THE
448     C     ABSORPTION COEFFICIENT.
449     C
450           SUBROUTINE ABSV02(V,BOUND,I7,I1,P,NALFA,ETA,ALFAD)
451           REAL NALFA
452           COMMON/Z/AD(4,5600),CAY
453     C
454     C     THE TWO FOLLOWING LOOPS DETERMINE WHICH ABSORPTION
455     C     LINES WILL BE USED TO CALCULATE THE ABSORPTION COEFFICIENT
456     C     AT THIS FREQUENCY.
457     C
458           I5=1
459           I6=I1
460           DO 14 I=1,I1
461           IF(V-BOUND-AD(1,I))12,12,14
462     12    I5=I
463           GO TO 15
464     14    CONTINUE
465     15    DO 19 K=I7,I1
466           IF(V+BOUND-AD(1,K))17,19,19
467     19    CONTINUE
468     17    I6 = K - 1
469     25    CAY1=0.0
470           CAY2=0.0
471           CAY3=0.0
472           DN2=ALOG(2.)
473           DN1=SQRT(DN2)
474     C
475     C     THE FOLLOWING LOOP SUMS THE CONTRIBUTIONS FROM
476     C     ALL THE ABSORPTION LINES.
477     C
478           DO 46 I=I5,I6
479           Y=ABS(V-AD(1,I))
480     C
481     C     THE FOLLOWING INSTRUCTION CORRECTS THE LORENTZ
482     C     HALFWIDTH FOR PRESSURE.
483     C
484           PT=AD(3,I)*P
485     C
486     C     THE FOLLOWING STATEMENT CALCULATES THE DOPPLER WIDTH.
487     C
488           ALFD=AD(1,I)*ALFAD
489           XV=DN1*Y/ALFD
490     C
491     C     IF ABSORPTION LINE IS FAR AWAY FROM CALCULATION
492     C     FREQUENCY, USE LORENTZ SHAPE REGARDLESS OF PRESSURE
```

```
      C     BUT IF LORENTZ HALFWIDTH IS LESS THAN FIVE TIMES
      C     THE DOPPLER HALFWIDTH, USE VOIGT LINESHAPE.
      C     OTHERWISE USE MODIFIED LORENTZ SHAPE.
      C
            IF(XV.GE.300.) GO TO 50
            IF(PT/ALFD.GE.5.)GO TO 50
            YV=PT/ALFD*DN1
      C
      C     CALCULATE THE VOIGT SHAPE
      C
            CAY3=CAY3+AD(2,I)*DN1/(SQRT(3.141592)*ALFD)*VOIGT(XV,YV)
            GO TO 46
      50    AWAY=NALFA*PT
            IF(Y-AWAY)36,36,42
      C
      C     CALCULATE THE LORENTZ LINE SHAPE FOR V NEAR LINE CENTER
      C
      36    SUM1=AD(2,I)*PT/(Y**2+(PT)**2)
            CAY1=CAY1+SUM1
            GO TO 46
      C
      C     CALCULATE MODIFIED LINE SHAPE FOR V)NALFA*AD(3,I)*P
      C
      42    AWAYSQ=AWAY*AWAY
            CK2=AD(2,I)*PT/(AWAYSQ+PT*PT)
            SUM2=CK2*(AWAY/Y)**ETA
            CAY2=CAY2+SUM2
      46    CONTINUE
      C
      C     SUMMATION OVER ALL LINES
      C
            CAY = 0.3183*(CAY1 + CAY2+CAY3)
      C
      C     ABSORPTION COEFF., CAY, HAS UNITS OF (MOL*CM-2)-1
      C
            RETURN
            END
      C
      C     THE FOLLOWING SUBROUTINE WRITES THE DATE AND TIME
      C     ON OUTPUT UNIT JJ (.TELETYPE OR .OUT FILE).
      C
            SUBROUTINE CLOCK
            COMMON JJ
            DIMENSION ITIME(3),IDATE(3)
            CALL GETDAT(IDATE)
            CALL GETTIM(ITIME)
            WRITE(JJ,10)IDATE,ITIME
      10    FORMAT(' DATE '3A3' TIME '3A3/)
            RETURN
            END
      C
      C     THE FOLLOWING SUBROUTINE EVALUATES THE VOIGT
      C     PROFILE EXPRESSION.  SUBROUTINE WAS PROVIDED
      C     BY CHARLES YOUNG.
      C
```

```
      FUNCTION VOIGT (XIN,YIN)
      DIMENSION RA(32),CA(32),RB(32),CB(32),B(44),AK(5),AM(5),DY(4)
     1,HH(2),XX(2,A(42)
      DATA    HH    /.8049141,.8131283E-01/,XX    /.5246476,1.650680/,A
     1  /0.0,.2,0.,-.184,0.0,.15584,0.0,-.121664,0.0,.8770816E-1,0.0,-.5
     2  851412E-1,0.0,.3621573E-1,0.0,-.2084976E-1,0.0,.1119601E-1,0.0,-
     3  .5623190E-2,0.0,.2648763E-2,0.0,-.1173267E-2,0.0,.4899520E-3,0.0
     4 ,-.1933631E-3,0.0,.7228775E-4,0.0,-.2565551E-4,0.0,.8662074E-5,0.
     5  0,-.2787638E-5,0.0,.8566874E-6,0.0,-.2518434E-6,0.0,.7093602E-7/
      X=XIN
      Y=YIN
      X2=X*X
      Y2=Y*Y
      IF (X-7.) 200,201,201
  200 IF (Y-1.) 202,202,203
  203 RA(1)=0.
      CA(1)=0.
      RB(1)=1.
      CB(1)=0.
      RA(2)=X
      CA(2)=Y
      RB(2)=.5-X2+Y2
      CB(2)=-2.*X*Y
      CB1=CB(2)
      UV1=0.
      DO 250 J=2,31
      JMINUS=J-1
      JPLUS=J+1
      FLOATJ=JMINUS
      RB1=2.*FLOATJ+RB(2)
      RA1=-FLOATJ*(2.*FLOATJ-1.)/2.
      RA(J+1)=RB1*RA(J)-CB1*CA(J)+RA1*RA(J-1)
      CA(J+1)=RB1*CA(J)+CB1*RA(J)+RA1*CA(JMINUS)
      RB(J+1)=RB1*RB(J)-CB1*CB(J)+RA 1*RB(J-1)
      CB(J+1)=RB1*CB(J)+CB1*RB(J)+RA1*CB(J-1)
      UV=(CA(JPLUS)*RB(JPLUS)-RA(JPLUS)*CB(JPLUS))/(RB(JPLUS)**2+
     1 CB(JPLUS)*CB(JPLUS))
      IF(ABS(UV-UV1)-1.E-6)251,250,250
  250 UV1=UV
  251 VOIGT=UV/1.772454
      RETURN
  202  IF(X-2.)301,301,302
  301 AINT = 1.
      MAX=12.+5.*X2
      KMAX=MAX-I
      K0=0
      DO 303 K=K0,KMAX
      AJ=MAX-K
  303 AINT=AINT*(-2.*X2)/(2.*AJ+1.)+1.
      U=-2.*X*AINT
      GO TO 304
  302     IF (X-4.5) 305,306,306
  305 B(43)=0.
      B(44)=0.
```

```
602           J=42
603           DO 307K=1,42
604           B(J)=.4*X*B(J+1)-B(J+2)+A(J)
605       307 J=J-1
606           U=B(3)-B(1)
607           GO TO 304
608       306 AINT=1.0
609           MAX=2.+40./X
610           AMAX=MAX
611           DO 308 K=1,MAX
612           AINT=AINT*(2.*AMAX-1.)/(2.*X2)+1.
613       308 AMAX=AMAX-1.
614           U=-AINT/X
615       304 V=1.772454*EXP(-X2)
616           H=.02
617           JM=Y/H
618           IF(JM)310,311,310
619       311 H=Y
620       310 Z=0.
621           L=0
622           DY(1)=0.
623       312 DY(2)=H/2.
624           DY(3)=DY(2)
625           DY(4)=H
626       318 AK(1)=0.
627           AM(1)=0.
628           DO 313 J=1,4
629           YY=Z+DY(J)
630           UU=U+.5*AK(J)
631           VV=V+.5*AM(J)
632           AK(J+1)= 2.*(YY*UU+X*VV)*H
633           AM(J+1)=-2.*(1.+X*UU-YY*VV)*H
634           IF(J-3) 313,314,313
635       314 AK(4)=2.*AK(4)
636           AM(4)=AM(4)+AM(4)
637       313 CONTINUE
638           Z=Z+H
639           L=L+1
640           U=U+.1666667*(AK(2)+2.*AK(3)+AK(4)+AK(5))
641           V=V+.1666667*(AM(2)+AM(3)+AM(3)+AM(4)+AM(5))
642           IF(JM) 315,320,315
643       315 IF(L-JM) 318,317,320
644       317 AJM=JM
645           H=Y-AJM*H
646           GO TO 312
647       320 VOIGT=V/1.772454
648           RETURN
649       201 F1=0.
650           DO 330 J=1,2
651       330 F1=F1+HH(J)/(Y2+(X-XX(J))*(X-XX(J)))+HH(J)/(Y2+(X+XX(J))*(X+XX(J))
652          1)
653           VOIGT=Y*F1/3.1415927
654           RETURN
655           END
```

B. Spectra Calculation Program

A listing of the program is given on pages 169 to 182. This program was also written to operate on the Ohio State University ElectroScience Laboratory timesharing system and contains some of the special statements described in Part A for the single frequency calculation program. Not used are the ESC, COMDFL and COMD subroutines.

The data storage requirements are somewhat relaxed with this program. At any given calculation frequency V, the computer requires data for the absorption lines having a frequency between V-BOUND and V+BOUND. There is storage in the program for data from 2500 absorption lines. Thus if BOUND is set at 20 cm^{-1}, then there may be no more than 2500 absorption lines in any 40 cm^{-1} interval. The absorption line density per 40 cm^{-1} interval on the AFCRL tape is less than 2500 except near 9.6 microns where there are many ozone lines. For calculating spectra in that region either BOUND must be reduced or the calculation must be performed on a larger computer.

Some modifications have been made to the subroutine ABSV03 which calculates the absorption coefficient at each frequency, so that it operates faster than the subroutine used in the single frequency calculation program or the subroutine ABSCOE written by Deutschmann and Calfee [16]. Each time the subroutine is called, it must first search the data storage array AD(J,K) to determine what range of K will cover the absorption lines with frequency between V-BOUND and V+BOUND. In ABSCOE (Deutschmann and Calfee) and in the subroutine in the single frequency calculation program, this search always starts at K=1. ABSV03 was changed so the search starts at the values of K determined the last time the subroutine was called. This saves time since the frequency is increased by only a small amount each time the subroutine is called.

Note in proof: It has been discovered that for low-pressure, this program can produce "glitches" in the final plots. The difficulty is associated with the transition from Lorentz to Voigt line shapes within an individual plot. This in turn is controlled by the program logic in statements 533 to 542. Future versions of the program will include a fix for this problem. Please contact R. K. Long, Ohio State University ElectroScience Laboratory for further information.

```
C
C     PROGRAM NAME: TRANSPLOT
C
C     COPYRIGHT 1975 THE OHIO STATE UNIVERSITY
C
C     THIS PROGRAM CALCULATES THE LOG OF THE ABSORPTION
C     COEFFICIENT VERSUS FREQUENCY FROM THE AFCRL LINE DATA
C     TAPE.  OUTPUT IS IN A SERIES OF PLOTS TEN INCHES WIDE.
C
C     PROGRAM AUTHORS: G. L. TRUSTY AND F. S. MILLS
C                      THE OHIO STATE UNIVERSITY
C                      ELECTROSCIENCE LABORATORY
C                      1320 KINNEAR ROAD
C                      COLUMBUS, OHIO 43212
C
C
C     LASER LINE FREQUENCIES MUST BE ARRANGED IN
C     STRICTLY ASCENDING ORDER, 125 MAXIMUM.  IF
C     FEWER THAN 125, LAST LINE MUST BE 0.0
C
      OPTIONS 32K
      LOGICAL ENDATA,FIRST
      DIMENSION IDATE(3),BX(7),CX(7),TITLEA(7),TITLEP(7)
      DIMENSION Y(1001),VLINE(125),PP(7),B(7),M(7),ITIM(3)
      COMMON/Z/AD(3,2500),NABS(2500),IP,I5,I6
      COMMON/A/PE(7),W(7),PL,AD,A1,A2,VL,VH,CAVV,ALFAD(7)
      COMMON/D/ENDATA,FIRST,NSUB(7),NUMBR,CSI,CS2(7),CA(7),ISOTOP(7)
      DATA IY2/1H /,BOUND/20.0/,TEMP0/296.0/,SLOW/.1E-26/
      DATA IYES/3HYES/
      DATA CX/.62,.58,0.5,0.5,0.5,0.5,0.5/
      DATA BX/1.5,1.0,1.5,1.0,1.0,1.5,1.0/
      DATA M/18,44,48,44,28,16,32/
      CALL FERR(0)
      CALL CLOCK
C
C     NUMBER IS THE TOTAL NUMBER OF SUBSTANCES TO BE CONSIDERED. (I.E. FOR
C     CO2 AND H2O NUMBER EQUALS 2)
C     NUMPLT IS THE NUMBER OF PLOTS THAT WILL BE MADE WITH EACH PLOT
C     CONTAINING AN INCREMENT OF 1000.*DELV1 WAVENUMBERS
C
      WRITE(8,2000)
      READ(8,-)NUMBR,NUMPLT
      WRITE(8,3000)
      READ(8,-) V1, DELV1
      V2=V1+NUMPLT*DELV1
      DELV1=DELV1/1000.
C
C     READ THE TOTAL PRESSURE IN TORR
C
      WRITE(8,4000)
      READ(8,-)PRESS
      PPLOT=PRESS
      PL=1000.
      WRITE(8,6000)
```

```
      C
      C     READ TEMPERATURE IN DEG F
      C
            READ(8,-)T
  983       TPLOT=T
      C
      C     CONVERT TEMPERATURE TO DEG K
      C
            TEMP=273.2+5./9.*(T-32.)
      C
      C     GET ID NUMBER, ISOTOPE, PARTIAL PRESSURE, AND BROADENING
      C     COEFFICIENT FOR EACH ABSORBER.
      C
            WRITE(8,4100)
            DO 400 I=1,NUMBR
             WRITE(8,4900)I
             READ(8,-)NSUB(I)
             J=NSUB(I)
             WRITE(8,4950)
             READ(8,-)ISOTOP(J)
             WRITE(8,5000)
      C
      C      READ ABSORBER PRESSURE IN TORR
      C
             READ(8,-)PP(J)
             WRITE(8,5500)
      C
      C      READ SELF BROADENING COEFFICIENT
      C
             READ(8,-)B(J)
  400       CONTINUE
      C
      C     REQUEST CONTINUUM INFORMATION.
      C
            WRITE(8,6100)
            READ(8,8500)IIN
            IF(IIN.NE.IYES) GO TO 140
            WRITE(8,6200)
            READ(8,-)A0
            WRITE(8,6300)
            READ(8,-)A1
            WRITE(8,6400)
            READ(8,-)A2
            WRITE(8,6500)
            READ(8,-)VL,VH
            GO TO 150
  140       A0=0.
            A1=0.
            A2=0.
      C
      C     GET TITLE INFORMATION FOR PLOTS
      C
  150       WRITE(8,4200)
            READ(8,1011)TITLEA
```

```
      READ(8,1011)TITLEP
C
C     REQUEST LOCATION OF ABSORPTION LINE DATA
C
      WRITE(8,950)
      WRITE(8,1100)
      READ(8,1010)FILED
      CALL ASSIGN(FILED,0,0,0)
      WRITE(8,9400)
      READ(8,-)NFILE,NRKD
      NFILE=NFILE-1
      NRKD=NRKD-1
C
C     REQUEST TAPE UNIT NUMBER FOR WRITING PLOT TAPE.
C
      WRITE(8,1200)
      WRITE(8,1100)
      READ(8,1010)FILEP
      CALL ASSIGN(FILEP,0,0,2)
      WRITE(8,1300)
      READ(8,-)NPFILE
      NPFILE=NPFILE-1
C
C     REQUEST LOCATION OF LASER LINE DATA.
C
      WRITE(8,9500)
      WRITE(8,1000)
      READ(8,1010)FILEL
      READ(8,1010)USERL
C
C     SHOULD PROGRAM BE RUN OFF-LINE?
C
      WRITE(8,8700)
      READ(8,8500)IIN
      IBAKGN=0
      IF(IIN.EQ.IYES)IBAKGN=1
C
C     COMPUTE ABSORBER CONCENTRATION(MOL*CM-2) FOR EACH ABSORBER
C
      DO 310 I=1,NUMBR
       J=NSUB(I)
       W(J)=9.65726E20*PP(J)*PL/TEMP
310   CONTINUE
C
C     COMPUTE EFFECTIVE PRESSURE FOR EACH ABSORBER.
C
      DO 300 I=1,NUMBR
       J=NSUB(I)
       PE(J)=(PRESS+(B(J)-1.)*PP(J))/760.
300   CONTINUE
C
C     COMPUTE CS1
C
      CS1=(TEMPS-TEMP)/(TEMPS*TEMP*.6951)
C
```

```
C      COMPUTE CS2 AND CA FOR EACH SUBSTANCE
C
       DO 410 I=1,7
        CS2(I)=(TEMP0/TEMP)**SX(I)
        CA(I)=(TEMP0/TEMP)**CX(I)
410    CONTINUE
C
C      COMPUTE DOPPLER HALF-WIDTH FOR EACH SUBSTANCE
C
       DO 420 I=1,7
        ALFAD(I)=3.5812E-7*SQRT(TEMP/M(I))
420    CONTINUE
C
C      POSITION TAPES PROPERLY
C
       REWIND 0
       CALL TPFILE(0,NFILE)
       CALL TPRKD(0,NRKD)
       WRITE(8,8800)
       REWIND 2
       CALL TPFILE(2,NPFILE)
       CLOSE 2
       WRITE(8,8900)
       ENDATA=.FALSE.
       FIRST =.TRUE.
       IARI=1
C
CCCCC  READ THE LASER LINES INTO VLINE FROM FILEL,USERL
C
       CALL CLSE(4)
       CALL ASSIGN(FILEL,USERL,4)
       DO 110 JF=1,125
       READ(4,8600)VLINE(JF)
       IF(VLINE(JF).EQ.0.0)GO TO 170
110    CONTINUE
170    CONTINUE
       IF(IBAKGN.EQ.1)CALL DEASSN
       CALL ASNPLT(512,2,FILEP)
       DO 700 N=1,NUMPLT
        DO 500 I=1,1001
         Y(I)=0.
500     CONTINUE
        DO 600 I=1,1001
         V=V1+(I-1)*DELV1
C
C      CALL DATA TO MAKE SURE THERE IS ENOUGH DATA TO DO THE
C      CALCULATION.
C
          CALL DATA(V,BOUND,V1,V2,IBAKGN,SLOW)
C
C      CALL ABSV03 TO CALCULATE THE ABSORPTION COEFFICIENT.
C
          CALL ABSV03(V,BOUND)
          Y(I)=Y(I)+CAYW
600     CONTINUE
```

```
219           DO 610 I=1,1001
220            Y(I)=ALOG10(Y(I))
221     610   CONTINUE
222     C
223     C     FIND BIGGEST Y(I)
224     C
225           YMAX=-1.E35
226           DO 620 I=1,1001
227            IF(Y(I).GT.YMAX)YMAX=Y(I)
228     620   CONTINUE
229           IYMAX=YMAX
230           IF(YMAX.GT.0)IYMAX=IYMAX+1
231     C
232     C     FIND SMALLEST Y(I)
233     C
234           YMIN=1.E35
235           DO 630 I=1,1001
236            IF(Y(I).LT.YMIN)YMIN=Y(I)
237     630   CONTINUE
238           IYMIN=YMIN
239           IF(YMIN.LT.0)IYMIN=IYMIN-1
240     C
241     C     SUBTRACT IYMIN FROM ALL Y(I)
242     C
243           DO 640 I=1,1001
244            Y(I)=Y(I)-IYMIN
245     640   CONTINUE
246           IYMAX=IYMAX-IYMIN
247     C
248     C     NORMALIZE Y FOR PLOTTING
249     C
250           DO 650 I=1,1001
251            Y(I)=6.5*Y(I)/IYMAX
252     650   CONTINUE
253     C
254     C     THE NEXT LOOP PLOTS THE CALCULATED DATA
255     C
256     C
257     C     FIRST A DIVERSION TO GET THE PEN WRITING
258     C
259           CALL PLOT(0.0,-1.,3)
260           CALL PLOT(4.0,-I.,2)
261           CALL PLOT(0.0,-I.,2)
262     C
263           DO 59 IN=1,1001
264           X=0.01*(IN-1)
265           YP=Y(IN)
266           IF(IN.EQ.1)CALL PLOT(X,YP,3)
267           CALL PLOT(X,YP,2)
268     59    CONTINUE
269           CALL PLOT(0.0,0.0,3)
270     210   IF(VLINE(IARI).GT.V1+DELVI*1000. ) GO TO 220
271           IF(VLINE(IARI).EQ.0.0)GO TO 220
272           IF(VLINE(IARI).LT.V1)GO TO 215
273           X = (VLINE(IARI) - V1)/DELVI/100.
```

```
      CALL PLOT(X,0.0,2)
      CALL PLOT(X,6.5,2)
      CALL PLOT(X,0.0,3)
215   IAR1=IAR1+1
      GO TO 210
220   CALL PLOT(10.0,0.0,3)
      CALL PLOT(0.,6.5,3)
230   CALL PLOT(10.0,6.5,2)
C
C     PLOT TITLE INFORMATION
C
      CALL SYMBOL(0.0,6.8,0.1,15HTEMP (DEG F)=  ,0.0,15)
      CALL NUMBER(1.50,6.8,0.1,TPLOT,0.0,1)
      CALL SYMBOL(0.0,7.0,0.1,15HAMOUNT (TORR)= ,0.0,15)
      CALL SYMBOL(1.50,7.0,0.1,TITLEP,0.0,42)
      CALL SYMBOL(0.0,7.2,0.1,16HABSORBERS=     ,0.0,16)
      CALL SYMBOL(1.50,7.2,0.1,TITLEA,0.0,42)
      CALL SYMBOL(7.1,7.0,0.1,23HTOTAL PRESSURE (TORR)= ,0.0,23)
      CALL CHANGE(PPLOT,DUM)
      CALL SYMBOL(9.4,7.0,0.1,DUM,0.0,5)
      CALL GETDAT(IDATE)
      CALL SYMBOL(7.1,7.2,0.1,IDATE,0.0,9)
C
CCCCC
      DYS=IYMAX/6.5
      SPC=1.0
      XNT=100.*DELV1
      IF(XNT.LT..7)SPC=2.0
      CALL AXIS(0.0,0.0,10HWAVENUMBER,-10,10.0,0.0,V1,XNT,10.0,-1)
      CALL AXIS(0.0,0.0,IY2,-1,-10.0,0.0,0.0,1.0,SPC,1)
      CALL FACTOR(0.5)
      CALL AXIS(0.0,0.0,IY2,-1,-20.,0.0,0.0,1.0,0.4,1)
      CALL FACTOR(1.0)
      YMIN=10.**IYMIN
      CALL LGAXS(10.,0.,IY2,-1.,-6.5,90.0,YMIN,DYS)
      CALL LGAXS(0.0,0.0,18HABS. COEFF. (KM-1),18,6.5,90.0,YMIN,DYS)
      CALL PLOT(12.0,0.0,-3)
      CALL PLOT(0.0,0.0,999)
      CALL ASNPLT(512,2,FILEP)
      V1=V1+1000.*DELV1
C
C     WRITE MESSAGE IN MSG,3271A TELLING DATE AND TIME EACH
C     CALCULATION WAS COMPLETED.
C
      CLOSE 7
      CALL ASSIGN(4HMSG ,5H3271A,7)
      CALL GETTIM(ITIM)
      WRITE(7,9000)N,ITIM,IDATE
      CLOSE 7
700   CONTINUE
      CALL EXIT
C
C     FORMATS
C
950   FORMAT(' WHERE IS THE ABSORPTION LINE DATA?')
```

```
 9400  FORMAT(' ENTER TAPE START POINT: FILE NUMBER AND RECORD NUMBER')
 9500  FORMAT(' WHERE IS THE LASER LINE DATA?')
 1000  FORMAT(' ENTER FILE AND USER NAME ON TWO LINES.'/)
 1010  FORMAT(A6)
 1011  FORMAT(7A6)
 1100  FORMAT(' ENTER .MTO OR .MTI')
 1200  FORMAT(' WHICH TAPE UNIT WILL PLOT DATA BE WRITTEN ON?')
 1300  FORMAT(' ENTER NUMBER OF FIRST FILE TO BE WRITTEN.')
C      NUMBR OF ABSORBERS = NUMBR
C      NUMBER OF PLOTS = NUMPLT
 2000  FORMAT(' ENTER THE NUMBER OF ABSORBERS AND THE NUMBER OF PLOTS')
 3000  FORMAT(' ENTER THE BEGINNING WAVENUMBER'/
     1' AND THE WAVENUMBER/PLOT.')
 4000  FORMAT(' ENTER THE TOTAL PRESSURE IN TORR.')
 4100  FORMAT(' ENTER ID NUMBER, PARTIAL PRESSURE, AND BROADENING'/
     1       ' COEFFICIENT FOR EACH ABSORBER.'/)
 4200  FORMAT('ENTER ABSORBER DESCRIPTION INFORMATION ON TWO LINES'/
     1       ' OF UP TO 42 CHARACTERS EACH.  THE FIRST LINE WILL'/
     2       ' APPEAR IMMEDIATELY TO THE RIGHT OF ABSORBERS: '/
     3       ' THE SECOND LINE WILL APPEAR TO THE RIGHT OF'/
     4       ' AMOUNT(TORR): AND IMMEDIATELY BELOW THE FIRST LINE.'/)
 4900  FORMAT(' ENTER ID NUMBER OF ABSORBER NO.'I1/
     1       ' 1=H2O 2=CO2 3=O3 4=N2O 5=CO 6=CH4 7=O2'/)
 4950  FORMAT(' ENTER NUMBER OF DESIRED ISOTOPE.'/
     1       ' IF ALL ISOTOPES ARE DESIRED ENTER 0.')
 5000  FORMAT(' ENTER THE ABSORBER AMOUNT IN TORR.')
 5500  FORMAT(' ENTER THE SELF-BROADENING COEFFICIENT.')
 5600  FORMAT(' ENTER THE PATH LENGTH IN METERS.')
 6000  FORMAT(' ENTER THE TEMPERATURE IN DEGREES F.')
 6100  FORMAT(' DO YOU WISH A CONTINUUM?')
 6200  FORMAT(' ENTER THE COEFFICIENTS FOR THE POLYNOMIAL'/
     1       ' K(V)=A0+A1*V+A2*V**2, WHERE K IS IN KM-1 AND'/
     2       ' V IS WAVENUMBER.'/
     3       ' A0= ')
 6300  FORMAT(' A1= ')
 6400  FORMAT(' A2= ')
 6500  FORMAT(' ENTER FREQUENCY LIMITS FO CONTINUUM, VL AND VH'/)
 8500  FORMAT(A3)
 8600  FORMAT(F12.0)
 8700  FORMAT(' DO YOU WISH TO RUN THIS PROGRAM IN BACKGROUND?')
 8800  FORMAT('THE DATA TAPE IS POSITIONED.')
 8900  FORMAT('THE PLOT TAPE IS POSITIONED.')
 9000  FORMAT('PLOT 'I3' FINISHED AT '3A3', '3A3)
       END
C
C      THE FOLLOWING SUBROUTINE READS DATA FROM TAPE AND
C      MODIFIES IT FOR USE IN THE PROGRAM.  IT ALSO CHECKS BEFORE
C      EACH CALCULATION IS MADE TO MAKE SURE THERE IS SUFFICIENT
C      DATA TO PERFORM THE CALCULATION.
C
       SUBROUTINE DATA(V,BOUND,V1,V2,IBAKGN,SLOW)
       LOGICAL ENDATA,FIRST
       COMMON/Z/AD(3,2500),NABS(2500),IH,I5,I6
       COMMON/D/ENDATA,FIRST,NSUB(7),NUMBR,CS1,CS2(7),CA(7),ISOTOP(7)
```

```
      C
      C     IF THIS IS THE FIRST TIME THIS SUBROUTINE HAS BEEN CALLED
      C     GO IMMEDIATELY TO INPUT.
      C
            IF(FIRST)GO TO 500
      C
      C     IF THERE IS ENOUGH DATA IN AD(J,K) AND NABS(K) TO PERFORM
      C     THE CALCULATION AT THIS FREQUENCY, OR IF THE END OF THE
      C     AFCRL DATA TAPE HAS BEEN REACHED, RETURN.
      C
            IF((AD(1,IH).GT.(V+BOUND)).OR.ENDATA)RETURN
      C
      C     IF MORE DATA IS NEEDED TO PERFORM THE CALCULATION AT THIS
      C     FREQUENCY, FIRST MOVE THE DATA IN AD(J,K) AND NABS(K)
      C     WHICH IS STILL NEEDED FROM HIGH K TO LOW K.
      C
      CCCCCCCCCCCCCCCCCCCCCCCCCCCCCCCCCCCCCCCCCCCCCC
            DO 100 I=IH,1,-1
             IF(AD(1,I).LT.(V-BOUND))GO TO 200
      100   CONTINUE
      200   I=I+1
            K=1
            DO 400 J=I,IH
             DO 300 M=1,3
              AD(M,K)=AD(M,J)
      300    CONTINUE
             NABS(K)=NABS(J)
             K=K+1
      400   CONTINUE
            GO TO 600
      CCCCCCCCCCCCCCCCCCCCCCCCCCCCCCCCCCCCCCCCCCCCCC
      500   K=1
            FIRST=.FALSE.
            VLOW=V1-BOUND
            VHIGH=V2+BOUND
            GO TO 600
      C
      C     NOW READ THE DATA INTO AD(J,K) AND NABS(K) UNTIL AD(J,K)
      C     IS FULL OR ENOUGH DATA HAS BEEN READ TO COMPLETE ALL
      C     THE DESIRED CALCULATIONS OR THE END OF THE AFCRL DATA
      C     TAPE HAS BEEN REACHED.
      C
      C     FOR AN ABSORPTION LINE K, AD(1,K) IS THE FREQUENCY,
      C     AD(2,K) IS THE LINE STRENGTH, AD(3,K) IS THE HALF-WIDTH,
      C     EPP IS ENERGY OF THE LOWER STATE OF THE TRANSITION,
      C     ISTOP IS THE ISOTOPE IDENTIFICATION, AND NABS(K)
      C     IS THE SUBSTANCE IDENTIFICATION NUMBER.
      C
      590   CLOSE 0
      600   READ(0,1000,END=590)AD(1,K),AD(2,K),AD(3,K),EPP,ISTOP,NABS(K)
      C
      C     DOES THIS LINE HAVE A LOWER FREQUENCY THAN IS NEEDED
      C     FOR THE CALCULATION, OR IS THE LINE STRENGTH TOO LOW?
      C
            IF((AD(1,K).LT.(V-BOUND)).OR.(AD(2,I).LT.SLOW))GO TO 600
```

```
C
C      IS THIS THE END OF THE DATA TAPE?
C
       IF(AD(1,K).EQ.12075.863)GO TO 790
C
C      DOES THIS LINE HAVE A HIGHER FREQUENCY THAN IS NEEDED
C      FOR THE CALCULATION?
C
       IF(AD(1,K).GT.VHIGH)GO TO 880
C
C      IS THIS SUBSTANCE TO BE CONSIDERED IN THE CALCULATION?
C
  690  DO 700 I=1,NUMBR
       IF(NSUB(I).EQ.NABS(K))GO TO 800
  700  CONTINUE
  710  IF(.NOT.ENDATA)GO TO 600
       GO TO 890
  790  ENDATA=.TRUE.
       GO TO 690
  800  J=NABS(K)
C
C      IS THIS ISOTOPE TO BE CONSIDERED IN THE CALCULATION?
C
       IF(ISOTOP(J).EQ.0)GO TO 810
       IF(ISOTOP(J).NE.ISTOP)GO TO 710
C
C      CORRECT THE LINE STRENGTH FOR TEMPERATURE.
C
  810  AD(2,K)=AD(2,K)*CS2(J)*EXP(-EPP*CS1)
C
C      CORRECT THE HALF-WIDTH FOR TEMPERATURE.
C
       AD(3,K)=AD(3,K)*CA(J)
       IF(ENDATA)GO TO 900
       K=K+1
       IF(K.LE.2500)GO TO 600
       GO TO 890
  880  ENDATA=.TRUE.
  890  K=K-1
  900  IH=K
       I5=1
       I6=1
C
C      IF PROGRAM IS ON-LINE TYPE MESSAGE ON THE TELETYPE THAT
C      DATA HAS BEEN READ IN.
C
       IF(IBAKGN.EQ.0)WRITE(8,2000)
       RETURN
 1000  FORMAT(2E10.4,F5.3,F10.3,38X,I4,I3)
 2000  FORMAT('ONE SET OF DATA HAS BEEN READ.')
       END
CCCCCCCCCCCCCCCCCCCCCCCCCCCCCCCCCCCCCCCCCCCCCCCCCCCCCCCCCCCCCCCCCCCCCCCCC
C
C      THE FOLLOWING SUBROUTINE CALCULATES THE ABSORPTION
C      COEFFICIENT.
```

```
493     C
494           SUBROUTINE ABSV03(V,BOUND)
495           COMMON/Z/AD(3,2500),NABS(2500),IH,I5,I6
496           COMMON/A/PE(7),W(7),PL,A0,A1,A2,VL,VH,CAYW,ALFAD(7)
497     C
498     C     THE FOLLOWING LOOPS DETERMINE WHICH ABSORPTION LINES
499     C     WILL BE USED TO CALCULATE THE ABSORPTION COEFFICIENT AT THIS
500     C     FREQUENCY.
501     C
502           DO 20 I=I5,IH
503            IF(V-BOUND-AD(1,I))10,10,20
504     10     I5=I
505            GO TO 30
506     20    CONTINUE
507     30    DO 50 K=I6,IH
508            IF(V+BOUND-AD(1,K))40,50,50
509     50    CONTINUE
510     40    I6=K-1
511     55    CAY1=0.0
512           CAY2=0.0
513           CAY=0.0
514           DN2=ALOG(2.)
515           DN1=SQRT(DN2)
516     C
517     C     THE FOLLOWING LOOP SUMS THE CONTRIBUTIONS FROM ALL THE
518     C     ABSORPTION LINES.
519     C
520           DO 80 I=I5,I6
521            J=NABS(I)
522            Y=ABS(V-AD(1,I))
523     C
524     C     CORRECT THE DOPPLER HALFWIDTH FOR FREQUENCY.
525     C
526            ALFD=AD(1,I)*ALFAD(J)
527            XV=DN1*Y/ALFD
528     C
529     C     THE FOLLOWING STATEMENT CORRECTS THE LORENTZ HALF-WIDTH
530     C     FOR PRESSURE.
531     C
532            ALFL=AD(3,I)*PE(J)
533     C
534     C     IF THE ABSORPTION LINE IS FAR AWAY FROM CALCULATION
535     C     FREQUENCY, USE LORENTZ SHAPE REGARDLESS OF PRESSURE;
536     C     BUT IF LORENTZ HALF-WIDTH IS LESS THAN FIVE TIMES THE
537     C     DOPPLER WIDTH, USE THE VOIGT LINE SHAPE.  OTHERWISE
538     C     USE THE LORENTZ SHAPE.
539     C
540            IF(XV.GE.300.) GO TO 59
541            IF(ALFL/ALFD.GE.5.)GO TO 59
542            YV=ALFL/ALFD*DN1
543     C
544     C     CALCULATE THE VOIGT SHAPE
545     C
546            SUM3=AD(2,I)*W(J)*DN1/(SQRT(3.141592)*ALFD)*VOIGT(XV,YV)
```

```
            CAY=CAY+0.3183*SUM3
            GO TO 80
 59         IF(Y-3.)60,60,70
 C
 C      CALCULATE THE LORENTZ LINE SHAPE FOR V NEAR LINE CENTER
 C
 60         SUM1=AD(2,I)*AD(3,I)/(Y*Y+AD(3,I)*AD(3,I)*PE(J)*PE(J))
            SUM1=SUM1*PE(J)*W(J)*0.3183
            CAY1=CAY1+SUM1
            GO TO 80
 C
 C      CALCULATE THE LORENTZ LINE SHAPE FOR V FAR FROM LINE
 C      CENTER, IGNORING THE HALF-WIDTH SQUARED TERM IN THE
 C      DENOMINATOR FOR INCREASED CALCULATION SPEED.
 C
 70         SUM2=AD(2,I)*AD(3,I)/(Y*Y)
            SUM2=SUM2*PE(J)*W(J)*0.3183
            CAY2=CAY2+SUM2
 80     CONTINUE
 C
 C      SUMMATION OVER ALL LINES.
 C
        CAYW=CAY1+CAY2+CAY
 C
 C      THE FOLLOWING ALLOWS A CONTINUUM WHICH IS A FUNCTION OF
 C      FREQUENCY TO BE ADDED TO THE LOCAL LINE ABSORPTION SPECTRUM.
 C      THE POLYNOMIAL WHICH EXPRESSES THE CONTINUUM IS K(V), WHERE
 C      K IS IN KM-1 AND V IS WAVENUMBER.  THE TERM PL*1E-3 CONVERTS
 C      KM-1 TO M-1.
 C
        IF((V.LT.VL).OR.(V.GT.VH))RETURN
        CAYW=CAYW+(AC+A1*V+A2*V*V)*PL*1.E-3
        RETURN
        END
CCCCCCCCCCCCCCCCCCCCCCCCCCCCCCCCCCCCCCCCCCCCCCCCCCCCCCCCCCCCCCCCCCC
C
C       THE FOLLOWING SUBROUTINE PRINTS DATE AND TIME ON THE TELETYPE.
C
        SUBROUTINE CLOCK
C
C
        DIMENSION ITIME(3),IDATE(3)
        CALL GETDAT(IDATE)
        CALL GETTIM(ITIME)
        WRITE(8,10)IDATE,ITIME
10      FORMAT(' DATE '3A3' TIME '3A3/)
        RETURN
        END
CCCCC
C       SUBROUTINE CHANGE FOR F10.4 TO A5 CONVERSION
C       FOR NUMBERS IN THE RANGE 9999.9999 TO .0001
C
        SUBROUTINE CHANGE(FNUM,A5)
        INTEGER FIVA1(5),A10(10),SCR(4)
C
```

```
C      FIND DECIMAL POINT LOCATION. LOC WILL BE NUMBER OF
C      DIGITS TO LEFT OF DEC IF POSITIVE.
C
       LOC=ALOG10(FNUM)+1.00001
       LFTLOC=5-LOC
       IF(LFTLOC.GT.5)LFTLOC=5
       ENCODE(10,1000,SCR)FNUM
       DECODE(10,2000,SCR)A10
C
C      PUT THE 5 DESIRED CHARACTERS INTO FIVA1
C
       DO 100 I=1,5
       J=LFTLOC+I
       FIVA1(I)=A10(J)
100    CONTINUE
C
C
C      CHANGE FROM 5A1 TO A5
C
       ENCODE(6,3000,SCR)FIVA1
       DECODE(6,4000,SCR)A5
1000   FORMAT(F10.4)
2000   FORMAT(10A1)
3000   FORMAT(5A1)
4000   FORMAT(A5)
       RETURN
       END
C
C      THE FOLLOWING SUBROUTINE EVALUATES THE VOIGT PROFILE
C      EXPRESSION.
C      SUBROUTINE WAS PROVIDED BY CHARLES YOUNG.
C
       FUNCTION VOIGT (XIN,YIN)
       DIMENSION RA(32),CA(32),RB(32),CB(32),B(44),AK(5),AM(5),DY(4)
      1,HH(2),XX(2),A(42)
       DATA   HH   /.8049141..8131283E-01/,XX   /.5246476,1.650680/,A
      1  /0.0,.2,0.,-.184,0.0,.15584,0.0,-.121664,0.0,.8770816E-1,0.0,-.5
      2  8514125-1,0.0,.3621573E-1,0.0,-.2084976E-1,0.0,.1119601E-1,0.0,-
      3  .5623190E-2,0.0,.2648763E-2,0.0,-.1173267E-2,0.0,.4899520E-3,0.0
      4 ,-.1933631E-3,0.0,.7228775E-4,0.0,-.2565551E-4,0.0,.8662074E-5,0.
      5  0,-.2787638E-5,0.0,.8566874E-6,0.0,-.2518434E-6,0.0,.7093602E-7/
       X=XIN
       Y=YIN
       X2=X*X
       Y2=Y*Y
       IF (X-7.) 200,201,201
  200  IF (Y-1.) 202,202,203
  203  RA(1)=0.
       CA(1)=0.
       RB(1)=1.
       CB(1)=0.
       RA(2)=X
       CA(2)=Y
       RB(2)=.5-X2+Y2
       CB(2)=-2.*X*Y
```

```
      CB1=CB(2)
      UV1=0.
      DO 250 J=2,31
      JMINUS=J-1
      JPLUS=J+1
      FLOATJ=JMINUS
      RB1=2.*FLOATJ+RB(2)
      RA1=-FLOATJ*(2.*FLOATJ-1.)/2.
      RA(J+1)=RB1*RA(J)-CB1*CA(J)+RA1*RA(J-1)
      CA(J+1)=RB1*CA(J)+CB1*RA(J)+RA1*CA(JMINUS)
      RB(J+1)=RB1*RB(J)-CB1*CB(J)+RA 1*RB(J-1)
      CB(J+1)=RB1*CB(J)+CB1*RB(J)+RA1*CB(J-1)
      UV=(CA(JPLUS)*RB(JPLUS)-RA(JPLUS)*CB(JPLUS))/(RB(JPLUS)**2+
     1 CB(JPLUS)*CB(JPLUS))
      IF(ABS(UV-UV1)-1.E-6)251,250,250
  250 UV1=UV
  251 VOIGT=UV/1.772454
      RETURN
  202  IF(X-2.)301,301,302
  301 AINT = 1.
      MAX=12.+5.*X2
      KMAX=MAX-1
      K0=0
      DO 303 K=K0,KMAX
      AJ=MAX-K
  303 AINT=AINT*(-2.*X2)/(2.*AJ+1.)+1.
      U=-2.*X*AINT
      GO TO 304
  302     IF (X-4.5) 305,306,306
  305 B(43)=0.
      B(44)=0.
      J=42
      DO 307K=1,42
      B(J)=.4*X*B(J+1)-B(J+2)+A(J)
  307 J=J-1
      U=B(3)-B(1)
      GO TO 304
  306 AINT=1.0
      MAX=2.+40./X
      AMAX=MAX
      DO 308 K=1,MAX
      AINT=AINT*(2.*AMAX-1.)/(2.*X2)+1.
  308 AMAX=AMAX-1.
      U=-AINT/X
  304 V=1.772454*EXP(-X2)
      H=.02
      JM=Y/H
      IF(JM)310,311,310
  311 H=Y
  310 Z=0.
      L=0
      DY(1)=0.
  312 DY(2)=H/2.
      DY(3)=DY(2)
      DY(4)=H
```

```
      318 AK(1)=0.
          AM(1)=0.
          DO 313 J=1,4
          YY=Z+DY(J)
          UU=U+.5*AK(J)
          VV=V+.5*AM(J)
          AK(J+1)= 2.*(YY*UU+X*VV)*H
          AM(J+1)=-2.*(1.+X*UU-YY*VV)*H
          IF(J-3) 313,314,313
      314 AK(4)=2.*AK(4)
          AM(4)=AM(4)+AM(4)
      313 CONTINUE
          Z=Z+H
          L=L+1
          U=U+.1666667*(AK(2)+2.*AK(3)+AK(4)+AK(5))
          V=V+.1666667*(AM(2)+AM(3)+AM(3)+AM(4)+AM(5))
          IF(JM) 315,320,315
      315 IF(L-JM) 318,317,320
      317 AJM=JM
          H=Y-AJM*H
          GO TO 312
      320 VOIGT=V/1.772454
          RETURN
      201 F1=0.
          DO 330 J=1,2
      330 F1=F1+HH(J)/(Y2+(X-XX(J))*(X-XX(J)))+HH(J)/(Y2+(X+XX(J))*(X+XX(J))
         1)
          VOIGT=Y*F1/3.1415927
          RETURN
          END
```

APPENDIX C

OPTICS DESIGN PROGRAM LISTING

```
C     F. S. MILLS   NOVEMBER 2,1972
C
C     FM101
C
C     LASER SPOT SIZE PROGRAM
C
C     THIS PROGRAM USES THE EQUATIONS ON WHICH THE COLLINS
C     CHART IS BASED.  REFERENCE:  S. A. COLLINS, JR.,
C     APPL. OPT. 3, 1263(1964)
C
C     THIS PROGRAM CALCULATES THE SPOT SIZE FOR A PLANE-
C     SPHERICAL RESONATOR. UP TO 10 FOCUSING MIRRORS OR LENSES MAY
C     BE PLACED ANYWHERE. THE OUTPUT OF THE LASER IS
C     CONSIDERED TO BE FROM THE SPHERICAL MIRROR.
C     DISTANCES ARE SPECIFIED WITH RESPECT TO THE PLANE MIRROR.
C     THE USER SPECIFIES THE RADIUS OF CURVATURE OF THE OUTPUT
C     MIRROR, ITS INDEX OF REFRACTION, THE MIRROR SEPARATION,
C     AND THE LOCATION AND FOCAL LENGTH OF THE FOCUSING
C     ELEMENTS.
C     WHEN ALL PARAMETERS ARE SPECIFIED, THE PROGRAM WILL
C     TYPE 'ENTER LOCATION'
C     AND THE USER TYPES THE LOCATION OF A POINT OF INTEREST
C     WITH RESPECT TO THE PLANE MIRROR OF THE LASER.  THE PROGRAM
C     TYPES THE SPOT SIZE AND THE DISTANCE TO THE FOCUS
C     OF THE BEAM.  THE PROGRAM THEN TYPES 'ENTER LOCATION' AGAIN
C     AND THE USER MAY PROCEED.
C
      DIMENSION BI(12),ZM1(12),ZM2(12),FM(10)
      CALL ESC($10)
      ZM1(1)=0.
      ZM2(1)=0.
10    WRITE(8,20)
20    FORMAT(/'LASER SPOT SIZE PROGRAM'///
     1'ENTER OUTPUT MIRROR RADIUS, INDEX, MIRROR SEPARATION'/)
      READ(8,-) B1,RN,ZM1(2)
      WRITE(8,35)
35    FORMAT('ENTER WAVELENGTH'/)
      READ(8,-)WAVE
      WRITE(8,25)
25    FORMAT('ENTER NUMBER OF ELEMENTS'/)
      READ(8,-)N
      DO 33 I=1,N
      WRITE(8,30)I
30    FORMAT('ENTER POSITION, FOCAL LENGTH OF ELEMENT NO. '
     1,I2/)
      READ(8,-)ZM1(I+2),FM(I)
33    CONTINUE
C
C     B1 IS OUTPUT MIRROR RADIUS OF CURVATURE
C     RN IS INDEX OF REFRACTION OF OUTPUT MIRROR MATERIAL
C     ZM1(2) IS MIRROR SEPERATION
C     ZM1 IS POSITION OF FOCUSING MIRROR OR LENS
C     WAVE IS THE WAVELENGTH OF THE LASER
C     FM IS FOCAL LENGTH OF FOCUSING MIRROR OR LENS
C
```

```
C     THE INTERSECTION POINT OF THE R=B1 LINE AND THE
C     CONSTANT DISTANCE CIRCLE DESCRIBED BY Z=Z1 IS GIVEN
C     BY THE COORDINATES
      X1=SQRT((1./2./ZM1(2))**2-(1./B1-1./2./ZM1(2))**2)
      Y1=1./B1
C
C     THE B CIRCLE WHICH ALSO INTERSECTS THIS POINT IS GIVEN BY
      BI(1)=(X1**2+Y1**2)/2./X1
C
C     THE OUTPUT MIRROR ACTS LIKE A NEGATIVE LENS OF FOCAL
C     LENGTH F1=-B1/(RN-1.)
      F1=-B1/(RN-1.)
C
C     THE LENS EFFECT OF THE MIRROR CAUSES Y1 TO BE DECREASED
C     BY 1./F1.  X1 REMAINS THE SAME.  JUST OUTSIDE THE MIRROR
      X2=X1
      Y2=Y1-1./F1
C
C     THE NEW B CIRCLE IS GIVEN BY
      BI(2)=(X2**2+Y2**2)/2./X2
C
C     THE NEW Z REFERENCE IS GIVEN BY
      ZM2(2)=Y2/(X2**2+Y2**2)
      DO 40 I=1,N
C
C     AT THE FOCUSING ELEMENT, ALPHA IS GIVEN BY
      ALPHA=ATAN(2.*(ZM1(I+2)-ZM1(I+1)+ZM2(I+1))*BI(I+1))
C
C     AT THE FOCUSING ELEMENT THE Y-VALUE IS GIVEN BY
      YM=BI(I+1)*SIN(2.*ALPHA)
C
C     AND THE X-VALUE IS
      XM=BI(I+1)+BI(I+1)*COS(2.*ALPHA)
C
C     THE FOCUSING ELEMENT DECREASES YM BY 1./FM
      YM=YM-1./FM(I)
C
C     THE NEW B CIRCLE IS GIVEN BY
      BI(I+2)=(XM**2+YM**2)/2./XM
C
C     THE NEW Z REFERENCE IS GIVEN BY
      ZM2(I+2)=YM/(XM**2+YM**2)
 40   CONTINUE
C
C     THE CALCULATION PORTION STARTS HERE
C
 60   WRITE(8,70)
 70   FORMAT(/'ENTER LOCATION')
      READ(8,-)Z
C
C     CHECK TO SEE WHERE IN THE OPTICAL SYSTEM Z IS
C
      M=N+1
      DO 75 I=1,M
      IF(Z.GT.ZM1(I+1))GO TO 75
```

```
      GO TO 76
75    CONTINUE
C
C     ALPHA IS GIVEN BY
76    ALPHA=ATAN(2*(Z-ZM1(I)+ZM2(I))*BI(I))
C
C     X IS GIVEN BY
      X=BI(I)+BI(I)*COS(2.*ALPHA)
C
C     THE SPOT SIZE IS GIVEN BY
      XO=SQRT(WAVE/3.1415926/X)
      Z=-(Z-ZM1(I)+ZM2(I))
      WRITE(8,80)XO,Z
80    FORMAT('THE SPOT SIZE IS ',G11.4,/'THE FOCUS IS ',G11.4,
     1'UNITS AWAY')
      GO TO 60
      END$
```

APPENDIX D

MASS SPECTROMETER MEASUREMENTS OF HDO CONCENTRATION

A small mass spectrometer residual gas analyzer was used to monitor the concentration of HDO relative to H_2O in the absorption cell. First the mass spectrometer was baked out using a heat lamp and heating tape to remove as much residual water as possible. After baking, the pressure in the mass spectrometer system was 10^{-8} torr. Next a sample of water containing 6.22% HDO was admitted to the absorption cell by completely evaporating a small amount of the enriched water contained in a bottle, and nitrogen was added to a total pressure of 760 torr. The sample was allowed to mix for one hour, and then a mass spectrum of the sample was recorded. The portion of this spectrum between 16 and 19 is the bottom curve in Fig. 75. The sample was admitted to the spectrometer through a small leak valve and continuously pumped out through the diffusion pump. The spectrum was recorded at a pressure of approximately 10^{-5} torr. In Fig. 75 mass number 16 corresponds to oxygen, 17 to OH, 18 to H_2O and OD, and 19 to HDO.

Next the absorption cell was closed off from the mass spectrometer, and the sample was allowed to remain in the cell and mix over night. During this time the mass spectrometer was again baked out in order to remove the residual water from the first sample. After baking, the mass spectrometer was again at a pressure of 10^{-8} torr. The next day another mass spectrum was recorded the same way as the first. The portion of this spectrum from mass number 16 to 19 is the top curve in Fig. 75.

The amplitude of the peaks at mass number 18 and 19, corresponding to H_2O and HDO, is greater in the second spectrum than in the first. However, in both cases the ratio of the amplitude of the peak at 18 to the amplitude of the peak at 19 is about 10 or 12. Therefore the ratio of HDO concentration to H_2O concentration did not change although 20 hours elapsed between the time the first spectrum was recorded and the time the second spectrum was recorded. The conclusion then is that the absorption cell walls do not absorb one water isotope more than the other.

It was not possible to determine the absolute concentration of HDO compared to H_2O. It was only possible to determine that the concentration did not change while the sample was in the cell. The absolute concentration must still be determined from the amounts of D_2O and H_2O used to mix the water sample, and the known equilibrium constants.

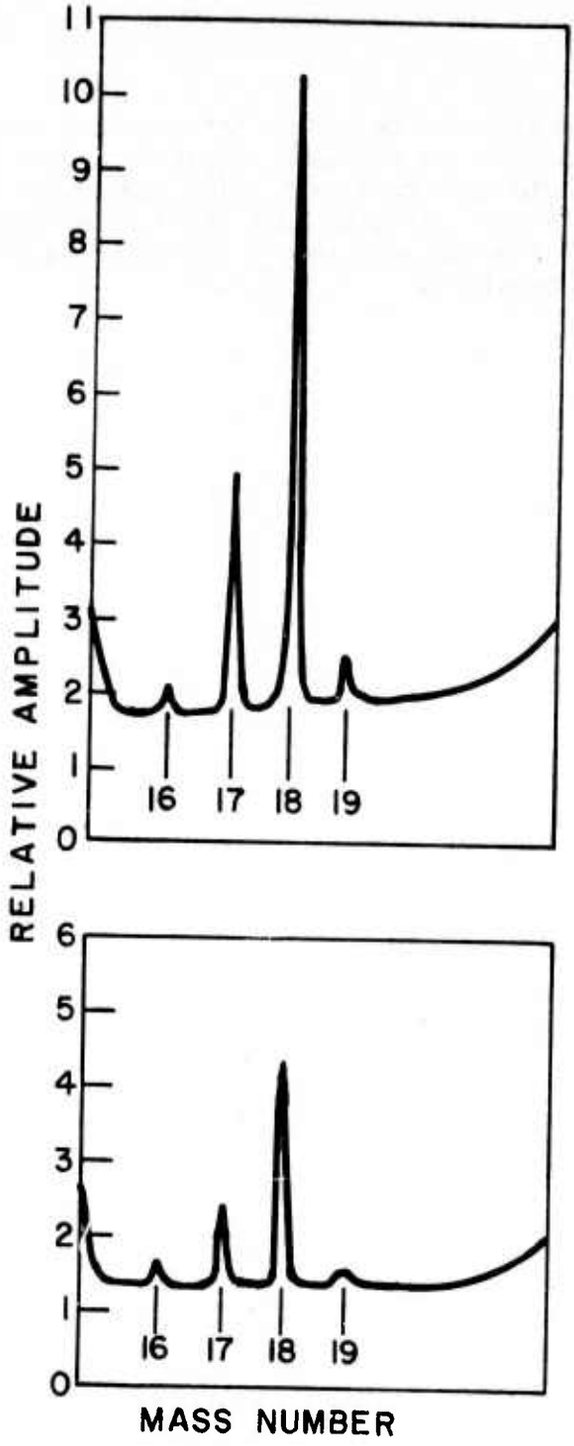

Fig. 75. Mass spectrum recordings of HDO concentration. Bottom curve, one hour after filling absorption cell. Top curve, 21 hours after filling absorption cell.

REFERENCES

1. J. H. Shaw, Ohio Journal of Science 53, 258 (1953).

2. J. L. Streete, "Atmospheric Attenuation of Electromagnetic Radiation in the Infrared Spectral REgion," Ph.D. Dissertation, University of Florida, August 1967.

3. R. A. McClatchey, W. S. Benedict, S. A. Clough, D. E. Burch, R. F. Calfee, K. Fox, L. S. Rothman, and J. S. Garing, "AFCRL Atmospheric Absorption Line Parameters Compilation," Air Force Cambridge Research Laboratory Technical Report AFCRL-TR-73-0096, January 1973.

4. D. E. Burch, D. A. Grynak, and J. D. Pembrook, "Investigation of the Infrared Radiation by Atmospheric Gases: Water, Nitrogen, Nitrous Oxide," Philco-Ford Aeronutronic Division Report U-4784, (AFCRL-71-0124), January 1974.

5. G. Herzberg, Molecular Spectra and Molecular Structure II. Infrared and Raman Spectra of Polyatomic Molecules, Van Nostrand Reinhold, New York, (1945).

6. W. S. Benedict, R. Herman, G. E. Moore, and S. Silverman, Canadian Jour. Phys. 34, 830 (1956).

7. H. A. Lorentz, The Theory of Electrons, Stechert and Co., New York (1910).

8. D. E. Burch, E. G. Singleton, and D. Williams, Appl. Opt. 1, 359 (1962).

9. W. S. Benedict and L. D. Kaplan, J. Chem. Phys. 30, 388 (1959).

10. E. M. Deutschman, and R. F. Calfee, "Two Computer Programs to Produce Theoretical Absorption Spectra of Water Vapor and Carbon Dioxide," ESSA Technical Report IER31-ITSA31 (AD 816 369), April 1967.

11. D. K. Rice, "Carbon Monoxide Spectral Line Selection Studies," Northrop Corporation Report NLSD72-13R, August 1972.

12. R. K. Long, F. S. Mills and G. L. Trusty, "Experimental Absorption Coefficients for Eleven CO Laser Lines," Report 3271-5, The Ohio State University ElectroScience Laboratory (RADC-TR-73-126) (AD 760 140), March 1973.

13. W. S. Benedict, R. Herman, G. E. Moore, and S. Silverman, Astrophys. J. 135, 277 (1962).

14. S. S. Penner, Addison-Wesley, Reading, Mass. (1959).

15. C. Young, J. Quant. Spectrosc. Radiat. Transfer 5, 549 (1965).

16. R. A. McClatchey, R. W. Fenn, J. E. A. Selby, F. E. Volz, and J. S. Garing, "Optical Properties of the Atmosphere (Third Edition)," Air Force Cambridge Research Laboratories Technical Report AFCRL-72-0487, August 1972.

17. W. Heath, W. B. Roh, K. N. Rao, F. S. Mills and R. K. Long, "DF and HF Laser Spectra," presented at the Thirtieth Symposium on Molecular Structure and Spectroscopy, Columbus, Ohio, June 16-20, 1975.

18. C. J. Ultee, The Review of Scientific Instruments 42, 1174, (1971).

19. C. J. Ultee, Private Communication, United Technologies Research Center, Hartford, Conn.

20. S. A. Collins, Jr., Appl. Opt. 3, 1263 (1964).

21. G. L. Trusty, Absorption Measurments of the 10.4 Micron Region Using a CO_2 Laser and a Spectrophone," Report 2819-4, The Ohio State University ElectroScience Laboratory (AFAL-TR-72-413) (AD 907 549) January 1973.

22. R. K. Long, "Absorption of Laser Radiation in the Atmosphere," Ph.D. Dissertation, The Ohio State University, 1963.

23. J. U. White, J. Opt. Soc. Am. 32, 285 (1942).

24. D. J. Spencer, G. C. Denault, and H. H. Takimoto, Appl. Opt. 13, 2855 (1974).

25. T. F. Deaton, D. A. Depatie, T. W. Walker, Appl. Phys. Lett. 26, 300 (1975).

26. J. C. Peterson, Private Communcation, The Ohio State University ElectroScience Laboratory, Columbus, Ohio.

27. G. L. Trusty, "Laser Propagation Investigation," Final Report 2819-5, Ohio State University ElectroScience Laboratory, Internal Final Report, January 1973.

28. E. K. Damon, J. C. Peterson, F. S. Mills and R. K. Long, "Spectrophone Measurement of the Water Vapor Continuum at DF Laser Frequencies," Report 4054-1, The Ohio State University ElectroScience Laboratory, July, 1975.

29. W. S. Benedict, Private Communication, University of Maryland.

30. O. E. Myers, Private Communication, General Dynamics Convair Aerospace, San Diego, California.

31. Enhalt and Ostlund, Journal of Geophysical Research, Vol. 75, No, 12, 1970.

32. D. L. Ford, F. S. Mills, and R. K. Long, "Laser Absorption in the 5 Micron Band," Report 3271-3, The Ohio State Universtiy ElectroScience Laboratory, (RADC-TR-72-195) (AD 748 437) July 1972.

33. R. K. Long, F. S. Mills and G. L. Trusty, "Calculated Absorption Coefficients for DF Laser Frequencies," Report 3271-7, The Ohio State University ElectroScience Laboratory, (RADC-TR-73-389) (AD 775 373/46I).

34. R. F. Calfee, "A Note on Terminologies used in Gaseous Absorption Processes," NOAA Technical Report ERL211-WPL 15, August 1971.

35. Handbook of Chemistry and Physics, 48th Edition, pp F158 and F210, A10, and Rear Coverpiece, Chemical Rubber Co., Cleveland (1967).

36. Smithsonian Meteorological Tables, Smithsonian Institution, 1951.

MISSION
of
Rome Air Development Center

RADC is the principal AFSC organization charged with planning and executing the USAF exploratory and advanced development programs for information sciences, intelligence, command, control and communications technology, products and services oriented to the needs of the USAF. Primary RADC mission areas are communications, electromagnetic guidance and control, surveillance of ground and aerospace objects, intelligence data collection and handling, information system technology, and electronic reliability, maintainability and compatibility. RADC has mission responsibility as assigned by AFSC for demonstration and acquisition of selected subsystems and systems in the intelligence, mapping, charting, command, control and communications areas.